# TOWARDS A BETTER CHARACTERIZATION OF MORPHOLOGICAL PLASTICITY AND BIOMASS PARTITIONING OF TREES IN STRUCTURAL DYNAMICS OF MANGROVE FORESTS

Adewole Olagoke

N°: 2016 AGPT XXXX

# Doctorat AgroParisTech

## T H È S E

**pour obtenir le grade de docteur délivré par**

## L'Institut des Sciences et Industries du Vivant et de l'Environnement

## (AgroParisTech)

### Spécialité : Ecosystèmes et Sciences Agronomiques

*présentée et soutenue publiquement par*

**Adewole OLAGOKE**

le 5 Décembre 2016

# VERS UNE MEILLEURE CARACTÉRISATION DE LA PLASTICITÉ MORPHOLOGIQUE ET DU PARTITIONNEMENT DE LA BIOMASSE DES PALÉTUVIERS POUR L'ÉTUDE DE LA DYNAMIQUE DES FORÊTS DE MANGROVES

Directeur de thèse : **Prof. Dr. Uta BERGER**
Co-encadrement de la thèse : **Dr. Christophe PROISY**

**Jury**

| | |
|---|---|
| **M. Daniel IMBERT**, Maître de Conférences, Univ. des Antilles (France) | Rapporteur |
| **M. Martin ZIMMER**, Professeur, Leibniz – ZMT, Univ. of Bremen (Allemagne) | Rapporteur |
| **M. Hauke REUTER**, Chercheur, Leibniz – ZMT, Univ. of Bremen (Allemagne) | Rapporteur |
| **M. Jürgen PRETZSCH**, Professeur, Technische Univ. Dresden (Allemagne) | Examinateur |
| **M. Loïc BRANCHERIAU**, Chercheur, CIRAD-UR BioWooEB, Montpellier (France) | Examinateur |
| **Mme Uta BERGER**, Professeur, Technische Univ. Dresden (Allemagne) | Directrice de thèse |
| **M. Christophe PROISY**, Chercheur, IRD-UMR AMAP / IFP, Pondichéry (Inde) | Co-directeur de thèse |

**AgroParisTech**
**IRD – UMR AMAP**
CIRAD - TA A51/PS2, 34398 Montpellier cedex 5

TECHNISCHE UNIVERSITÄT DRESDEN

**Faculty of Environmental Sciences** Department of Forest Sciences

Institute of Forest Growth and Forest Computer Sciences, Chair of Forest Biometrics and Systems Analysis

# TOWARDS A BETTER CHARACTERIZATION OF MORPHOLOGICAL PLASTICITY AND BIOMASS PARTITIONING OF TREES IN STRUCTURAL DYNAMICS OF MANGROVE FORESTS

**Adewole OLAGOKE**
Born on: 18.05.1982

## DISSERTATION

to achieve the academic degree

**DOCTOR RERUM SILVATCARUM (DR. RER. SILV.)**

Supervisors
**Prof. Dr. Uta BERGER**
**Dr. Christophe PROISY**

Referees
**Prof. Dr. Martin ZIMMER**
**PD. Dr. Hauke REUTER**
**Dr. Daniel IMBERT**

Submitted on:

Defended on:

**Title:** Towards a better characterization of morphological plasticity and biomass partitioning of trees in structural dynamics of mangrove forests

**Keywords:** Plant plasticity, Biomass allocation, Tree allometry, Forest structure, Coastal dynamics, Mechanistic ecological modelling, Mangrove ecosystems

**Abstract:**

Changing environmental conditions often impose stressful growing conditions in plant communities. Until now, morphological plasticity, i.e. polymorphic growth physiognomies of plants, has not been sufficiently studied as a pivotal strategy for the whole ecosystem adaptation to environmental stress. We consider mangrove ecosystems as suitable models to provide insights on this subject.

In the thesis, I investigate the ecological significance of tree morphological plasticity in the structural development and the dynamics of mangrove forests. I conducted field experiments in two regions located on both sides of the Amazon River mouths i.e. in French Guiana and North Brazil. Forest inventories were carried out in contrasting mangrove stands in both regions. The thesis combines empirical analysis of field data, terrestrial laser scanning (TLS), and mechanistic, individual-based computer simulations.

We published results that proved the TLS-based analysis of individual tree structure useful for a better knowledge on biomass allocation between trunk and branches in tall and large *Avicennia germinans* mangrove trees reaching 45 m high and 125 cm of trunk diameter. Combining structural descriptions of *A. germinans* trees found in both sites, I highlighted the site-specific differences in tree allometries. The study suggests that regional differences in mangrove tree structure and function could be captured through better description of crown metrics, and that selected indicators of local morphological plasticity and consequent stand structure could generate a plus-value in the understanding of mangrove stand dynamics across contrasting coastal environments. Beyond extension of allometric models to large *Avicennia* trees, we proposed new biomass equations with improved predictive power when crown metrics is taken into account. Additionally, we developed a novel software tool, named *Lollymangrove*, based on the AMAPStudio suite of software, with the objective of maximizing the potential of further field descriptions and modeling works. *Lollymangrove* allows standardized forest data capture, 3D visualization of structural data, aboveground biomass computations from a configurable and export formats for forest dynamics and remote sensing models.

Simulation experiments were conducted by means of the spatially explicit, individual-based stand model BETTINA_IBM. This model describes the important mechanism of water uptake limited by salt stress, and revealed insights into the relation between environmental conditions, allometric variations and biomass partitioning of mangrove trees, and stand characteristics. The simulation results suggest close matches with observed ecological patterns (e.g., tree allometries, mortality distributions, and self-thinning trajectories) under higher salinity. In low salinity conditions, however, the current parameterization underestimates the maximum tree height and diameter, and consequently, aboveground biomass and self-thinning trajectories of forest stands. This suggests that the morphology of trees under low levels of salinity are explained by further regulation mechanism(s) that still need to be addressed in a subsequent model improvement.

Overall, this work has essentially pointed out the need to elucidate how morphological plasticity relates with structural development of forest stands. It establishes that TLS measurements and structural data analysis associated to efforts for integrative software and mechanistic modelling works could link mangrove dynamics to fast-changing coastal processes.

**Titre :** Vers une meilleure caractérisation de la plasticité morphologique et du partitionnement de la biomasse des palétuviers pour l'étude de la dynamique des forêts de mangroves

**Mots clés :** Morphologie des plantes, allocation de biomasse, allometries, structure forestière, modélisation écologique, écosystèmes de mangrove, dynamique côtière

**Résumé :**

Les changements environnementaux sont souvent sources de stress pour la croissance des plantes. Jusqu'à présent, la plasticité morphologique des arbres, c'est à dire leur capacité à produire des physionomies différentes, n'a été que peu envisagée comme stratégie d'adaptation du peuplement forestier à un environnement stressant. Etant donné la variabilité des physionomies de palétuviers observée y compris au sein d'une même espèce, l'étude des mangroves nous apparait pertinente à la fois pour aborder la question de l'adaptation des formes de plantes à des environnements changeants mais également pour apprendre sur le fonctionnement de cet écosystème soumis en permanence à des changements environnementaux.

J'ai donc cherché à caractériser l'importance de la plasticité morphologique des palétuviers dans la structuration et la dynamique des forêts de mangroves. Pour cela, j'ai réalisé des expérimentations de terrain dans deux grandes régions de mangroves situées de part et d'autre de l'embouchure de l'Amazone, à savoir, la Guyane Française et la péninsule de Bragança, dans l'état du Pará au Brésil. Le travail de thèse a combiné à la fois des analyses empiriques de données forestières, l'acquisition et le traitement de données issues d'un scanner laser terrestre (TLS) utilisées pour décrire la physionomie d'arbres adultes et de la modélisation écologique.

Nous avons publié des résultats qui attestent du potentiel de données TLS pour obtenir une meilleure connaissance de la distribution de biomasse entre le tronc et les branches dans le cas de grands et larges palétuviers de l'espèce *Avicennia germinans*, pouvant atteindre 45 m de haut et 125 cm de diamètre de tronc. En combinant les descriptions de structure arborée acquises sur nos deux sites d'étude, nous avons mis en évidence des différences nettes dans les allométries décrivant la croissance de cette espèce. J'ai proposé de nouvelles équations allométriques qui intègrent des paramètres descriptifs de houppiers. En parallèle, nous avons développé un nouvel outil, nommé Lollymangrove, intégré à la suite de logiciels AMAPStudio dans l'objectif de maximiser le potentiel des futures descriptions et travaux de modélisation. Lollymangrove permet de saisir des données d'inventaires forestiers, de visualiser les faciès forestiers sous la forme de peuplements 3D en 'sucettes', de faire des calculs de biomasse épigée à partir d'une interface configurable proposant la plupart des modèles allométriques de la littérature et d'exporter dans des formats utilisables par les modèles de dynamique forestière et de télédétection.

En parallèle, des simulations ont été réalisées avec le modèle BETTINA_IBM. Ce modèle individu centré et spatialement explicite décrit les mécanismes d'absorption de l'eau sous contraintes de salinité. Il permet d'appréhender les relations entre les conditions environnementales, les variations allométriques, le partitionnement de biomasse dans les palétuviers et la structuration des peuplements forestiers. En conditions de forte salinité, les résultats sont en bonne adéquation avec des processus écologiques simples (allométries, trajectoires d'auto-éclaircie, densité de mortalité, etc.). Dans des conditions de faible salinité, le paramétrage actuel sous-estime la hauteur et le diamètre maximaux observés. Les mécanismes de régulation à faible niveau de salinité doivent donc être mieux décrits dans le modèle utilisé.

Pour résumer, ce travail de thèse insiste sur le besoin d'élucider comment la plasticité morphologique des palétuviers influence le développement structural et le fonctionnement des forêts de mangroves. Il a établi que la combinaison de mesures TLS et d'analyses de données de structure forestière associée à des efforts de modélisation écologique pouvait fournir des éléments indispensables pour lier dynamique des mangroves et dynamique des processus côtiers.

## ACKNOWLEDGEMENTS

This doctoral thesis was realized between September 2013 and November 2016, thanks to the FONASO fellowship, which was funded by the European Commission's Erasmus Mundus Joint Doctorate programme (EMJD). I am grateful for the travelling grants and research supports provided by the Graduate Academy of the TU Dresden, the CREC (Coastal Research Network on Environmental Changes) project of the TU Dresden, the French Institut de recherche pour le développement (IRD), and the Centre National de la Recherche Scientifique (CNRS) research program - "Incubator for interdisciplinary research projects in French Guiana". Also, credits are due to the IRD Cayenne and the UFPA Bragança, Brazil for hosting me during my field studies. Prof. Dr. Ulrich-Saint Paul granted us access to a utility vehicle for the field campaign in Bragança, thanks a lot.

I have benefited from the support, contributions, companionship and goodwill of a number of people in the course of my doctoral studies. In particular, I am very grateful to my thesis supervisors Prof. Uta Berger and Dr. Christophe Proisy. Thanks for your untiring patience, enthusiasms, regular guidance, and most importantly, for providing a conducive and resourceful learning environment. My sincere appreciation also goes to Prof. Sven Wagner, Dr. Isabella Chuine, and Dr. Raphaël Manlay for your time and contributions to the PhD committee. My sincere thanks to Prof. Jürgen Pretzsch, Prof. Martin Zimmer, PD Dr. Hauke Reuter, Dr. Daniel Imbert and Dr. Loïc Branchériau for accepting and making time to participate in the evaluation and jury of my thesis.

I am indebted to a host of collaborators and consultees, especially the co-authors of my published articles and manuscripts. Drs. Ronny Peters, Jean-Baptiste Féret, François Fromard, Ulf Mehlig, Moirah Menezes, Valdenira dos Santos, and François de coligny are well acknowledged. I appreciate the advice and contributions of Profs. Morag McDonald, Karl-Heinz Feger, Heinz Röhle, S.O. Akindele, Victor Adekunle and Jonathan Onyekwelu. Mrs. Claudia Wenzel was very helpful in many respects. Aor Pranchai and Micheal Jenke made the field studies in Bragança a delightful one. I am glad to acknowledge the fellowship and supports from members of the Forest Growth and Forest Informatics, TU Dresden (Dr. Juliane Vogt, Dr. Ronny Peters, Dr. Robert Schlicht, Dr. Alejandra Vovides, Martin Werisch, Hans Hamkens, Soledad Luna, Mrs. Gisela Metzig, Mrs. Sabine Schenk, Mrs. Ursula Behr and others), and the AMAP team, Montpellier (Dr. Pierre Couteron, Dr. Raphael Pellissier, Dr. Nicola Barbier, Pierre Ploton, Emil Cherrington and others). I would not forget the kindness of various amazing people I met or contacted in different parts of the world during my studies, thanks to you all.

Thanks due to all my kinsmen and friends, especially my parents Gabriel and Victoria Olagoke for their supports and patience, and for always believing in me.

Last but not the least, kudos to Sade and 'Demi for accompanying me through this tasking, yet a highly rewarding journey. You rock my world!

# TABLE OF CONTENTS

# LIST OF FIGURES

# LIST OF TABLES

# 1 GENERAL INTRODUCTION

*This chapter presents the main motivation for the current work and the research objectives addressed in the course of my doctoral studies. Specifically, I present a concise note on the impetus to analyze the ecological significance of trees and forests' adaptations to environmental change, with a focus on mangrove ecosystems. I briefly introduce the complementary nature of empirical studies, mechanistic modelling and the prospects of remote sensing techniques in addressing the target study, and in the end, I present the research objectives, scope and organization of the chapters covered in the thesis.*

## 1.1 Main motivation and challenges

### *1.1.1 Forests and plants adaptations to environmental change*

Our environment is constantly changing, and the understanding and prediction of the ecological feedbacks on plants and forest communities have arguably assumed an active area of investigations among the contemporary ecologists. For about 370 million years, plants and forest ecosystems (e.g. Stein et al. (2007)) have interacted with climate and environmental conditions (e.g. Retallack (1997)). They are now composed in complex ecosystems, with varying echelons of responses, adaptations, resilience or other capabilities to cope with local and global environmental changes (Thompson et al., 2009). Accordingly, plants have evolved allometric patterns characteristics of diverse selection pressures and constraints, and these patterns scale from the individual levels to explain many emergent behaviours being observed at the population or community levels (Weiner, 2004). In a bid to optimize resource acquisition, utilization and growth under changing environment, plants do develop structural features that are characteristic of the growing environment. Through plasticity in growth forms and biomass allocation, for example, plants adapt to ambient conditions, or changes that occur in the course of their development. Thus, the signatures placed by the past and/ or currently prevailing environmental conditions are conspicuously readable in the characteristic plant morphological traits. Exploring this morphological plasticity[1] and the ecological significance across contrasting environments thus becomes fundamental to the understanding of the causes and consequences of environmental change in plant communities.

There are well-established allometric frameworks linking many aspects of forest structural and functional properties to the scaling of trees' morphological and physiological traits (Bohlman and Pacala, 2012; Muller-Landau et al., 2006; West et

[1] Morphological plasticity defines the phenomenon of a given plant genotype exhibiting divergent growth forms and allometric scaling under different selection pressures in variable environments (*Sensu*. Callaway *et al*. 2003; Weiner, 2004)

al., 2009). Such relationships are rooted in the power-based dimensional ratio of structure and function relationships (Huxley and Teissier, 1936). For these conceptual models, the morphological scaling in trees is simply presumed to converge in invariant allometric exponents (Enquist and Niklas, 2001; West et al., 1999). Consequently, many predictive models of tree form and functions across sites or regions are captured in simple allometric equations. Evidences however, suggest that the allometric relationships of the tree structure and function are not always linearly simple (Weiner, 2004), and can vary significantly both within and across sites (Feldpausch et al., 2011; O'Brien et al., 1995; Pretzsch et al., 2014); they are largely influenced by environmental constraints (Koch et al., 2004; Ryan and Yoder, 1997). For instance, the morphology of shoot in relation to the respective root systems in individual trees is fashioned in the sense that they meet individuals' peculiar functional need to obtain light, water or nutrients prevailing environmental cues (Franklin et al., 2012; Poorter et al., 2012). Traversing to the ecosystem level, the ecological significance of tree morphological plasticity for local tree interactions (Callaway et al., 2003) has to be clarified in the scope of their contributions to the structural dynamics and functioning of forest ecosystems in changing environments (Banin et al., 2012; Berg and Ellers, 2010). Such knowledge is quite fundamental to the prediction of forests and tree responses to environmental change (Nicotra et al., 2010; Richter et al., 2012), imperative for understanding ecological feedbacks to ever-changing climate. In the context of this thesis, the mangrove ecosystems were considered as the subject of investigations for reasons demonstrated in the following sections.

### *1.1.2 Mangrove ecosystems and the relevance for investigations of tree morphological plasticity and forest dynamics in changing environments*

Occupying the interface of land and oceans in the tropical and subtropical coastlines, the global distribution (Figure 1-1) of mangrove forests are restricted to regions under the combined influence from the continental and the oceanic climates (Wolanski et al., 2009), where the isotherm of seawater temperature approximate at 24°C and the air temperature of ca. 16°C isotherm (Chapman, 1977). When mangrove forests are viewed in the mirror of the tropical (terrestrial) rainforests, they are often classified as relatively simple in terms of species composition as well as the vertical stratification. They are mostly of few species in one dominant vertical layer with little or no understory scrubs and forbs (Alongi, 2009). The variety of mangrove forest structure rather becomes distinguishable by how the interactions of physical processes constrain the vigour and diversity of forest development (Wolanski et al., 2009).

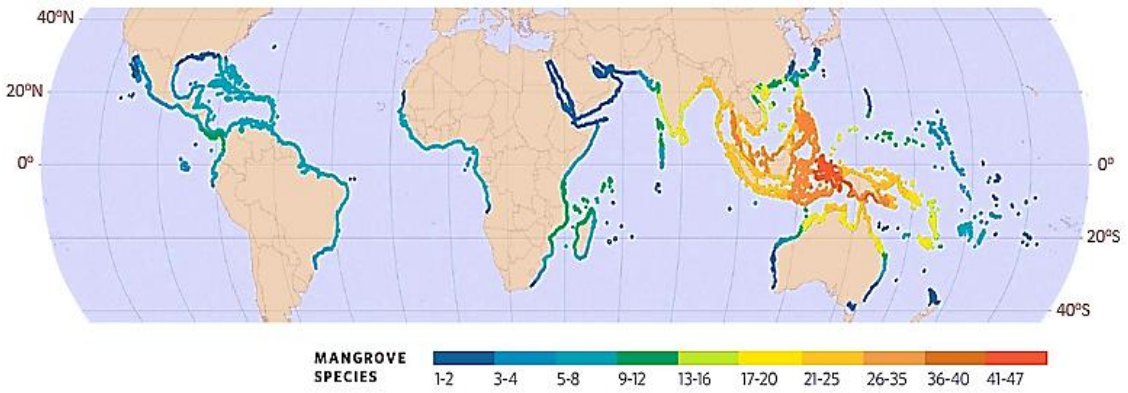


Figure 1-1: Global distribution of mangrove forests showing the coastal extent and species richness. *(Map adapted from http://roomthily.tumblr.com)*

For the heterogeneous nature and varying impacts of biophysical forcing functions like tidal currents, nutrients, multiple stressors including salt accumulation, drought and occasional disturbances such as typhoon and hurricanes across the world mangrove belt, the architecture of mangrove forests substantially differ in local and regional scales (Cintron and Schaeffer-Novelli, 1984). The fact thus remains that each mangrove stand at a local scale has possessed a unique signature reminiscent of the complex interplay of the temporal changes in coastal processes and geomorphology and the resulting trees' physiological tolerances and competitive interactions (Alongi, 2008). Indeed, it is less conservative to state that each mangrove forest has a unique story to show. As stress factors are high in mangrove forests, and the costs of specialization are significantly high, a crucial strategy for plants' survival remains high levels of plasticity in both phenotypic features and physiological traits (Feller et al., 2010).

Many empirical cases of morphological plasticity of mangrove trees are highlighted in different studies (Feller et al., 2010; Vovides et al., 2014). In some instances, single species were noted exhibiting divergent growth forms (polymorphism) in variable environments, ensuring their survival over a wide ecological range (Feller et al., 2010). A typical *Avicennia germinans* tree in the equatorial mangrove region can attain a height of ca. 45 m (Fromard et al., 1998), but then grow in dwarf or scrubby stands (examples in Figure 1-2) with a height of about 0.5 to 2 m in the sub-optimal habitats (Vogt et al., 2014a). Likewise, Lugo (1997) showed that *Rhizophora mangle* in the Neotropical forest can attain mature tree size between 0.5 m and 40 m high depending on habitat salinity. In other instances, cases of neotenized growth or precarious reproduction are documented (e.g., Dangremond and Feller (2016)). Additionally, mud-bank colonization of *A. germinans* in French Guiana display high local disparities in tree growth and morphology, which suggests that local and tenuous differences of mud elevations and hydrological patterns can significantly influence the initial stages of mangrove development (Proisy et al., 2009). These and

other examples of highly plastic mangrove structure resulting from other abiotic factors in variable environments (Dahdouh-Guebas et al., 2004; Lovelock et al., 2005) place mangrove forests in an unrivalled position in the understanding of trees and forests responses to environmental change.


Figure 1-2: Photographic illustration of polymorphic growth forms in Avicennia trees

The plastic growth forms in mangrove tree species directly relate with the preferential biomass partitioning to various tree components in the course of tree development in variable environments (Feller et al., 2003; Lira-Medeiros et al., 2010; Peters et al., 2014). In this case, an individual growing in a water or nutrient limited environment prioritizes biomass allocation to root development (Ball, 1988; Castañeda-Moya et al., 2011) in order to facilitate access to belowground soil resources. On the other hands, trees direct allocation of more biomass to the crown and leaf growth when light resource becomes limiting (Cintron and Schaeffer-Novelli, 1984; Clough, 1992). In spite of these available knowledge on the morphological plasticity of mangrove trees, the implications for structural development and dynamics at the stand scale remains less understood, and hence the contributions of the current thesis.

### *1.1.3 Forest dynamics modelling and the incorporation of morphological plasticity*

Forest simulation models are important tools in the investigations of complex interactions of different mechanisms underlying trees and forests adaptations to changing environment or habitat alterations (Berger et al., 2008). The beauty of forest simulators is showcased in the fact that the trees' or forests' properties under investigations may require large and costly to acquire datasets in natural systems (Berger et al., 2008). More so, simulation modelling has facilitated testing of hypotheses, in manipulated virtual experiments, concerning processes that could otherwise take years to become observable in field conditions (e.g. Fourcaud et al. (2008); Zurell et al. (2010)). Simulation models have attempted to demonstrate the extent to which constraints in local geomorphological settings, coastal processes and regional climatic forcing functions can influence the dynamics of mangrove forest structure (Proisy et al., 2016a; Twilley and Rivera-Monroy, 2005). Also, their usefulness in the understanding of how abiotic environments affect the colonization, growth, productivity and mortality of mangrove species have been demonstrated in various studies (Berger and Hildenbrandt, 2000; Berger et al., 2004; Chen and Twilley, 1998; Grueters et al., 2014). With the application of mangrove stand simulator, Piou et al. (2008) evaluated the importance of different perturbations intensity and abiotic conditions on post-hurricane forest recovery. In a similar manner, Vogt et al. (2013) and Vogt et al. (2014b) advanced the analysis of canopy disturbances and the significance for forest regeneration and structural heterogeneity in mangrove plantations. The work of Doyle and Girod (1997) is equally one example demonstrating how simulation model was employed to analyze the effect of hurricane histories on the structure and composition of mangrove forests at the landscape scales. In the analysis of forest restoration trajectories, the work of Twilley et al. (1999) was quite demonstrative. Beyond several applications in ecological studies, simulation models have also tested satisfactorily in planning and decision-making for management of mangrove forests (Fontalvo-Herazo et al., 2011; Rivera-Monroy et al., 2004; Twilley et al., 1998).

With capabilities to capture the mechanisms that explain mangrove forest dynamics, including the controlling role of stress factors, plant–environment interactions, and scenarios for the impacts of natural and anthropogenic disturbances at different scales, three major simulation models (FORMAN, MANGRO and KiWi) have received wide applications. Their predictive ability is albeit limited by their lack of provision for morphological plasticity of trees, among other factors (Grimm and Railsback, 2005; Berger et al. 2008). Mostly, the models rely on the use of static growth functions with deterministic relations between tree dimensional attributes such as stem diameter, tree height or canopy projection area, etc. More recently, the mesoFON model (Grueters et al., 2014) made a pioneering attempt to address issues of morphological plasticity in mangrove stand modelling while describing crown shift

related to light foraging of individual trees. Yet, the allometry relation of the tree structure in this model remains size-dependent. In the scope of the current thesis, we found the BETTINA single-tree model of Peters et al. (2014), that describes the adaptation and allometric change of individual trees to environmental change, a very promising to approach the simulation of structural development and dynamics of mangrove forests to changing habitat conditions in coastal environments.

### *1.1.4 The prospects of coupling forest simulation models and remote sensing techniques*

In the previous section, a concise overview of the importance and potential of forest simulation models was presented. Realizing an extensive validation of most models over large spatial and temporal scales is often difficult to achieve due to lack of multitemporal data of forest measurements. This step, perhaps, is required to meet the predict-and-test cycle and evaluation process in forest modelling (Shugart et al., 2015). Another aspect centers on realistic representation of tree architecture, biomass partitioning and adaptive growth behaviors (Peters et al., 2014). Until now, explicit representation of phenotypic plasticity in plants is lacking in the available models (Grimm and Railsback, 2005). Meanwhile, remote sensing techniques have potential to complementary role in extending modelling capabilities.

First, recent remote sensing facilities are providing opportunity to capture large-scale datasets on forest structure, including detailed tree properties and biomass, which allows for validation of forest models' predictions (Shugart et al., 2015). More so, remote sensing instruments have the potential for acquisition of forest and tree properties that are difficult to achieve through ground measurements (Feliciano et al., 2014; Kasischke and Christensen Jr, 1990). In general, remote sensing observations have proved useful in providing multi-decadal data to support monitoring of vegetation cover and changes mangrove shorelines (e.g. Nascimento Jr et al. (2013); Walcker et al. (2015)). Such types of data are currently not wholly integrated into the existing forest modelling framework (Proisy et al., 2016a), even when they can support our understanding of the structural dynamics of mangrove forests to changing coastal processes. Remote sensing techniques, in turn, have much to gain for fine-tune calibration through a connection to forest models (Proisy et al., 2016b; Shugart et al., 2015). This thesis highlighted the prospects of connecting these two domains in realizing the set objectives.

## 1.2 Research objectives

The contributions of the current thesis are encapsulated in threefold objectives. These include: 1) improved characterization of tree morphology and biomass partitioning of mangrove trees, 2) empirical analyses of cross-regional differences in tree morphological allometries and subsequent impacts on stand aboveground biomass dynamics, and 3) simulation of the effects of plastic tree morphology and

biomass partitioning on the emergent structure and dynamics of mangrove forests under varying environmental conditions. Considering the challenges of field measurements in the mangrove environment, the novelty of this work commences with the application of terrestrial laser scanning techniques (TLS) to describe the structure and biomass partitioning of mangrove trees, up to the very large stems that are practically not feasible for direct cut-and-weight method. On top of the empirical analyses of the significance of morphological plasticity for cross-regional aboveground biomass dynamics, an integrated software for capturing structural data and 3D visualization of mangrove forests was proposed. The augmentation of the field studies with a mechanistic-based modelling approach, where morphological plasticity and dynamic biomass partitioning were integrated, to simulate the interplays of environmental (abiotic) factors, local competitive interactions and growth forms of individual mangrove trees on the emergent forest structure, marks a significant milestone. For simplicity's sake, the context of environmental factors was restricted to a gradient of habitat salinity and water stress conditions with the scope of this thesis.

## 1.3 Study areas and datasets

### *1.3.1 Description of study sites*

For the purpose of this thesis, we have conducted field studies in the Amazon-influenced mangrove forests in French Guiana, a French department located 500 km north of the Amazon River mouth and in the Bragança peninsula located about 150 km southeast of the Amazon River mouth, in the Pará state, Brazil. Figure 1-3 shows the map of the study areas outlining the specific location of the sample plots. These sites demonstrated a good ability to inform on coastal changes (Fromard and Proisy, 2010; Fromard et al., 2004; Lara and Cohen, 2006; Souza Filho et al., 2006). The sites are characterized by the dominance of two mangrove species (*Avicennia germinans* and *Rhizophora ssp.*) as key structural components, and distinctive coastal settings.

The French Guiana mangroves stretch along a 350 km coastline, primarily covered by sediment dispersal from the Amazon River (Baltzer et al., 2004). The spatio-temporal distribution of mangroves is controlled by a succession of rapid and acute erosion and accretion phases resulting from the drift of giant mudbanks to the northwest (Allison and Lee, 2004; Gardel and Gratiot, 2004). Mangrove forests are distinctly structured in varying growth stages, and patchily distributed across the coastal landscape (Proisy et al., 2007). The French Guiana coast can be considered as a pristine coast as industrial activities are still not extensively developed and aquaculture does not exist.

The Bragança mangrove region, located in the Caeté estuary, extends over ~300 km southeast of the Amazon estuary, near the city of Bragança (Menezes et al., 2008).

The forests form riverine/ fringe mangroves in a 166-km² peninsula, crossed by several tidal channels with macrotides of ~4 m range and strong oscillating currents reaching ~1.5 m $s^{-1}$ velocities for spring tides (Lara and Cohen, 2006; Lara, 2003). Highly dynamic sediment transport, with areas of rapid mud erosion and deposition, forming similar geomorphologic features and the development of analogous mangroves, and the correlation found between tree height and topography-dependent inundation frequency (Cohen and Lara, 2003; Cohen et al., 2004) are some of the intrinsic features of Bragança mangroves.

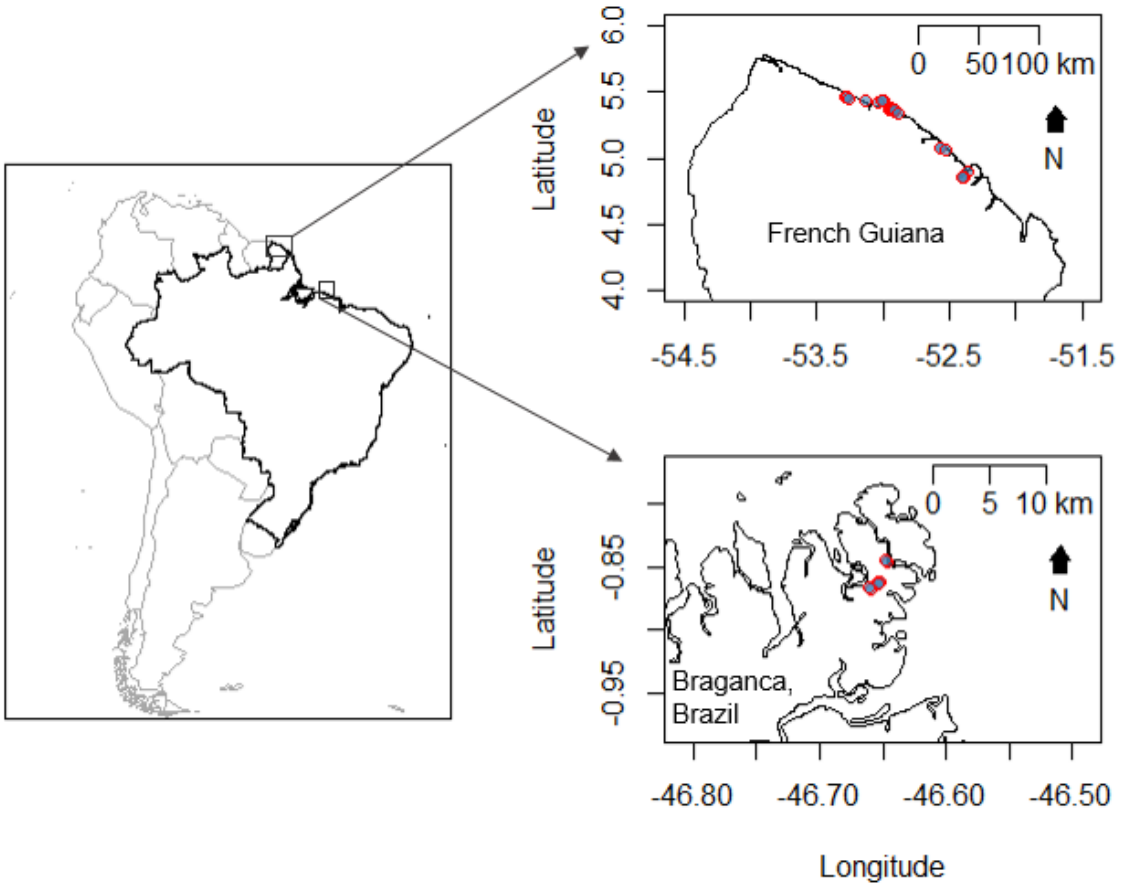


Figure 1-3: Map of study locations in the Amazon-influenced coasts of French Guiana (upper-right) and the Caeté estuary (lower-right) near Bragança (North Brazil). *Experimental plots are marked in coloured polygons.*

### 1.3.2 *Data collection*

We conducted two field studies in the frame of my PhD work. The first one was realized in Bragança (North Brazil) between January and April 2014 (3 months) and the second field campaign took place in French Guiana from August to September 2014 (2 months). Complementing data from these field studies are the time-series datasets of forest structure from 46 sample plots in French Guiana. These datasets, obtained from 2001 to 2012, were made available for use in the current thesis by Dr. Christophe Proisy. During the field campaigns, the measurement procedures were cascaded into two levels: the stand structure descriptions and tree scale

measurements. Other than the variations in plot sizes and the choice of device for non-destructive characterization of three-dimensional (3D) mangrove tree structure and biomass, nearly the same sampling strategies and measurement protocols were deployed in all field studies.

*Stand level measurements*

The stand selection follows a purposeful sampling strategy. We have chosen to concentrate on *A. germinans* as a focal species to test methods and thus, stands were selected to ensure the presence and dominance of this species. We considered to sample stands of varying DBH sizes and growth forms, species mixture and forest structure across a range of habitat conditions where they commonly occur, both in Bragança and the French Guiana. Once stands were located, we mapped all trees of DBH greater than 5cm. The position within the plot, DBH, total height, crown dimensions, and species name were recorded to describe the stand structure. In the case of the French Guiana, the selection of sample stands was designed to capture different forest types over a range of development stages, as classified by (Fromard et al., 1998). *A. germinans* trees were found in the early colonization (pioneer) and old-growth forests, spanning a wide range of growth stages. These growth stages are patchily distributed across the coastal landscape with clusters of young trees, sometimes in close vicinity to decaying stands (Proisy et al., 2007). In essence, the selected plots also covered from predominantly monospecific *Avicennia* stands to the most diverse mixed stands (containing mostly 3 mangrove species - *A. germinans, R. mangle* and *L. racemosa*, and other associates).

*Tree scale measurements*

The 3D architectural measurements were completed on 51 selected mangrove trees across sample plots in the French Guiana using the FARO Focus3D X330 terrestrial laser scanning (TLS) and a total-station laser tacheometer. Figure 1-4 illustrates a typical set-up of the TLS device for tree measurements during the field studies in French Guiana. Detailed descriptions of the scanning procedures and subsequent analyses are provided in the Chapter 2 of this thesis. In Bragança, we used a rangefinder device (LaserACE 1000) to characterize the 3D tree shape/ skeleton, tree and trunk height (m), stem diameter (cm), crown dimensions (m) and projection area ($m^2$), and volume of biomass in trunk and branch components, from 26 dominant (top height) trees systematically distributed across five mangrove forest stands. Additionally, wood density measurements were obtained from representative trees and the mean values of all observations were estimated accordingly for each species encountered in all forest plots.


Figure 1-4: Setting up the FARO 3D X330 laser scanner on a tripod in the mangrove forests

## 1.4 Organization of the thesis

This thesis is structured into six distinct, but complementary chapters. The current chapter introduces the entire work, covering the main motivation and challenges, research objectives and scope, and the thesis structure.

In Chapter 2, I present a method developed for non-destructive characterization of the 3D aboveground morphology and biomass of mangrove trees, using terrestrial laser technology. The chapter elaborated on the need for applying remote measurement techniques in the study of mangrove structure and functioning while showcasing a practical application to the measurements of *A. germinans* trees, including the very large individuals (often difficult for direct field measurements) in French Guiana. More so, I attempted the decomposition of tree biomass into main constituent parts (trunk, branches, and leaves), towards the analysis of shifting biomass allocation in mangrove species. The biomass data so obtained were applied to extend the calibration and validation domains of biomass allometric models to large trees. The main outcomes of this study were presented in the SilviLASER conference (France) in 2015, and subsequently published in the journal, *Trees – Structure and Function*.

Chapter 3 provides an empirical cross-regional analysis of tree morphological changes and the implications for the dynamics of aboveground biomass in the Amazon-influenced mangrove forests. In the study, I highlighted the extent of local variations in tree morphology using ensemble inventory data from contrasting mangrove forests in Bragança (North Brazil) and French Guiana. Here, I proposed the inclusion of crown metrics in biomass allometric models to account for local

morphological variation in biomass estimates. The study further extends to the determination of collective plastic structural attributes that can explain the variation of stand aboveground biomass from local to regional scales.

Chapter 4 centers on the description of a standardized platform, which was proposed to facilitate the acquisition, processing and visualization of structural data of mangrove forests. In this chapter, I demonstrate the capability of the software tool to address site-specific variation in biomass allometric models through the provision of a configurable biomass module. Furthermore, the application of the platform towards an extensive data preparation for calibration and validation of forest dynamics and remote sensing models was advanced.

In Chapter 5, I present a study on the application of mechanistic simulation modelling to complement empirical data in investigating the consequences of morphological plasticity and dynamic biomass partitioning for the structural development of mangrove forests under variable environmental conditions. The emphasis was on model description, and the evaluation based on field measurements and other benchmarks, including known ecological patterns in scientific literature. An example application of the model for canopy-based biomass analysis and the significance for remote sensing studies was presented.

Chapter 6, finally, presents a summarizing discussion and the synthesis of the main findings of this thesis, focusing on the contributions, potentials and limitations of the different aspects, and perspectives regarding the study of structural dynamics and functioning mangrove forests in changing coastal environments.

## 1.5 References

Allison, M. A., and Lee, M. T. (2004). Sediment exchange between Amazon mudbanks and shore-fringing mangroves in French Guiana. *Marine Geology* **208**, 169-190.

Alongi, D. M. (2008). Mangrove forests: Resilience, protection from tsunamis, and responses to global climate change. *Estuarine, Coastal and Shelf Science* **76**, 1-13.

Alongi, D. M. (2009). "The Energetics of Mangrove Forests," Springer Science + Business Media, Dordrecht, The Netherlands.

Ball, M. (1988). Salinity Tolerance in the Mangroves *Aegiceras corniculatum* and *Avicennia marina*. I. Water Use in Relation to Growth, Carbon Partitioning, and Salt Balance. *Functional Plant Biology* **15**, 447-464.

Baltzer, F., Allison, M., and Fromard, F. (2004). Material exchange between the continental shelf and mangrove-fringed coasts with special reference to the Amazon–Guianas coast. *Marine Geology* **208**, 115-126.

Banin, L., Feldpausch, T. R., Phillips, O. L., Baker, T. R., Lloyd, J., Affum-Baffoe, K., Arets, E. J. M. M., Berry, N. J., Bradford, M., Brienen, R. J. W., Davies, S., Drescher, M., Higuchi, N., Hilbert, D. W., Hladik, A., Iida, Y., Salim, K. A., Kassim, A. R., King, D. A., Lopez-Gonzalez, G., Metcalfe, D., Nilus, R., Peh, K. S. H., Reitsma, J. M., Sonké, B., Taedoumg, H., Tan, S., White, L., Wöll, H., and Lewis, S. L. (2012). What controls tropical forest architecture? Testing environmental, structural and floristic drivers. *Global Ecology and Biogeography* **21**, 1179-1190.

Berg, M. P., and Ellers, J. (2010). Trait plasticity in species interactions: a driving force of community dynamics. *Evolutionary Ecology* **24**, 617-629.

Berger, U., and Hildenbrandt, H. (2000). A new approach to spatially explicit modelling of forest dynamics: spacing, ageing and neighbourhood competition of mangrove trees. *Ecological Modelling* **132**, 287-302.

Berger, U., Hildenbrandt, H., and Grimm, V. (2004). Age-related decline in forest production: modelling the effects of growth limitation, neighbourhood competition and self-thinning. *Journal of Ecology* **92**, 846-853.

Berger, U., Rivera-Monroy, V. H., Doyle, T. W., Dahdouh-Guebas, F., Duke, N. C., Fontalvo-Herazo, M. L., Hildenbrandt, H., Koedam, N., Mehlig, U., Piou, C., and Twilley, R. R. (2008). Advances and limitations of individual-based models to analyze and predict dynamics of mangrove forests: A review. *Aquatic Botany* **89**, 260-274.

Bohlman, S., and Pacala, S. (2012). A forest structure model that determines crown layers and partitions growth and mortality rates for landscape-scale applications of tropical forests. *Journal of Ecology* **100**, 508-518.

Callaway, R. M., Pennings, S. C., and Richards, C. L. (2003). Phenotypic plasticity and interactions among plants. *Ecology* **84**, 1115-1128.

Castañeda-Moya, E., Twilley, R. R., Rivera-Monroy, V. H., Marx, B. D., Coronado-Molina, C., and Ewe, S. M. L. (2011). Patterns of Root Dynamics in Mangrove Forests Along Environmental Gradients in the Florida Coastal Everglades, USA. *Ecosystems* **14**, 1178-1195.

Chapman, V. J. (1977). "Wet coastal ecosystems," V.J. Chapman/Ed. Elsevier.

Chen, R., and Twilley, R. R. (1998). A gap dynamic model of mangrove forest development along gradients of soil salinity and nutrient resources. *Journal of Ecology* **86**, 37-51.

Cintron, G., and Schaeffer-Novelli, Y. (1984). Methods for studying mangrove structure. *In* "The mangrove ecosystem: research methods" (S. C. Snedaker and J. G. Snedaker, eds.), pp. 91-113. United Nations Educational, Scientific and Cultural Organization (UNESCO), Paris.

Clough, B. F. (1992). Primary Productivity and Growth of Mangrove Forests. *In* "Tropical Mangrove Ecosystems", pp. 225-249. American Geophysical Union.

Cohen, M. C. L., and Lara, R. J. (2003). Temporal changes of mangrove vegetation boundaries in Amazônia: Application of GIS and remote sensing techniques. *Wetlands Ecology and Management* **11**, 223-231.

Cohen, M. C. L., R.J. Lara, R. J., Szlafsztein, C., and Dittmar, T. (2004). Mangrove inundation and nutrient dynamics from a GIS perspective. *Wetlands Ecology and Management* **12**, 81-86.

Dahdouh-Guebas, F., De Bondt, R., Abeysinghe, P. D., Kairo, J. G., Cannicci, S., Triest, L., and Koedam, N. (2004). Comparative Study of the Disjunct Zonation Pattern of the Grey Mangrove Avicennia Marina (Forsk.) Vierh. in Gazi Bay (Kenya). *Bulletin of Marine Science* **74**, 237-252.

Dangremond, E. M., and Feller, I. C. (2016). Precocious reproduction increases at the leading edge of a mangrove range expansion. *Ecology and Evolution* **6**, 5087-5092.

Doyle, T. W., and Girod, G. F. (1997). The Frequency and Intensity of Atlantic Hurricanes and Their Influence on the Structure of South Florida Mangrove Communities. *In* "Hurricanes: Climate and Socioeconomic Impacts" (H. F. Diaz and R. S. Pulwarty, eds.), pp. 109-120. Springer-Verlag Berlin Heidelberg.

Enquist, B. J., and Niklas, K. J. (2001). Invariant scaling relations across tree-dominated communities. *Nature* **410**, 655-660.

Feldpausch, T. R., Banin, L., Phillips, O. L., Baker, T. R., Lewis, S. L., Quesada, C. A., Affum-Baffoe, K., Arets, E. J. M. M., Berry, N. J., Bird, M., Brondizio, E. S., de Camargo, P., Chave, J., Djagbletey, G., Domingues, T. F., Drescher, M., Fearnside, P. M., França, M.

B., Fyllas, N. M., Lopez-Gonzalez, G., Hladik, A., Higuchi, N., Hunter, M. O., Iida, Y., Salim, K. A., Kassim, A. R., Keller, M., Kemp, J., King, D. A., Lovett, J. C., Marimon, B. S., Marimon-Junior, B. H., Lenza, E., Marshall, A. R., Metcalfe, D. J., Mitchard, E. T. A., Moran, E. F., Nelson, B. W., Nilus, R., Nogueira, E. M., Palace, M., Patiño, S., Peh, K. S. H., Raventos, M. T., Reitsma, J. M., Saiz, G., Schrodt, F., Sonké, B., Taedoumg, H. E., Tan, S., White, L., Wöll, H., and Lloyd, J. (2011). Height-diameter allometry of tropical forest trees. *Biogeosciences* **8**, 1081-1106.

Feliciano, E. A., Wdowinski, S., and Potts, M. D. (2014). Assessing Mangrove Above-Ground Biomass and Structure using Terrestrial Laser Scanning: A Case Study in the Everglades National Park. *Wetlands* **34**, 955-968.

Feller, I., Whigham, D., McKee, K., and Lovelock, C. (2003). Nitrogen limitation of growth and nutrient dynamics in a disturbed mangrove forest, Indian River Lagoon, Florida. *Oecologia* **134**, 405-414.

Feller, I. C., Lovelock, C. E., Berger, U., McKee, K. L., Joye, S. B., and Ball, M. C. (2010). Biocomplexity in Mangrove Ecosystems. *Annual Review of Marine Science* **2**, 395-417.

Fontalvo-Herazo, M. L., Piou, C., Vogt, J., Saint-Paul, U., and Berger, U. (2011). Simulating harvesting scenarios towards the sustainable use of mangrove forest plantations. *Wetlands Ecology and Management* **19**, 397-407.

Fourcaud, T., Zhang, X., Alexia Stokes, A., Hans Lambers, H., and Körner, C. (2008). Plant Growth Modelling and Applications: The Increasing Importance of Plant Architecture in Growth Models. *Annals of Botany* **101**, 1053–1063.

Franklin, O., Johansson, J., Dewar, R. C., Dieckmann, U., McMurtrie, R. E., Brännström, Å., and Dybzinski, R. (2012). Modeling carbon allocation in trees: a search for principles. *Tree Physiology* **32**, 648-666.

Fromard, F., and Proisy, C. (2010). Coastal dynamics and its consequences for mangrove structure and functioning in French Guiana. *In* "Revised World Atlas of Mangrove for Conservation and Restoration of Mangrove Ecosystems" (M. Spalding, M. Kainuma and L. Collins, eds.), pp. 229-232. Earthscan Ltd, London, UK.

Fromard, F., Puig, H., Mougin, E., Marty, G., Betoulle, J. L., and Cadamuro, L. (1998). Structure, above-ground biomass and dynamics of mangrove ecosystems: new data from French Guiana. *Oecologia* **115**, 39-53.

Fromard, F., Vega, C., and Proisy, C. (2004). Half a century of dynamic coastal change affecting mangrove shorelines of French Guiana. A case study based on remote sensing data analyses and field surveys. *Marine Geology* **208**, 265-280.

Gardel, A., and Gratiot, N. (2004). Monitoring of coastal dynamics in French Guiana from 16 years of SPOT satellite images. *Journal of Coastal Research* **SI 39**.

Grimm, V., and Railsback, S. F. (2005). "Individual-based Modelling and Ecology," Princeton University Press, Princeton, NY.

Grueters, U., Seltmann, T., Schmidt, H., Horn, H., Pranchai, A., Vovides, A. G., Peters, R., Vogt, J., Dahdouh-Guebas, F., and Berger, U. (2014). The mangrove forest dynamics model mesoFON. *Ecological Modelling* **291**, 28-41.

Huxley, J. S., and Teissier, G. (1936). Terminology of Relative Growth. *Nature* **137**, 780-781.

Kasischke, E. S., and Christensen Jr, N. L. (1990). Connecting forest ecosystem and microwave backscatter models. *International Journal of Remote Sensing* **11**, 1277-1298.

Koch, G. W., Sillett, S. C., Jennings, G. M., and Davis, S. D. (2004). The limits to tree height. *Nature* **428**, 851-854.

Lara, R., and Cohen, M. (2006). Sediment porewater salinity, inundation frequency and mangrove vegetation height in Bragança, North Brazil: an ecohydrology-based empirical model. *Wetlands Ecology and Management* **14**, 349-358.

Lara, R. J. (2003). Amazonian mangroves – A multidisciplinary case study in Pará State, North Brazil: Introduction. *Wetlands Ecology and Management* **11**, 217-221.

Lira-Medeiros, C. F., Parisod, C., Fernandes, R. A., Mata, C. S., Cardoso, M. A., and Ferreira, P. C. G. (2010). Epigenetic Variation in Mangrove Plants Occurring in Contrasting Natural Environment. *PLoS ONE* **5**, e10326.

Lovelock, C. E., Feller, I. C., McKee, K. L., and Thompson, R. (2005). Variation in mangrove forest structure and sediment characteristics in Bocas del Toro, Panama. *Caribbean Journal of Science* **41**, 456-464.

Lugo, A. E. (1997). Old-growth mangrove forests in the United States. *Conservation Biology* **11**, 11-20.

Menezes, M. P. M., Berger, U., and Mehlig, U. (2008). Mangrove vegetation in Amazonia: a review of studies from the coast of Pará and Maranhão States, north Brazil. *Acta Amazonica* **38**, 403-420.

Muller-Landau, H. C., Condit, R. S., Harms, K. E., Marks, C. O., Thomas, S. C., Bunyavejchewin, S., Chuyong, G., Co, L., Davies, S., Foster, R., Gunatilleke, S., Gunatilleke, N., Hart, T., Hubbell, S. P., Itoh, A., Kassim, A. R., Kenfack, D., LaFrankie, J. V., Lagunzad, D., Lee, H. S., Losos, E., Makana, J.-R., Ohkubo, T., Samper, C., Sukumar, R., Sun, I. F., Nur Supardi, M. N., Tan, S., Thomas, D., Thompson, J., Valencia, R., Vallejo, M. I., Muñoz, G. V., Yamakura, T., Zimmerman, J. K., Dattaraja, H. S., Esufali, S., Hall, P., He, F., Hernandez, C., Kiratiprayoon, S., Suresh, H. S., Wills, C., and Ashton, P. (2006). Comparing tropical forest tree size distributions with the predictions of metabolic ecology and equilibrium models. *Ecology letters* **9**, 589-602.

Nascimento Jr, W. R., Souza-Filho, P. W. M., Proisy, C., Lucas, R. M., and Rosenqvist, A. (2013). Mapping changes in the largest continuous Amazonian mangrove belt using object-based classification of multisensor satellite imagery. *Estuarine, Coastal and Shelf Science* **117**, 83-93.

Nicotra, A. B., Atkin, O. K., Bonser, S. P., Davidson, A. M., Finnegan, E. J., Mathesius, U., Poot, P., Purugganan, M. D., Richards, C. L., Valladares, F., and van Kleunen, M. (2010). Plant phenotypic plasticity in a changing climate. *Trends in Plant Science* **15**, 684-692.

O'Brien, S. T., Hubbell, S. P., Spiro, P., Condit, R., and Foster, R. B. (1995). Diameter, Height, Crown, and Age Relationship in Eight Neotropical Tree Species. *Ecology* **76**, 1926-1939.

Peters, R., Vovides, A. G., Luna, S., Grüters, U., and Berger, U. (2014). Changes in allometric relations of mangrove trees due to resource availability – A new mechanistic modelling approach. *Ecological Modelling* **283**, 53-61.

Piou, C., Berger, U., Hildenbrandt, H., and Feller, I. C. (2008). Testing the intermediate disturbance hypothesis in species poor systems: a simulation experiment for mangrove forests. *Journal of Vegetation Science* **19**, 417-424.

Poorter, H., Niklas, K. J., Reich, P. B., Oleksyn, J., Poot, P., and Mommer, L. (2012). Biomass allocation to leaves, stems and roots: meta-analyses of interspecific variation and environmental control. *New Phytologist* **193**, 30-50.

Pretzsch, H., Biber, P., Schütze, G., Uhl, E., and Rötzer, T. (2014). Forest stand growth dynamics in Central Europe have accelerated since 1870. *Nat Commun* **5**.

Proisy, C., Couteron, P., and Fromard, F. (2007). Predicting and mapping mangrove biomass from canopy grain analysis using Fourier-based textural ordination of IKONOS images. *Remote Sensing of Environment* **109**, 379-392.

Proisy, C., Degenne, P., Anthony, E., Berger, U., Blanchard, E., Fromard, F., Gardel, A., Olagoke, A., Santos, V. F., Walcker, R., and Lo Seen, D. (2016a). A multiscale simulation approach for linking mangrove dynamics to coastal proceesses using remote sensing observations. *Journal of Coastal Research*, 810-814.

Proisy, C., Féret, J.-B., Lauret, N., and Gastellu-Etchegorry, J.-P. (2016b). Mangrove forest dynamics using very high spatial resolution optical remote sensing. *In* "Remote

sensing of Land Surfaces: Urban and coastal area" (N. Baghdadi and M. Zribi, eds.), Vol. 5, Chapter 7. ELSEVIER, London. In press.

Proisy, C., Gratiot, N., Anthony, E. J., Gardel, A., Fromard, F., and Heuret, P. (2009). Mud bank colonization by opportunistic mangroves: A case study from French Guiana using lidar data. *Continental Shelf Research* **29**, 632-641.

Retallack, G. J. (1997). Early Forest Soils and Their Role in Devonian Global Change. *Science* **276**, 583-585.

Richter, S., Kipfer, T., Wohlgemuth, T., Calderón Guerrero, C., Ghazoul, J., and Moser, B. (2012). Phenotypic plasticity facilitates resistance to climate change in a highly variable environment. *Oecologia* **169**, 269-279.

Rivera-Monroy, V. H., Twilley, R. R., Bone, D., Childers, D. L., Coronado-Molina, C., Feller, I. C., Herrera-Silveira, J., Jaffe, R., Mancera, E., Rejmankova, E., Salisbury, J. E., and Weil, E. (2004). A conceptual framework to develop long-term ecological research and management objectives in the wider Caribbean region. *BioScience* **54**, 843-856.

Ryan, M. G., and Yoder, B. J. (1997). Hydraulic Limits to Tree Height and Tree Growth. *BioScience* **47**, 235-242.

Shugart, H. H., Asner, G. P., Fischer, R., Huth, A., Knapp, N., Le Toan, T., and Shuman, J. K. (2015). Computer and remote-sensing infrastructure to enhance large-scale testing of individual-based forest models. *Frontiers in Ecology and the Environment* **13**, 503-511.

Souza Filho, P. W. M., Farias Martins, E. S., and da Costa, F. R. (2006). Using mangroves as a geological indicator of coastal changes in the Braganca macrotidal flat, Brazilian Amazon: A remote sensing data approach. *Ocean & Coastal Management* **49**, 462-475.

Stein, W. E., Mannolini, F., Hernick, L. V., Landing, E., and Berry, C. M. (2007). Giant cladoxylopsid trees resolve the enigma of the Earth's earliest forest stumps at Gilboa. *Nature* **446**, 904-907.

Thompson, I., Mackey, B., McNulty, S., and Mosseler, A. (2009). "Forest Resilience, Biodiversity, and Climate Change. A synthesis of the biodiversity/resilience/stability relationship in forest ecosystems," Montreal.

Twilley, R. R., R. Gottfried, R., Rivera-Monroy, V. H., Zhang, W., Montano Armijos, M., and Bodero, A. (1998). An approach and preliminary model of integrating ecological and economic constraints of environmental quality in the Guayas River estuary, Ecuador. *Environmental Science & Policy* **1**, 271-288.

Twilley, R. R., and Rivera-Monroy, V. H. (2005). Developing performance measures of mangrove wetlands using simulation models of hydrology, nutrient biogeochemistry, and community dynamics. *Journal of Coastal Research*, 79-93.

Twilley, R. R., Rivera-Monroy, V. H., Chen, R., and Botero, L. (1999). Adapting an Ecological Mangrove Model to Simulate Trajectories in Restoration Ecology. *Marine Pollution Bulletin* **37**, 404-419.

Vogt, J., Kautz, M., Fontalvo Herazo, M. L., Triet, T., Walther, D., Saint-Paul, U., Diele, K., and Berger, U. (2013). Do canopy disturbances drive forest plantations into more natural conditions? — A case study from Can Gio Biosphere Reserve, Viet Nam. *Global and Planetary Change* **110, Part B**, 249-258.

Vogt, J., Lin, Y., Pranchai, A., Frohberg, P., Mehlig, U., and Berger, U. (2014a). The importance of conspecific facilitation during recruitment and regeneration: A case study in degraded mangroves. *Basic and Applied Ecology* **15**, 651-660.

Vogt, J., Piou, C., and Berger, U. (2014b). Comparing the influence of large- and small-scale disturbances on forest heterogeneity: A simulation study for mangroves. *Ecological Complexity* **20**, 107-115.

Vovides, A. G., Vogt, J., Kollert, A., Berger, U., Grueters, U., Peters, R., Lara-Domínguez, A. L., and López-Portillo, J. (2014). Morphological plasticity in mangrove trees: salinity-related changes in the allometry of Avicennia germinans. *Trees* **28**, 1413-1425.

Walcker, R., Anthony, E. J., Cassou, C., Aller, R. C., Gardel, A., Proisy, C., Martinez, J.-M., and Fromard, F. (2015). Fluctuations in the extent of mangroves driven by multi-decadal changes in North Atlantic waves. *Journal of Biogeography* **42**, 2209-2219.

Weiner, J. (2004). Allocation, plasticity and allometry in plants. *Perspectives in Plant Ecology, Evolution and Systematics* **6**, 207-215.

West, G. B., Brown, J. H., and Enquist, B. J. (1999). A general model for the structure and allometry of plant vascular systems. *Nature* **400**, 664-667.

West, G. B., Enquist, B. J., and Brown, J. H. (2009). A general quantitative theory of forest structure and dynamics. *Proceedings of the National Academy of Sciences* **106**, 7040-7045.

Wolanski, E., Brinson, M. M., Cahoon, D. R., and Perillo, G. M. E. (2009). Coastal wetlands: A synthesis. *In* "Coastal Wetlands: An Integrated Ecosystem Approach" (Perillo G.M.E., E. Wolanski, D. R. Cahoon and M. M. Brinson, eds.), Vol. Chapter 1, pp. 1-62. Elsevier Press, The Netherlands.

Zurell, D., Berger, U., Cabral, J. S., Jeltsch, F., Meynard, C. N., Münkemüller, T., Nehrbass, N., Pagel, J., Reineking, B., Schröder, B., and Grimm, V. (2010). The virtual ecologist approach: simulating data and observers. *Oikos* **119**, 622-635.

# 2 CHARACTERIZING THE STRUCTURE AND BIOMASS OF MANGROVE SPECIES USING TERRESTRIAL LIDAR DATA, AND THE APPLICATION IN EXTENDING BIOMASS ALLOMETRIC EQUATIONS TO LARGE TREES[1]

Olagoke Adewole[1,2,3], Christophe Proisy[2], Jean-Baptiste Féret[4], Elodie Blanchard[2], François Fromard[5,6], Ulf Mehlig[7], Moirah Machado de Menezes[7], Valdenira Ferreira dos Santos[8], Uta Berger[1]

[1]Institute of Forest Growth and Computer Sciences, Technische Universität, Dresden, Germany adewole.olagoke@tu-dresden.de, uta.berger@tu-dresden.de
[2]IRD, UMR-AMAP, 34000 Montpellier, France christophe.proisy@ird.fr, elodie.blanchard@ird.fr
[3]Institut des sciences et industries du vivant et de l'environnement (AgroParisTech), Campus d'Agropolis International, 648 rue Jean-François Breton, 34093 Montpellier, France
[4]IRSTEA, UMR-TETIS, 500 rue J.F. Breton, 34093 Montpellier Cedex 5, France jb.feret@teledetection.fr
[5]Université de Toulouse; INP, UPS; EcoLab, 118 Route de Narbonne, 31062 Toulouse, France
[6]CNRS; EcoLab; 31062 Toulouse, France francois.fromard@univ-tlse3.fr ;
[7]Instituto de Estudos Costeiros, Universidade Federal do Pará, Campus de Bragança, Brazil ulf@ufpa.br, moirah@ufpa.br
[8]Instituto de Pesquisas Científicas e Tecnológicas do Estado do Amapá (IEPA), Macapá, Brazil valdeniraferreira@gmail.com

## Abstract

*Accurately determining biomass of large trees is crucial for reliable biomass analyses in most tropical forests, but most allometric models calibration are deficient in large trees data. This issue is a major concern for high-biomass mangrove forests, especially when their role in the ecosystem carbon storage is considered. As an alternative to the fastidious cutting and weighing measurement approach, we explored a non-destructive terrestrial laser scanning approach to estimate the aboveground biomass of large mangroves (diameters reaching up to 125 cm). Because of buttresses in large trees, we propose a pixel-based analysis of the composite 2D flattened images, obtained from the successive thin segments of stem point-cloud data to estimate wood volume. Branches were considered as successive best-fitted primitive of conical frustums. The product of wood volume and height-decreasing wood density yielded biomass estimates. This approach was tested on 36 A. germinans trees in French Guiana, considering available biomass models from the same region as references. Our biomass estimates reached ca. 90% accuracy and a correlation of 0.99 with reference biomass values. Based on the results, new tree biomass model, which had $R^2$ of 0.99 and RSE of*

[1] *A modified version of this chapter was published as:*
Olagoke, A., Proisy, C., Féret, J.-B., Blanchard, E., Fromard, F., Mehlig, U., de Menezes, M. M., dos Santos, V. F., and Berger, U. (2016). Extended biomass allometric equations for large mangrove trees from terrestrial LiDAR data. *Trees* **30**, 935-947.

*87.6 kg of dry matter. This terrestrial LiDAR-based approach allows the estimates of large tree biomass to be tractable, and opens new opportunities to improve biomass estimates of tall mangroves. The method could also be tested and applied to other tree species.*

**Keywords:** Aboveground biomass; Coastal blue carbon; French Guiana; Mangrove; Terrestrial LiDAR; Tree allometry

## 2.1 Introduction

Recent studies have demonstrated the importance of large trees as keystone ecological elements (Lindenmayer et al., 2012; Lutz et al., 2013) in forest ecosystems. Their significance extends beyond the characteristic contribution to regeneration as mother trees and the provision of food and shelter for many living organisms, because they also represent essential structures that shape ecosystem biomass productivity and recurrent forest dynamics (Slik et al., 2013). In terms of wood volume, biomass, and carbon stocks, they dominate the forest structure and this may explain variations in biomass distribution across forest landscapes (Bastin et al., 2015a). Thus, an accurate estimation of the biomass of large trees is crucial for obtaining reliable estimates of the total biomass in such forests.

One key challenge is that the biomass data of large tropical tree are generally scarce (e.g. only ca. 7% of the available pantropical tree biomass dataset, Chave et al. (2014)) . This is also the case for the tall mangroves that grow in the equatorial region. Although the species diversity of mangroves is low compared with rainforests, the variability in the tree structure of *Avicennia* species, for example, is higher. *Avicennia* trees may exhibit a wide range of growth forms, from small to large/ tall trees, depending on the habitat condition. Considering this variation in tree structure, available models may actually fall short in their predictive power for out-of-sample application. This situation may also limit the extent to which the existing general pantropical biomass allometric models can be applied to mangrove trees, without significant bias in the resulting estimates.

Meanwhile, there is a growing interest in attaining highly precise estimates of biomass and carbon stock of tropical forests (Gibbs et al., 2007; Pistorius, 2012), including mangroves, as in the case of the *blue carbon* projects. This necessitates the refinement of the available methods, like the commonly used allometric models, for biomass measurement. All the same, the available biomass models for mangrove trees (Komiyama et al., 2008) only cover a range of small - medium sized trees (DBH ≤ 50 cm) and are deficient in respect of large trees. Collecting data, using the conventional cutting and weighing method, to validate mangrove biomass models for large trees is however difficult in the tidal environment.

The terrestrial laser scanning (TLS), also knowns as terrestrial LiDAR (light detection and ranging), offers a remote sensing technology that allows capturing the high resolution three-dimensional (3D) structure of trees with relatively low time and labour requirements. Earlier applications in the forest sciences and ecological studies include the description of forest structural parameters (Strahler et al., 2008), assessment of canopy metrics and gaps (Bayer et al., 2013; Hilker et al., 2010), individual tree volume and biomass estimation (e.g., Calders et al. (2015); Dassot et al. (2012)), to the application in estimating leaf area and foliage properties (Béland et al., 2014). Interestingly, various approaches have tested satisfactorily in the estimation of individual tree volume and biomass from TLS point cloud data: from tree features extraction (Kankare et al., 2013; Pueschel et al., 2013), shape reconstruction and primitive fittings (e.g., Raumonen et al. (2013)) to voxelization (Hauglin et al., 2013).

Some automatic techniques have been proposed for reconstructing and modelling of tree structure and topology (Åkerblom et al., 2015; Hackenberg et al., 2015; Raumonen et al., 2013), and they achieved notably good results with regular, cylindrical shaped tree trunks, and mostly in leaf-off conditions. Since such methods are based on segmental geometric primitive fits, irregularities in the shape of large tropical trees like mangroves remain challenging for direct application of such automatic tree reconstruction. For irregular trunk shapes, we presume that automatic techniques may require a combination with (semi-)manual interactive steps. In any case, the application of TLS in the study of mangrove species remains largely unexplored; the only pilot attempt was limited to mangrove trees with DBH < 43 cm (Feliciano et al., 2014). In the present study, our aims were (1) to describe and evaluate the performance of a simple TLS-based method for estimating the wood volume and biomass of large mangrove trees, and (2) to propose revised allometric models for the widespread mangrove tree species *Avicennia germinans* (L.) L. with a validation domain extended to very large trees.

## 2.2 Methods

### 2.2.1 *Study area*

The study was performed in French Guiana (hereafter referred to as FG) where mangroves stretch along a 320 km coastline (Figure 2-1), to cover an approximate area of 70,000 ha. This coast can be considered as pristine, because there are still no extensive industrial activities, and aquaculture and tree exploitation are not present. It is subjected primarily to sediment dispersal from the Amazon River (Baltzer et al., 2004). The spatiotemporal distribution of mangroves is controlled by a succession of rapid and acute erosion and accretion phases caused by the drifting of giant mud-banks to the northwest of the coastline (Anthony et al., 2010).

The mangrove forests encompass new colonization on the freshly consolidated mud-banks up to mature forests located several kilometers inland at the limit of tidal influence. In this area, mangroves are unaffected by coastal instability (Anthony et al., 2010) and this allows trees to reach their largest potential stature. Fromard et al. (1998) described the different mangrove forest types of FG; *A. germinans* (L.) L. is represented from pioneer to old-growth forest, spanning a wide range of growth stages. These growth stages are patchily distributed across the coastal landscape with clusters of young trees, sometimes in close vicinity to decaying stands (Proisy et al., 2007).

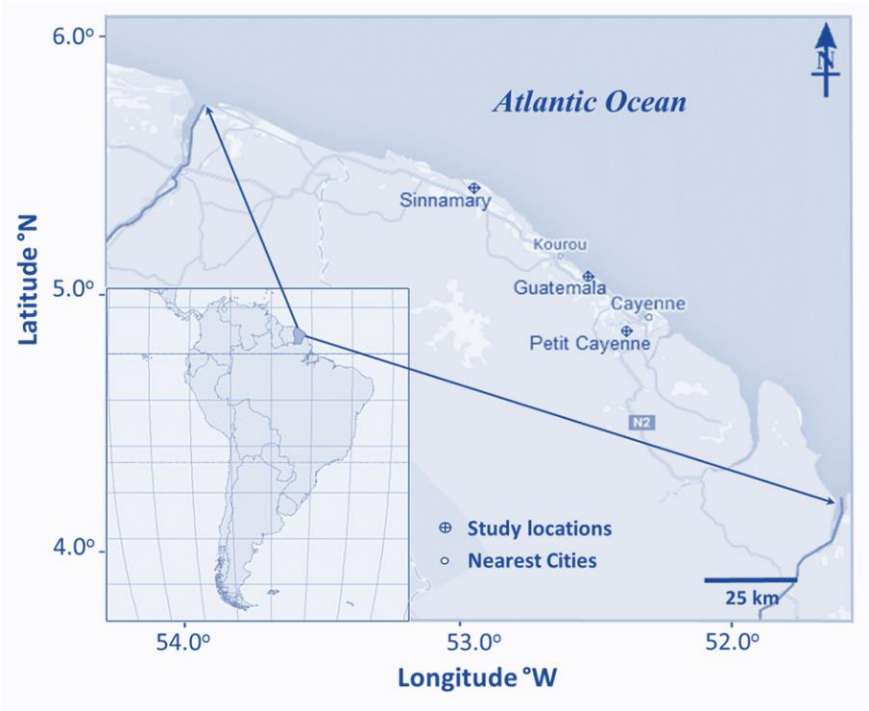


Figure 2-1: Map of the coastline of French Guiana showing the locations of the study sites

The sampling locations were selected in order to capture data from trees distributed over a wide *DBH* range. This *DBH* range was distributed in three distinct forest stands, as noted in Figure 2-1. First, a mixed old-growth *Avicennia–Rhizophora* forest stand near Petit Cayenne 10 km upstream of the Cayenne river, with a stand density of 504 trees per hectare, total basal area of 26.2 $m^2.ha^{-1}$ and *A. germinans* trees reaching a mean *DBH* of 56.2 cm. The second stand, located at about 3 km from the actual mangrove shoreline along Guatemala road, was made up of small-medium size and scattered large *A. germinans* trees. The tree density in this stand was 3733 trees per hectare with a total basal area of 25.5 $m^2.ha^{-1}$, and average *DBH* of 15 cm.

The third stand, we considered an even-aged *A. germinans* forest located 6 km backward of the mangrove seafront in the Sinnamary region. This stand contained mainly *A. germinans* in a density of 1132 trees per hectare with basal area totalling 21.8 $m^2.ha^{-1}$.

### 2.2.2 *Essential features of Avicennia germinans (L.) L.*

In this study, we employed *A. germinans* as a proxy species to test a new method for estimating the biomass of mangrove trees using TLS data. This is a keystone species and the most dominant mangrove species on the FG coast (Fromard et al., 1998; Fromard et al., 2004). *A. germinans* trees vary greatly in size and growth form. The species grows from low-scrubby (ca. 0.4–1.5 m tall) in the sub-optimal habitats (Vogt et al., 2014) to large trees approaching 42 m height and 125 cm diameter in favorable and stable growth conditions, as found in some parts of French Guiana. Trunks are roughly cylindrical to slightly angled or even canaliculated and may develop buttresses and short fascicles of aerial roots. The trees reiterate to produce coppice shoots when the main stem is damaged, resulting in frequently contorted stem development.

*Existing biomass allometric models for A. germinans*

Fromard et al. (1998) developed biomass allometric models for aboveground biomass (*AGB*) of mangrove trees in French Guiana. The models for *A. germinans* followed a power function, with two coefficients (Table 2-1). They were calibrated using data obtained from small to medium-sized trees with *DBH* of 4 – 42 cm and corresponding *AGB* between 4.8 and 1543.7 kg of dry matter, respectively. These models conformed to the biomass allometric model developed for the same species in Guadeloupe (Imbert and Rollet, 1989). Other mangrove biomass models applicable to *A. germinans* are the two generic equations develped by Chave et al. (2005) and Komiyama et al. (2005), which were also calibrated with trees *DBH* < 60 cm. An independent dataset obtained by direct cutting and weighing of sample trees (Fromard et al., 1998) at the same study locations as ours jointly with the predicted biomass estimates of currently sampled trees, using the allometric models of Fromard et al. (1998), were used for reference to evaluate the TLS-based biomass values and new models in this study.

Table 2-1: Reference models from Fromard et al. (1998) for *A. germinans* trees (DBH ≤ 42 cm) based on power function of the tree diameter ($\alpha.DBH^{\beta}$)

| Model ID | $\alpha$ | $\beta$ | $R^2$ | n |
|---|---|---|---|---|
| *AGB* tree biomass ($AGB_{ref}$) | 0.14 | 2.40 | 0.97 | 25 |
| Trunk biomass ($BTR_{ref}$) | 0.07 | 2.59 | 0.97 | 25 |
| Branch biomass ($BBR_{ref}$) | 0.03 | 2.33 | 0.97 | 25 |
| Leaf biomass ($BLeaf_{ref}$) | 0.04 | 1.77 | 0.91 | 25 |
| *The coefficients $\alpha$ (intercept) and $\beta$ (slope) are constant parameters, and n is the number of sample trees.* | | | | |

*Wood density (WD) measurements at different heights*

In most studies of allometric relationships, the *WD* is estimated at breast height. To our knowledge, no *WD* measurements have been reported at different heights along the main axis for *A. germinans* so far. Thus, we initiated an experiment that involved coring *A. germinans* trees at different heights in various mangrove regions throughout French Guiana. We climbed 20 trees (10 < *DBH* < 110 cm) and used hand-powered drills to extract 52 samples. The wood core samples measured 4.3 mm in diameter with lengths of 2–13 cm over bark. The core heights along the stem axis ranged from 0.3 m for all trees up to 23 m for tall trees, corresponding to diameters varying from 4.8 cm, at the top of small trees, up to 110 cm at the base of large trees. All core samples were dried at a constant temperature of 105°C for several days until constant mass, and subsequently weighted in relation to wood volume to obtain *WD* as dry weight. High variability in the *WD* was observed at heights below 10 m, and also around the breast height. The distribution of wood density along the main stem vs. sampling height and diameter was fitted using a linear mixed effects model, with the individual tree as random factor. This analysis was based on *WD* density data from the outer wood core samples, since the outer wood density values are known to strongly correlate to the *WD* values from any point along the radial spectrum, without a significant bias (Bastin et al., 2015b).

### 2.2.3 *TLS measurements and data processing*

The TLS measurements used in this study were collected with a FARO Focus$^{3D}$ X330 device between August and September 2014. The instrument operates using a 1.55 µm class 1 laser signal. The distance between the scanner and the object is determined by analyzing the shift in the wavelength of the return beam. The device can scan objects at a distance of up to 330 m; and with an accuracy of < 0.25 mm for dark objects at a distance of 25 m. The vertical and horizontal fields of view are 300° and 360°, respectively. Several scanning resolutions can be used for collecting point cloud data from the focal surface. However, we chose the second finest scanning configuration able to achieve complete scanning at about 20 min with a distance accuracy reaching ±3 mm over a horizontal range of 90° as the finest scan required more than 1 hour for an accuracy slightly improved to ±2 mm over the same distance. A flowchart that illustrates the procedure for data acquisition and subsequent processing is presented in Figure 2-2. Further methodical descriptions are provided in the subsequent sections.

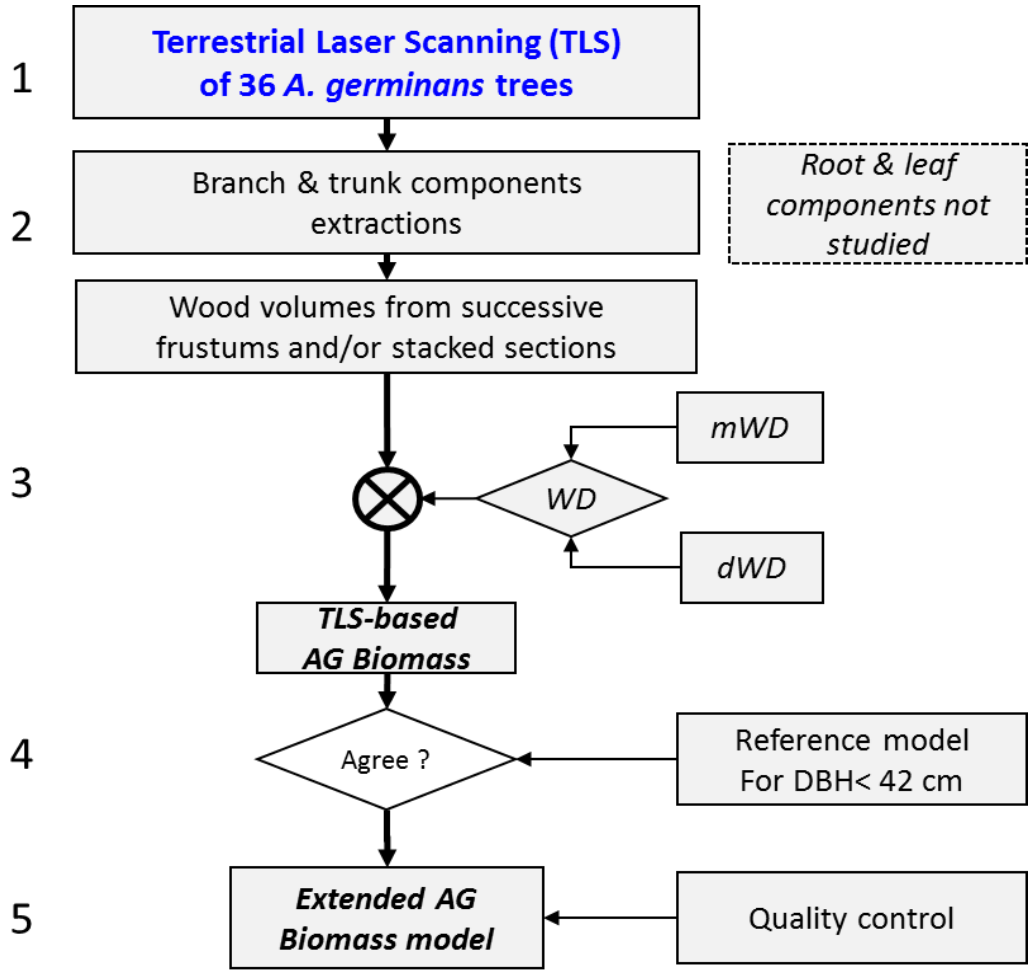


Figure 2-2: Scheme showing the procedure employed for TLS data acquisition and processing for biomass estimation of mangrove trees. AG = aboveground, WD = wood density, mWD = mean WD value at tree DBH, and dWD = decreasing WD value with stem height

*Mangrove tree scanning*

The number of trees selected for each scanning operation ranged from a single (large) tree to a group of six individual (small to medium-sized) trees. Before placing the instrument, several viewpoints were identified for TLS placement around selected individual(s), and subsequently distribution of the target spheres (reference objects to aid merging/ alignment of multiscans). This was a crucial step because it directly affected the quality of the 3D description of the focal mangrove tree(s). In this experiment, five white target spheres were positioned in the foreground and background surrounding the focal trees at different heights ranging from 0–2 m using stands made of metal rods and pipes, at a minimum distance of ca. 3 m from the tree base (Figure 2-3).

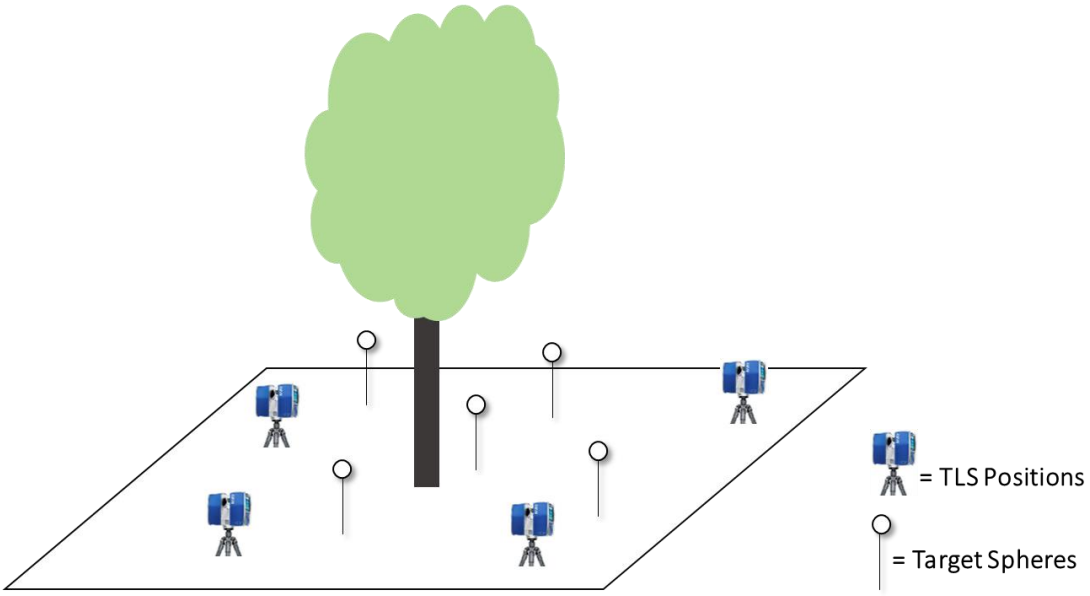


Figure 2-3: Schematic representation showing the multi-scan analysis of a tree, involving four placements for the TLS instrument and five white reference spheres (target spheres mounted on metal rods)

The TLS instrument was mounted on a sturdy tripod stand, with additional support from reinforced metal frames (ca. 60 cm long) embedded in the muddy sediment. One can adapt the length of these support metal frames as required, until adequate stability is reached before mounting the LiDAR system. The number of scan positions was selected as a function of the horizontal and vertical projections of the target trees. To minimize the chance of occlusions or missing parts in the 3D tree structure, it was essential to scan large individual trees with buttresses from at least 5 viewpoints at high scanning resolution. Table 2-2 provides the summary attributes of the sample trees.

*Extraction of trunk and branches from point-cloud data*

The TLS data processing comprised merging of multiple scans, filtering or removal of background vegetation, and generating point clouds for individual trees of interest. This process was conducted using the FARO SCENE 5.2 software. The process took from ca. 1 - 12 working hours to complete one large tree, depending on its structure. The main trunk and primary branches (in the case of large trees) were manually separated, and the 3D coordinates of the point cloud were exported for subsequent processing. The computation routine for wood volume and biomass was implemented in MATLAB. For control, we also fitted successive geometric primitives on point cloud data of trunks and branches (> 4 cm at the branch base) using the least squares method.

Table 2-2: Descriptive metrics of sample trees selected for the TLS experiments

| Site ID | Location coordinates | Forest type | No. of trees | Tree ID | *DBH* (cm) | Total height (m) |
|---|---|---|---|---|---|---|
| Guatemala | 5.07 N, 52.54 W | Small – medium size *A. germinans* stands with uneven ages | 17 | GUA1 | 13.4 | 14.8 |
| | | | | GUA2 | 15.8 | 17.2 |
| | | | | GUA3 | 16.0 | 21.0 |
| | | | | GUA4 | 16.0 | 20.1 |
| | | | | GUA5 | 16.1 | 18.5 |
| | | | | GUA6 | 17.6 | 21.8 |
| | | | | GUA7 | 17.9 | 21.6 |
| | | | | GUA8 | 18.7 | 20.3 |
| | | | | GUA9 | 20.9 | 23.8 |
| | | | | GUA10 | 22.7 | 20.4 |
| | | | | GUA11 | 24.1 | 23.0 |
| | | | | GUA12 | 26.0 | 21.3 |
| | | | | GUA13 | 28.0 | 24.1 |
| | | | | GUA14 | 28.5 | 22.3 |
| | | | | GUA15 | 32.1 | 21.1 |
| | | | | GUA16 | 50.0 | 18.4 |
| | | | | GUA17 | 54.0 | 14.7 |
| Sinnamary | 5.41 N, 52.96 W | Medium size *A. germinans* stand with similar ages | 6 | SIN1 | 26.8 | 23.8 |
| | | | | SIN2 | 33.5 | 29.7 |
| | | | | SIN3 | 35.3 | 31.5 |
| | | | | SIN4 | 35.0 | 29.7 |
| | | | | SIN5 | 35.7 | 31.2 |
| | | | | SIN6 | 44.9 | 33.4 |
| Petit Cayenne | 4.86 N, 52.40 W | Mixed old-growth *Avicennia* and *Rhizophora* | 13 | CAY1 | 47.8 | 34.0 |
| | | | | CAY2 | 54.6 | 36.5 |
| | | | | CAY3 | 56.4 | 35.3 |
| | | | | CAY4 | 58.5 | 32.1 |
| | | | | CAY5 | 64.0 | 32.5 |
| | | | | CAY6 | 69.2 | 34.1 |
| | | | | CAY7 | 70.5 | 34.0 |
| | | | | CAY8 | 81.0 | 37.9 |
| | | | | CAY9 | 91.6 | 36.1 |
| | | | | CAY10 | 93.5 | 38.2 |
| | | | | CAY11 | 94.0 | 36.4 |
| | | | | CAY12 | 99.7 | 37.9 |
| | | | | CAY13 | 124.5 | 41.3 |

### 2.2.4 *Computation of the trunk and branch volumes*

Two volume computation procedures were performed for the trunks: (1) volume estimation of successive best-fitted geometric shapes (primitive fitting), and (2) an

automatic pixel count on 2D flattened projection of segmented thin trunk sections. The trunk volume estimates from the composite primitive shapes fitted on the selected trunks served for the validation of the pixel-based analysis. The determination of the volume of tree branches was restricted to manual primitive shape fittings in this study due to computational complexity.

*Stem volume estimation by primitive fitting*

For each tree, sets of conical frustums were extracted that corresponded to the main trunk and each branch. The diameters at the base (*Db*) and the top (*Dt*), and the height (*Hc*) of each solid shape were recorded. Thereafter, the geometrical volume (*Vc* for trunk and *Vcb* for branches) of each primitive shape was estimated as a truncated cone, as given by equation 1.

$$Vc_i = \frac{\pi \cdot Hc_i}{12} \cdot \left( Db_i^{\,2} + Db_i \cdot Dt_i + Dt_i^{\,2} \right), \quad (1)$$

All of the *Vc* values in a trunk were summed to obtain the trunk volume ($VTr_{cone}$). The addition of the component *Vcb* of each branch yielded the branch volume.

*Trunk volume estimation with the pixel-based method*

We implemented a program routine that decomposed 3D trunk shapes into successive thin sections (Figure 2-4, a–c). The height of each section to the ground level was recorded. These sections were converted into two-dimensional (2D) binary images to obtain their flattened plan projections. Different segmentation heights (section thickness), ranging from 1 cm to 1 m, were tested to find a trade-off between complete shape outline and gaps in the 2D plan. When open shapes occurred in the point cloud (due to occlusion on trunk part during scanning), they were filled automatically by fitting a simple convex envelope around the missing region. The area covered by the boundary of the section was then divided into a grid of 1 $cm^2$ pixels. The number of pixels in the flattened image of each section was summed to obtain its surface area, and the volume was obtained as the product of the surface area and its thickness, and the trunk volume was obtained as the total stacked constituent sections. These trunk volume estimates were compared with the volume obtained from primitive fittings (described above) to validate the pixel-based method.

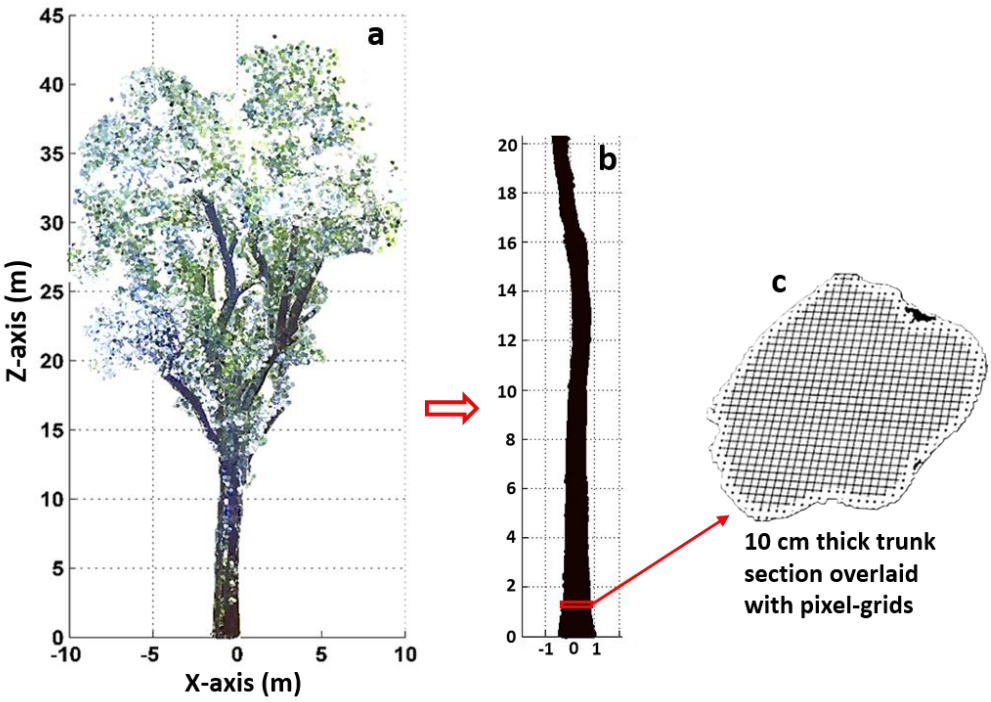


Figure 2-4: Trunk segmentation and sectioning for stem volume computation. a) Typical view of a large mangrove tree. b) A trunk with DBH = 93.5 cm. c) Typical flattened projection of a trunk section extracted at a height of 1.3 m

### 2.2.5 *Biomass estimation from TLS-derived wood volume*

*Conversion of stem volume to biomass*

In this study, we systematically obtained two biomass estimates: the first used a mean *WD* derived from our wood density sampling; and the second employed a decreasing *WD* relative to height along the stem axis derived from the respective linear mixed-effects model. In the latter case, we interpolated the height *WD* model to obtain specific *WD* at each section height by reference to the bottom of the tree. The biomass estimates for each of the trunk ($BTR_{TLS}$) and the branch ($BBR_{TLS}$) components were obtained as the sum of the products of each section volume and the corresponding *WD*. The sum of the branch and trunk biomass of each tree provided its TLS-derived aboveground woody biomass ($AGBW_{TLS}$). The leaf biomass was only considered in this study as a proportional relation following the model of Fromard et al. (1998) in Table 2-1, although it constituted an insignificant share of the *AGB* estimates.

*Evaluation of TLS biomass estimates for trees DBH < 42 cm*

We applied a cross-validation procedure to evaluate the accuracy of the TLS-derived trunk volume and biomass estimates of trees within the *DBH* range of the reference data (Fromard et al., 1998). We calculated the root mean squared error (*RMSE*) and the accuracy using equations 2 and 3, respectively:

$$RMSE = \sqrt{\frac{\sum_{i=1}^{n}(FF_i - TLS_i)^2}{n}}, \quad (2)$$

$$\%RMSE = 100 \cdot \frac{RMSE}{mean(FF)}, \quad (3)$$

where $FF_i$ denotes the reference values based on Fromard et al. (1998), $TLS_i$ is the corresponding TLS-derived estimate, and $n$ is the number of trees.

### 2.2.6 *Fitting of allometric models using TLS-derived biomass data*

*Model calibration*

We employed TLS-derived data for calibrating easily applicable biomass allometric models. Based on tree diameter–biomass relationship of *A. germinans*, we fitted a new non-linear *AGB* model with *DBH* as the predictive variable using a maximum likelihood regression approach (AGB.M1, equation 4). The coefficients $\alpha$ and $\beta$ are parameters that characterized the new biomass models we obtained. As suggested by Chave et al. (2005) and Komiyama et al. (2005), we considered other models (AGB.M2–AGB.M4) that incorporated *WD* (denoted as ρ in the allometric equations) and/or tree height (*H*), as given by equations 5 – 7:

AGB.M1: $$AGB = \alpha \cdot DBH^{\beta} + \varepsilon, \quad (4)$$

AGB.M2: $$AGB = \alpha \cdot \rho DBH^{\beta} + \varepsilon, \quad (5)$$

AGB.M3: $$AGB = \alpha \cdot (DBH^2 H)^{\beta} + \varepsilon, \quad (6)$$

AGB.M4: $$AGB = \alpha \cdot \rho (DBH^2 H)^{\beta} + \varepsilon, \quad (7)$$

where ε is the model error, which considers factors that may explain the difference in biomass between two trees with the same DBH and H dimensions. The branch (*BBR.M*) and trunk (*BTR.M*) models were fitted according to the model formulated in AGB.M1. All of the variables in these models were considered as logarithmic transformed variables to eliminate *heteroscedasticity*. To obtain biomass values by back-transformation, we applied the correction factor (CF) described by Sprugel (1983), which relies on the residual standard error (RSE) of the models, as given in equation 8, thereby adjusting for the systematic bias associated with log-transformations of data.

$$CF = \exp\left(\frac{RSE^2}{2}\right) \quad (8)$$

*Evaluation of the biomass models*

A thorough validation of a new model normally requires the use of independent empirical datasets (Vanclay and Skovsgaard, 1997). However, due to the relatively small sample size and paucity of separate validation datasets, we decided to employ goodness-of-fit statistics, Akaike's information criterion (AIC) for multi-model inference, and graphical analysis to assess the performances of the new models in comparison to the previous models produced by Fromard et al. (1998). All of the model fitting procedures and statistical evaluation were performed using MATLAB.

## 2.3 Results

Height-dependent wood density

*WD* values ranged from 595 to 790 kg $m^{-3}$ (Figure 2-5) for trees over a DBH range of 10.4 – 110 cm, with a mean value of 728.7 ± 8.91 kg $m^{-3}$ around the breast height. The LME model fitted for WD as a function of sample height and tree *DBH*, with the individual tree as random factor, demonstrated a decreasing trend along the stem axis. From the tree base to the top, each increase the sampling height resulted in a 0.7% decrease in the basal mean *WD* value of 731.5 ± 17.2 kg $m^{-3}$. The inclusion of a measure of individual tree *DBH* in the model resulted in ca. 0.08% increase in the predicted ($P$ = 0.076). Thus, individual tree effect was not a significant factor in the total effects found in the distribution of wood density along the stem axis.

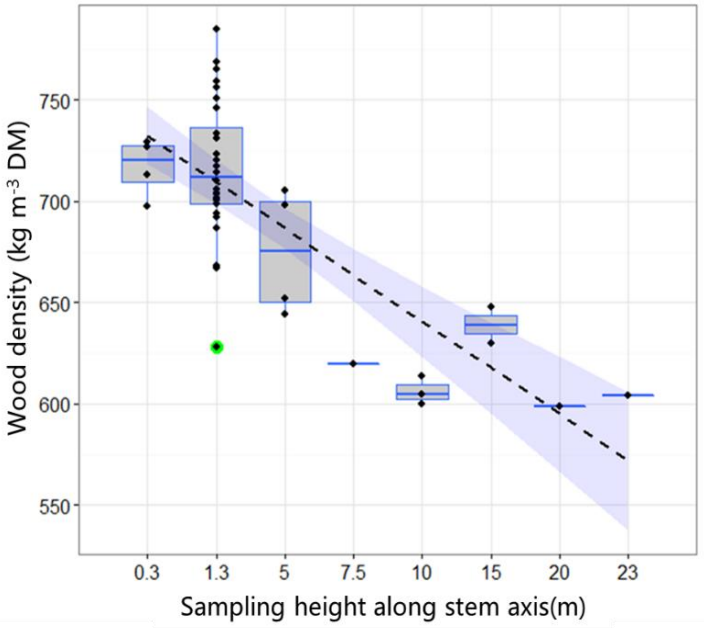


Figure 2-5: Decreasing wood density at different heights along the stem axis: black dots denote the wood density values from tree samples; the green dot was consider an outlier; and the dashed line shows the linear model with a 95% confidence interval

### 2.3.1 *Accuracy of pixel-based trunk volume estimation from TLS data*

Based on the performance test of the pixel-based method, the best results were achieved at a trunk section height of 10 cm during volume computation. These trunk volume estimates were compared with the geometric volume based on successive conical frustums for the analyzed trees (Figure 2-6, a & b). The *RMSE* between these two methods reached 6.7% of the mean value for 18 trees with no pronounced buttresses. The linear fit ($R^2$ = 0.99) of the trunk volume estimates nearly overlaid the one-to-one line for the small, almost straight bole trees (Figure 2-6a). Higher volume estimates were obtained from trees with more pronounced buttresses, with the *RMSE* value increased to 16.7% of the mean value and the $R^2$ decreased to 0.96 for larger trees (Figure 2-6b). Overall, the pixel-based method produced trunk volume with an accuracy of ca. 90%.

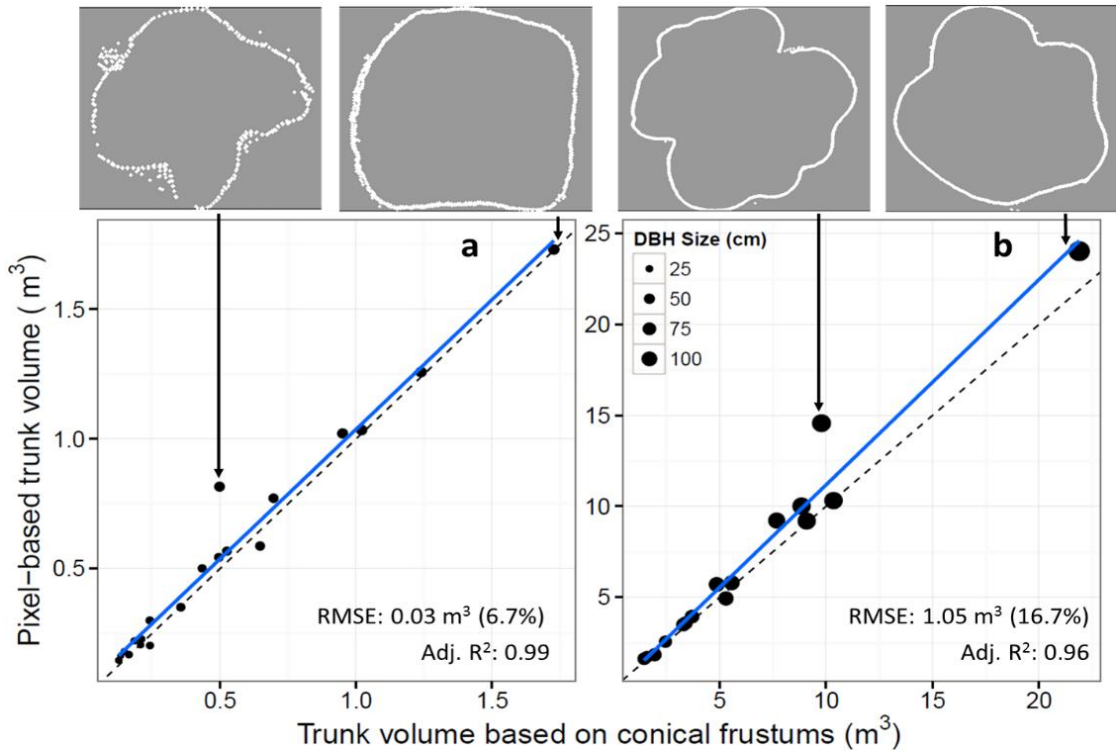


Figure 2-6: Comparison of the trunk volumes estimated using the automatic pixel-based analysis of TLS data and the successive trunk-fitted conical frustums for trees with DBH < 42 cm (a) and > 42 cm (b). Outline of girth form of typical trunks are shown in white with a grey background (arrows 1–4). The dashed line depicts a one-to-one relationship and the blue solid line corresponds to linear fit.

### 2.3.2 *Accuracy of TLS-based tree volume-to-biomass conversion*

The two specific *WD* values were combined with the pixel-based trunk volume estimates to produce biomass of trees in the diameter range of the reference data. The mean value of *WD* yielded a mean deviation of 16.5% (dry matter) compared with the reference biomass values for tree *DBH* < 42 cm. The *dWD* values lowered the mean deviation of the TLS-derived trunk biomass to 6.7% for the trees analysed in this study. Overall, the *dWD*-based biomass estimates strongly correlated with the reference values (R = 0.99), where the RMSE was 41.23 kg (14.21%) for the trunk biomass, 48.6 kg (13.6%) for the aboveground woody components, and 48.5 kg (13.5%) for the total *AGB* (Figure 2-7, a–c), with biomass values ranging from ca. 70 to 900 kg (dry matter).

### 2.3.3 *Aboveground woody biomass of large A. germinans trees*

The sum of the TLS-derived branch and trunk biomass yielded the aboveground woody biomass of large trees. These values ranged from 1242 kg for a tree with a *DBH* of 44.9 cm to 17,367 kg for a tree with a *DBH* of 124.5 cm. The branch biomass composition was almost uniform in small to medium-sized trees, i.e., 15–20% of the tree biomass. For large trees, the branch biomass varied from ca. 20% to almost 50% of the tree *AGB* in some cases (see Appendix).

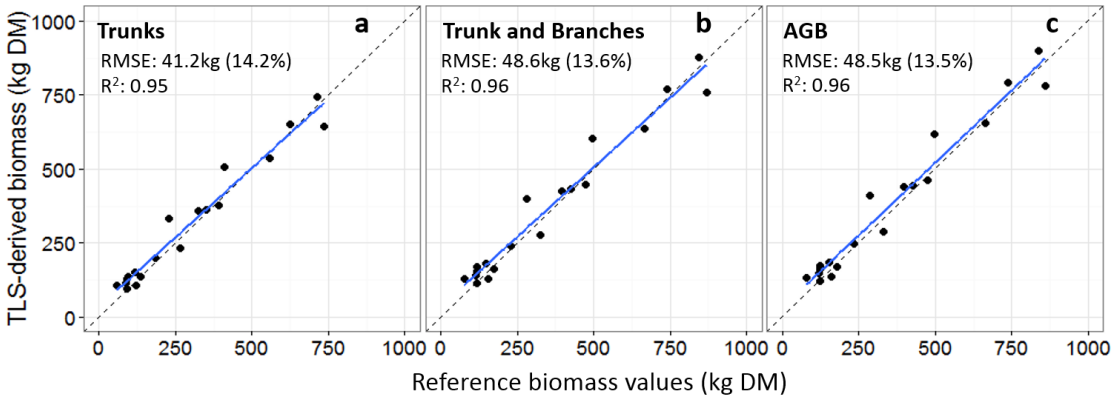


Figure 2-7: Comparison of the TLS method relative to the estimates to the reference values for the trunk DBH<42 cm (a), trunk and branches (b), and total biomass estimates (c). The dots correspond to the biomass values of the sample trees (cf. Fromard et al. 1998), the dashed line is a 1:1 relationship, and the blue solid line indicates the linear fit

### 2.3.4 *Revised allometric models of A. germinans trees*

Using the new TLS-derived tree biomass and the available tree weight dataset, revised allometric models' parameters were proposed (Table 2-3). For the tree branch biomass (*BBR.M*), we obtained a model with the same intercept coefficient ($\alpha$ = 0.03) as the reference model ($BBR_{ref}$). Meanwhile, the model parameter $\beta$ and $R^2$ changed from 2.33 and 0.90 to 2.41 and 0.98, respectively. The curve describing

*BBR.M* clearly shifted upward for trees larger than the diameter range of $BBR_{ref}$ (Figure 2-8a), indicating that the $BBR_{ref}$ underestimated the branch biomass of large trees. Our model for trunk biomass (*BTR.M*) was characterized by the model parameters $\alpha = 0.11$ and $\beta = 2.46$, which yielded a clear power curve deflection below the reference model (Figure 2-8b). The $R^2$ also increased from 0.95 in the reference model ($BTR_{ref}$) to 0.99 in the BTR.M. We obtained the best fit for a total *AGB* (AGB.M1) model, which has *DBH* as an explanatory variable (Table 2-3, Figure 2-8c). The model clearly had different parameters, where $R^2 = 0.99$ and corrected AIC were significantly lower compared with the reference model ($AGB_{ref}$), but the corresponding residual standard error (RSE) only decreased by 1.2 kg (1.4%). With the exception of AGB.M2, which is similar to AGB.M1 in terms of model parameter and statistical attributes, AGB.M3 and AGB.M4 models with additional variable(s) (tree height and wood density) yielded higher residual standard errors compared with the $AGB_{ref}$.

Table 2-3: Descriptions of the revised allometric models and associated statistical parameters

| Model ID | Model Form* | *DBH* range (cm) | Number of trees | $\alpha$ | $\beta$ | RSE (kg) | $R^2$ | AIC |
|---|---|---|---|---|---|---|---|---|
| ***Branch Models*** | | | | | | | | |
| $BBR_{ref}$ | $\alpha.DBH^{\beta}$ | 4 – 42 | 25 | 0.03 | 2.33 | 65.4 | 0.90 | 56.36 |
| *BBR.M* | | 4 – 125 | 60 | 0.03 | 2.41 | 54.7 | 0.98 | 40.14 |
| ***Trunk Models*** | | | | | | | | |
| $BTR_{ref}$ | $\alpha.DBH^{\beta}$ | 4 – 42 | 25 | 0.07 | 2.59 | 122.6 | 0.95 | 30.08 |
| *BTR.M* | | 4 – 125 | 60 | 0.11 | 2.46 | 60.9 | 0.99 | 27.44 |
| ***AGB Models*** | | | | | | | | |
| $AGB_{ref}$ | $\alpha.DBH^{\beta}$ | 4 – 42 | 25 | 0.14 | 2.40 | 88.6 | 0.97 | 12.3 |
| AGB.M1 | | 4 – 125 | 60 | 0.16 | 2.42 | 87.4 | 0.99 | –3.86 |
| AGB.M2 | $\alpha.\rho DBH^{\beta}$ | 4 – 125 | 60 | 0.23 | 2.41 | 87.9 | 0.99 | –3.82 |
| AGB.M3 | $\alpha(DBH^2H)^{\beta}$ | 4 – 125 | 60 | 0.072 | 0.91 | 118.5 | 0.99 | 2.76 |
| AGB.M4 | $\alpha(\rho DBH^2H)^{\beta}$ | 4 – 125 | 60 | 0.099 | 0.91 | 117.5 | 0.99 | 2.57 |

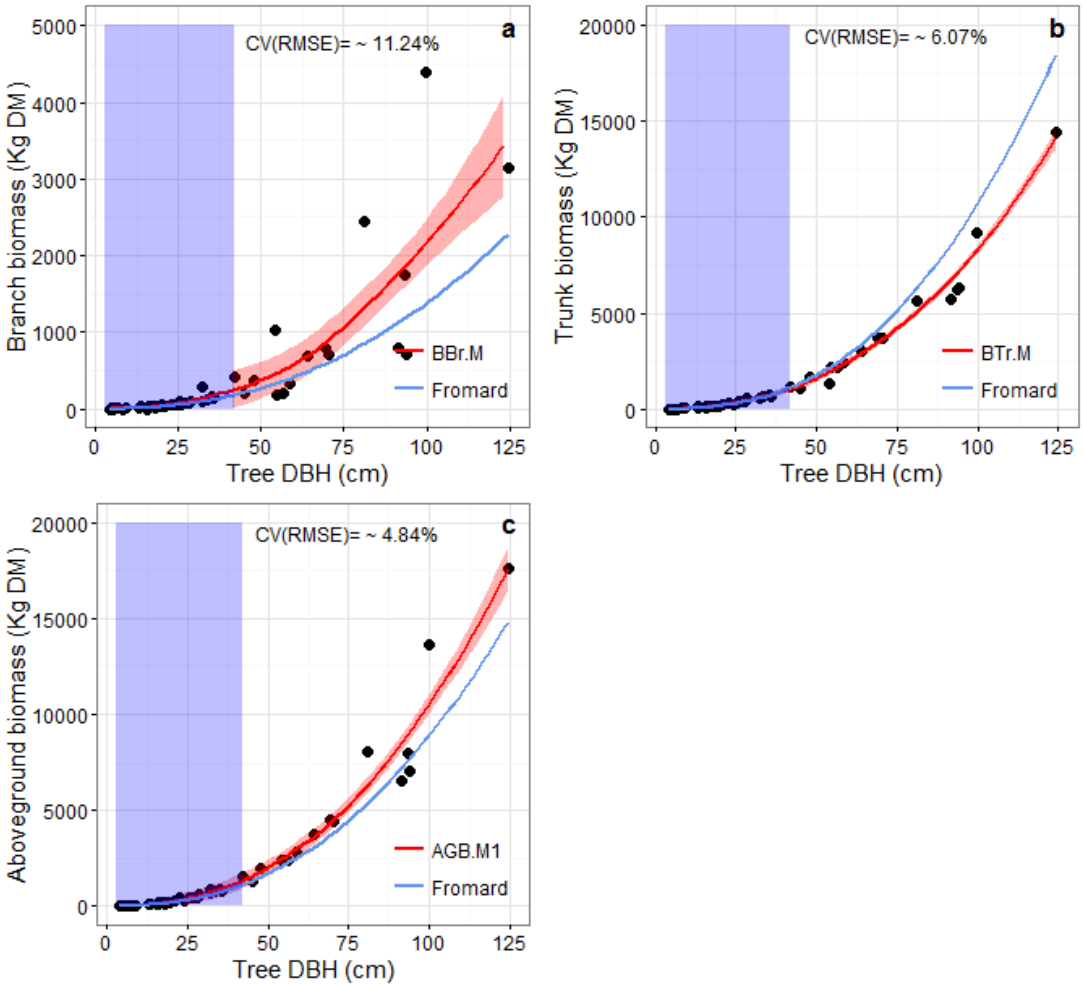


Figure 2-8: Comparison of the TLS-based biomass functions and the reference models for *A. germinans*. The branch (a), trunk (b), and total AGB (c) are distinguished. The *red line* and the surrounding *shade* represent the new model and confidence interval. The *blue line* is the prediction from the reference model, calibrated over the *DBH* range in the *shaded area*

## 2.4 Discussion

In this study, we evaluated the possible use of TLS for estimating the *AGB* of large mangrove trees (*A. germinans*) to facilitate the development of improved, non-destructive measurement procedures and to achieve higher precision in allometric models.

### *2.4.1 Accuracy of the TLS-derived mangrove tree biomass*

The results of the TLS-based biomass estimates reliably compare to the tree biomass weighed in the field for *DBH*<42cm. In particular, the estimates for the small to medium-sized trees had an accuracy of near 90% and they were highly correlated (R = 0.99) with the reference biomass. Interestingly, the accuracy of results produced using our simplified TLS data analysis achieved a comparable accuracy with results reported in previous studies (e.g., Calders et al. (2015); Raumonen et al. (2013)). That

the presence of buttresses in trees (Nogueira et al., 2006) may influence the overall accuracy of the TLS-derived biomass estimates justified the consideration for a pixel-based analysis adopted in this study. This approach respects the real shape of buttressed trees, making it particularly suitable for biomass measurement in large mangroves trees where basal protuberances are present.

Additionally, the careful selection of thickness for trunk sections in the segmentation process, as well as the consideration for the *WD* variations along the stem axis during the biomass conversion contributed to a high precision of the TLS-derived biomass estimates. Notwithstanding, the approach that dwells on primitive shape fitting may be sufficient when trees are near perfect shaped cylinder or conical forms, as is with the case of small and medium sized trees. Overall, it is possible that the TLS-based measurements insignificantly underestimate the actual tree biomass, especially for the crown biomass where the omission of fine twigs may likely occur.

### 2.4.2 *Modelling mangrove tree biomass with TLS-derived data*

Given the significance of large-diameter trees in allometric models, the new sets of biomass equations obtained in this study, which extend to very large trees, should improve biomass analyses of mangrove forests. The models do not yield significantly different predictions; model AGB.M1 where only *DBH* was used as an explanatory variable was shown to produce the best results according to the evaluation parameters. The TLS-based allometric models yielded new model parameters with higher predictive power, especially for the aboveground tree components of large trees. It should be noted that the overestimation of the trunks of large trees in relation to the reference models was complemented by the corresponding underestimation from the branch model in the total *AGB* estimates, with the new model yielding only slightly lower *AGB* estimates for trees *DBH* > 42 cm. Contrary to our expectations, the current results thus suggest that the reference model presents considerably good estimates for the total *AGB*, even for the very large trees.

The distinction in the behaviour of our models for the branch and trunk biomass and the reference models can be explained by the variations in the pattern of biomass partitioning in the aboveground tree components beyond the *DBH* range of the reference models. Fromard et al. (1998) confirmed that the small-medium size trees used to produce their models mostly had allocated the largest share of the *AGB* to their trunks, which was also demonstrated in our current study. The trees in these growth stages usually exhibit continuous growth in height and consistent natural pruning with no pronounced crown size. This growth pattern is likely related to survival strategies for fast-growing trees in competitive growing conditions. Later, trees will reach approach asymptotically a height where only secondary growth in the tree girth and the crown development continue, and large trees may prioritize

biomass distribution to the branches on the assumption of as a means for canopy space-filling, and to ensure mechanical stability.

Since the allocation of biomass to different tree components is subject to environmental effects, we suggest that considering the plasticity of tree morphology in mangrove allometric models may greatly facilitate improved biomass prediction in a range of environmental conditions. Indeed, Peters et al. (2014) have demonstrated such an environment-related plasticity in a mechanistic approach in their BETTINA model. This and similar models can be parameterized with TLS-derived data to achieve a framework for accurate biomass analyses from natural scrubby to tall mangrove forests.

In this study, the allometric model where mean *WD* was incorporated slightly increased the residual error of the biomass predictions compared with the base model. Since the *WD* varies with the individual tree size, but also at different heights within an individual *A. germinans* tree, the use of global or site-specific mean values may likely result in more biased estimates. Nevertheless, this factor has greater importance when parameterizing allometric models for species-specific comparisons among different sites or in multispecies applications (Chave et al., 2005; Chave et al., 2014). In addition, the inclusion of tree height as an additional variable in the current allometric models incurred higher residual error to biomass estimates. More so that this variable is not always available and not easy to measure, we suggest that the allometric model based only on the *DBH* is sufficient for estimating the biomass of *A. germinans* trees under optimal growth conditions.

### *2.4.3 Challenges affecting the wider application of TLS in mangrove studies*

The TLS provides an attractive, indirect method for the estimation of forest biomass, but several challenges need to be addressed to maximize its usability in mangrove studies. Deflection of tree crowns by the wind occurred during measurements in some of our scanning operations, especially with small to medium-sized trees. Thus, avoiding scanning during windy periods may reduce the likelihood of errors in such conditions.

In addition, large mangrove trees occasionally have hollow trunks due to rotting of the heartwood. This may lead to significant errors in the biomass estimates obtained for large trees based on indirect non-destructive measurements (Nogueira et al., 2006). However, it is questionable whether it is, in a real world scenario, feasible to reliably capture the necessary information on hollow trees, even from conventional destructive sampling. Without knowledge of the average volume of the cavities in the different tree size classes and the respective probability of their occurrence, subsequent estimation of biomass from regression models relying on *DBH* surveys

will consequently fail, regardless of the calibration technique applied. Advances in the application of ultrasonic tomography (Brancheriau et al., 2008) and Resistograph measurements (Rinn et al., 1996) demonstrate non-destructive detection of volume of cavities in trees. Integrating these measurements with the TLS-based method in the future could address the uncertainty caused by the possible presence of tree cavities. Meanwhile, in the current study, we have carefully avoided hollow trunks by a systematic restriction of sampling to physically sound trees (i.e., without signs of crack or rotten parts).

By considering the individual architecture of trees, our proposed TLS-based method could have wide applicability to other mangrove species. The work of Feliciano et al. (2014) already demonstrated a workaround for TLS application to *Rhizophora* species, considering the prop roots as toroidal objects to estimate their volumes and biomass. Their approach and the one presented here are fundamental towards ensuring the wider applicability of the TLS method for the studies on mangrove tree architecture and ecosystem functioning. The approaches could also be supported by tree architecture studies, which are scarce for mangroves at present, for example, for species developing prop roots, or aerial appendages.

Conclusively, the TLS data analysis provides a viable substitute for the destructive biomass measurement and allows estimates of large mangrove trees to be tractable. This opens new research opportunities in mangroves studies with respect to tree architecture, 'biomass productivity and ecosystem functioning. Our current allometric models may facilitate accurate determinations of the biomass for the aboveground parts with potential benefit to the success of the coastal blue carbon projects for conservation of mangrove forests. To advance the TLS method to other mangrove forests, a fully automatic procedure for volume and biomass estimation is desirable for use in the natural scrubby to tall mangrove forests, and this may require further refinement of our current procedure for TLS data collection and processing.

**Acknowledgements**

This research was conducted under the framework of the MANGWATCH project funded by the French *Centre National de la Recherche Scientifique* (CNRS) research program "Incubator for interdisciplinary research projects in French Guiana." Adewole Olagoke received doctoral fellowship from the European Commission under the Erasmus Mundus Joint Doctorate programme, *Forest and Nature for Society* (FONASO), and travel grants from the CNRS and Technische Universität Dresden Graduate Academy (Germany). Jean-Baptiste Féret is grateful to the French *Centre National d'Etudes Spatiales* (CNES) for supporting a postdoctoral fellowship. We thank the TOSCA program of the CNES for providing a grant to develop a 3D mock-up of mangrove trees within the framework of the BIOMASS mission

preparation. This study is dedicated to the memory of Michael Guéroult, our friend and colleague, who passed away all too soon. We greatly appreciate the two anonymous reviewers for their insightful and constructive comments.

## 2.5 References

Åkerblom, M., Pasi, R., Kaasalainen, M., and Casella, E. (2015). Analysis of Geometric Primitives in Quantitative Structure Models of Tree Stems. *Remote Sensing* **7**, 4581.

Anthony, E. J., Gardel, A., Gratiot, N., Proisy, C., Allison, M. A., Dolique, F., and Fromard, F. (2010). The Amazon-influenced muddy coast of South America: A review of mud-bank-shoreline interactions. *Earth-Science Reviews* **103**, 99-121.

Baltzer, F., Allison, M., and Fromard, F. (2004). Material exchange between the continental shelf and mangrove-fringed coasts with special reference to the Amazon–Guianas coast. *Marine Geology* **208**, 115-126.

Bastin, J. F., Barbier, N., Réjou-Méchain, M., Fayolle, A., Gourlet-Fleury, S., Maniatis, D., de Haulleville, T., Baya, F., Beeckman, H., Beina, D., Couteron, P., Chuyong, G., Dauby, G., Doucet, J. L., Droissart, V., Dufrêne, M., Ewango, C., Gillet, J. F., Gonmadje, C. H., Hart, T., Kavali, T., Kenfack, D., Libalah, M., Malhi, Y., Makana, J. R., Pélissier, R., Ploton, P., Serckx, A., Sonké, B., Stevart, T., Thomas, D. W., De Cannière, C., and Bogaert, J. (2015a). Seeing Central African forests through their largest trees. *Scientific Reports* **5**, 13156.

Bastin, J. F., Fayolle, A., Tarelkin, Y., Van den Bulcke, J., de Haulleville, T., Mortier, F., Beeckman, H., Van Acker, J., Serckx, A., Bogaert, J., and De Canniere, C. (2015b). Wood Specific Gravity Variations and Biomass of Central African Tree Species: The Simple Choice of the Outer Wood. *PLoS One* **10**, e0142146.

Bayer, D., Seifert, S., and Pretzsch, H. (2013). Structural crown properties of Norway spruce (Picea abies [L.] Karst.) and European beech (Fagus sylvatica [L.]) in mixed versus pure stands revealed by terrestrial laser scanning. *Trees* **27**, 1035-1047.

Béland, M., Baldocchi, D. D., Widlowski, J.-L., Fournier, R. A., and Verstraete, M. M. (2014). On seeing the wood from the leaves and the role of voxel size in determining leaf area distribution of forests with terrestrial LiDAR. *Agricultural and Forest Meteorology* **184**, 82-97.

Brancheriau, L., Lasaygues, P., Debieu, E., and Lefebvre, J. P. (2008). Ultrasonic tomography of green wood using a non-parametric imaging algorithm with reflected waves. *Annals of Forest Science* **65**, 712-712.

Calders, K., Newnham, G., Burt, A., Murphy, S., Raumonen, P., Herold, M., Culvenor, D., Avitabile, V., Disney, M., Armston, J., Kaasalainen, M., and McMahon, S. (2015). Nondestructive estimates of above-ground biomass using terrestrial laser scanning. *Methods in Ecology and Evolution* **6**, 198-208.

Chave, J., Andalo, C., Brown, S., Cairns, M. A., Chambers, J. Q., Eamus, D., Folster, H., Fromard, F., Higuchi, N., Kira, T., Lescure, J.-P., Nelson, B. W., Ogawa, H., Puig, H., Riéra, B., and Yamakura, T. (2005). Tree allometry and improved estimation of carbon stocks and balance in tropical forests. *Oecologia* **145**, 87-99.

Chave, J., Rejou-Mechain, M., Burquez, A., Chidumayo, E., Colgan, M. S., Delitti, W. B., Duque, A., Eid, T., Fearnside, P. M., Goodman, R. C., Henry, M., Martinez-Yrizar, A., Mugasha, W. A., Muller-Landau, H. C., Mencuccini, M., Nelson, B. W., Ngomanda, A., Nogueira, E. M., Ortiz-Malavassi, E., Pelissier, R., Ploton, P., Ryan, C. M., Saldarriaga, J. G., and Vieilledent, G. (2014). Improved allometric models to estimate the aboveground biomass of tropical trees. *Glob Chang Biol* **20**, 3177-90.

Dassot, M., Colin, A., Santenoise, P., Fournier, M., and Constant, T. (2012). Terrestrial laser scanning for measuring the solid wood volume, including branches, of adult standing trees in the forest environment. *Computers and Electronics in Agriculture* **89**, 86-93.

Feliciano, E. A., Wdowinski, S., and Potts, M. D. (2014). Assessing Mangrove Above-Ground Biomass and Structure using Terrestrial Laser Scanning: A Case Study in the Everglades National Park. *Wetlands* **34**, 955-968.

Fromard, F., Puig, H., Mougin, E., Marty, G., Betoulle, J. L., and Cadamuro, L. (1998). Structure, above-ground biomass and dynamics of mangrove ecosystems: new data from French Guiana. *Oecologia* **115**, 39-53.

Fromard, F., Vega, C., and Proisy, C. (2004). Half a century of dynamic coastal change affecting mangrove shorelines of French Guiana. A case study based on remote sensing data analyses and field surveys. *Marine Geology* **208**, 265-280.

Gibbs, H. K., Brown, S., O Niles, J. O., and Foley, J. A. (2007). Monitoring and estimating tropical forest carbon stocks: making REDD a reality. *Environmental Research Letters* **2**, 1-13.

Hackenberg, J., Wassenberg, M., Spiecker, H., and Sun, D. (2015). Non Destructive Method for Biomass Prediction Combining TLS Derived Tree Volume and Wood Density. *Forests* **6**, 1274-1300.

Hauglin, M., Astrup, R., Gobakken, T., and Næsset, E. (2013). Estimating single-tree branch biomass of Norway spruce with terrestrial laser scanning using voxel-based and crown dimension features. *Scandinavian Journal of Forest Research* **28**, 456-469.

Hilker, T., van Leeuwen, M., Coops, N., Wulder, M., Newnham, G., Jupp, D. B., and Culvenor, D. (2010). Comparing canopy metrics derived from terrestrial and airborne laser scanning in a Douglas-fir dominated forest stand. *Trees* **24**, 819-832.

Imbert, D., and Rollet, B. (1989). Phytomasse aerienne et production primaire dans la mangrove du Grand Cul-de-Sac Marin (Guadeloupe, Antilles francaises). *Bulletin d'Ecologie* **20**, 27-39.

Kankare, V., Holopainen, M., Vastaranta, M., Puttonen, E., Yu, X., Hyyppä, J., Vaaja, M., Hyyppä, H., and Alho, P. (2013). Individual tree biomass estimation using terrestrial laser scanning. *ISPRS Journal of Photogrammetry and Remote Sensing* **75**, 64-75.

Komiyama, A., Ong, J. E., and Poungparn, S. (2008). Allometry, biomass, and productivity of mangrove forests: A review. *Aquatic Botany* **89**, 128-137.

Komiyama, A., Poungparn, S., and Kato, S. (2005). Common allometric equations for estimating the tree weight of mangroves. *Journal of Tropical Ecology* **21**, 471-477.

Lindenmayer, D. B., Laurance, W. F., and Franklin, J. F. (2012). Global Decline in Large Old Trees. *Science* **338**, 1305-1306.

Lutz, J. A., Larson, A. J., Freund, J. A., Swanson, M. E., and Bible, K. J. (2013). The Importance of Large-Diameter Trees to Forest Structural Heterogeneity. *PLoS ONE* **8**, e82784.

Nogueira, E. M., Nelson, B. W., and Fearnside, P. M. (2006). Volume and biomass of trees in central Amazonia: influence of irregularly shaped and hollow trunks. *Forest Ecology and Management* **227**, 14-21.

Peters, R., Vovides, A. G., Luna, S., Grüters, U., and Berger, U. (2014). Changes in allometric relations of mangrove trees due to resource availability – A new mechanistic modelling approach. *Ecological Modelling* **283**, 53-61.

Pistorius, T. (2012). From RED to REDD+: the evolution of a forest-based mitigation approach for developing countries. *Current Opinion in Environmental Sustainability* **4**, 638-645.

Proisy, C., Couteron, P., and Fromard, F. (2007). Predicting and mapping mangrove biomass from canopy grain analysis using Fourier-based textural ordination of IKONOS images. *Remote Sensing of Environment* **109**, 379-392.

Pueschel, P., Newnham, G., Rock, G., Udelhoven, T., Werner, W., and Hill, J. (2013). The influence of scan mode and circle fitting on tree stem detection, stem diameter and

volume extraction from terrestrial laser scans. *ISPRS Journal of Photogrammetry and Remote Sensing* **77**, 44-56.

Raumonen, P., Kaasalainen, M., Åkerblom, M., Kaasalainen, S., Kaartinen, H., Vastaranta, M., Holopainen, M., Disney, M., and Lewis, P. (2013). Fast Automatic Precision Tree Models from Terrestrial Laser Scanner Data. *Remote Sensing* **5**, 491-520.

Rinn, F., Schweingruber, F.-H., and Schaer, E. (1996). RESISTOGRAPH and X-ray density charts of wood comparative evaluation of drill resistance profiles and X-ray density charts of different wood species. *Holzforschung* **50**, 303-311.

Slik, J. W. F., Paoli, G., McGuire, K., Amaral, I., Barroso, J., Bastian, M., Blanc, L., Bongers, F., Boundja, P., Clark, C., Collins, M., Dauby, G., Ding, Y., Doucet, J.-L., Eler, E., Ferreira, L., Forshed, O., Fredriksson, G., Gillet, J.-F., Harris, D., Leal, M., Laumonier, Y., Malhi, Y., Mansor, A., Martin, E., Miyamoto, K., Araujo-Murakami, A., Nagamasu, H., Nilus, R., Nurtjahya, E., Oliveira, Á., Onrizal, O., Parada-Gutierrez, A., Permana, A., Poorter, L., Poulsen, J., Ramirez-Angulo, H., Reitsma, J., Rovero, F., Rozak, A., Sheil, D., Silva-Espejo, J., Silveira, M., Spironelo, W., ter Steege, H., Stevart, T., Navarro-Aguilar, G. E., Sunderland, T., Suzuki, E., Tang, J., Theilade, I., van der Heijden, G., van Valkenburg, J., Van Do, T., Vilanova, E., Vos, V., Wich, S., Wöll, H., Yoneda, T., Zang, R., Zhang, M.-G., and Zweifel, N. (2013). Large trees drive forest aboveground biomass variation in moist lowland forests across the tropics. *Global Ecology and Biogeography* **22**, 1261-1271.

Sprugel, D. (1983). Correcting for bias in log-transformed allometric equations. *Ecology* **64**, 209–210.

Strahler, A. H., Jupp, D. L. B., Woodcock, C. E., Schaaf, C. B., Yao, T., Zhao, F., Yang, X., Lovell, J., Culvenor, D., Newnham, G., Ni-Miester, W., and Boykin-Morris, W. (2008). Retrieval of forest structural parameters using a ground-based lidar instrument (Echidna®). *Canadian Journal of Remote Sensing* **34**, S426-S440.

Vanclay, J. K., and Skovsgaard, J. P. (1997). Evaluating forest growth models. *Ecological Modelling* **98**, 1-12.

Vogt, J., Lin, Y., Pranchai, A., Frohberg, P., Mehlig, U., and Berger, U. (2014). The importance of conspecific facilitation during recruitment and regeneration: A case study in degraded mangroves. *Basic and Applied Ecology* **15**, 651-660.

## 2.6 Appendix

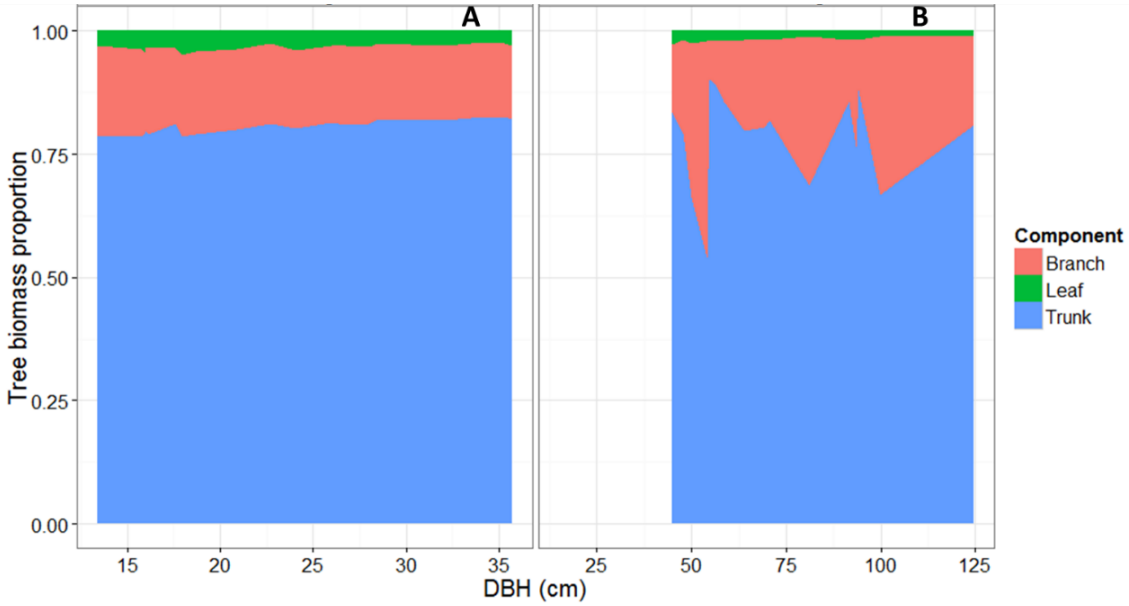


Appendix 2- I: Contribution of different tree components to total aboveground biomass of *Avicennia germinans* (*A. near uniform distribution in small trees (DBH< 42 cm); B. Variability of branch biomass in large trees (DBH> 42 cm))*

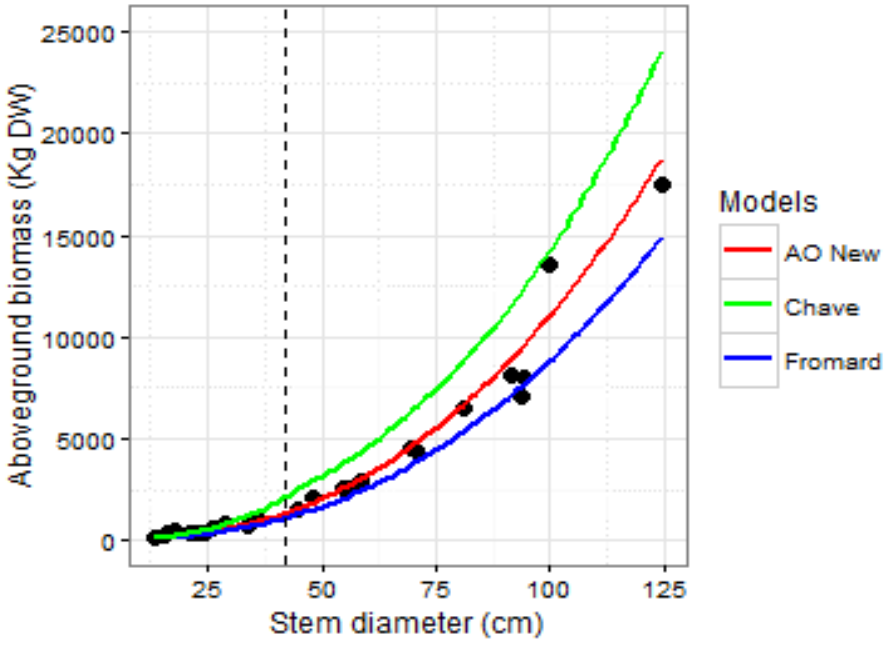


Appendix 2- II: TLS-derived allometric model for estimating aboveground biomass of *Avicennia germinans* in comparison to models of Fromard et al (1998) and Chave et al. (2005)

# 3 COLLECTIVE PLASTIC TREE ATTRIBUTES EXPLAIN THE DYNAMICS OF ABOVEGROUND BIOMASS IN CONTRASTING AMAZON-INFLUENCED MANGROVE FORESTS[1]


## Abstract

*In an attempt to elucidate on how the cross-regional variations in mangrove tree morphology relate to the dynamics forest structure, we investigated the relative contribution of plastic tree attributes to the divergence of aboveground biomass in the Amazon-influenced mangrove forests. Datasets from 45 plots of contrasting tree morphology and stand structure in French Guiana (FG) and Bragança, state of Pará, North Brazil were considered for this study. Using Avicennia germinans as a test species, we highlighted the site-specific differences in tree allometries, thanks to the analysis of covariance (ANCOVA) covering the dimensional relations of total height – stem diameter, height-to-crown base – stem diameter and crown – stem diameter in comparison to their respective cross-regional models. Marked differences in the tree crown dimensions clearly suggest regional-scale allometric differences among mangrove forests in FG and Bragança. To identify how far site-dependent tree allometries can influence aboveground biomass at the tree scale, we optimized a diameter-biomass allometry using height and crown dimensions as covariate explanatory variables. Scaling to the stand level, selected collective indicators of local variation in tree morphology and forest structure were considered in developing parsimonious stand aboveground biomass (AGB.ha) models, allowing us to explain the cross-regional divergence of aboveground biomass across the Amazon-influenced forests. The potential of the models were tested in contrasting mangrove stands with distinct tree morphology. Our results showed that local variation in tree allometries reflected up to ca. 30% coefficient of variations in the tree-scale aboveground biomass predictions from tall forests in FG to medium-height forests in Bragança. Models based on the stand basal area (SBA.ha), quadratic mean stem diameter (Dq), maximum stem diameter (Dmax) and height (Hmax) explained ca. 90% of local variation in the AGB.ha. The best-fitted model (noted SM.4), with SBA.ha, Dq and Dmax as explanatory variables, predicted the AGB.ha of mangrove forests in Bragança to the root mean square (RMSE) of 13.9%. Conclusively, the site-specific variation in mangrove tree morphology led to divergent allometric relations and that strongly impedes the application of any cross-regional allometric model. The biomass allometric model incorporating crown metrics apparently provided a measure of site-dependent variations at the tree scale. This study thus suggests that regional differences in mangrove tree structure and function could be captured through better description of crown metrics, and that selected indicators of local morphological plasticity and consequent stand structure could generate a plus-value in the understanding of mangrove stand dynamics across contrasting coasts.*


[1] *Manuscript in preparation*

## 3.1 Introduction

Many aspects of forest structural and functional properties directly relate to the allometric scaling of trees' morphological and physiological traits (Bohlman and Pacala, 2012; West et al., 2009). Such relationships are well established in allometric framework (Muller-Landau et al., 2006; West et al., 2009), which are rooted on the power-based dimensional ratio of structure and function relationships (Huxley and Teissier, 1936). In the purview of these conceptual models, the morphological scaling of tree species are simply presumed to converge in invariant allometric exponents (Enquist and Niklas, 2001; West et al., 1999). Most general allometric models are hinged on similar assumptions that tree form and functions across sites or regions could be captured in simple allometric equations. Evidences however suggest that the allometric relationships of tree structure and function are not always linearly simple (Weiner, 2004), and can vary significantly from local to regional scales (Feldpausch et al., 2011; O'Brien et al., 1995; Pretzsch et al., 2014); they are largely influenced by environmental constraints (Koch et al., 2004; Ryan and Yoder, 1997). This being that individual trees are shaped to maximize fitness and optimized function in response to exacting abiotic stress and competitive interactions with neighbouring others (Callaway et al., 2003; Chapin et al., 1987).

For instance, the morphology of shoot in relation to the respective root systems in individual trees are fashioned in the sense that they meet individuals' peculiar functional need to obtain light, water or nutrients prevailing environmental cues (Franklin et al., 2012; Poorter et al., 2012). Further support for allometric plasticity rested on the assumption of increasing cost of hydraulic limitation with reduced water availability, whereby trees respond with restricted height growth with no corresponding change in stem diameter (Feldpausch et al., 2011). In a similar manner, studies have shown that the average tree height in the tropical forests decreases with increasing altitude (Grubb, 1977) as well as latitude (Méndez-Alonzo et al., 2008), and the stem diameter less responsive in a comparable magnitude. The question thus remains whether allometric relations of tree dimensions to the respective functionalities (for example, biomass accumulation) hold constants or rather converge in constant slopes at a regional scale, especially for tree species exhibiting morphological plasticity.

In mangrove forests, numerous cases of morphological plasticity have been documented (*sensu.* Feller et al. (2010); Vovides et al. (2014)) and this makes an unrivalled opportunity to shed light to the understanding of changes in tree allometric relations and the implications for biomass predictions across scales of environmental/ coastal conditions. Local variations in abiotic conditions – hydroperiod, salinity and resource distribution – and regional environmental settings (Twilley and Rivera-Monroy, 2005) often do lead to diverse morphological

expression within a single mangrove species. While a typical *A. germinans* tree in equatorial mangrove region can attain a height of ca. 45 m (Fromard et al., 1998; Olagoke et al., 2016), a dwarfy individual of the same species in an adverse environment rarely exceed a height range of 0.5 m to 2 m (Vogt et al., 2014). Likewise, Lugo (1997) showed that *R. mangle* in the Neotropical forest can attain mature tree size between 0.5 m and 40 m high depending on habitat salinity. The differential biomass partitioning to various tree components in the course of growth development is mainly attributed with structural plasticity of mangrove trees in variable environments (Feller et al., 2003; Lira-Medeiros et al., 2010; Peters et al., 2014). In this case, an individual growing in a water or nutrient limited environment prioritizes biomass allocation to root development (Ball, 1988; Castañeda-Moya et al., 2011) in order to facilitate access to belowground soil resources. A reverse trend comes to play when light resource becomes limiting, as trees are disposed to increasing competition for light, and by implication direct more biomass proportion to crown and leaf growth (Cintron and Schaeffer-Novelli, 1984; Clough, 1992). Despite the knowledge of allometric plasticity in mangrove trees, the influence of stand level structure and function is rarely explored (Vovides et al., 2014).

Earlier studies have highlighted the importance of allometric models in the study of mangrove structure and functions (e.g. Fromard et al. (1998); (Komiyama et al., 2002); Ong et al. (2004); Soares and Schaeffer-Novelli (2005)). Many of these works pointed to the fact that allometric relations are site-dependent, leading to regular proliferation of local mangrove diameter-biomass allometric models (Komiyama et al., 2008). Of the available models, only a few studies have advanced common or general biomass allometric models (Chave et al., 2005; Komiyama et al., 2002; Komiyama et al., 2005), which are supposedly applicable for tree biomass estimation in every mangrove regions. It however remains uncertain that specific wood gravity, which appears the only precursor of environment conditions in such models is sufficient to capture the variability being observed in nature. Beyond the tree scale, the modelling attempts by Saenger and Snedaker (1993) and Hutchison et al. (2014) tend to capture regional or global patterns in stand biomass, though they achieved models that explained only ca. 7.6% and 13.9% of stand biomass variations respectively using local latitude and/ or biophysical parameters. The above notwithstanding, the common practice remains the application of common allometric models to forests in the same region and beyond, especially where no local allometric equations are available (Fourqurean et al., 2014). We opine that the implication of local variations in tree allometries could impacts significantly on the accuracy of biomass estimation at the tree scale, as well as the stand level estimates of forest structure. Given this assumption, applying a common diameter-allometric biomass models to sites beyond the region of calibration could result in gross

systematic errors over the stand-scale biomass estimates (Fourqurean et al., 2014), as equally demonstrated in the tropical rainforest studies (Chave et al., 2004).

Accounting for site-specific allometric variations in biomass models is obviously challenging and perhaps the reason for paucity of cross-regional biomass models. Forests with largely distinct structural properties may indeed culminate in nearly the same aboveground biomass estimates (Proisy et al., 2012; Proisy et al., 2016b). This factor also limits the prospects of many sophisticated remote sensing techniques in accurately mapping of mangrove forest biomass (e.g. Réjou-Méchain et al. (2014)). As a practical contribution to the identification of variables that can explain structural dynamics of mangrove forests, we analysed in this study the allometric differences among amazon-influenced mangrove forests and the implications for aboveground biomass estimation both at the tree scale and stand level. Our key aim is to advance parsimonious models that can explain the cross-regional dynamics in the aboveground biomass using site-dependent plastic tree indicators. In specific terms, we addressed three important questions:

1. Do variations in mangrove tree morphology lead to convergence in allometric relations in the Amazon-influenced regions?
2. If not, how much does the local variation reflected in the diameter-biomass allometry across the regions?
3. To what extent can a parsimonious model explain the dynamics of aboveground biomass across the amazon-influenced mangrove forests?

## 3.2 Materials and methods

### *3.2.1 Study locations*

This work presents data from a series of mangrove forests located in contrasting/ diverse sites along the coasts of French Guiana and Bragança, North Brazil (Figure 3-1), all in the Amazon-influenced regions. In total, we have assembled tree dimensions and forest structure data from 46 mangrove forest plots (39 in French Guiana and 7 in Bragança), with sizes ranging from 0.03 to 1 ha (depending on tree density). The sites are generally distinct in local environmental conditions, tree growth forms and forest structure. Although the study was pre-designed to represent contrasting *Avicennia germinans* dominated forests, some of the sites contained sparse proportion of *Rhizophora mangle* and *Laguncularia racemosa* in varying compositions. Further descriptions of the sites, forest structure and species compositions are provided in the subsequent sections.

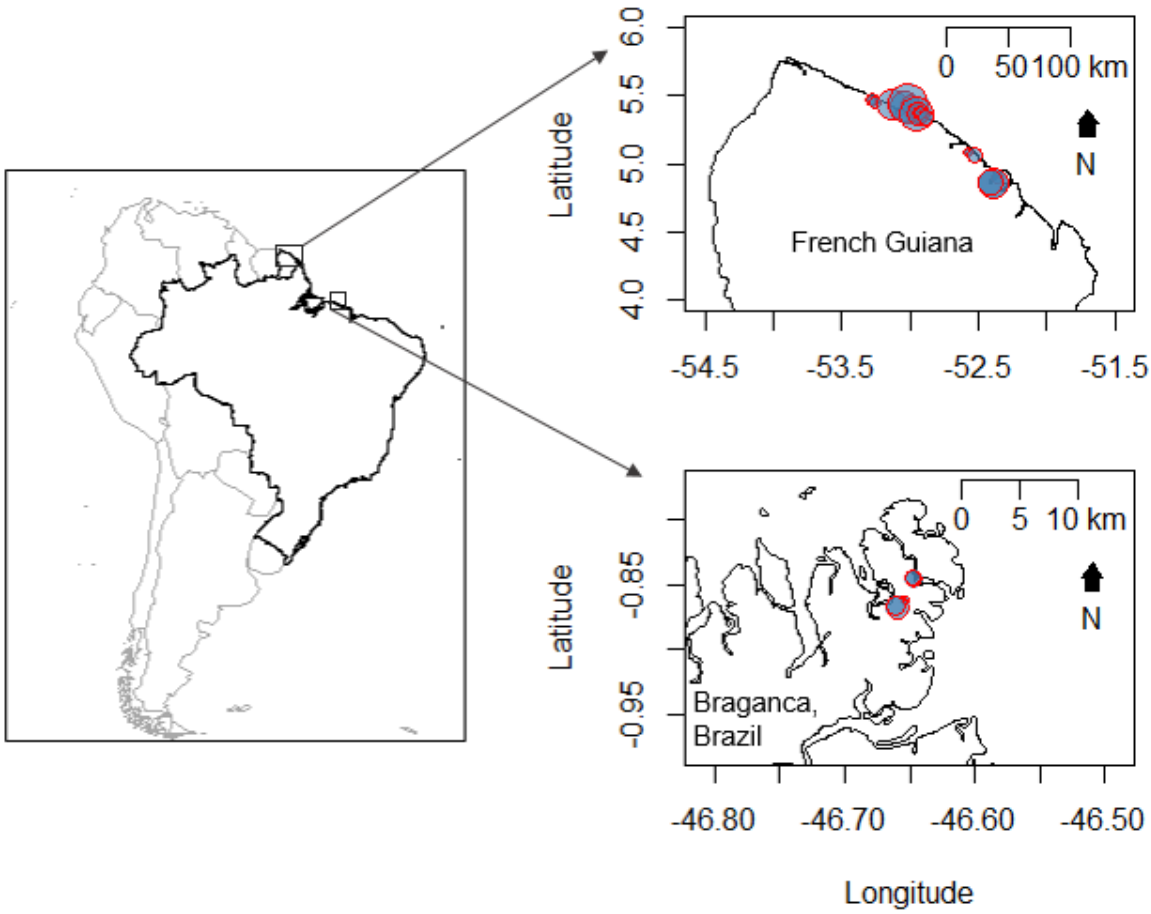


Figure 3-1: Location of study sites in French Guiana coast and Bragança (North Brazil), with selected plots in filled circles in the scale proportional to aboveground biomass per hectare.

In French Guiana (FG), the study plots are distributed along the 350 km mangrove coastline, which is primarily exposed to the influence of sediment dispersal from the Amazon River (Baltzer et al., 2004). The spatio-temporal distribution of mangroves in this area is controlled by a succession of rapid and acute erosion and accretion phases resulting from the drift of giant mudbanks to the northwest (Allison and Lee, 2004; Gardel and Gratiot, 2004). The main successional growth stages are distributed in patchy forest mosaics across the coastal landscape, with clusters of young trees sometimes occurring in close vicinity to decaying areas (Fromard et al., 1998; Proisy et al., 2007). Here, the positioning of study plots specifically represents the span of different developmental stages as characterized by their forest structure and aboveground biomass ranging from 50 to ca. 400 Mg DM/ ha, with site salinity between 10 – 20 ppt.

In Bragança (North Brazil), our plots are located within the mangrove peninsula around the Caeté bay, which extends over ~300 km southeast of the Amazon estuary (Lara and Cohen, 2006). The forests form riverine/ fringe mangroves in a 166 $km^2$ peninsula, crossed by several tidal channels with macrotides height range of ca. 4 m and strong oscillating currents reaching ~1.5 m $s^{-1}$ velocities for spring tides (Lara,

2003). Highly dynamic sediment transport, with areas of rapid mud erosion and deposition, forming similar geomorphologic features and the development of analogous mangroves, and the correlation found between tree height and topography-dependent inundation frequency are some of the intrinsic features characterizing the mangrove forests in this area (Cohen and Lara, 2003; Cohen et al., 2004). Here, we have selected seven study plots covering a range of *Avicennia* tree height profile: from 2-11 m Medium Avicennia stand (BragM, 3 plots) through 5-25 m in the mixed stand (BragMix, 2 sample plots) and ca. 5-30 m in the Tall *Avicennia* stand (BragT, 2 plots). More so, the classification based on tree height profile equally matched a gradient of sediment salinity, from low (30 ppt) in the Tall *Avicennia* stand to ca. 60 ppt in the Medium stand.

### 3.2.2 *The datasets*

*Forest structure*

We provide the summary descriptions of the forest stands presented in this study in the Table 3-1 below. In French Guiana, the selected plots covered forest stands with mean diameter ranging from 5.9 to 73.5 cm and mean height, from 10.2 to 35.7 m. In this area, the maximum stem diameter and height reached respective values of ca. 125 cm and ca. 45 m. The corresponding aboveground biomass per hectare (estimated as presented in section 3.2.3 below) ranged from 57.5 to 481.9 Mg DM/ha. For the sites in Bragança, the mean stem diameter ranged between 9.5 and 12.9 cm in the BragM, 16.7 and 22.7 cm in the BragT, and 24.5 to 36.7 cm in the BragMix. Across the Bragança sites, we recorded stand aboveground biomass ranging from 90.2 to 288.8 Mg DM/ha.

The Dq in each plots was determined from the stem diameter measurements $D_{i,\ i\ =\ 1\ldots N}$ of all individual trees (N) in the plot using the formula:

$$D_q = \sqrt{\frac{\sum_{i=1} D_i^2}{N}},$$

and the Hq represented the corresponding mean height of trees with stem diameter the nearest Dq (Pretzsch, 2009). We estimated stand basal area for each forest plot as:

$$SBA.ha = pi \times \sum_{i=1}^{N} \frac{D_i^2}{200} \times \frac{plot\,size}{10000},$$

The stand aboveground biomass (AGB.ha) for each forest area correspond to the sum of the component trees' aboveground biomass (AGB), with individual tree AGB estimated using allometric models as detailed in 3.2.3 below.

Table 3-1: Important structural attributes and habitat salinity range characterizing the selected forest plots, including quadratic mean stem diameter (Dq), median stem diameter (Dm), quadratic mean height (Hq), median height (Hm), maximum height (Hmax), maximum stem diameter (Dmax), number of individuals per hectare (N.ha), stand basal area (SBA), stand aboveground biomass (AGB.ha). Values denote range obtained from plots within the same site categories.

| | Forest sites | | | |
|---|---|---|---|---|
| variables | French Guiana | Bragança Tall | Brag Medium | Brag Mixed |
| Dq (cm) | 5.90 – 73.53 | 16.72 – 22.68 | 9.51 – 12.90 | 24.51 – 36.88 |
| Dm (cm) | 5.40 – 69.50 | 12.48 – 15.65 | 7.40 – 8.80 | 10.48 – 18.05 |
| Dmax (cm) | 8.50 – 124.50 | 35.70 – 43.10 | 24.65 – 24.70 | 92.00 – 95.60 |
| Hq (m) | 10.23 – 35.66 | 13.46 – 17.11 | 5.68 – 6.53 | 12.90 – 17.27 |
| Hm (m) | 9.44 – 36.31 | 12.27 – 16.58 | 5.36 – 6.13 | 9.81 – 19.10 |
| Hmax (m) | 14.21 – 42.39 | 23.80 – 29.20 | 8.08 – 11.01 | 23.97 – 24.58 |
| N.ha (stems/ ha) | 44 – 1599 | 533 – 888 | 1122 – 1411 | 256 – 533 |
| SBA ($m^2$/ha) | 7.00 – 65.56 | 19.52 – 21.56 | 10.03 – 14.46 | 25.17 – 27.30 |
| AGB.ha (Mg DM/ha) | 57.5 – 481.9 | 216.2 – 242.1 | 90.2 – 118.6 | 274.5 – 288.8 |
| Salinity (ppt) | 10 – 20 | 30 – 35 | 55 – 65 | 35 – 50 |

*Tree scale measurements*

The datasets include measurements of stem diameter (D), crown diameter (CD), height-to-crown-base (HCb) and total height (Ht) from 341 individual mangrove trees encountered in the studied plots, both in FG and Bracança. We selected only data of all living trees in the studied plots with stem diameter greater than 5 cm measured at breast height (1.3 m) in most cases, or 0.5 m above buttresses or stilt root formations where necessary. Complementing these data are 3D measurements of 51 selected trees in FG using the terrestrial laser scanning (TLS) and total-station laser tacheometer. The description of the TLS measurements and subsequent analysis was provided in details in Olagoke et al. (2016). In Bragança, we described simplified 3D structure of 26 individual trees described using a classic rangefinder (LaserACE 1000). Additionally, wood density measurements were obtained from representative trees and the mean values of all observations were estimated accordingly for each species encountered in all forest plots.

*Tree AGB estimations*

We applied the species-specific allometric models of Fromard et al. (1998) to estimate the AGB of trees in FG to the diameter limit of the models' calibration data. For *Avicennia* species larger than 42 cm diameter (the maximum diameter of Fromard et al. (1998)), we used the model of (Olagoke et al., 2016) that extended to large trees reaching 125 cm. For the trees in Bragança plots, we based our biomass estimates on the model type proposed by Ploton et al. (2016), which decomposes AGB measures into trunk mass and crown mass, using the 3D mangrove tree measurements and tree weight presented in the previous chapter. Specifically, this model optimized a diameter-biomass allometric model using crown dimensions as covariate explanatory variables. The model was selected on the rationale that crown measures provide good indicator of local morphological plasticity in tree allometry (Vovides et al 2014). Using mean wood density (ρ) of 730 kg/m$^3$, the parameterized biomass model is written as:

$$AGB = \exp(-1.767 + (0.305 \times \ln(\rho \times D^2 \times HCb)) + (0.015 \times (\ln(\rho \times D^2 \times CD)^2)),$$

$$R^2 = 0.98$$

### 3.2.3 *Data analyses and statistics*

*Tree allometric relationships*

We consider the use of allometric relationships to explore the variation of mangrove tree morphology across sites in FG and Brazil, using *A. germinans* as a case study. The analysis covered the allometries of tree height (Ht), height-to-crown-base (HCb), crown diameter (CD) with stem diameter (D) in logarithmic scale as explanatory variable. With each pair of variables, we first proceeded with sets of cross-regional (joint) models using aggregated data from all sites while ignoring the site-specific differences in tree morphology and the local variation in tree allometries. The general form of cross-regional models is written as:

$$Y_i \sim N\left(\beta_0 + \beta_1 \cdot \ln(X_i), \sigma^2\right),$$

with $Y_i$ as estimate of a response variable (Ht, HCb and CD) for tree i from the corresponding $X_i$ stem diameter, $\beta$ as model parameters with residuals normally distributed ($N$) against zero variance, $\sigma^2$.

In order to estimate and test whether the local morphological scaling could result in significant statistical differences in the allometric slope values among sites, we considered partitioning the datasets into regional categories through analyses of covariance (ANCOVA) in nested generalized linear model design:

$$Y_i \sim (ForestID \ / \ \ln(X_i) - 1),$$

with *Forest ID* as the categorical variable for regional partitioning. The standard analysis of variance with *F*-statistics of the resulting cross-regional model and corresponding ANCOVA model allowed us to infer on the significance of local variation in intercepts and slopes across the regional categories. In addition, we compared the estimates from the fitted cross-regional models and the site-specific counterpart to obtain the deviation terms in root mean square deviation (RMSD) as provided in 2.3.2 below.

*Effect of site-dependent morphology on AGB estimates*

We compared the diameter-biomass allometry and the estimate of the reparameterized Ploton et al (2015) model to isolate the effect of changing tree morphology on AGB estimates within the amazon-influenced mangrove forests. The inference was based on the coefficient of variation (CV) of the root mean square deviation (RMSD) of the two estimates. The RMSD was estimated as:

$$RMSD = \left( \frac{\sqrt{\sum_{i=1}^{N} (\hat{y}_i - y_i)^2}}{N} \right),$$

where $\hat{y}_i$ and $y_i$ are the respective allometric predicted and site-specific estimates. The corresponding CV computed as:

$$CV(\hat{y}_i - y_i) = \frac{RMSD}{\bar{y}} \times 100$$ , with $\bar{y}$ as the mean value from all $y_i$ .

*Morphological plasticity in stand AGB modelling*

As a preliminary analysis, we assessed the linkages of some collective indicators of local variation in tree morphology and forest structure to the aboveground biomass at the stand level (AGB.ha). The variables tested include quadratic mean stem diameter (Dq), median stem diameter (Dm), quadratic mean height (Hq), median height (Hm), maximum height (Hmax), maximum stem diameter (Dmax), number of individuals per hectare (N.ha), stand basal area (SBA). We selected variables with strong correlation to the AGB.ha to advance the parsimonious stand aboveground biomass models that could serve to explain the cross-regional divergence of aboveground biomass across the Amazon-influenced forests. The fitting of models of the models considered are expressed as:

$$AGB.ha_i \sim N\left(\exp\left(\beta_0 + \beta_1 \cdot \ln(X_{1i}) + \beta_2 \cdot \ln(X_{2i})\right), \sigma^2\right),$$

as in models tagged SM.1 and SM.2, and

$$AGB.ha_i \sim N\left(\exp\left(\beta_0 + \beta_1 \cdot \ln\left(X_{1i}\right) + \beta_2 \cdot \ln\left(X_{2i}\right) + \beta_3 \cdot \ln\left(X_{3i}\right)\right), \sigma^2\right),$$

in models with code SM.3 and SM.4. The $Xn_i$ corresponds to a specific explanatory variable for AGB.ha in forest stand i. In this case, we tested varying combination of selected indicators of site-specific variation in tree allometry including SBA, Dq, Dmax and Hmax as explanatory variables in four different models as presented in Table 3-3 below. The percentage variance explained by individual explanatory variable in each model was computed as:

$$\frac{SS_{Xn}}{SS_{Total}} \times 100,$$

where $SS_{Xn}$ corresponds to sum-of-squares for variable Xn, and the sum of all $SS_{Xn\ and}$ residual term yielded the $SS_{Total}$. The sum of variance (%) of all variables provided the total explained variance while the percentage value of sum of square error marked the total unexplained variance. All statistical analyses and modelling presented in this study were realized in R software 3.2.2 (R Core Team, 2015).

## 3.3 Results

### *3.3.1 Regional differences in tree morphological allometries*

The variations in the allometries of mangrove tree morphology across the investigated study locations in the Amazon-influenced mangrove regions are summarized in Figure 3-2. In the first step, the joint models (in reds) based on aggregated cross-regional datasets show significant relationships between 1) tree height (Ht) and stem diameter (D), 2) height-to-crown-base and stem diameter, and 3) crown diameter and stem diameter, with respective $R^2$ values of 0.77, 0.60 and 0.76 (Table 3-2). These joint models are characterized by slope of 12.11 (CI[2] [11.39, 12.83]) and intercept of -18.55 (CI [-20.69, -16.39]) for the Ht – D, slope of 4.91 (CI [4.45, 5.36]) and intercept of -7.03 (CI [-8.37, -5.70]) for the HCb – D, and slope of 4.07 (CI [3.79, 4.36]) and intercept of -5.59 (CI [-6.39, -4.79]) for the CD – D relationships, respectively.

By controlling for the local variation in morphological scaling across the investigated sites, the ANCOVA models indicated significantly divergent slopes and intercepts for all allometric relationships (Table 3-2). Trees in FG forests are significantly higher than trees of equivalent diameters in the tall mangrove forests in Bragança, which are equally substantially higher that the counterparts in the medium-height forests in Bragança. The differences in the site-specific ANCOVA models and the counterpart

[2] CI indicates lower and upper intervals at 95 percent confidence level

cross-regional joint models resulted in variable coefficient of variations (CV) for the estimates obtained from both models across the region. For the Ht – D relationships, the CV of the estimates ranged from ca. 16% in tall FG forests to ca. 84% in the medium height forests in Bragança. The CV of 18.30% and 19.72% of the HCb – D marked a comparable trunk ratio (height-crown-base) for trees in FG and Bragança tall forests, while nearly a six-fold deviation (111.91) in trunk ratio was recorded in the Bragança medium-height forests. For the crown allometry, the estimates from both the joint models and the site-specific models yield the CV of 20.82% in FG forests compare to 8.49% and 31.69% in Bragança tall and medium-height forests respectively.

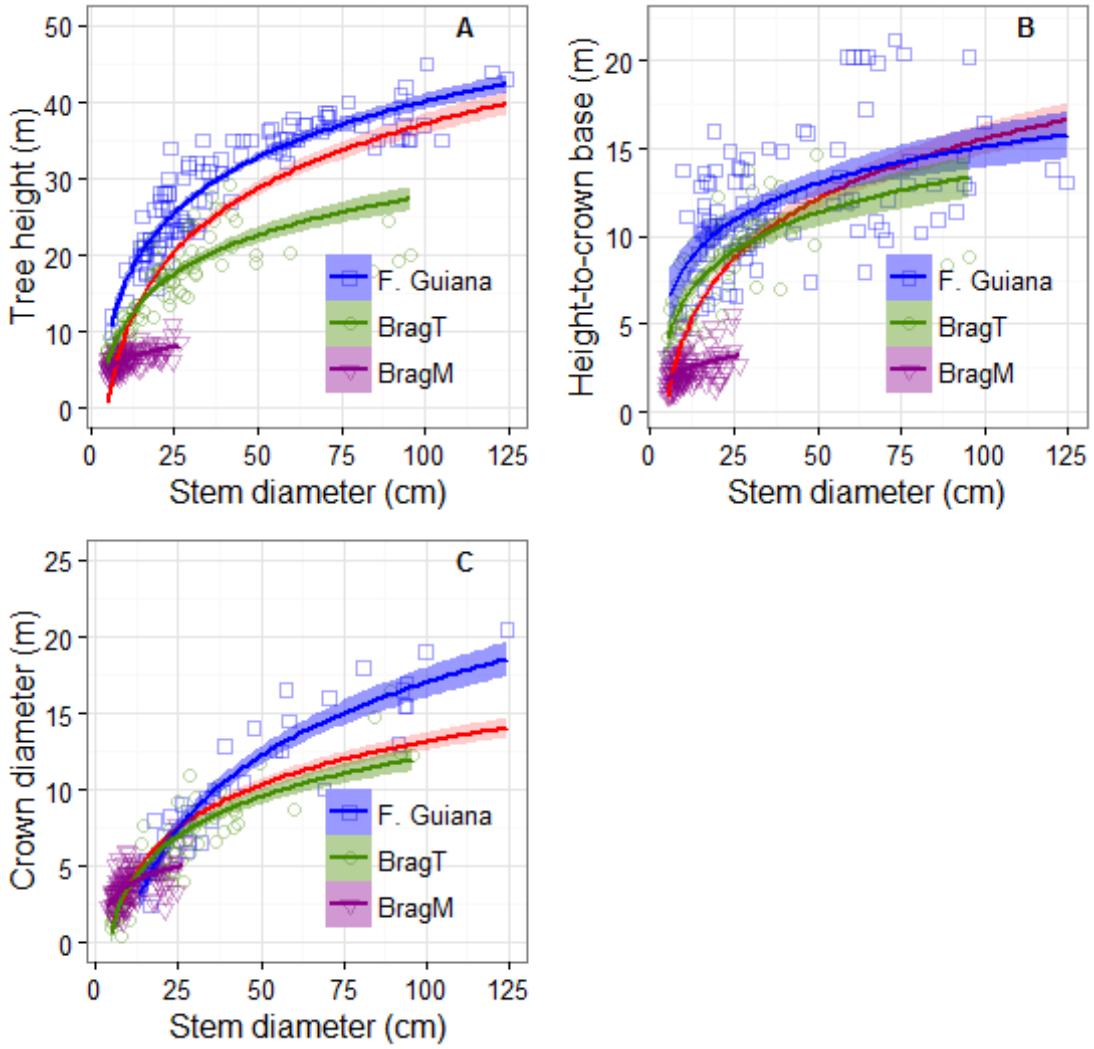


Figure 3-2: Comparison of tree allometric relationships in the French Guiana, Bragança tall (BragT) and medium-height (BragM) sites, all in the Amazon-influenced mangrove regions. The red curves indicate cross-regional (joint) models from the aggregated datasets.

Table 3-2: Comparison of site-based (Nested ANCOVA) and cross-regional (Joint) tree allometries in contrasting Amazon-influenced mangrove forests across French Guiana (FG) and Bragança. Specific allometric relationships tested include total height – stem diameter (Ht – D), height-to-crown base – stem diameter (HCb – D), and crown diameter – stem diameter (CD – D). Sites considered in Bragança were classified as tall (BragT) and medium-height (BragM) forest stands. The SE represents the standard error of the parameter estimates.

| Allometry | Model type | Forest ID | Intercept (SE) | Slope (SE) | Test | CV (%) of estimates |
|---|---|---|---|---|---|---|
| Ht – D | Nested ANCOVA | FG | -8.29 (1.26) | 10.52 (0.35) | Nested ($R^2$=0.98) vs Joint ($R^2$=0.77) | 16.32 |
| | | BragT | -5.80 (0.94) | 7.27 (0.33) | | 25.19 |
| | | BragM | 2.00 (1.24) | 1.86 (0.52) | | 84.32 |
| | Joint | All | -18.55 (1.10) | 12.11 (0.37) | $p< 2.2x10^{-16}$ | - |
| HCb – D | Nested ANCOVA | FG | 1.28 (1.08) | 3.00 (0.31) | Nested ($R^2$=0.94) vs Joint ($R^2$=0.60) | 18.30 |
| | | BragT | -0.82 (1.06) | 3.11 (0.36) | | 19.72 |
| | | BragM | 0.37 (1.03) | 0.86 (0.44) | | 111.91 |
| | Joint | All | -7.03 (0.68) | 4.91 (0.23) | $p< 2.2x10^{-16}$ | - |
| CD – D | Nested ANCOVA | FG | -14.70 (1.09) | 6.89 (0.30) | Nested ($R^2$=0.96) vs Joint($R^2$=0.76) | 20.82 |
| | | BragT | -4.89 (0.51) | 3.69 (0.17) | | 8.49 |
| | | BragM | 0.70 (0.61) | 1.32 (0.26) | | 31.69 |
| | Joint | All | -5.59 (0.40) | 4.07 (0.14) | $p< 2.2x10^{-16}$ | - |

### *3.3.2 Morphological plasticity and aboveground biomass allometry*

Common diameter – biomass allometric models in the study area (Fromard et al., 1998; Olagoke et al., 2016) resulted in similar estimates for all sites, indicating the lack of capability to isolate the effect of morphological plasticity at the local scale. Decomposing the tree structure into trunk and crown components provided indicators to account for local variations in tree aboveground biomass, using the model of Ploton et al. (2016) parameterized and validated for mangrove species (see Appendix). The results revealed substantially higher aboveground biomass for trees in French Guiana than trees of similar diameter in the counterpart tall forests in Bragança, which had trees with higher biomass than in Bragança medium height forests. For trees of equivalent stem diameters, the aboveground biomass estimates from this parameterized model yielded coefficient of variation of ca. 10% between tall forests in French Guiana and Bragança, and this increased to ca. 31% between French Guiana and Bragança medium-height forests. The deviations in tree aboveground biomass were detectable from trees with stem diameter greater than ca. 10 cm and 20 cm in the Bragança medium-height and tall forest stands respectively (Figure 3-3).

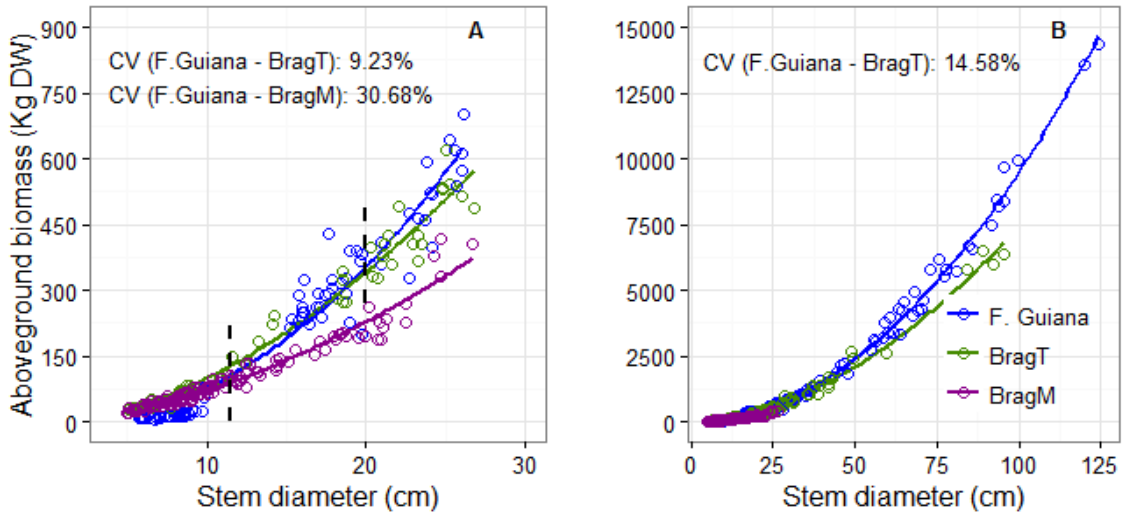


Figure 3-3: Differential diameter-biomass allometries as reflected by local differences in morphological (trunk and crown) scaling in the Amazon-influenced mangrove forests. 3-3A compared trees in Bragança medium-height stands (BragM) with equivalent diameter sizes in Bragança tall (BragT) and French Guiana forests, while 3-3B extends to the large trees in the tall forests. The *dashed lined* marked the point of deviation of tree biomass between sites.

### *3.3.3 Dynamics of stand aboveground biomass in divergent mangrove forests*

Based on datasets from French Guiana forests, we built a correlation network (as shown in Figure 3-4) that identifies the strength (measured by correlation coefficient, r) of the link of selected indicators of site-specific variation in tree morphology and stand structure to the characteristic stand aboveground biomass (AGB.ha). The results revealed that variables including stand basal area (SBA), quadratic mean stemdiameter (Dq), maximum stem diameter (Dmax), quadratic mean height (Hq) and maximum height (Hmax) show strong positive relationships with the AGB.ha, as the Pearson correlation coefficient (r) ranked well above 0.5. While number of trees per hectare (N.ha) had strong negative relationship with stand biomass, other variables including median stem diameter (Dm) and height (Hm) showed relatively weaker correlation ($r \leq 0.5$).

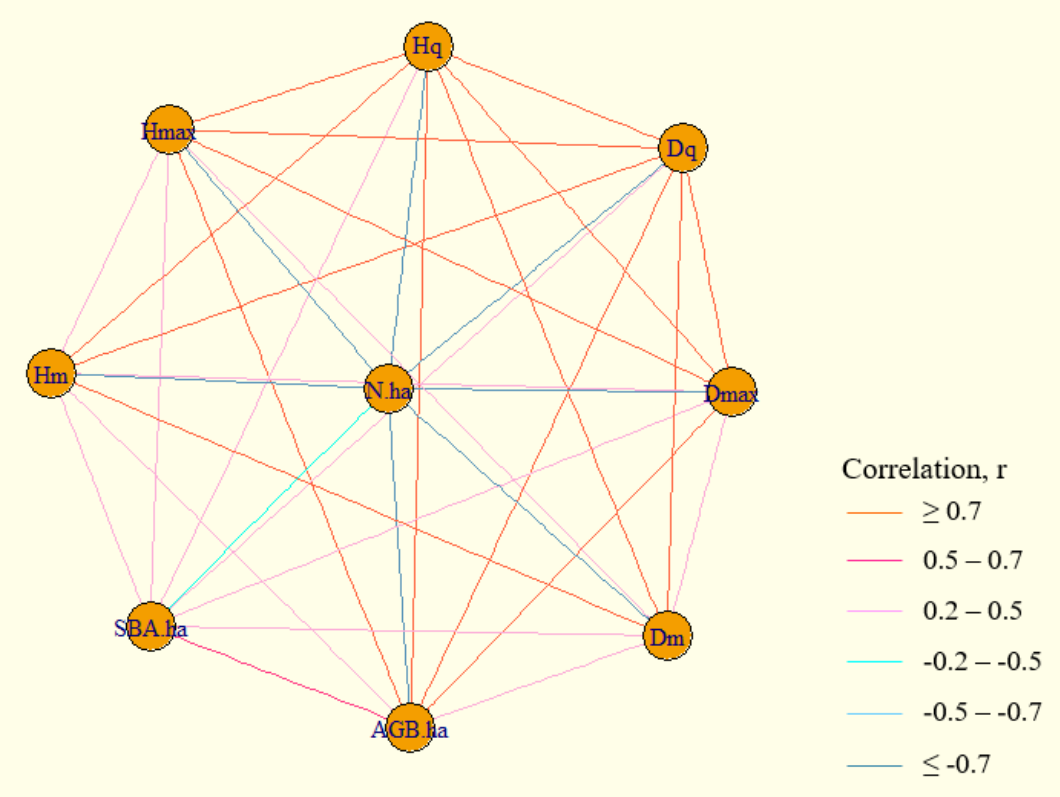


Figure 3-4: Relationships of collective plastic tree and stand attributes to stand aboveground biomass (AGB.ha), based on data from diverse French Guiana mangrove forests. *Variables tested include quadratic mean stem diameter (Dq), median stem diameter (Dm), quadratic mean height (Hq), median height (Hm), maximum height (Hmax), maximum stem diameter (Dmax), number of individuals per hectare (N.ha), stand basal area (noted as SBA.ha).*

In attempting to explain the dynamics of stand aboveground biomass in forests characterized by varying morphology and structural attributes, we explored the models presented in Table 3-3. While the model tagged SM.1 explained ca. 86% of the total variations observed in the stand biomass, the model SM.4 reached ca. 90% credible performance. According to the Akaike's information criterion (AIC), a model with the least AIC value provide the best fit. In this case, the performances of the fitted models are ranked in the decreasing order as:

SM.4 (AIC [-22.97]) > SM.2 (AIC [-21.08]) > SM.3 (AIC [-21.08]) > SM.1 (AIC [-12.72])

From the total variance explained by all models, we found that stand basal area (SBA) made a relative contribution of ca. 55% as shown in Figure 3-5. In model SM.1, SM.3 and SM.4, the quadratic mean stem diameter (Dq) contributed ca. 31% of the total variance. While dominant stem diameter (Dmax) explained ca. 34% of total variance in SM.2, the contribution was lowered to ca. 3% in SM.4 where the Dq was incorporated.

Table 3-3: Models linking the dynamics of stand aboveground biomass to parsimonious collective plastic tree and forest structural attributes. The alphabets a – d are the model parameters and the SE represents standard error of parameter estimates. Model selections are based performance inference measured by the $R^2$, residual standard error (RSE) and the Akaike's information criterion (AIC).

| | Explanatory variables | | | Model parameters | | | | Performance | | |
|---|---|---|---|---|---|---|---|---|---|---|
| Model | ln(X1) | ln(X2) | ln(X3) | a (SE) | b (SE) | c (SE) | d (SE) | $R^2$ | RSE | AIC |
| SM.1 | SBA | Dq | - | 1.57 (0.27) | 0.62 (0.09) | 0.56 (0.06) | - | 0.86 | 0.19 | -12.72 |
| SM.2 | SBA | Dmax | - | 1.51 (0.24) | 0.54 (0.08) | 0.53 (0.05) | - | 0.89 | 0.17 | -21.08 |
| SM.3 | SBA | Dq | Hmax | 0.12 (0.66) | 0.53 (0.09) | 0.32 (0.12) | 0.72 (0.30) | 0.88 | 0.18 | -16.55 |
| SM.4 | SBA | Dq | Dmax | 1.49 (0.24) | 0.54 (0.08) | 0.36 (0.10) | 0.21 (0.11) | 0.90 | 0.17 | -22.97 |

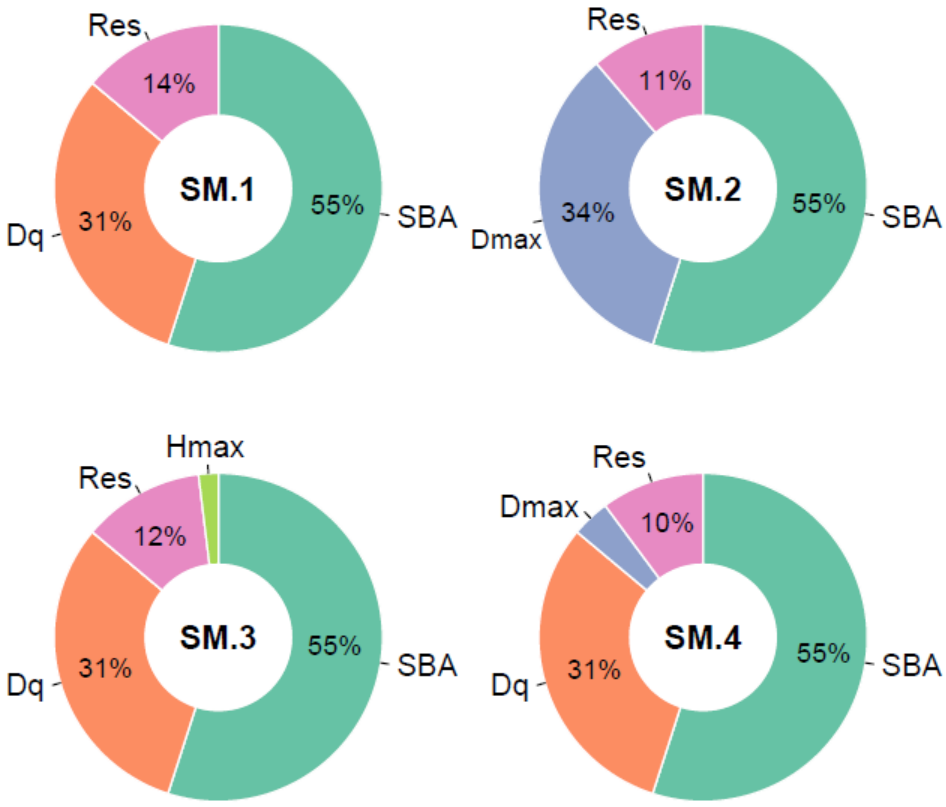


Figure 3-5: Relative contribution of tree attributes as explanatory variables for dynamics of aboveground biomass per hectare in contrasting mangrove forests. *SM.1 – SM.4 are models based on different combinations of stand basal area (SBA), quadratic mean stem diameter (Dq), median stem diameter (Dm), maximum height (Hmax), maximum stem diameter (Dmax).*

Both as a measure of evaluation and application, the models were tested against independent datasets from forests of contrasting tree morphology and structural attributes in Bragança. The results showed that SM.2 and SM.4 explained nearly 90%

variation of aboveground biomass in forests of diverse tree and stand structure (Figure 3-6), with coefficient of variation (CV) standing at 14.57% and 13.90% respectively.

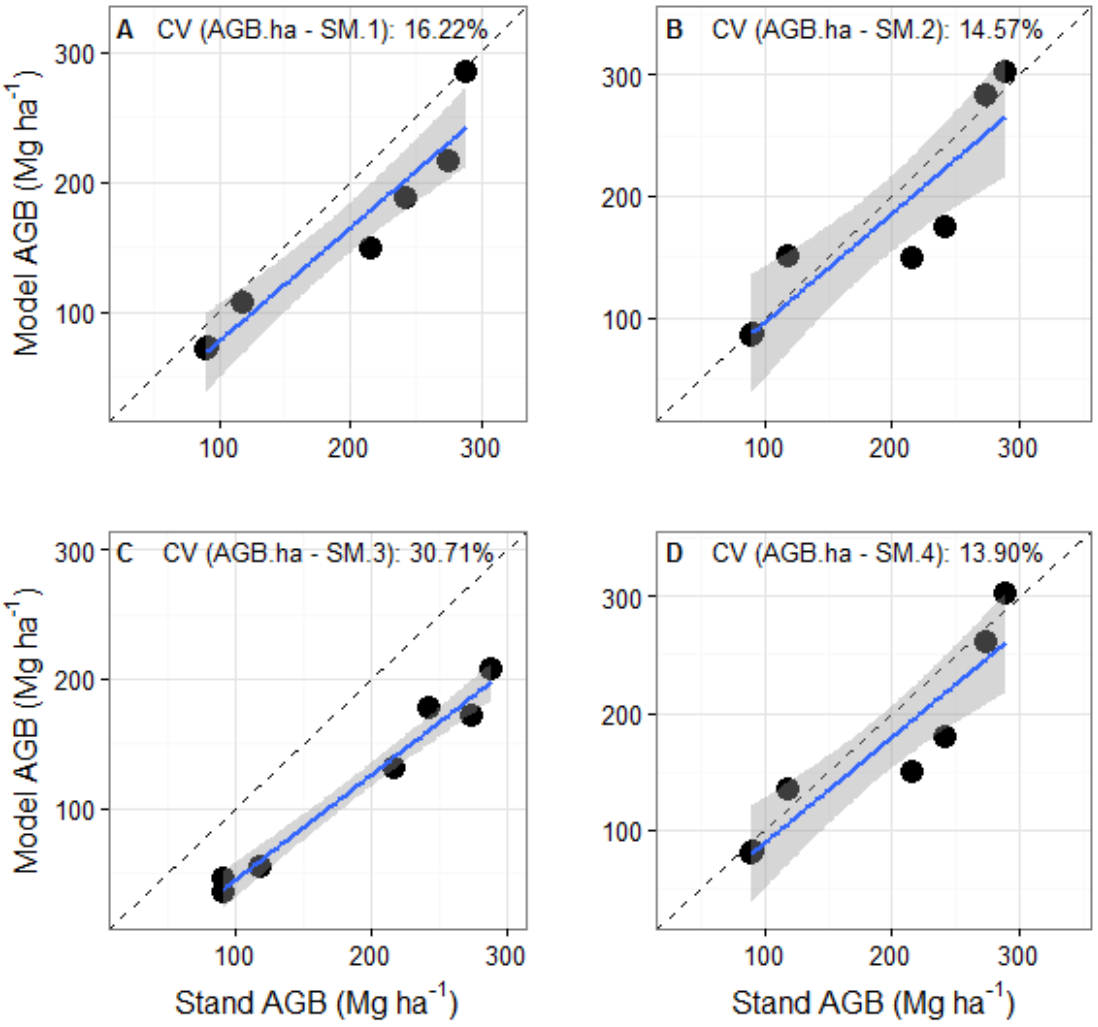


Figure 3-6: Comparison of stand aboveground estimates in Bragança forests to the corresponding predicted values using models (SM.1 – SM.4) fitted on FG data. *Common to all models is the stand basal area (SBA), while other explanatory variables include quadratic mean diameter (Dq) in SM.1, SM.3 and SM.4; Hmax in SM.3; and Dmax in SM.2 and SM.4.*

## 3.4 Discussion

Our first intention in this study aimed at investigating whether local variations in tree morphology between mangrove forests in French Guiana and Bragança converge in cross-regional allometries, with no significant impacts on the estimates of tree aboveground biomass. Our findings demonstrate that trees display markedly distinct allometries between forests stands in French Guiana and Bragança, reflecting a substantial measure of allometric plasticity (Vovides et al., 2014). Interestingly, the significant differences recorded in tree allometries seemed preserved in the crown – stem diameter relations across the investigated sites. We demonstrate how the

divergence in tree allometries could restrain the application of diameter-biomass allometric models calibrated for French Guiana (Fromard et al., 1998; Olagoke et al., 2016) to other mangrove forests in the Amazon-influenced coasts, but a biomass model incorporating crown metrics as a measure of local plasticity has a greater prospect for cross-regional application. For the second objective, we explored to what extent some collective indicators of tree plasticity and local variations in forest structure can explain the cross-regional dynamics of aboveground biomass in the contrasting Amazon-influenced mangrove forests. Our results showed that a model (SM.4) based on stand basal area (noted as SBA.ha), quadratic mean diameter (Dq) and dominant tree diameter (Dmax) in French Guiana accounted for ca. 90 % of variation in the stand aboveground biomass (noted as AGB.ha). This model reached a coefficient of variations of only 13.9% on application to sites of distinct tree morphology and forest structure in Bragança. We expatiate on these findings in the following discussion.

Of the two models (power function and logarithmic model) tested for the investigated tree allometries, we selected the model based on the logarithmic transformation of stem diameter. The reasons being that: 1) while power function resulted in over prediction of large tree height and crown diameter, the logarithmic model displayed a good fit for the asymptotic nature of tree growth (Feldpausch et al., 2011; Olagoke et al., 2016); 2) the logarithmic model returned much lower error estimates for trees in the lower and larger diameter size classes than the power model. Apparently, our nested ANCOVA (site-dependent) models of allometric relations differed significantly from the joint models obtained through data aggregated from across the study sites. This reestablishes that cross-regional models stand the chance to propagate significant error margin if the local site conditions are not properly accounted for.

From the analyses of height – diameter allometric relations, tall trees in Bragança were nearly 30% shorter that the equivalent diameter sized trees in the French Guiana. Of the likely hypotheses for tree height growth in mangrove forests (Alongi, 2009; Clough et al., 1997; Twilley and Rivera-Monroy, 2005), one clear explanation for allometric differences in the case of our study sites is the markedly different pore water salinity. As Reef and Lovelock (2015) acknowledged, increasing soil salinity limits the availability of utilizable belowground water resource for plant growth. More so, the high salinity conditions come with high cost of water transport (hydraulic conductivity) (Koch et al., 2004; Lovelock et al., 2006), possibly leading to restricted height growth or crown recession as we noted in some mangrove trees in Braganca. Another important explanation relates to the plastic and preferential allocation of biomass/ carbon to organ(s) responsible for acquisition of limiting resources (Ball and Passioura, 1995; Peters et al., 2014). By implications, trees

growing in hypersaline conditions allocate more biomass to root region, and consequently display shorter stem than individuals growing under intense-moderate competition for light. These explanations however may not undermine the fact that forest history, local coastal processes (Fromard et al., 2004; Proisy et al., 2016a) and sediment biogeochemistry (Clough, 1992; Twilley and Rivera-Monroy, 2005) might have contributed to the allometric variations observed among the study sites. Specifically, Twilley and Rivera-Monroy (2005) pointed that sediment biogeochemistry and associated processes can equally relate to the regional divergence in the tree structure, and resulting allometries. Since the current study is lacking in data on sediment quality, and the relative contribution of such factors to the regional differences in tree allometries in the Amazon-influenced coasts contexts could not ascertained.

The crown – stem diameter allometry was largely congruent to the tree height – diameter allometric relations in terms of variations, from French Guiana to the two forest classifications in Bragança. Our results revealed that the trees in French Guiana yielded higher crown scaling ratio than trees from both the tall and medium-height forests in Bragança, with the least value in the latter. These results largely agree with previous findings suggesting variant crown – stem diameter allometric scaling in mangrove trees (e.g. Vovides et al. (2014)), though in a clear contradiction to predicted convergent scaling of the metabolic theory of ecology (Brown et al., 2004; West et al., 1997) as largely demonstrated in studies with focus on terra-firme forests (Blanchard et al., 2016; Clark et al., 2015; Poorter et al., 2006). Similar to tree height allometry, both the available empirical and theoretical studies (e.g. Vovides et al. (2014); Peters et al. (2014); Grueters et al. (2014)) supported the hypothesis that mangrove trees prioritize dimensional growth such that the allometry of crown proportion in relation to stem diameter reduces with increasing water and nutrient limitations, where the need for increasing root extension to allow for extended resource foraging prevails over crown development. By implication of these results, it may suffice to point that remote sensing techniques linking crown – diameter allometry or other tree allometric relations in the measurements of forest biomass and other forest parameters (e.g. ; Proisy et al. (2007); Fatoyinbo and Simard (2013)) in mangrove ecosystems stand could gain improved accuracy with fine-scale morphological variations adequately accounted for.

As expected, we found that local variations in tree morphology significantly impact on aboveground biomass estimates when we considered diameter – biomass allometric models calibrated for French Guiana mangroves for sites of contrasting tree structure in Bragança, even when sites are located in the same geographical region. Applying the model of Ploton et al. (2016) – parameterized for mangrove tree species – that reflected a measure of morphological variations through the

incorporation of crown metrics, our results revealed that both Fromard et al. (1998) and Olagoke et al. (2016) diameter – biomass allometric models from the French Guiana yielded coefficient of variation of ca. 15 % and ca. 31 % for trees in the tall and medium-height mangrove forests in Bragança respectively. Further than the explanation rooted on latitudinal variation in tree biomass (Twilley et al., 1992), morphological plasticity here appears an important factor in the diameter – biomass relationship. Where no site-specific diameter – biomass allometric models are available, it may be worthwhile to consider using crown metrics in the biomass allometric model to account for local morphological variations, which would certainly reduce error propagation. The values presented here, however, may need to be treated with cautions as they are yet to be validated with direct biomass measurements in Bragança sites, but rather show estimates via the method of Ploton et al. (2016) that was validated using data of tree weight and terrestrial laser measurements from French Guiana.

At the forest stand scale, we investigated the relative contribution of various collective indicators of morphological plasticity (*Sensu* Vovides et al. (2014)) in explaining the dynamics of aboveground biomass across the Amazon-influenced mangrove forests. We found that the stand aboveground biomass considerably correlated with stand basal area, mean quadratic diameter, diameter and height of the dominant trees, but more weakly linked to the median stem diameter and height, and number of trees within the stand (stand density). The negative correlation of stand density with the aboveground biomass is rather not unfounded, given their generally known relationships in the context of self-thinning processes (West et al., 2009; Yoda et al., 1963). Of all the selected variables, we identified stand basal area as the most important explanatory variable for the stand aboveground biomass, being that it contributed ca. 55% of the total variance in all tested models. This perhaps directly relate to the point highlighted by Feldpausch et al. (2011) that stand basal area could be indicative of local height – stem diameter allometry. The results equally align with the findings of Vovides et al. (2014), where the authors suggested an analogous trend for both stand basal area and height – stem diameter allometry from forests of contrasting site conditions. Other than the stand basal area, both the quadratic mean stem diameter (Dq) and dominant tree diameter (Dmax) accounted for 31% and 34% of the total variance in models where they are separately considered. Meanwhile the contribution of Dmax was reduced to ca. 4% in the model where Dq was jointly included (SM.4). Even when this model behavior is partly explained by the strong correlation between Dmax and Dq in the French Guiana region, our motivation to retain them in a single model is predicated on the fact that forests with the same Dq could differ in their Dmax and vice versa in forests of contrasting environmental cues, and/or local history.

The validation and application of the models presented in this work is still of limited scope given the paucity of primary data on tree attributes and biomass required. Nonetheless, the performance of the model integrating SBA and Dq (SM.2), and the other adding Dmax to these two variables (SM.4) yielded satisfactory results on application to independent and contrasting sites in Bragança. A comparison of our biomass estimates and model predictions to the values presented in Hutchinson et al. 2013, the stand aboveground biomass estimates from our models were ca. 1.5 - 2 fold higher than predicted by the model of Hutchison et al. (2014), which used only precipitation and temperature as explanatory variables. It is most likely that our current approach, which is based on collective indicators of local morphological plasticity, lead the path accurate biomass mapping over large scale, from regional to global level (Fatoyinbo and Simard, 2013; Hutchison et al., 2014; Proisy et al., 2012; Saenger and Snedaker, 1993), especially when biophysical parameters as applied in Hutchison et al. (2014) are considered in the modelling framework. The main challenge to this task thus remains the remote retrieval of the plastic tree attributes across diverse mangrove environments.

## 3.5 Conclusion

In general, this study has provided a 'snapshot' demonstration that a significant variation in the tree allometries of mangrove species can be recorded from local to regional levels, and cross-regional biomass model can result in substantial error margin when no consideration is made for local variations. Interestingly, we noted that crown allometry preserve local variation and a model incorporating captured local variations way above the diameter-biomass allometry. Scaling to the stand level, models based on collective indicators of local morphological plasticity provided viable explanatory variables capable of explaining the dynamics of aboveground biomass in contrasting mangrove forests. Although the validation of the models presented here over more extensive ground-truth data from diverse site conditions are still underway, we are optimistic that the current approach may be informative towards achieving accurate mapping landscape patterns in aboveground biomass of mangrove forests, from regional to global scale.

## 3.6 References

Allison, M. A., and Lee, M. T. (2004). Sediment exchange between Amazon mudbanks and shore-fringing mangroves in French Guiana. *Marine Geology* **208**, 169-190.

Alongi, D. M. (2009). Paradigm shifts in mangrove biology. *In* "Coastal Wetlands: An Integrated Ecosystem Approach" (Perillo G.M.E., E. Wolanski, D. R. Cahoon and M. M. Brinson, eds.), Vol. Chapter 22, pp. 615-640. Elsevier Press, The Netherlands.

Ball, M. (1988). Salinity Tolerance in the Mangroves *Aegiceras corniculatum* and *Avicennia marina*. I. Water Use in Relation to Growth, Carbon Partitioning, and Salt Balance. *Functional Plant Biology* **15**, 447-464.

Ball, M. C., and Passioura, J. B. (1995). Carbon Gain in Relation to Water Use: Photosynthesis in Mangroves. *In* "Ecophysiology of Photosynthesis" (E.-D. Schulze and M. M. Caldwell, eds.), pp. 247-259. Springer Berlin Heidelberg, Berlin, Heidelberg.

Baltzer, F., Allison, M., and Fromard, F. (2004). Material exchange between the continental shelf and mangrove-fringed coasts with special reference to the Amazon–Guianas coast. *Marine Geology* **208**, 115-126.

Blanchard, E., Birnbaum, P., Ibanez, T., Boutreux, T., Antin, C., Ploton, P., Vincent, G., Pouteau, R., Vandrot, H., Hequet, V., Barbier, N., Droissart, V., Sonké, B., Texier, N., Kamdem, N. G., Zebaze, D., Libalah, M., and Couteron, P. (2016). Contrasted allometries between stem diameter, crown area, and tree height in five tropical biogeographic areas. *Trees*, 1-16.

Bohlman, S., and Pacala, S. (2012). A forest structure model that determines crown layers and partitions growth and mortality rates for landscape-scale applications of tropical forests. *Journal of Ecology* **100**, 508-518.

Brown, J. H., Gillooly, J. F., Allen, A. P., Savage, V. M., and West, G. B. (2004). Toward a metabolic theory of ecology. *Ecology* **85**, 1771-1789.

Callaway, R. M., Pennings, S. C., and Richards, C. L. (2003). Phenotypic plasticity and interactions among plants. *Ecology* **84**, 1115-1128.

Castañeda-Moya, E., Twilley, R. R., Rivera-Monroy, V. H., Marx, B. D., Coronado-Molina, C., and Ewe, S. M. L. (2011). Patterns of Root Dynamics in Mangrove Forests Along Environmental Gradients in the Florida Coastal Everglades, USA. *Ecosystems* **14**, 1178-1195.

Chapin, F. S., Bloom, A. J., Field, C. B., and Waring, R. H. (1987). Plant Responses to Multiple Environmental Factors. *BioScience* **37**, 49-57.

Chave, J., Andalo, C., Brown, S., Cairns, M. A., Chambers, J. Q., Eamus, D., Folster, H., Fromard, F., Higuchi, N., Kira, T., Lescure, J.-P., Nelson, B. W., Ogawa, H., Puig, H., Riéra, B., and Yamakura, T. (2005). Tree allometry and improved estimation of carbon stocks and balance in tropical forests. *Oecologia* **145**, 87-99.

Chave, J., Condit, R., Aguilar, S., Hernandez, A., Lao, S., and Perez, R. (2004). Error propagation and scaling for tropical forest biomass estimates. *Philosophical Transactions of the Royal Society of London, Series B* **359**, 409-420.

Cintron, G., and Schaeffer-Novelli, Y. (1984). Methods for studying mangrove structure. *In* "The mangrove ecosystem: research methods" (S. C. Snedaker and J. G. Snedaker, eds.), pp. 91-113. United Nations Educational, Scientific and Cultural Organization (UNESCO), Paris.

Clark, D. B., Hurtado, J., and Saatchi, S. S. (2015). Tropical Rain Forest Structure, Tree Growth and Dynamics along a 2700-m Elevational Transect in Costa Rica. *PLoS ONE* **10**, e0122905.

Clough, B. F. (1992). Primary Productivity and Growth of Mangrove Forests. *In* "Tropical Mangrove Ecosystems", pp. 225-249. American Geophysical Union.

Clough, B. F., Dixon, P., and Dalhaus, O. (1997). Allometric relationships for estimating biomass in multi-stemmed mangrove trees. *Australian Journal of Botany* **45,** 1023-1031.

Cohen, M. C. L., and Lara, R. J. (2003). Temporal changes of mangrove vegetation boundaries in Amazônia: Application of GIS and remote sensing techniques. *Wetlands Ecology and Management* **11,** 223-231.

Cohen, M. C. L., R.J. Lara, R. J., Szlafsztein, C., and Dittmar, T. (2004). Mangrove inundation and nutrient dynamics from a GIS perspective. *Wetlands Ecology and Management* **12,** 81-86.

Enquist, B. J., and Niklas, K. J. (2001). Invariant scaling relations across tree-dominated communities. *Nature* **410**, 655-660.

Fatoyinbo, T. E., and Simard, M. (2013). Height and biomass of mangroves in Africa from ICESat/GLAS and SRTM. *International Journal of Remote Sensing* **34**, 668-681.

Feldpausch, T. R., Banin, L., Phillips, O. L., Baker, T. R., Lewis, S. L., Quesada, C. A., Affum-Baffoe, K., Arets, E. J. M. M., Berry, N. J., Bird, M., Brondizio, E. S., de Camargo, P., Chave, J., Djagbletey, G., Domingues, T. F., Drescher, M., Fearnside, P. M., França, M. B., Fyllas, N. M., Lopez-Gonzalez, G., Hladik, A., Higuchi, N., Hunter, M. O., Iida, Y., Salim, K. A., Kassim, A. R., Keller, M., Kemp, J., King, D. A., Lovett, J. C., Marimon, B. S., Marimon-Junior, B. H., Lenza, E., Marshall, A. R., Metcalfe, D. J., Mitchard, E. T. A., Moran, E. F., Nelson, B. W., Nilus, R., Nogueira, E. M., Palace, M., Patiño, S., Peh, K. S. H., Raventos, M. T., Reitsma, J. M., Saiz, G., Schrodt, F., Sonké, B., Taedoumg, H. E., Tan, S., White, L., Wöll, H., and Lloyd, J. (2011). Height-diameter allometry of tropical forest trees. *Biogeosciences* **8**, 1081-1106.

Feller, I., Whigham, D., McKee, K., and Lovelock, C. (2003). Nitrogen limitation of growth and nutrient dynamics in a disturbed mangrove forest, Indian River Lagoon, Florida. *Oecologia* **134**, 405-414.

Feller, I. C., Lovelock, C. E., Berger, U., McKee, K. L., Joye, S. B., and Ball, M. C. (2010). Biocomplexity in Mangrove Ecosystems. *Annual Review of Marine Science* **2**, 395-417.

Fourqurean, J., Johnson, B., Kauffman, J. B., Kennedy, H., Lovelock, C., Saintilan, N., Alongi, D. M., Cifuentes, M., Copertino, M., Crooks, S., Duarte, C., Fortes, M., Howard, J., Hutahaean, A., Kairo, J., Marbà, N., Daniel Murdiyarso, Pidgeon, E., Ralph, P., and Serrano, O. (2014). Field Sampling of Vegetative Carbon Pools in Coastal Ecosystems. *In* "Coastal Blue Carbon: Methods for assessing carbon stocks and emissions factors in mangroves. tidal marshes. and seagrass meadows" (J. Howard, S. Hoyt, K. Isesnsee, M. Telszewski and E. Pidgeon, eds.), pp. 67-108. Conservation International, Intergovernmental Oceanographic Commission of UNESCO, International Union for Conservation of Nature.

Franklin, O., Johansson, J., Dewar, R. C., Dieckmann, U., McMurtrie, R. E., Brännström, Å., and Dybzinski, R. (2012). Modeling carbon allocation in trees: a search for principles. *Tree Physiology* **32**, 648-666.

Fromard, F., Puig, H., Mougin, E., Marty, G., Betoulle, J. L., and Cadamuro, L. (1998). Structure, above-ground biomass and dynamics of mangrove ecosystems: new data from French Guiana. *Oecologia* **115**, 39-53.

Fromard, F., Vega, C., and Proisy, C. (2004). Half a century of dynamic coastal change affecting mangrove shorelines of French Guiana. A case study based on remote sensing data analyses and field surveys. *Marine Geology* **208**, 265-280.

Gardel, A., and Gratiot, N. (2004). Monitoring of coastal dynamics in French Guiana from 16 years of SPOT satellite images. *Journal of Coastal Research* **SI 39**.

Grubb, P. J. (1977). Control of Forest Growth and Distribution on Wet Tropical Mountains: with Special Reference to Mineral Nutrition. *Annual Review of Ecology and Systematics* **8**, 83-107.

Grueters, U., Seltmann, T., Schmidt, H., Horn, H., Pranchai, A., Vovides, A. G., Peters, R., Vogt, J., Dahdouh-Guebas, F., and Berger, U. (2014). The mangrove forest dynamics model mesoFON. *Ecological Modelling* **291**, 28-41.

Hutchison, J., Manica, A., Swetnam, R., Balmford, A., and Spalding, M. (2014). Predicting Global Patterns in Mangrove Forest Biomass. *Conservation Letters* **7**, 233-240.

Huxley, J. S., and Teissier, G. (1936). Terminology of Relative Growth. *Nature* **137**, 780-781.

Koch, G. W., Sillett, S. C., Jennings, G. M., and Davis, S. D. (2004). The limits to tree height. *Nature* **428**, 851-854.

Komiyama, A., Jintana, V., Sangtiean, T., and Kato, S. (2002). A common allometric equation for predicting stem weight of mangroves growing in secondary forests. *Ecological Research* **17**, 415-418.

Komiyama, A., Ong, J. E., and Poungparn, S. (2008). Allometry, biomass, and productivity of mangrove forests: A review. *Aquatic Botany* **89**, 128-137.

Komiyama, A., Poungparn, S., and Kato, S. (2005). Common allometric equations for estimating the tree weight of mangroves. *Journal of Tropical Ecology* **21**, 471-477.

Lara, R., and Cohen, M. (2006). Sediment porewater salinity, inundation frequency and mangrove vegetation height in Bragança, North Brazil: an ecohydrology-based empirical model. *Wetlands Ecology and Management* **14**, 349-358.

Lara, R. J. (2003). Amazonian mangroves – A multidisciplinary case study in Pará State, North Brazil: Introduction. *Wetlands Ecology and Management* **11**, 217-221.

Lira-Medeiros, C. F., Parisod, C., Fernandes, R. A., Mata, C. S., Cardoso, M. A., and Ferreira, P. C. G. (2010). Epigenetic Variation in Mangrove Plants Occurring in Contrasting Natural Environment. *PLoS ONE* **5**, e10326.

Lovelock, C. E., Ball, M. C., Feller, I. C., Engelbrecht, B. M. J., and Ling Ewe, M. (2006). Variation in hydraulic conductivity of mangroves: influence of species, salinity, and nitrogen and phosphorus availability. *Physiologia Plantarum* **127**, 457-464.

Lugo, A. E. (1997). Old-growth mangrove forests in the United States. *Conservation Biology* **11**, 11-20.

Méndez-Alonzo, R., López-Portillo, J., and Rivera-Monroy, V. H. (2008). Latitudinal Variation in Leaf and Tree Traits of the Mangrove Avicennia germinans (Avicenniaceae) in the Central Region of the Gulf of Mexico. *Biotropica* **40**, 449-456.

Muller-Landau, H. C., Condit, R. S., Chave, J., Thomas, S. C., Bohlman, S. A., Bunyavejchewin, S., Davies, S., Foster, R., Gunatilleke, S., Gunatilleke, N., Harms, K. E., Hart, T., Hubbell, S. P., Itoh, A., Kassim, A. R., LaFrankie, J. V., Lee, H. S., Losos, E., Makana, J.-R., Ohkubo, T., Sukumar, R., Sun, I. F., Nur Supardi, M. N., Tan, S., Thompson, J., Valencia, R., Muñoz, G. V., Wills, C., Yamakura, T., Chuyong, G., Dattaraja, H. S., Esufali, S., Hall, P., Hernandez, C., Kenfack, D., Kiratiprayoon, S., Suresh, H. S., Thomas, D., Vallejo, M. I., and Ashton, P. (2006). Testing metabolic ecology theory for allometric scaling of tree size, growth and mortality in tropical forests. *Ecology letters* **9**, 575-588.

O'Brien, S. T., Hubbell, S. P., Spiro, P., Condit, R., and Foster, R. B. (1995). Diameter, Height, Crown, and Age Relationship in Eight Neotropical Tree Species. *Ecology* **76**, 1926-1939.

Olagoke, A., Proisy, C., Féret, J.-B., Blanchard, E., Fromard, F., Mehlig, U., de Menezes, M. M., dos Santos, V. F., and Berger, U. (2016). Extended biomass allometric equations for large mangrove trees from terrestrial LiDAR data. *Trees* **30**, 935-947.

Ong, J. E., Gong, W. K., and Wong, C. H. (2004). Allometry and partitioning of the mangrove, Rhizophora apiculata. *Forest Ecology and Management* **188**, 395-408.

Peters, R., Vovides, A. G., Luna, S., Grüters, U., and Berger, U. (2014). Changes in allometric relations of mangrove trees due to resource availability – A new mechanistic modelling approach. *Ecological Modelling* **283**, 53-61.

Ploton, P., Barbier, N., Takoudjou Momo, S., Réjou-Méchain, M., Boyemba Bosela, F., Chuyong, G., Dauby, G., Droissart, V., Fayolle, A., Goodman, R. C., Henry, M., Kamdem, N. G., Mukirania, J. K., Kenfack, D., Libalah, M., Ngomanda, A., Rossi, V., Sonké, B., Texier, N., Thomas, D., Zebaze, D., Couteron, P., Berger, U., and Pélissier, R. (2016). Closing a gap in tropical forest biomass estimation: taking crown mass variation into account in pantropical allometries. *Biogeosciences* **13**, 1571-1585.

Poorter, H., Niklas, K. J., Reich, P. B., Oleksyn, J., Poot, P., and Mommer, L. (2012). Biomass allocation to leaves, stems and roots: meta-analyses of interspecific variation and environmental control. *New Phytologist* **193**, 30-50.

Poorter, L., Bongers, L., and Bongers, F. (2006). Architecture of 54 moist-forest tree species: Traits, trade-offs, and functional groups. *Ecology* **87**, 1289-1301.

Pretzsch, H. (2009). "Forest Dynamics, Growth and Yield: From Measurement to Model," Springer-Verlag Berlin Heidelberg.

Pretzsch, H., Biber, P., Schütze, G., Uhl, E., and Rötzer, T. (2014). Forest stand growth dynamics in Central Europe have accelerated since 1870. *Nat Commun* **5**.

Proisy, C., Barbier, N., Guéroult, M., Pélissier, R., Gastellu-Etchegorry, J.-P., Grau, E., and Couteron, P. (2012). Biomass prediction in tropical forests: the canopy grain approach. *In* "Remote Sensing of Biomass: Principles and Applications / Book 1" (T. E. Fatoyinbo, ed.). INTECH publisher.

Proisy, C., Couteron, P., and Fromard, F. (2007). Predicting and mapping mangrove biomass from canopy grain analysis using Fourier-based textural ordination of IKONOS images. *Remote Sensing of Environment* **109**, 379-392.

Proisy, C., Degenne, P., Anthony, E., Berger, U., Blanchard, E., Fromard, F., Gardel, A., Olagoke, A., Santos, V. F., Walcker, R., and Lo Seen, D. (2016a). A multiscale simulation approach for linking mangrove dynamics to coastal proceesses using remote sensing observations. *Journal of Coastal Research*, 810-814.

Proisy, C., Féret, J.-B., Lauret, N., and Gastellu-Etchegorry, J.-P. (2016b). Mangrove forest dynamics using very high spatial resolution optical remote sensing. *In* "Remote sensing of Land Surfaces: Urban and coastal area" (N. Baghdadi and M. Zribi, eds.), Vol. 5, Chapter 7. ELSEVIER, London. In press.

Reef, R., and Lovelock, C. E. (2015). Regulation of water balance in mangroves. *Annals of Botany* **115**, 385-395.

Réjou-Méchain, M., Muller-Landau, H. C., Detto, M., Thomas, S. C., Le Toan, T., Saatchi, S. S., Barreto-Silva, J. S., Bourg, N. A., Bunyavejchewin, S., Butt, N., Brockelman, W. Y., Cao, M., Cárdenas, D., Chiang, J. M., Chuyong, G. B., Clay, K., Condit, R., Dattaraja, H. S., Davies, S. J., Duque, A., Esufali, S., Ewango, C., Fernando, R. H. S., Fletcher, C. D., Gunatilleke, I. A. U. N., Hao, Z., Harms, K. E., Hart, T. B., Hérault, B., Howe, R. W., Hubbell, S. P., Johnson, D. J., Kenfack, D., Larson, A. J., Lin, L., Lin, Y., Lutz, J. A., Makana, J. R., Malhi, Y., Marthews, T. R., McEwan, R. W., McMahon, S. M., McShea, W. J., Muscarella, R., Nathalang, A., Noor, N. S. M., Nytch, C. J., Oliveira, A. A., Phillips, R. P., Pongpattananurak, N., Punchi-Manage, R., Salim, R., Schurman, J., Sukumar, R., Suresh, H. S., Suwanvecho, U., Thomas, D. W., Thompson, J., Uríarte, M., Valencia, R., Vicentini, A., Wolf, A. T., Yap, S., Yuan, Z., Zartman, C. E., Zimmerman, J. K., and Chave, J. (2014). Local spatial structure of forest biomass and its consequences for remote sensing of carbon stocks. *Biogeosciences* **11**, 6827-6840.

Ryan, M. G., and Yoder, B. J. (1997). Hydraulic Limits to Tree Height and Tree Growth. *BioScience* **47**, 235-242.

Saenger, P., and Snedaker, S. C. (1993). Pantropical trends in mangrove above-ground biomass and annual litter fall. *Oecologia* **96**, 293 - 299.

Soares, M. L. G., and Schaeffer-Novelli, Y. (2005). Above-ground biomass of mangrove species. I. Analysis of models. *Estuarine, Coastal and Shelf Science* **65**, 1-18.

Twilley, R. R., Chen, R. H., and Hargis, T. (1992). Carbon sinks in mangroves and their implications to carbon budget of tropical coastal ecosystems. *Water, Air, and Soil Pollution* **64**, 265-288.

Twilley, R. R., and Rivera-Monroy, V. H. (2005). Developing performance measures of mangrove wetlands using simulation models of hydrology, nutrient biogeochemistry, and community dynamics. *Journal of Coastal Research*, 79-93.

Vogt, J., Lin, Y., Pranchai, A., Frohberg, P., Mehlig, U., and Berger, U. (2014). The importance of conspecific facilitation during recruitment and regeneration: A case study in degraded mangroves. *Basic and Applied Ecology* **15**, 651-660.

Vovides, A. G., Vogt, J., Kollert, A., Berger, U., Grueters, U., Peters, R., Lara-Domínguez, A. L., and López-Portillo, J. (2014). Morphological plasticity in mangrove trees: salinity-related changes in the allometry of Avicennia germinans. *Trees* **28**, 1413-1425.

Weiner, J. (2004). Allocation, plasticity and allometry in plants. *Perspectives in Plant Ecology, Evolution and Systematics* **6**, 207-215.

West, G. B., Brown, J. H., and Enquist, B. J. (1997). A General Model for the Origin of Allometric Scaling Laws in Biology. *Science* **276**, 122-126.

West, G. B., Brown, J. H., and Enquist, B. J. (1999). A general model for the structure and allometry of plant vascular systems. *Nature* **400**, 664-667.

West, G. B., Enquist, B. J., and Brown, J. H. (2009). A general quantitative theory of forest structure and dynamics. *Proceedings of the National Academy of Sciences* **106**, 7040-7045.

Yoda, K., Kira, T., Ogawa, H., and Hozumi, K. (1963). Self-thinning in overcrowded pure stands under cultivated and natural conditions. *Journal of Biology, Osaka City University* **14**, 107-129.

## 3.7 Appendix

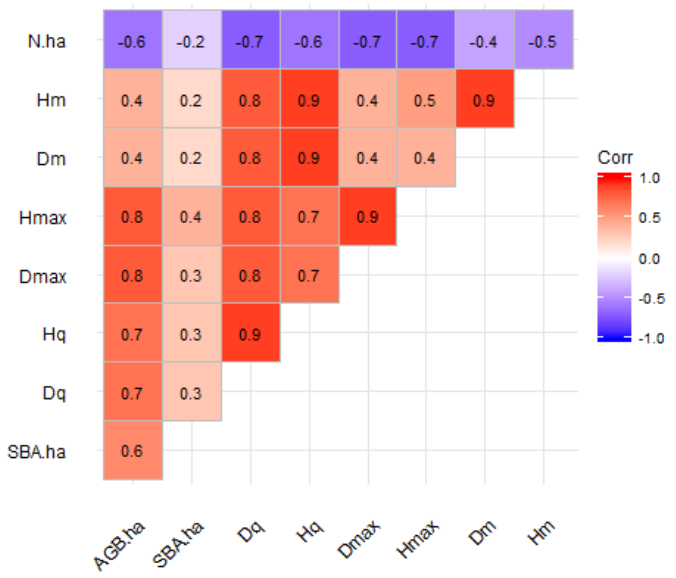


Appendix 3- I: Correlation matrix of selected forest structural attributes

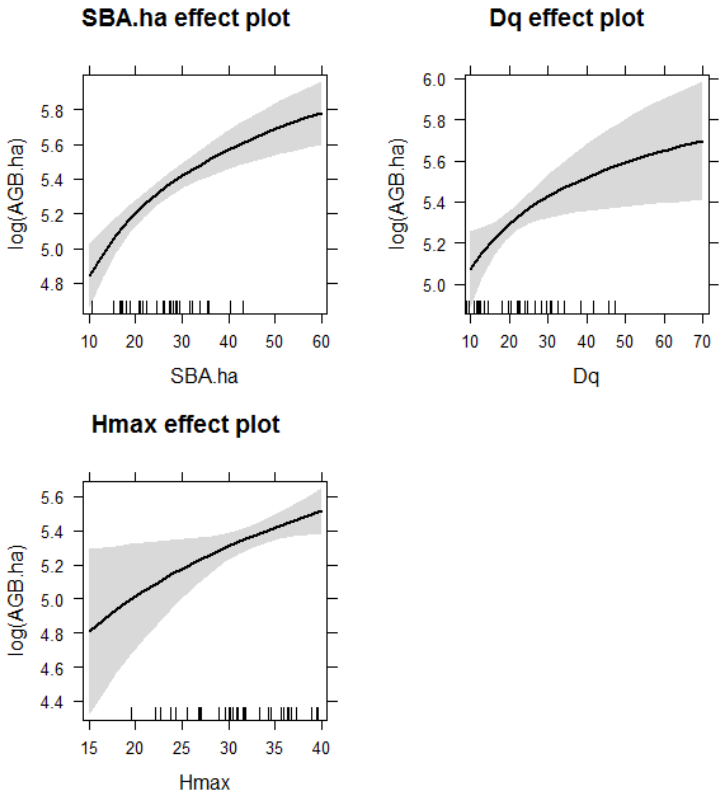


Appendix 3- II: Effects of different variables tested in the selected models

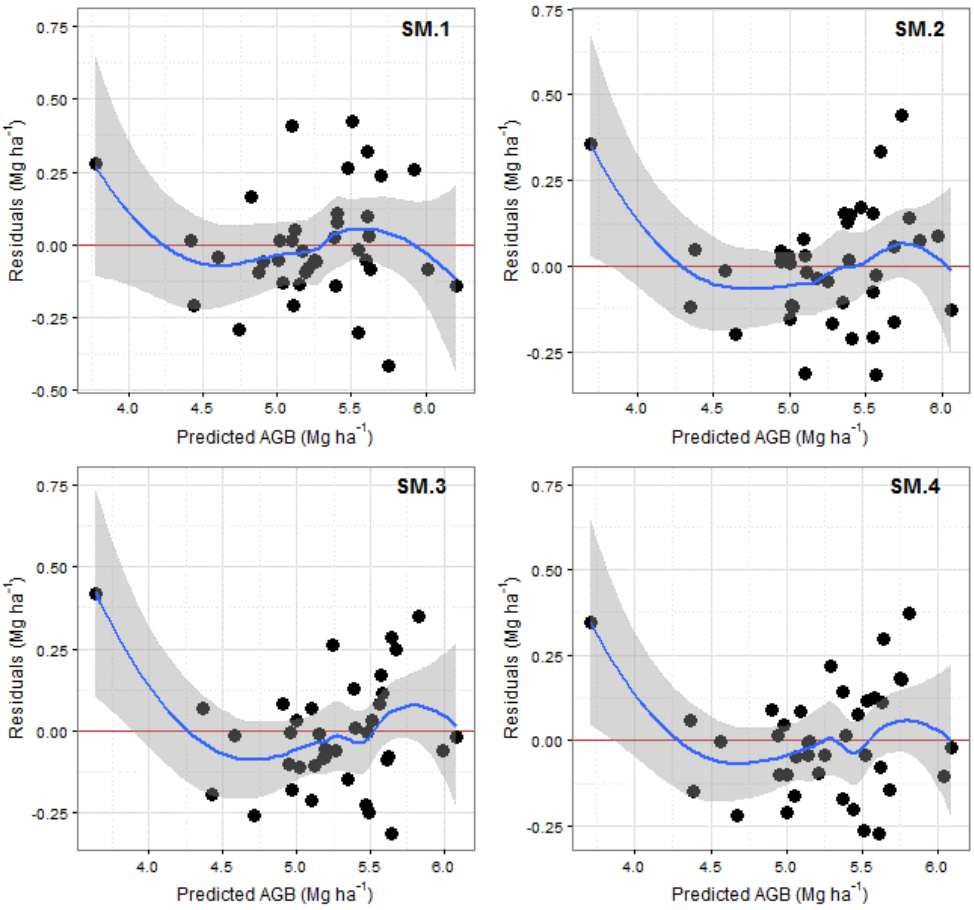


Appendix 3- III: Residuals against predicted values in log scale

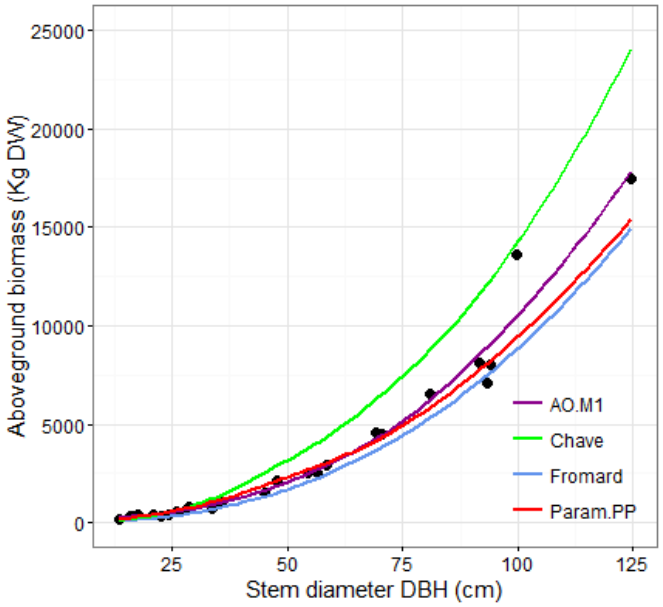


Appendix 3- IV: Comparison of parameterized biomass model with existing allometric models

# 4 *LOLLYMANGROVE* SOFTWARE: A STANDARDIZED TOOL FOR DATA ACQUISITION AND 3D DESCRIPTION OF MANGROVE FOREST STRUCTURE[1]

A. Olagoke[1,2], C. Proisy[1], U. Berger[2], S. Costa Neto[3], G. Estrada[4], F. Facundes[3], R. Peters[2], M. Soares[4], V. Santos[3], F. de Coligny[6]

1. *IRD-UMR AMAP, Boulevard de la Lironde, Montpellier, France*
2. *Institute of Forest Growth and Computer Science, Technische Universität, Dresden, Germany*
3. *Instituto de Pesquisas Científicas e Tecnológicas do Estado do Amapá (IEPA), Macapá, Amapá, Brazil*
4. *Faculdade de Oceanografia, Departamento de Oceanografia Biológica, Universidade do Estado do Rio de Janeiro, Rio de Janeiro, Brazil*
5. *Cartography and Remote Sensing Study Program, Faculty of Geography, Universitas Gadjah Mada, Bulaksumur, Yogyakarta, Indonesia*
6. *INRA-UMR AMAP, Boulevard de la Lironde, Montpellier, France*

**Software availability**

**Package**: Lollymangrove is embedded in the forest scene implantation manager (SIMEO) available in the AMAPStudio software platform dedicated to the study of plant architecture http://amapstudio.cirad.fr/

**Description**: Software package for collecting forest inventory data made in mangroves, visualizing 'lollypop-like' mangrove stands and biomass computations using preselected or configurable allometric equations.

**Availability**: via email contact to: christophe.proisy@ird.fr

**Cost**: Free.

**License:** LGPL

**Required software:** Java 1.7; Linux or Windows

**Required hardware**: Standard machine configurations are enough.

[1] Manuscript in *preparation for submission to Environmental Modeling & Software journal*

**Abstract**

*Consistent monitoring framework and good quality data are quite fundamental to our ability to predict the causes and consequences of environmental-induced changes in structure and functioning of mangrove forests. To that effect, large amount of data are becoming increasingly available from different part of the world. A perusal through however reveals that the designs for data collection and presentation are rarely harmonized, and thus forms a hindrance in achieving explicit comparison and modelling of structural development to changing coastal processes across spatial and temporal scale. In light of the foregoing, we developed a standardized software tool (Lollymangrove) to meet three-fold objectives: 1) improve protocol for collecting forest structural data on mangroves using a robust user interface, 2) workable platform for sharing structural data using predefined formats to a large scientific audience and decision makers in coastal management, and 3) robust data preparation for the parameterization of the forest dynamics and radiative transfer models. Implemented in the forest scene implementation manager (SIMEO) package of the AMAPSTUDIO plant architecture models suite, Lollymangrove integrated all available tree allometry and biomass models for ca. 40 mangrove species. In addition, we provided a configurable biomass allometry module that allows for adjusting parameters of proposed base models to account for local morphological variations in biomass computation across variable sites. Other than the capability of the software to input data in different formats, the editable 3D rendering module equally provided an interesting feature for visualization and mock-up export. Further descriptions and example application of the software are showcased in this paper.*

**Keywords**: Data standardization, Forest inventory, 3D forest visualization, mangrove biomass, SIMEO

## 4.1 Introduction

Our ability to model and predict the dynamics in the structural development and functioning of mangrove forests to fast changing local coastal processes invokes the demand for consistent monitoring framework and acquisition of good quality data over large spatial scales. Other than for modelling, the need for multi-temporal monitoring of mangrove forests also remains a major prerequisite in the planning and decision-making for early preemptive degradation detection, integrated management and conservation actions (Lewis III et al., 2016). Just like the responses and capabilities of mangrove tree species and forests to heterogeneous climatic forcing functions and human impacts are diverse, so also is the ecological feedbacks registered in the structure of different mangrove forests (Cintron and Schaeffer-Novelli, 1984). At the extreme of such pressure-induced responses, degradation or total collapse may results (Ellison, 2012; Lovelock et al., 2015); and once mangrove

are lost to degradation, a complete reversal may be costly or even less possible to achieve (Lewis III, 2005; Lewis III et al., 2016). Certainly, extensive monitoring schemes and acquisition of large datasets on mangrove forest structure has no compromise in this regards.

To date, large amount of data, especially on the structure and biomass distribution, on mangrove forests are available from different parts of the world. One clear issue that applies in most cases is, however, the lack of a standardized protocol for data collection and presentation. Individual authors tend to present data in a manner that addresses their interests or research goals as noted since early 80's in mangrove studies (Cintron and Schaeffer-Novelli, 1984), without a clear consideration for a common structure that can allow for easy understanding and collaborative data ensemble. Advancing a more fashionable and collective data presentation scheme in line with the recent "open movement" (Bakillah and Liang, 2016), or the open access database format (e.g. TRY (Kattge et al., 2011); DRYAD (Zanne et al., 2009)) appears decisive to match the research need in the current era of scientific cooperation and coordinated interdisciplinary studies in ecology.

On this note, we are present a standardized framework in the form of a software tool (named, *Lollymangrove*) that is capable of ensuring a common structure for data collection and representation for mangrove forests. Specifically, we describe in this study the structure and practically demonstrate the potential applications of the Lollymangrove software while addressing a threefold objective: i. the realization of a standard protocol for collecting structural data of mangrove forests using a robust user-friendly interface; ii. the advancement of predefined and ready formats for data visualization and biomass computation at both tree and stand scales; iii. Provision of versatile interface that allows for preparing and exporting data directly usable for the parameterization forest dynamics and radiative transfer simulation models or other relevant computer-aided study platforms.

## 4.2 Background and fundamentals

### *4.2.1 Sampling designs for characterizing mangrove forest structure*

Scientists and forest managers working in mangrove ecosystems often embark on forest measurements for different purposes or research goals, using diverse sampling designs and inventory methods. Because of the differing measurement techniques, the comparative value of forest structure data available in many published mangrove studies appears less impressive (Cintron and Schaeffer-Novelli, 1984). For many authors (e.g. Di Nitto et al. (2014); Dahdouh-Guebas et al. (2004); Piou et al. (2006)) whose primary aims are mostly rapid assessment of forest structure in relatively small areas, plotless methods such as point sampling or distance-based sampling like point-centered quarter method (PCQM) are favored

basically because of ease of application, time and cost effectiveness. The work of Dahdouh-Guebas and Koedam (2006) and Hijbeek et al. (2013) highlighted the reliability of PCQM among other methods for mangrove studies, especially for tree density estimation. These methods are however not without problems in some circumstances. First, they are liable to biased results in highly heterogeneous mangrove forests where local conditions usually culminate in diverse tree and forest architecture. The accuracy is equally limited where inter-tree distances are wide and uneven, though this could be compensated for by increasing the number of sampling points (up to 50 sampling points in spatially random forests, Khan et al. (2016)) at an increasing expense of time requirements.

When it comes to extensive characterization of forest structure over large-scale temporal and spatial extents, the common practice in classical forestry remains the establishment of forest plots (either circular or polygonal shapes) where variables, including tree trunk diameters, tree height, tree positions, and other stand characteristics are systematically measured (Couteron et al., 2012). From the preliminary knowledge of canopy analysis (e.g. Proisy et al. (2007); Proisy et al. (2012)) or satellite-based remote sensing (e.g. Fatoyinbo et al. (2008); Simard et al. (2008)) in mangrove forests, polygonal plot areas are positioned more representative of the beneath forest stand structure. These polygonal plots are widely applied, especially in studies dealing with structural attributes, inter-tree interactions (competition) and forest dynamics modelling (e.g. Berger et al. (2006); Vogt et al. (2013)), but also biomass and carbon measurements in mangrove ecosystems (e.g. Howard et al. (2014); Kauffman and Donato (2012)).

We postulate that sampling in polygonal areas hold greater benefits in studies aimed at understanding the nature and extent of ecological processes and complex interactions in mangrove forests. Although most forest inventories in mangrove forests are limited to small plot areas, and sometimes include only stem diameter measurements and possibly with stem mapping in X, Y Cartesian coordinates, due to the expensive nature (both time and cost) of comprehensive plot-based forest inventory. Such restricted measurements and small plot areas could sometimes become less representative of local forest structure. The gain here is that recent advancements in the area of physical modelling showcase good possibilities in the realization of explicit three-dimensional (3D) virtual forest structure (e.g. Barbier et al. (2012); Proisy et al. (2016)) from parsimonious forest measurements. We expanded such capability in the framework of *Lollymangrove* software.

### *4.2.2 Tree and biomass allometric models*

Numerous studies have highlighted the importance of allometric models in studies with focus on structure and functions of mangrove forests (e.g. Fromard et al. (1998); (Komiyama et al., 2002); Ong et al. (2004); Soares and Schaeffer-Novelli

(2005)). From such allometric models, tree dimensions that are difficult or not cost-effective to measure are conveniently estimated. Certainly, the application of these allometric models forms the basis for a rapid rendering three-dimensional forest structure (3D mock-ups) advanced in the *Lollymangrove* software. Since tree crown dimensions are rarely measured in classical forest inventories, workable diameter-crown allometries for specific sites are scarce. Besides, our analysis in the previous chapter together with available literature (e.g. Vovides et al. (2014)) pointed the fact that diameter-crown allometries are more variable from local to regional scale, lowering the chance to transfer allometric model between sites. To this end, the *Lollymangrove* software offers the possibility for a user-defined adjustment of parameters to realize suitable mock-ups for specific site conditions.

For biomass measurements, allometric models are usually established from the relationships of tree weights of representative sets of trees to the corresponding easy-to-measure tree dimensions, e.g. stem diameter or tree height. While there are many site-specific diameter – biomass allometric models (Komiyama et al., 2008), only a few integrated other tree variables like height or wood density to achieve general allometric models (Chave et al., 2005; Komiyama et al., 2002; Komiyama et al., 2005). These kind of general allometric models found application in every mangrove regions. Although the complexity of local structural variations in mangrove forests challenges the application of 'general purpose' allometric models, the common practice remains the application of such allometric models to other regions outside the domain of their calibration when appropriate local models are not available. Meanwhile, forests with contrasting structural properties may yield very similar aboveground biomass estimates (Proisy et al., 2012; Proisy et al., 2016). This factor, perhaps poses a major limitation to the application of sophisticated remote sensing techniques in accurately mapping of mangrove forest biomass (e.g. Réjou-Méchain et al. (2014)) till date.

Towards achieving a flexible and versatile platform for estimating forest biomass, we address the above issues in two distinct, but complementary ways in the *Lollymangove* software. First, the software compiled available allometric models and delivered an interface through which the user could indicate a choice of model relevant for site-specific application. Secondly, we proposed a set of generic and configurable model forms (Table 4-1) that allows for easy parameterization to site-specific use using parameters estimated from input field measurements. On top, the software offer possibility for a rapid comparison of outputs from different model forms. Until now, the form of biomass models provided in the software is not so exhaustive, and hence the need to validate and compare model outputs.

Table 4-1: Configurable allometric models for estimating biomass of mangrove trees

| Model ID | Aboveground biomass (AGB) model forms | Example parameters | References |
|---|---|---|---|
| 1 | $a_0 + a_1 \times DBH^{a_2} \times \rho^{a_3} \times H^{a_4}$ | $a_0$=0; $a_1$=0.14; $a_2$=2.4; $a_3$=0; $a_4$=0 | *A. germinans* Fromard *et al.* (1998) |
| 2 | $a_1 \times \exp\,(a_2 + a_3 \times \log(DBH))$ | $a_1$=1.00; $a_2$=0.25; $a_3$=0.91 | *A. marina* Kairo *et al.* (2009) |
| 3 | $a_1 \times \exp\left(a_2 \times DBH\right)$ | $a_1$=3.25; $a_2$=0.07 | *General (all species)* Sitoe *et al.* (2014) |
| 4 | $a_1 + (a_2 \times \log(DBH))^2 + (a_3 \times \log(CrV))$ | $a_1$=2.13; $a_2$=0.90; $a_3$=0.18 | *A. germinans* Ross *et al.* (2001) |
| 5 | $a_1 + CrD^{a_2} + H^{a_3}$ | $a_1$=1.83; $a_2$=2.00; $a_3$=1.02 | *A. marina* Fu and Wu (2011) |
| 6 | $\rho \times \exp[a_1 + a_2 \times \log(DBH) + a_3 \times (\log(DBH))^2 + a_4 \times (\log(DBH))^3]$ | $a_1$=-1.35; $a_2$=1.98; $a_3$=0.21; $a_4$=-0.03 | *General (all species)* Chave *et al.* (2005) |

***Units:***

*AGB: aboveground biomass (kg); DBH: diameter at breast height (cm); ρ: wood density (kg/ m³); H: tree height (m); CrD: crown diameter (m); CrV: crown volume (m³)*

***Note:***

- *A number of models originally use the natural logarithm 'ln' instead of the decimal logarithm 'log'. Coefficients must be divided by ln(10) according to:*
  *log(x) = ln(x) / ln(10) .*
- *0, 1 or a fitted real value can be assigned to any of the $a_i$ coefficient in order to adjust both the number of variables and the equation form. Please refer to examples given in the table to understand parameter settings for the highlighted models.*

## 4.3 Description of the software package

The *Lollymangrove* is a software application integrated in the AMAPstudio suite for plants architecture modelling (Griffon and de Coligny, 2014), more specifically in the SIMEO framework for trees architecture modelling at the forest scale. SIMEO makes it possible to build simulators / tools for natural forests, plantations or smaller groups of trees interacting in the same stand, to study their structure or growth with possibly the fine architecture of each tree.

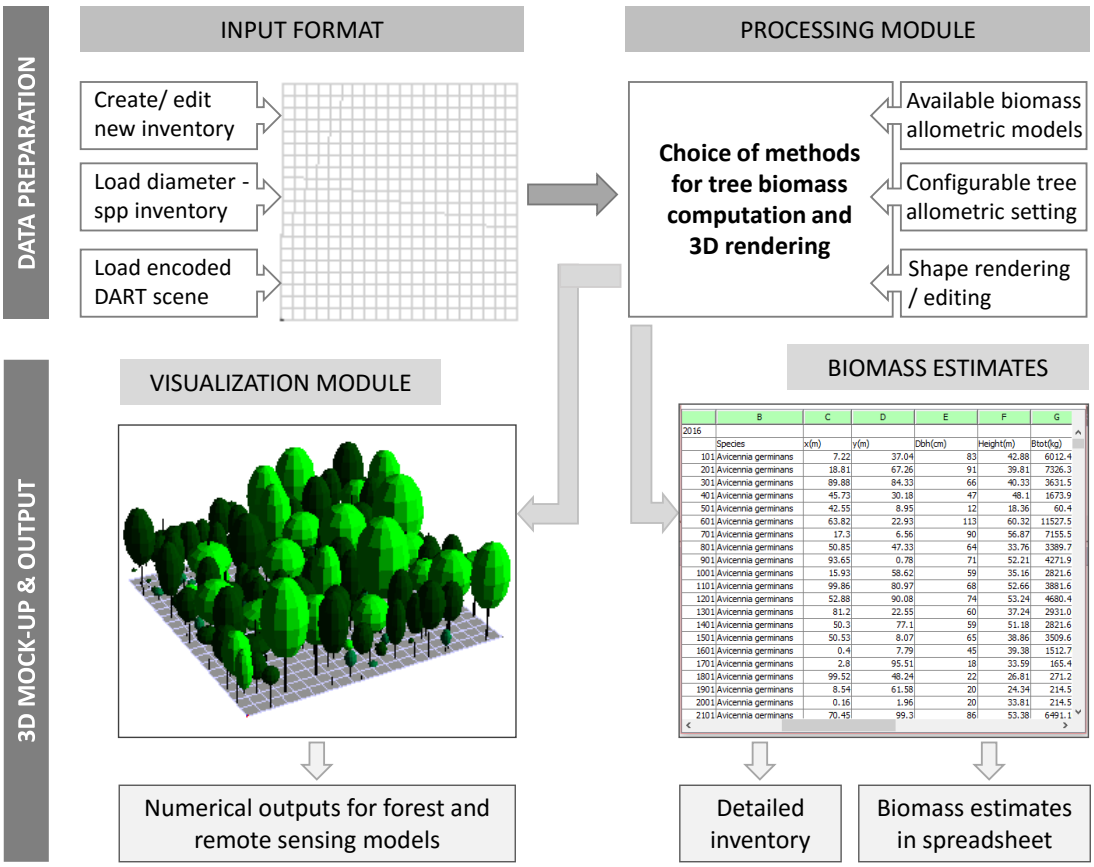


Figure 4-1: The basic structure of the *Lollymangrove* software, outlining main component modules and output formats.

The software offers a simplified graphical user interaction interface providing dialogs and comments in all component steps. Figure 4-1 provides the basic structure of the *Lollymangrove* software with an outline of the main modules. At initialization, the main interface features the menu items comprising project panel, which allows access to the file import, export and save tabs; the selection panel that facilitates isolation and edit of mock-up polygons; the tools panel for controlling CSV (comma-separated values) file viewer and tree rendering; and most importantly the help menu where a user can access guide to all component modules. Additionally, the scene for 3D view and rendering adjustment tools are embedded in the main graphical user interface (GUI). We provide an overview of the main modules of *Lollymangrove* software in the following sub-sections.

### 4.3.1 *Input module*

The input module starts with the opening and defining the name of a new project. At the first step, the GUI allows for specification of general parameters including species properties (among a list of 42 species registered with predefined coded names), and biomass model types, and then the choice of input formats. Currently, the *Lollymangrove* takes inputs in three different ways: 1) creation of a new inventory, 2) loading a species-diameter inventory, and 3) importation of an encoded DART (Discrete Anisotropic Radiative Transfer, Gastellu-Etchegorry et al. (2015)) compatible scene. Option 1 provides the possibility for direct input of data into the *Lollymangrove* in-situ during forest data collection. In this case, the user can enter forest parameters and tree variables as provided in Table 4-2. While option 2 loads spreadsheet where tree species and the stem diameter are provided in CSV format, the option 3 works with an encoded DART files. Added to the input GUI is the path for loading and editing an existing detailed inventory file in text-tab delimited format.

Table 4-2: A template table for a detailed inventory data layout in the Lollymangrove

| # Lollymangrove detailed inventory, date: Wed Aug 28, 2016 | | | | | | | | | |
|---|---|---|---|---|---|---|---|---|---|
| Plot Name = | | | | | | | | | |
| Plot XSize = 100 m | | | | | | | | | |
| Plot YSize = 100 m | | | | | | | | | |
| Species Code: AVge = *Avicennia germinans, LAra = Laguncularia racemosa, etc* | | | | | | | | | |
| # Trees | Species Code | Status | Diameter | Tree position | | Tree height | | Crown diameter | |
| stemId | | | Dbh (cm) | X (m) | Y (m) | H1b (m) | Htot (m) | Axis – A (m) | Axis – B (m) |
| 1 | AVge | alive | 36 | 57.4 | 29.8 | 15.9 | 30.7 | 11.4 | 11.3 |
| 2 | AVge | alive | 38 | 40.4 | 117.5 | 16.0 | 30.9 | 11.9 | 12.0 |
| 3 | AVge | alive | 5 | 107.1 | 17.4 | 14.8 | 24.5 | 2.9 | 2.8 |
| 4 | AVge | alive | 5 | 124.0 | 106.9 | 14.9 | 23.5 | 3.3 | 3.3 |
| 5 | AVge | alive | 5 | 56.9 | 35.0 | 14.8 | 25.1 | 2.9 | 3.0 |

### 4.3.2 *Processing module*

Once data are imported, the processing module provides the user with dialog tools to indicate choice of data processing methods in the processing module. Here, the user may opt for existing allometric models (compiled from published literature) relevant for local site application, or supply parameters for configurable model forms (Table 4-1) for biomass computation. Embedded comments in this module guide the user with examples on how to adjust parameters for local site application. Moreover, the crown-diameter allometry for the rendering of 3D mock-up can be modulated

accordingly. The rendering function also allows for adjustment of forest scene size to suit user's need through the interpolation or extrapolation of the input data. For example, a user can generate a 1-hectare forest scene from measurements available from 0.1-hectare plot forest data.

### *4.3.3 Visualization module*

The visualization module provides an interface that allows the user to visualize the 3D tree mock-ups characteristics of their forest plots. These mock-ups are generated from the tree dimensions input and the integrated allometric relationships. For now, forest scenes are modelled in geometric constructions with trunks represented in cylindrical shapes corresponding to stem diameter, and crowns as ellipsoidal objects. The position of each mock-up mimics the x- and y-coordinate position of each stem as supplied in the forest data. Where such stem position data are not available, the *Lollymangrove* software offers a built-in automatic 'random forest' generator able to supply random position for component trees based on other forest properties.

### *4.3.4 Output module*

With the output module, the user is able to specify and follow through the dialog to export results at the completion of all processing and analyses. Basically, the *Lollymangrove* software generates four types of output for export: 1) the image (snapshot) of forest mock-ups, 2) Numerical encode (DART output) in ASC or TXT file format, to meet input requirements for forest models, 3) detailed inventory data in spreadsheet, and 4) biomass estimates from choice models. Thus, the user can optionally request output given the specific needs or interests.

## 4.4 Example applications in South America

We illustrate the potential of the *Lollymangrove* software through example applications to data from contrasting mangrove forest stands in the Amazon-influenced coasts (South America). The data were obtained from plots of varying sizes from 0.1 to 1-hectare forest plots, depending on the number of trees per unit area in the sampling plots. We benefitted from the capability of the *Lollymangrove* to standardize all plot data to achieve 1-hectare forest scene, representative of the sample forest stands (Figure 4-2). Tree species were discriminated in different colors: *Avicennia germinans* (light green), *Rhizophora mangle* (copper brown), and *Laguncularia racemosa* (gray). The forest scene, marked GU1 represents a young *Avicennia* stand near Guatemala (French Guiana), TC1 connotes an Old-growth mixed mangrove stand in Petit Cayenne (French Guiana), the medium-height and tall *Avicennia* dominated mangrove forests in Bragança (Brazil) are respectively tagged BR1 and BR6, while the SU4 and SU5 are *Avicennia-Rhizophora mixed* mangrove forest stands in Amapá (Brazil). From these modelled forest scenes, the variation in

forest structure, tree density, species and size distribution are considerably discernible.

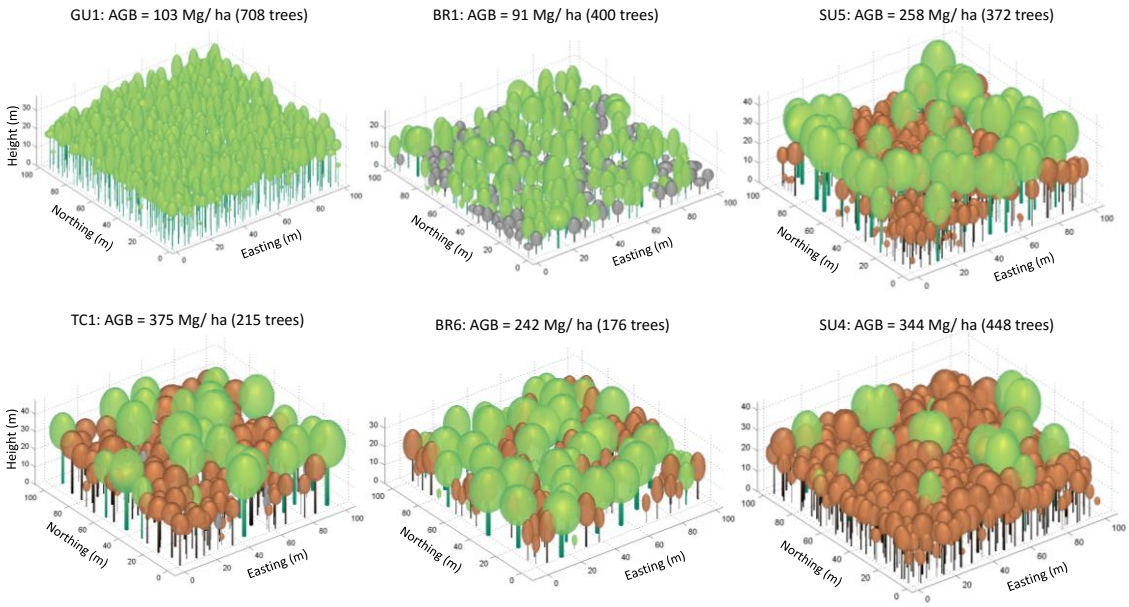


Figure 4-2: Examples 3D forest scene (mock-ups) of forest stands from contrasting mangrove ecosystems in the Amazon-influenced (South America)

## 4.5 Coupling with ecological and remote-sensing models

One key goal of the efforts demonstrated in this study centers on facilitating our capability to maximize field measurements of forest structure in the parameterization of ecological models, but also calibration of remote sensing signals, in the overall objective of capturing variability in forest structural parameters and canopy characteristics. With forest dynamics models, we stand to gain insights into the ecological processes underlying structural patterns being observed in nature. At the same time, formatted ensembles of multitemporal forest structure observations from the *Lollymangrove* software can conveniently be connected to forest models for rapid parameterization and subsequent modelling. The example provided in Figure 4-3 forms the basis for linking field observations of forest structure to remotely sensed information, like canopy analysis through Very High Spatial Resolution (VHSR) satellite images (Proisy et al., 2012). Certainly, the integration of modelled forest scenes and the simulated canopy images stands to facilitate the interpretation of remote sensing images, and further the analysis of remotely acquired structural data of mangrove forests (Kasischke and Christensen Jr, 1990; Proisy et al., 2016; Viennois et al., 2016). Efforts are currently underway to decipher the influence of ontogenetic- and species-specific crown porosity, leaf clumping and canopy reflectance under variable environments, in order to achieve

fine parameterization of DART models (Féret and Asner, 2011; Gastellu-Etchegorry et al., 2015) from current parsimonious descriptions of mangrove forest structure.

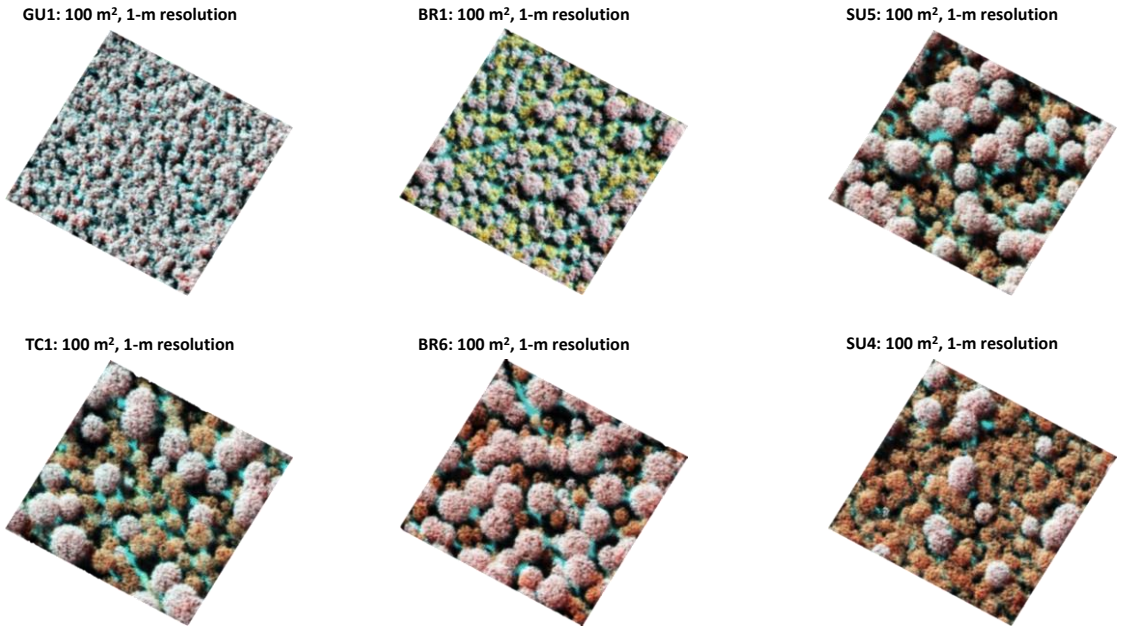


Figure 4-3: Simulated canopy images (from DART model) of the forest scenes presented in the Figure 4-2. Each image corresponds to a multi-spectral (RGB-colored composite) WorldView-2 image acquisition at the configuration of 22.4° Zenith angle and 210° Azimuth angle.

## 4.6 Conclusion and perspectives

This chapter presents the *Lollymangrove* software (specifically designed for mangrove forests), which offers a standardized platform with capability to facilitate data collection, visualization and sharing of forest structure descriptions among mangrove ecologists. While the software provides a flexible and configurable approach to localized biomass computation over the regular site-specific and general allometric models, the extension for data preparation in compatible formats for integration into forest simulation models gives a greater prospect in advancing data acquisition, modelling and validation towards better understanding and monitoring of structural development and dynamics of mangrove forests. By the time an extensive validation and refinement are realized, this software would meet to advance the calibration and parameterization of our simulation modelling and remote sensing techniques, with prospects of simulating the consequences of environmental change on mangrove forest dynamics. Certainly, the approach presented here can be extended to find applications in other forest ecosystems.

**Acknowledgements**

This research was conducted under the framework of the MANGWATCH project funded by the French *Centre National de la Recherche Scientifique* (CNRS) research program "Incubator for interdisciplinary research projects in French Guiana."

Adewole Olagoke received doctoral fellowship from the European Commission under the Erasmus Mundus Joint Doctorate programme, *Forest and Nature for Society* (FONASO), and travel grants from the CNRS and Technische Universität Dresden Graduate Academy (Germany).

## 4.7 References

Bakillah, M., and Liang, S. (2016). Open geospatial data, software and standards. *Open Geospatial Data, Software and Standards* **1**, 1-2.

Barbier, N., Couteron, P., Gastelly-Etchegorry, J.-P., and Proisy, C. (2012). Linking canopy images to forest structural parameters: potential of a modeling framework. *Annals of Forest Science* **69**, 305-311.

Berger, U., Adams, M., Grimm, V., and Hildenbrandt, H. (2006). Modelling secondary succession of neotropical mangroves: Causes and consequences of growth reduction in pioneer species. *Perspectives in Plant Ecology, Evolution and Systematics* **7**, 243-252.

Chave, J., Andalo, C., Brown, S., Cairns, M. A., Chambers, J. Q., Eamus, D., Folster, H., Fromard, F., Higuchi, N., Kira, T., Lescure, J.-P., Nelson, B. W., Ogawa, H., Puig, H., Riéra, B., and Yamakura, T. (2005). Tree allometry and improved estimation of carbon stocks and balance in tropical forests. *Oecologia* **145**, 87-99.

Cintron, G., and Schaeffer-Novelli, Y. (1984). Methods for studying mangrove structure. *In* "The mangrove ecosystem: research methods" (S. C. Snedaker and J. G. Snedaker, eds.), pp. 91-113. United Nations Educational, Scientific and Cultural Organization (UNESCO), Paris.

Couteron, P., Barbier, N., Proisy, C., Pélissier, R., and Vincent, G. (2012). Linking Remote-Sensing Information to Tropical Forest Structure: The Crucial Role of Modelling. *Earthzine*.

Dahdouh-Guebas, F., and Koedam, N. (2006). Empirical estimate of the reliability of the use of the Point-Centred Quarter Method (PCQM): Solutions to ambiguous field situations and description of the PCQM+ protocol. *Forest Ecology and Management* **228**, 1-18.

Dahdouh-Guebas, F., Van Pottelbergh, I., Kairo, J. G., Cannicci, S., and Koedam, N. (2004). Human-impacted mangroves in Gazi (Kenya): Predicting future vegetation based on retrospective remote sensing, social surveys, and tree distribution. *Marine Ecology Progress Series* **272**, 77-92.

Di Nitto, D., Neukermans, G., Koedam, N., Defever, H., Pattyn, F., Kairo, J. G., and Dahdouh-Guebas, F. (2014). Mangroves facing climate change: landward migration potential in response to projected scenarios of sea level rise. *Biogeosciences* **11**, 857-871.

Ellison, J. C. (2012). "Climate Change Vulnerability Assessment and Adaptation Planning for Mangrove Systems," World Wildlife Fund (WWF), Washington, DC.

Fatoyinbo, T. E., Simard, M., Washington-Allen, R. A., and Shugart, H. H. (2008). Landscape-scale extent, height, biomass, and carbon estimation of Mozambique's mangrove forests with Landsat ETM+ and Shuttle Radar Topography Mission elevation data. *J. Geophys. Res.* **113**.

Féret, J.-B., and Asner, G. P. (2011). Spectroscopic classification of tropical forest species using radiative transfer modeling. *Remote Sensing of Environment* **115**, 2415-2422.

Fromard, F., Puig, H., Mougin, E., Marty, G., Betoulle, J. L., and Cadamuro, L. (1998). Structure, above-ground biomass and dynamics of mangrove ecosystems: new data from French Guiana. *Oecologia* **115**, 39-53.

Gastellu-Etchegorry, J.-P., Yin, T., Lauret, N., Cajgfinger, T., Gregoire, T., Grau, E., Feret, J.-B., Lopes, M., Guilleux, J., Dedieu, G., Malenovský, Z., Cook, B., Morton, D., Rubio, J.,

Durrieu, S., Cazanave, G., Martin, E., and Ristorcelli, T. (2015). Discrete Anisotropic Radiative Transfer (DART 5) for Modeling Airborne and Satellite Spectroradiometer and LIDAR Acquisitions of Natural and Urban Landscapes. *Remote Sensing* **7**, 1667.

Griffon, S., and de Coligny, F. (2014). AMAPstudio: An editing and simulation software suite for plants architecture modelling. *Ecological Modelling* **290**, 3-10.

Hijbeek, R., Koedam, N., Khan, M. N. I., Kairo, J. G., Schoukens, J., and Dahdouh-Guebas, F. (2013). An Evaluation of Plotless Sampling Using Vegetation Simulations and Field Data from a Mangrove Forest. *PLoS ONE* **8**, e67201.

Howard, J., Hoyt, S., Isensee, K., Pidgeon, E., and Telszewski, M., eds. (2014). "Coastal Blue Carbon: Methods for assessing carbon stocks and emissions factors in mangroves, tidal salt marshes, and seagrass meadows," pp. 1-184. Conservation International, Intergovernmental Oceanographic Commission of UNESCO, International Union for Conservation of Nature, Arlington, Virginia, USA.

Kasischke, E. S., and Christensen Jr, N. L. (1990). Connecting forest ecosystem and microwave backscatter models. *International Journal of Remote Sensing* **11**, 1277-1298.

Kattge, J., DÍAz, S., Lavorel, S., Prentice, I. C., Leadley, P., BÖNisch, G., Garnier, E., Westoby, M., Reich, P. B., Wright, I. J., Cornelissen, J. H. C., Violle, C., Harrison, S. P., Van Bodegom, P. M., Reichstein, M., Enquist, B. J., Soudzilovskaia, N. A., Ackerly, D. D., Anand, M., Atkin, O., Bahn, M., Baker, T. R., Baldocchi, D., Bekker, R., Blanco, C. C., Blonder, B., Bond, W. J., Bradstock, R., Bunker, D. E., Casanoves, F., Cavender-Bares, J., Chambers, J. Q., Chapin Iii, F. S., Chave, J., Coomes, D., Cornwell, W. K., Craine, J. M., Dobrin, B. H., Duarte, L., Durka, W., Elser, J., Esser, G., Estiarte, M., Fagan, W. F., Fang, J., FernÁNdez-MÉNdez, F., Fidelis, A., Finegan, B., Flores, O., Ford, H., Frank, D., Freschet, G. T., Fyllas, N. M., Gallagher, R. V., Green, W. A., Gutierrez, A. G., Hickler, T., Higgins, S. I., Hodgson, J. G., Jalili, A., Jansen, S., Joly, C. A., Kerkhoff, A. J., Kirkup, D., Kitajima, K., Kleyer, M., Klotz, S., Knops, J. M. H., Kramer, K., KÜHn, I., Kurokawa, H., Laughlin, D., Lee, T. D., Leishman, M., Lens, F., Lenz, T., Lewis, S. L., Lloyd, J., LlusiÀ, J., Louault, F., Ma, S., Mahecha, M. D., Manning, P., Massad, T., Medlyn, B. E., Messier, J., Moles, A. T., MÜLler, S. C., Nadrowski, K., Naeem, S., Niinemets, Ü., NÖLlert, S., NÜSke, A., Ogaya, R., Oleksyn, J., Onipchenko, V. G., Onoda, Y., OrdoÑEz, J., Overbeck, G., Ozinga, W. A., et al. (2011). TRY – a global database of plant traits. *Global Change Biology* **17**, 2905-2935.

Kauffman, J. B., and Donato, D. (2012). "Protocols for the measurement, monitoring and reporting of structure, biomass and carbon stocks in mangrove forests," Center for International Forestry Research (CIFOR), Bogor, Indonesia.

Khan, M. N. I., Hijbeek, R., Berger, U., Koedam, N., Grueters, U., Islam, S. M. Z., Hasan, M. A., and Dahdouh-Guebas, F. (2016). An Evaluation of the Plant Density Estimator the Point-Centred Quarter Method (PCQM) Using Monte Carlo Simulation. *PLoS ONE* **11**, e0157985.

Komiyama, A., Jintana, V., Sangtiean, T., and Kato, S. (2002). A common allometric equation for predicting stem weight of mangroves growing in secondary forests. *Ecological Research* **17**, 415-418.

Komiyama, A., Ong, J. E., and Poungparn, S. (2008). Allometry, biomass, and productivity of mangrove forests: A review. *Aquatic Botany* **89**, 128-137.

Komiyama, A., Poungparn, S., and Kato, S. (2005). Common allometric equations for estimating the tree weight of mangroves. *Journal of Tropical Ecology* **21**, 471-477.

Lewis III, R. R. (2005). Ecological engineering for successful management and restoration of mangrove forests. *Ecological Engineering* **24**, 403-418.

Lewis III, R. R., Milbrandt, E. C., Brown, B., Krauss, K. W., Rovai, A. S., Beever Iii, J. W., and Flynn, L. L. (2016). Stress in mangrove forests: Early detection and preemptive

rehabilitation are essential for future successful worldwide mangrove forest management. *Marine Pollution Bulletin*.

Lovelock, C. E., Cahoon, D. R., Friess, D. A., Guntenspergen, G. R., Krauss, K. W., Reef, R., Rogers, K., Saunders, M. L., Sidik, F., Swales, A., Saintilan, N., Thuyen, L. X., and Triet, T. (2015). The vulnerability of Indo-Pacific mangrove forests to sea-level rise. *Nature* **526**, 559-563.

Ong, J. E., Gong, W. K., and Wong, C. H. (2004). Allometry and partitioning of the mangrove, Rhizophora apiculata. *Forest Ecology and Management* **188**, 395-408.

Piou, C., Feller, I. C., Berger, U., and Chi, F. (2006). Zonation Patterns of Belizean Offshore Mangrove Forests 41 Years After a Catastrophic Hurricane1. *Biotropica* **38**, 365-374.

Proisy, C., Barbier, N., Guéroult, M., Pélissier, R., Gastellu-Etchegorry, J.-P., Grau, E., and Couteron, P. (2012). Biomass prediction in tropical forests: the canopy grain approach. *In* "Remote Sensing of Biomass: Principles and Applications / Book 1" (T. E. Fatoyinbo, ed.). INTECH publisher.

Proisy, C., Couteron, P., and Fromard, F. (2007). Predicting and mapping mangrove biomass from canopy grain analysis using Fourier-based textural ordination of IKONOS images. *Remote Sensing of Environment* **109**, 379-392.

Proisy, C., Féret, J.-B., Lauret, N., and Gastellu-Etchegorry, J.-P. (2016). Mangrove forest dynamics using very high spatial resolution optical remote sensing. *In* "Remote sensing of Land Surfaces: Urban and coastal area" (N. Baghdadi and M. Zribi, eds.), Vol. 5, Chapter 7. ELSEVIER, London. In press.

Réjou-Méchain, M., Muller-Landau, H. C., Detto, M., Thomas, S. C., Le Toan, T., Saatchi, S. S., Barreto-Silva, J. S., Bourg, N. A., Bunyavejchewin, S., Butt, N., Brockelman, W. Y., Cao, M., Cárdenas, D., Chiang, J. M., Chuyong, G. B., Clay, K., Condit, R., Dattaraja, H. S., Davies, S. J., Duque, A., Esufali, S., Ewango, C., Fernando, R. H. S., Fletcher, C. D., Gunatilleke, I. A. U. N., Hao, Z., Harms, K. E., Hart, T. B., Hérault, B., Howe, R. W., Hubbell, S. P., Johnson, D. J., Kenfack, D., Larson, A. J., Lin, L., Lin, Y., Lutz, J. A., Makana, J. R., Malhi, Y., Marthews, T. R., McEwan, R. W., McMahon, S. M., McShea, W. J., Muscarella, R., Nathalang, A., Noor, N. S. M., Nytch, C. J., Oliveira, A. A., Phillips, R. P., Pongpattananurak, N., Punchi-Manage, R., Salim, R., Schurman, J., Sukumar, R., Suresh, H. S., Suwanvecho, U., Thomas, D. W., Thompson, J., Uríarte, M., Valencia, R., Vicentini, A., Wolf, A. T., Yap, S., Yuan, Z., Zartman, C. E., Zimmerman, J. K., and Chave, J. (2014). Local spatial structure of forest biomass and its consequences for remote sensing of carbon stocks. *Biogeosciences* **11**, 6827-6840.

Simard, M., Rivera-Monroy, V. H., Mancera-Pineda, J. E., Castañeda-Moya, E., and Twilley, R. R. (2008). A systematic method for 3D mapping of mangrove forests based on Shuttle Radar Topography Mission elevation data, ICEsat/GLAS waveforms and field data: Application to Ciénaga Grande de Santa Marta, Colombia. *Remote Sensing of Environment* **112**, 2131-2144.

Soares, M. L. G., and Schaeffer-Novelli, Y. (2005). Above-ground biomass of mangrove species. I. Analysis of models. *Estuarine, Coastal and Shelf Science* **65**, 1-18.

Viennois, G., Proisy, C., J. B, F., x00E, ret, Prosperi, J., Sidik, F., Suhardjono, Rahmania, R., Long, N., x00E, x00E, Germain, O., and Gaspar, P. (2016). Multitemporal Analysis of High-Spatial-Resolution Optical Satellite Imagery for Mangrove Species Mapping in Bali, Indonesia. *IEEE Journal of Selected Topics in Applied Earth Observations and Remote Sensing* **PP**, 1-7.

Vogt, J., Kautz, M., Fontalvo Herazo, M. L., Triet, T., Walther, D., Saint-Paul, U., Diele, K., and Berger, U. (2013). Do canopy disturbances drive forest plantations into more natural conditions? — A case study from Can Gio Biosphere Reserve, Viet Nam. *Global and Planetary Change* **110, Part B**, 249-258.

Vovides, A. G., Vogt, J., Kollert, A., Berger, U., Grueters, U., Peters, R., Lara-Domínguez, A. L., and López-Portillo, J. (2014). Morphological plasticity in mangrove trees: salinity-related changes in the allometry of Avicennia germinans. *Trees* **28**, 1413-1425.

Zanne, A. E., Lopez-Gonzalez, G., Coomes, D. A., Ilic, J., Jansen, S., Lewis, S. L., Miller, R. B., Swenson, N. G., Wiemann, M. C., and Chave, J. (2009). Data from: Towards a worldwide wood economics spectrum. Dryad Data Repository.

# 5 SIMULATING THE INFLUENCE OF PLASTIC TREE MORPHOLOGY AND BIOMASS PARTITIONING ON THE STRUCTURAL DEVELOPMENT OF MANGROVE FORESTS[1]

Adewole Olagoke [1,2], Ronny Peters[1], Christophe Proisy[2] & Uta Berger[1]

[1]Institute of Forest Growth and Computer Sciences, Technische Universität, Dresden, Germany
[2]IRD, UMR-AMAP, 34000 Montpellier, France

## Abstract

*Morphological plasticity of trees relates to changes in the partitioning of above- and belowground biomass during growth, which is often a direct consequence of environmental stresses or limiting resources (e.g. light, water, or nutrients). The subsequent tree structure affects local neighbourhood interactions and the competitive strength of individual trees leading to a site-dependent forest stand structure. In order to understand these complex interactions, a mangrove stand simulator incorporating environment-dependent plastic tree morphology and biomass partitioning, was parameterized (using published data in literature and a few assumed parameters), and tested against field observations and published empirical forest patterns. Simulation experiments were conducted to analyze the importance of pore water salinity and related water stress on tree morphological scaling and the subsequent dynamics of mangrove forest structure. Selected stand characteristics matched well with observed ecological patterns (e.g., the growth trajectories of single trees, mortality distributions, self-thinning trajectories) confirming the dependence of mangrove tree growth and stand structural development on ambient environmental conditions. Meanwhile the current parameterization only yielded a considerable lower maximum tree height and diameter, but also aboveground biomass when compared to field measurements in low salinity conditions. The deviation of the simulated self-thinning trajectories from the slopes estimated for these low salinity sites also pointed the need for a further model improvement. Overall, the study demonstrates that an explicit consideration of tree morphological plasticity related to soil salinity and water availability is indeed important in the analysis of mangrove structural development in variable environments.*

**Keywords:** Morphological plasticity, forest structure and dynamics, self-thinning rule, density-dependent mortality, shifting tree allometry, biomass allocation

[1] *Manuscript in preparation*

## 5.1 Introduction

Recurrent changes in the abiotic factors or stresses surrounding plants and forest growth are frequently observed in the coastal mangrove environment. Prominent among these factors are hyper-salinity, anoxic soil conditions, water stress or nutrient limitations (Cintron and Schaeffer-Novelli, 1984; Twilley and Rivera-Monroy, 2005). As a means of adaptation to such factors, mangrove trees have exhibited plastic physiological processes as well as modification of morphological structures (Ball, 2002; Feller et al., 2010; Lovelock et al., 2006). Accordingly, a number of mangrove species, including *Avicennia germinans* and *Rhizophora spp* are known with ability to maximize the iconic "polymorphism" attribute resulting from plasticity to persist over a wide ecological range (Clough et al., 1997; Vogt et al., 2014; Vovides et al., 2014). This, according to Callaway et al. (2003), is consequent to individual trees restraining morphological formations to optimize resource acquisition, utilization and growth in the ambient environment. Thus, the expressed tree forms become characteristic of the growing environment (Weiner, 2004). To our knowledge, insights about the consequences of this environment-related plasticity in tree morphology and biomass partitioning for the structural development of mangrove forests are generally lacking and hence, the motivation for the current study.

Efforts demonstrated in the previous chapters provided empirical observations characterizing the dynamics of tree morphology and stand structure in contrasting mangrove forests with the use of laser techniques (e.g. Olagoke et al. (2016)), classical forest inventory, 3D modelling, etc. However precise, extending the approach at both temporal and spatial scales to explore how morphological plasticity and related ecological processes interplay to shape forest structure in variable environments would require more extensive datasets over long-term studies. More so, such approach and similar others are fairly limited when the identification and descriptions of the ecological processes causing the observed changes in tree and stand structure are subjects of investigations (Berger et al., 2008). It is thus worth to complement the earlier experimental approach with a spatially explicit mechanistic modelling, able to provide a forecast of stand characteristics based on the parameterization from parsimonious tree and stand measurements.

Spatially explicit forest stands simulators are recognized for modelling growth, yield and structural dynamics of mangrove forests over different temporal and spatial; scales (e.g., Berger and Hildenbrandt (2000); Twilley et al. (1999)). So far, no mangrove forest simulator exists, which is suitable for characterizing the processes underlying the plastic tree morphology and biomass partitioning in response to varying environmental cues. Most of the stand simulation models that have been

developed and tested for mangrove forests (e.g., KiWi, FORMAN, MANGO, etc.) rely on the use of static growth functions with deterministic relations between tree dimensional attributes such as stem diameter, tree height or canopy projection area, etc. The pioneering attempt to address issues of morphological plasticity in mangrove stand modelling is the recent mesoFON model (Grueters et al., 2014) that describes crown shift because of light foraging. Yet, the allometry relation of the tree structure in this model remains size-dependent.

The BETTINA model (Peters et al., 2014) seems promising in this regards, since it describes the factors controlling the individual tree's adaptation to environmental change mechanistically. Originally designed for single trees, the model captures the environment-sensitive internal processes driving biomass allocation to different tree compartments – leaves, branches, stem, fine and coarse roots. Based on the established water transport resistance approach (Thornley, 1996), BETTINA model derives the environmental-modulated tree dimensions expected for mangrove trees growing under diverse salinity conditions (Vovides et al., 2014). Until now, the model has been satisfactorily tested for theoretical response of simulated individual trees to variable environments (Peters et al., 2014), though no explicit parameterization and evaluation with ensemble empirical information. Given the currently mounting interest in the analysis of the how plants are responding and adapting to the changing environment and the consequences for forest stand dynamics, we consider it necessary to advance the parameterization of the BETTINA as a single-tree model and its incorporation into a spatially explicit stand simulator.

Therefore, the objectives of this study are: (1) to parameterize and evaluate the BETTINA_IBM mangrove stand simulator, which uses the earlier published BETTINA model to describe the growth of single trees; and (2) to apply the model to understand how the complex interactions of water stress and local competition influence individual tree growth and biomass partitioning, and the implications for the dynamics of forest structural development at the stand level. For simplicity, we restricted the simulation experiments to mono-specific stands of *A. germinans* in variable environments, though the effects apply more generally to other mangrove species too.

## 5.2 Methodology

### *5.2.1 Model description*

In this study, we used the model BETTINA_IBM that describes (1) the growth and allometric plasticity of individual trees to abiotic environmental conditions and (2) the local tree-tree interactions among neighbouring individuals. A simplified framework for integrating the environment-related tree development and biomass partitioning to different tree components into this individual-based mangrove stand

simulator is provided in the Figure 5-1. While the overview of component processes implemented in the model is presented in the succeeding sub-sections, a version with more explicit details following the standardized 'ODD' (Overview, Design concepts, and Details) protocol (Grimm et al., 2006; Grimm et al., 2010) provided in the annex. Model implementation was realized in the NetLogo (Version 5.3.1).

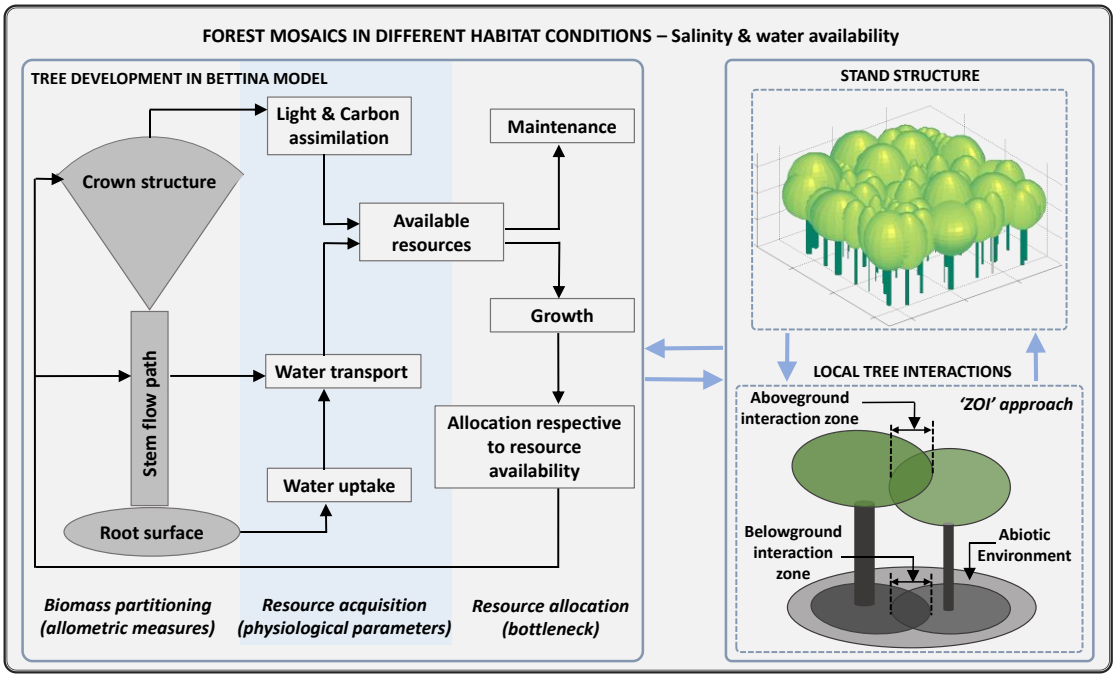


Figure 5-1: The modelling framework integrating environment dependent tree development and biomass partitioning (as represented in BETTINA model) for simulating stand structure of mangrove forests along a gradient of habitat salinity and water availability conditions. *The Zone-Of-Influence ('ZOI') underlined the process of local interactions with pairwise set of trees interacting in the overlapping areas.*

Using the mechanistic approach, as presented in BETTINA single-tree model (Peters et al., 2014), the BETTINA_IBM described explicitly the processes underlying the morphological development of individual trees and overcomes the empirical formulation of tree allometric relations. Thus, trees evolve divergent shape and biomass allocation patterns depending on the local environmental conditions (basically, salinity and water availability) and inter-individual competition for resources, below- and aboveground (two-dimensional neighbourhood interactions). For initialization, each tree started with its characteristic Cartesian coordinate ($x$,$y$) of stem position within the simulated forest area, crown radius ($r_{crown}$) describing the projected crown area (aboveground Zone-of-Influence[2], ZOI), and crown height ($h_{crown}$) corresponding to the leaf volume per unit area. Other initialization attributes include individual tree's stem radius ($r_{stem}$), stem height ($h_{stem}$), root-zone radius

[2] The zone-of-influence conceptually defines the area individual trees occupy, and compete for resources with neighboring other(s) in areas they overlap (Weiner et al., 2001).

($r_{root}$) that describes the belowground ZOI and root height ($h_{root}$), which corresponds to volume of fine root per unit area, as described in Table 5-1. The initial stem radius and root-zone radius were adjusted by local salinity (*sal*) condition to achieve an equilibrium in the above- and below-ground resources distribution using an auxiliary modifier, $k_{aux}$ (see details in the ODD provided in the annex).

Table 5-1: Initialization variables characterizing individual trees in the BETTINA_IBM model

| Variable | Unit | Description | Value | Behaviour |
|---|---|---|---|---|
| $x$ | m | Cartesian position - x | random | constant |
| $y$ | m | Cartesian position - y | random | constant |
| $r_{crown}$ | m | Crown radius | 0.3 | variable |
| $h_{crown}$ | $m^3.m^{-2}$ | Leaf volume per unit area | 0.004 | constant |
| $r_{stem}$ | m | Stem radius | estimated* | variable |
| $h_{stem}$ | m | Stem height | 0.0001 | variable |
| $r_{root}$ | m | Radius of root zone | estimated* | variable |
| $h_{root}$ | $m^3.m^{-2}$ | Fine root volume per unit area | 0.004 | constant |
| $r_{croot}$ | m | Radius of coarse root | $2^{-0.5}$ | constant |

***** *estimated from other measures at the initial state to achieve numerical stability.*

Accordingly, the allometric measures of each tree are updated sequel to the growth in dimensions at each growth cycle. Trees adapt growth to both the abiotic (salinity and water availability) and biotic (local neighbourhood interaction) environment. The shape of individual trees controls the prospect for resource acquisition, and vice versa, the growth is predicated upon the available resources. Overall, the population level features (e.g. the trajectories of plant mass-density relationships and tree spatial distribution (as measured by the Clark-Evans index) naturally emerged as trees grow and die over time, given the influence of resource availability and neighbourhood competition intensity in varying habitats.

*Individual tree growth*

The conceptualized outlining of individual trees growth and biomass allocation to component organs (leaf, branch, stem, fine- and coarse-root) is the core strength of the BETTINA model. Using the transport-resistance modelling approach, we used a number of numerical descriptions to obtain the volume of biomass distributed in different plant components based on the model parameters provided in Table 5-2. Our current parameterization is simply based on the literature studies, whereas some parameters were either estimated from field measurements or assumed. The

simulation commenced with each tree component simply conceptualized in an approximated cylindrical structure and the volume estimated based on the characteristic dimensions of the given component as stated in Table 5-1. The total tree volume $v_{tree}$ was obtained as the summation of the volume of all tree components. This process, being modulated by the resistances in the root zone and the stem flow path (see Figure 5-1, left-position), is repeated at every growth cycle.

Table 5-2: Parameters and values for simulating *Avicennia germinans* tree growth

| Variable | Unit | Description | Value | Source |
|---|---|---|---|---|
| $L_p \times k_{geom}$ * | kg.s$^{-1}$m$^{-4}$ | Fine root permeability × geom. constant | 0.04 | Estimated |
| $k_{f,\ sap}$ | kg.s$^{-1}$m$^{-2}$ | Xylem conductivity | 1.48 | Krauss et al. (2007); Muller et al. (2009) |
| $R_{solar} \times k_{rel}$ * | kg.s$^{-1}$m$^{-2}$ | Solar radiation × water resource factor | 0.038 | Assumed |
| $psi_{leaf}$ | MPa | Minimum leaf water potential | -7.86 | Lopez-Portillo et al. (2014) |
| $k_{maint}$ | kg.s$^{-1}$m$^{-3}$ | Maintenance cost per unit biomass | 0.28 | Assumed |
| $k_{r,\ halfmax}$ | - | Half of maximum height growth weight | 0.1 | Assumed |
| $sf_{sig,\ 1}$ | - | Scaling factor for sigmoid function 1 (growth allocation) | 0.02 | Assumed |
| $sf_{sig,\ 2}$ | - | Scaling factor for sigmoid function 2 (height growth) | 0.15 | Assumed |
| $K_{grow}$ | - | Scaling factor for tree growth | 0.10 | Assumed |
| *death.threshold* | - | Factor defining tree mortality | 0.5 | Assumed |

** these assumed parameters occur in combinations and thus condensed to a single value*

In the growth process, the resistances for water crossing the root surface ($r_1$) and the axial flow ($r_2$) towards the leaf area are sensitive to some species-specific parameters $L_p \times k_{geom}$ and $k_{f,\ sap}$, and the current allometric measures of the individual trees (*sensu* Peters et al. (2014)). We computed the root surface resistance ($r_1$) as:

$$r_1 = \frac{1}{L_p \times k_{geom} \cdot \pi \cdot r_{root}^2 \cdot h_{root}} \quad (1)$$

and the resistance for axial flow[3] ($r_2$) as:

$$r_2 = \frac{2 \cdot r_{crown} + h_{stem} + r_{croot} \cdot r_{root}}{k_{f,sap} \cdot \pi \cdot r_{stem}^2} \quad (2)$$

The resource acquisition by an individual tree was partitioned into two: the aboveground light interception and belowground water uptake. Both processes are influenced by the individual's above- and below-ground competitive strengths (*above_c* and *below_c*, respectively) to attain the optimal values, with the minimum values corresponding to the available resources. We calculated the allocation of aboveground light ($res_a$) and belowground water ($res_b$) using the formulae presented in equations 3 and 4 respectively. The part available resources ($res_{avail}$) allocated for total biomass growth (equation 5) is dependent on the proportion required for maintenance process.

$$res_a = above\_c \cdot k_{rel} \times R_{solar} \cdot \pi \cdot r_{crown}^2 \quad (3)$$

$$res_b = below\_c \cdot \frac{-\left(psi_{leaf} + (9.81 kPa \cdot m^{-1}) \cdot (h_{stem} + 2 \cdot r_{crown}) + (85 kPa \cdot ppt^{-1}) \cdot sal\right)}{(r_1 + r_2) \cdot (9.81 kPa \cdot m^{-1})} \quad (4)$$

$$biomass\ growth = k_{grow} \cdot (res_{avail} - k_{maint} \cdot v_{tree}) \quad (5)$$

We applied four weight measures (two in the above- and another two belowground) to distribute the *biomass growth,* such that the tree grows mainly to maximize the increase in specific allometric measures for improving subsequent resource acquisition at the bottleneck. In defining how strong the mechanism of either the above- ($wa_1$, $wa_2$) or below-ground ($wb_1$, $wb_2$) shall predominated, we set some standardized criteria, with corresponding equations as shown below:

i. check to what extent the tree is lacking either of the above- or below-ground resources, with the value $Q_{res}$ *set as:*

$$Q_{res} = \frac{res_a - res_b}{res_a + res_b} \quad (6)$$

ii. check which of the resistance component limits the water, with the value $Q_r$ *set as:*

$$Q_r = \frac{r_1 - r_2}{r_1 + r_2} \quad (7)$$

[3] The term in the formula's numerator correspond to the length of the xylem flow path

iii. where the area of projected crown overshadows the root zone, the aboveground competition is assumed dominating, and for this purpose, we set the variable $Q_{rad}$ to check the ratio of crown radius to root radius as:

$$Q_{rad} = \frac{r_{crown} - r_{root}}{r_{crown} + r_{root}} \quad (8)$$

The rules i – iii were implemented to define the weight measures for different tree components as shown below:

- the weight $wa_2$ modifies the rate of increment in stem height, $h_{stem}$

$$wa_2 = \frac{k_r, half\ \max}{1 + e^{-\frac{Q_{rad}}{sf_{sig,2}}}} \quad (9)$$

and the stem height growth ( $\Delta h_{stem}$ ) set as:

$$\Delta h_{stem} = \frac{wa_2 \cdot growth}{\pi \cdot r_{stem}^2} \quad (10)$$

- the crown radius ($r_{crown}$ ) increment modifier, weight $wa_1$ was defined as:

$$wa_1 = \frac{1 - wa_2}{1 + e^{-\frac{Q_{res}}{sf_{sig,1}}}} \quad (11)$$

while the crown radius increment ( $\Delta r_{crown}$ ) was set as:

$$\Delta r_{crown} = \frac{wa_1 \cdot growth}{2 \cdot \pi \cdot (r_{crown} \cdot h_{crown} \cdot r_{stem}^2)} \quad (12)$$

- the modifier for the growth of stem radius ($r_{stem}$), the weight $wb_2$ was estimated as:

$$wb_2 = \frac{1 - wa_1 - wa_2}{1 + e^{-\frac{Q_r}{sf_{sig,1}}}} \quad (13)$$

and the corresponding increment in the stem radius ( $\Delta r_{stem}$ ) computed as:

$$\Delta r_{stem} = \frac{wb_2 \cdot growth}{2 \cdot \pi \cdot r_{stem} \cdot (2 \cdot r_{crown} + h_{stem} + r_{croot} \cdot r_{root}^2)} \quad (14)$$

- the root radius ($r_{stem}$) growth modifier ($wb_1$) thus weighed as:

$$wb_1 = 1 - wa_1 - wa_2 - wb_2 \quad (15)$$

with the actual increment in the root radius ( $\Delta r_{root}$ ) set as:

$$\Delta r_{root} = \frac{wb_1 \cdot growth}{2 \cdot \pi \cdot r_{root} \cdot h_{root} + (r_{croot} \cdot \pi \cdot r_{stem}^2)} \quad (16)$$

*Tree-tree interactions*

The incorporation of two-dimensional ZOIs to the representation of each tree in order to describe local tree-to-tree interactions allowed the advancement of the original BETTINA single-tree model into a stand simulator, BETTINA_IBM. Basically, trees interacted in the BETTINA_IBM model while competing for growing space and light (aboveground), as well as they reach for belowground resources (e.g. water). The concept of competition among neighbouring trees was implemented through the resource sharing approach embedded in the Zone-Of-Influence ('ZOI', Weiner et al. (2001); May et al. (2009); (Lin et al., 2012)). We presented a simplified illustration scheme in the Figure 5-1 (bottom-right).The above- and below-ground 'ZOI' radii correspond to the $r_{crown}$ and $r_{root}$ respectively. Individual trees compete for resources with neighbouring other(s) in the overlapping parts of their 'ZOI'. We implemented disparate modes of competition in the aboveground canopy and the belowground root zones. For the aboveground interaction (marked with an index *above_c*), we applied a "completely asymmetric" competition, which mainly allows the taller individual of the competing neighbours to pre-empt the acquisition and utilization of the available resources at the expense of the overshadowed neighbouring trees. As an augmentation to the pure concept of "complete asymmetry" in tree competition (e.g. Lin et al. (2013)), a simple 'canopy light diffusion' module was included in the model to allow for the penetration of diffuse light through the canopy of a 'suppressed' tree depending on the availability and scale of gap mosaic(s) in the individual's vicinity. In the parallel, the belowground interaction mode (marked with an index *below_c*) was implemented as "completely symmetric" competition, where equity in resource sharing largely plays out among neighbouring individuals. In essence, neighbouring individuals can share the available belowground resources in equal proportions. Further details on the implementation procedure are highlighted in the appended ODD document.

*Tree mortality*

The process of natural mortality was programmed in connection to individual tree biomass productivity and growth repression, emerging in three distinct categories: i. suppressed growth due to competition ii. old age and the associated decline in biomass productivity and iii. water shortage and the increased cost of transport through the stem to the crown part (high maintenance cost). Trees die to any of the

indicated reasons when the biomass productivity falls below an assumed critical threshold. Specifically, when the tree volume increment at a particular time falls below a defined factor (mortality threshold) of one percent fraction of the accrual tree volume, such tree is designated for death. Once an individual is marked for death, the dimensions of the particular tree are recorded right before the eventual mortality takes place.

### 5.2.2 *Simulation settings*

We simulated monospecific forests of *A. germinans* in four contrasting mangrove environments (10 ppt, 30 ppt, 50 ppt and 70 ppt) to account for the effect of the interplay of salinity conditions and water stress on tree growth and structural development. The simulations ran for a span of 1000 time steps in 20 replications for each of the environmental settings (porewater salinity). In this study, porewater salinity essentially marks the degree of water stress in different habitat conditions. Further settings for the simulation experiments were cascaded into three levels: i. a scenario that mimicked the growth of an isolated (single) tree growing without any influence of a competing neighbouring individual ("solitary tree" scenario); ii. a scenario depicting the population of an even-aged tree cohorts where individual tree growth and mortality is co-influenced by its competitive strength and the local neighbourhood tree interactions ("plantation forest" scenario); and iii. a scenario that reflects the succession cycle of a population of trees competing with neighbouring others, natural mortality and recruitment of saplings, in resemblance of successional trajectories in natural forests ("natural forest" scenario).

During the simulation runs in the steps ii. and iii., the model was initialized by 8000 individual trees randomly distributed across an initially empty 1 hectare plot, to make an initial sapling density of 0.8 $m^{-2}$. In the case of step iii., 100 new individual saplings are randomly released for regeneration during each growth year. The chance of saplings' establishment largely depends on the Cartesian position at recruitment in relation to the local neighbourhood; only the saplings in the forest gaps and porous areas under crown boundaries become established while those completely overshadowed under the crown of existing trees died shortly after recruitment. For each simulated scenario, the growth metrics and the stem position of individual living trees were logged for subsequent data analyses. The logged data were analysed and compared to field measurements and selected benchmark ecological patterns in scientific literature.

### 5.2.3 *Benchmarks for model evaluation*

We have combined the use of the field measurements and some general patterns known to plant ecology, forestry and mangrove ecology as benchmark for evaluating the results from BETTINA_IBM model simulations against the empirical

and theoretical mangrove growth strategies in variable environments. Our evaluation procedure, which aimed at applying the model to reproduce known emergent tree growth and stand structural patterns, was cascaded into 3 levels as described under the simulation settings (1. individual tree level - "solitary tree" scenario, 2. stand structure of even-aged cohorts - "plantation forest" scenario, and 3. forest stand with regeneration - "natural forest" scenario).

The field measurements were obtained from the mangrove peninsula surrounding the Caeté bay, which extends over ~300 km southeast of the Amazon estuary near Bragança (Lara and Cohen, 2006), Pará (North Brazil). Our data collection efforts focussed on non-destructive characterization of 3D mangrove tree structure and biomass from contrasting growing conditions (at porewater salinity of 30 ppt and 50 – 70 ppt). The mangrove stands at the 30 ppt consisted mainly of tall *A. germinans* trees (ca. 30 -35 m high), while the plots characterized by 50 – 70 ppt were dominated by shorter individuals (max. height of 11 m). We used a rangefinder device (LaserACE 1000) to characterize the 3D tree shape/ skeleton, tree and trunk height (m), stem diameter (cm), crown dimensions (m) and projection area ($m^2$), and volume of biomass in trunk and branch components, from 26 dominant (top height) trees systematically distributed across five plots of 900 $m^2$ mangrove forest stands. In addition, the stem position, diameter, tree height and crown dimensions of all trees ≥ 5 cm diameter at the breast height were registered to characterize forest structure in the studied forest plots. We recorded ca. 17 – 25 % *Rhizophora mangle* and 6 – 10 % of *Laguncularia racemosa* individuals in the 30 ppt and 50 – 70 ppt mangrove stands respectively.

Specifically, model evaluation was based on the trends of height and diameter increments, biomass assimilation, root-to-shoot biomass partitioning, height-diameter relation (slenderness) of single tree growing under varying habitat conditions in comparison to the expected patterns, in similitude of the known tree responses to site quality in forestry (Berger and Hildenbrandt, 2003). At the stand level, we studied the environment-dependent trends of total accrued stand biomass over time (Berger et al., 2004); the trajectories of plant mass-density relation (the "self-thinning" process) as influenced by the environment-dependent plastic tree morphology and local interactions (Berger et al., 2002; Lin et al., 2013); and the "U-shaped" cumulative distribution of mortality across tree sizes. In addition, we used a selection of other forest structure indices as a further benchmark for the simulation results. The height-diameter relations of top trees at the end of simulations were compared to the field observations. The observed spatial point patterns using the pair correlation function of Baddeley and Turner (2005) and the Clark-Evans aggregation *R* index (Clark and Evans, 1954) were juxtaposed against the patterns recorded in the simulated stands.

### 5.2.4 *Data analyses and statistics*

At the individual tree level, we compared the patterns of tree development under varying salinity and water stress conditions. Specifically, we analysed the rate of stem diameter and height growth increments in relation to the stem diameter (often used as a surrogate for tree age), but also the increment in tree biomass assimilation over time. We obtained tree biomass as a product of model predicted tree volume and the specific wood gravity (730 kg.m$^{-3}$ of dry mass, in the case of *A. germinans*). For comparison sake, we considered the estimation of tree aboveground dry biomass from the tree stem diameter using the species-specific allometric models (Fromard et al., 1998; Olagoke et al., 2016). In addition, the trend of allometric relations of tree height and trunk height to the corresponding stem diameter (proxies for tree slenderness) in the course of tree development was considered.

To characterize the structure of simulated forest stands, we analysed a selection of indices across the studied scenarios. These include the trajectories of plant mass – tree density relations (self-thinning scaling) using the metabolic scaling theoretical value (West et al., 2009) as a reference, the relative distribution of tree mortality across size ranges over time, changes in the local tree interactions as measured by the Clark-Evans index for spatial aggregation (Clark and Evans, 1954). We computed the Clark-Evans, *R* index as:

$$R = \frac{\bar{r}_A}{\bar{r}_E} \cdots 0 \leq R \leq 2.15 \qquad (17)$$

where $\bar{r}_A$ represents the average distance from a tree to its nearest neighbour, with $\bar{r}_E$ as the mean expected value in a population at complete spatial randomness (CSR) where *R* = 1. The value of *R* < 1 results in tree clustering (spatial aggregation) while the structure shows increasing regular patterns as the value tend towards the upper limit of 2.15. We conducted the *Friedman's two-way* test to verify the statistical differences in all stand attributes over equivalent time-range (*sensu,* Davey and Flores (1993)) in the course of temporal stand development across the investigated salinity and water stress conditions.

As an example application of the BETTINA_IBM model, we considered to demonstrate that trees of similar crown sizes in contrasting environment (e.g. 30 ppt and 50 ppt) can develop with different quantity of aboveground tree biomass, depending on the environmental conditions, based on the hypothesis that the tree slenderness and diameter-crown allometric relation change with the prevailing abiotic environment. Thus, it makes a substantial implication for biomass estimations using remotely sensed aerial observations where pertinent information on the site factor is not properly resolved. The crown classes were defined dividing the crown

projection area (i.e., $CPA = \pi \cdot r_{crown}^2$). We carried out the Mann-Whitney U test to verify the statistical differences of the biomass distribution in different crown classes as influenced by the site factor (salinity and water stress).

All statistical analyses were conducted in R software 3.2.2 (R Core Team, 2015) using the packages: *spatstat* (Baddeley and Turner, 2005) to compute the pair correlation functions and the Clark-Evans *R* index and *pgirmess* (Giraudoux, 2016) for analysing the attributes of simulated forest stands.

## 5.3 Results

### *5.3.1 Model evaluation*

*Individual tree development*

From the analyses presented in Figure 5-2, we observed that adaptation of tree growth and biomass partitioning explicitly resulted from the parsimonious description of selected physiological and allocation processes in accordance to the current parameterization. Simulated trees showed a differential rate of realized periodic diameter increment in response to the prevailing ambient environmental conditions. For trees of similar stem diameters, the results revealed that the diameter increment was lowered by near 20% between a tree growing at simulated 10 ppt salinity condition and the counterpart in the 70 ppt habitat salinity (Figure 5-2a). Similarly, divergent rate of height growth was demonstrated for simulated trees of similar stem diameter when grown under contrasting salinity and water stressed habitat conditions. For instance, we recorded a periodic height increment of ca. 0.5 m a tree for a simulated tree at 10 ppt condition against the 0.1 m noted for corresponding sized tree at 70 ppt salinity over the same growth period. While the potential stem diameter and height climaxed at ca. 100 cm and 36 m respectively at 10 ppt salinity condition, we recorded the maximum of ca. 80 cm stem diameter and 14 m height under the 70 ppt condition (Figure 5-2c).

Individual tree in low salinity condition exhibited high stem slenderness, which decreased with increasing salinity. As individual in high salinity responded significantly to water limitation and increasing cost of water transportation, the tree shape showed adaptation with a maximum trunk height of ca. 3 - 4 m with an equivalent stem diameter sized tree reaching 15 m trunk height in the low salinity condition where no water shortage is encountered. Ditto to the intrinsic modification in tree forms, the simulated biomass assimilation and allocation patterns differed significantly in variable environmental conditions. Equivalent sized individuals displayed as high as a 50% difference in the biomass growth between low- and high salinity site conditions. Of the total tree biomass productivity, the root-shoot allocation ratio increased significantly from low- to high salinity habitats

(Figure 5-2f), demonstrating the adaptive tree root responses to limiting below-ground water supply.

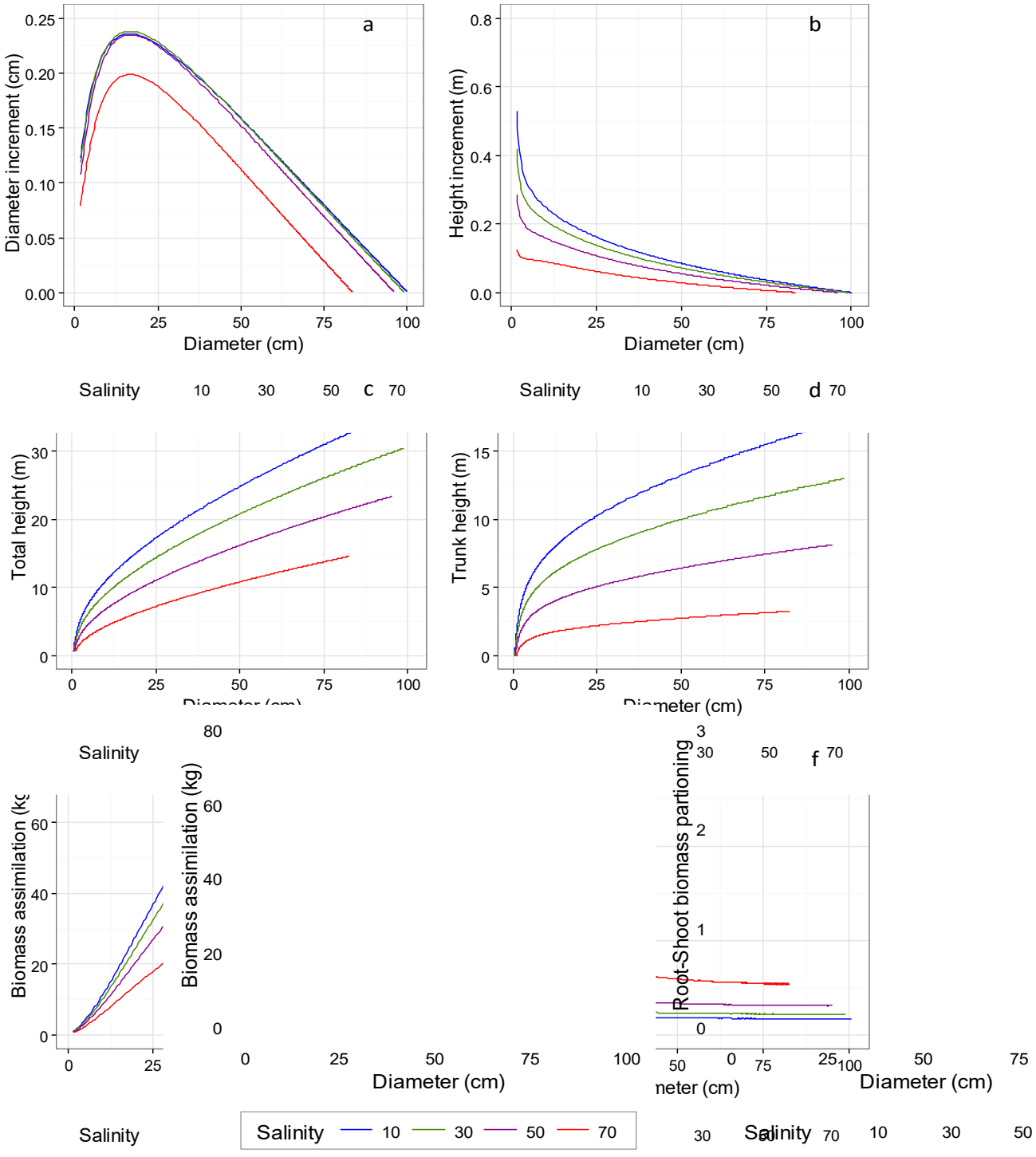


Figure 5-2: Divergent growth and biomass partitioning of simulated single trees (without competition) in relation to tree diameter under contrasting habitat salinity-water stress conditions

*Emergent patterns at the forest stand level*

Here, we aimed at scrutinizing the model performance in realistically reproducing the emergent forest structural patterns known to empirical observations in nature.

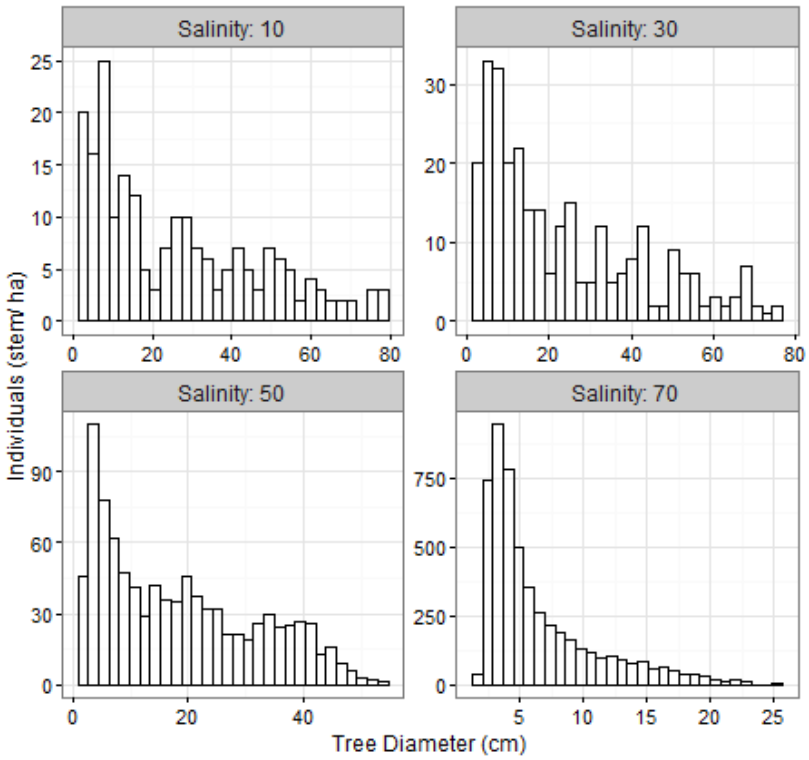


Figure 5-3: Diameter distribution of trees in the forest stands ("natural forest" scenario) under different salinity conditions at the final simulation time step

We observed that the diameter distribution of pooled trees in the simulated stands culminated in the general log-normal ("inverted-J") size-density structure of natural forest stands. Specifically, we recorded high proportion of small diameter trees and gradual decline with increasing tree sizes, until a relatively small proportion of the largest individuals in all investigated scenarios of stand salinity conditions (Figure 5-3). For low salinity conditions, few individuals of trees as large as 80 cm stem diameter were observed. In contrast, the largest individuals had stem diameters peaked at ca. 55 cm and 25 cm for stands simulated at 50 ppt and 70 ppt salinity conditions respectively.

Relatedly, we showed in Figure 5-4 that the maximum total height attained by the largest individuals decreased from ca. 38 m to 3 m in the order of simulated stand salinity conditions. The height-diameter allometry of all trees larger than 5 cm stem diameter at the final simulation period in the simulated stands in relation to the field measurement in stands of comparable salinity conditions (Figure 5-4). Most tree measurements from the two contrasting site salinity conditions (30 ppt and 50-70 ppt) clustered around the predicted curves fitted for trees in corresponding

simulated habitat conditions. The scaling exponent of tree height to a corresponding diameter decline from ca. 0.63 to 0.35 between the investigated low- and high salinity environments in comparison to 0.66 - 0.28 exponents recorded in the empirical observations.

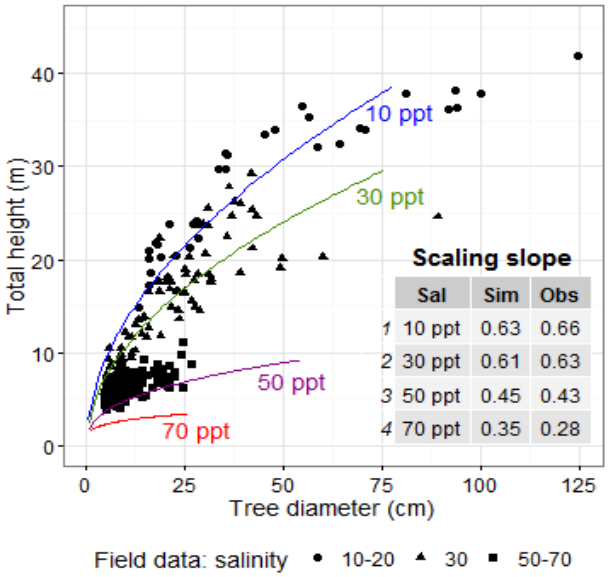


Figure 5-4: Height-diameter allometric relations of simulated stands ("natural forest" scenario) in comparison to the field observations under different site salinity and water limitations

We examined the temporal spatial structure of tree distribution to gain understanding into how the emergent patterns of local tree-to-tree interactions change in the course of time given the influence of the environment-induced plasticity of tree forms and biomass partitioning in the simulated stands (Figure 5-5).

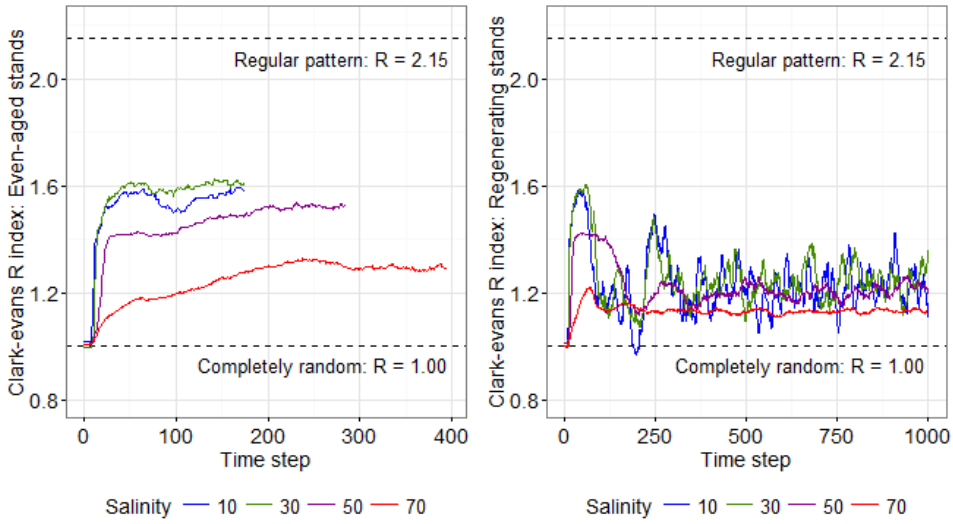


Figure 5-5: Temporal changes in the local tree-to-tree interactions (competition), as measured by the average Clark-Evans aggregation R index. *Left: even-aged cohort plantation, Right: dynamics in regenerating natural forest scenario*

The results of the Friedman test for comparison of Clark-Evans aggregation *R* index showed significant differences in competition intensities ($p < 0.001$) in the course of stand development under variable salinity conditions, both in the even-aged plantation and regenerating natural forest scenarios. On the average, the intensity of tree-to-tree local competition decreased with increasing ambient salinity in the simulated stands. The interactions of environment-induced tree forms and local competition intensity produced a significant effect on the trajectories of plant biomass-density relations, the so-called "self-thinning" process (i.e., how the number of trees in a particular stand changes with average biomass in the course of stand development) in the simulated stands. With reference to the theoretical slope of '-4/3' , we observed a clear shift in the self-thinning slope of the simulated even-aged plantation forest scenarios from -1.34 to -0.99 (Table 5-3) between the investigated low- and high salinity forest stands (Figure 5-6).

Table 5-3: Mean slopes and intercepts of plant biomass – density relations in simulated stands of contrasting habitat salinity and water stress conditions.

| Salinity (ppt) | Slope* | | | Intercept* | | |
|---|---|---|---|---|---|---|
| | Upper C.I. | Mean value | Lower C.I. | Upper C.I. | Mean value | Lower C.I. |
| 10 | -1.325 | -1.338 | -1.352 | 6.335 | 6.305 | 6.274 |
| 30 | -1.298 | -1.312 | -1.326 | 6.300 | 6.268 | 6.237 |
| 50 | -0.996 | -1.024 | -1.052 | 5.712 | 5.702 | 5.692 |
| 70 | -0.981 | -0.988 | -0.995 | 5.445 | 5.437 | 5.428 |

***** *Values were obtained from logarithmic transformed scale.*

Sequel to the 'self-thinning' phase, all stands seemed to attain the asymptotic stage where the decline in the number of trees and subsequent biomass change balanced out. This quasi-equilibrium stage in the plant biomass – density trajectories were reached at different periods under varying site salinity, marking the divergence of biomass growth rate and mortality from competition effect in different habitat conditions. From the current parameterization, the low salinity forest stands approached the asymptote after about 200 growth cycles, while the phase was delayed until ca. 400 and 600 growth cycles in the 50 ppt and 70 ppt high salinity forest stands respectively. When systematic field observations from the 30 – 60 ppt salinity conditions were distributed around the corresponding self-thinning lines, the data from 10-20 ppt forest stands suggest a steeper slope in the approximate range of Yoda "-3/2" self-thinning rule (Yoda et al., 1963).

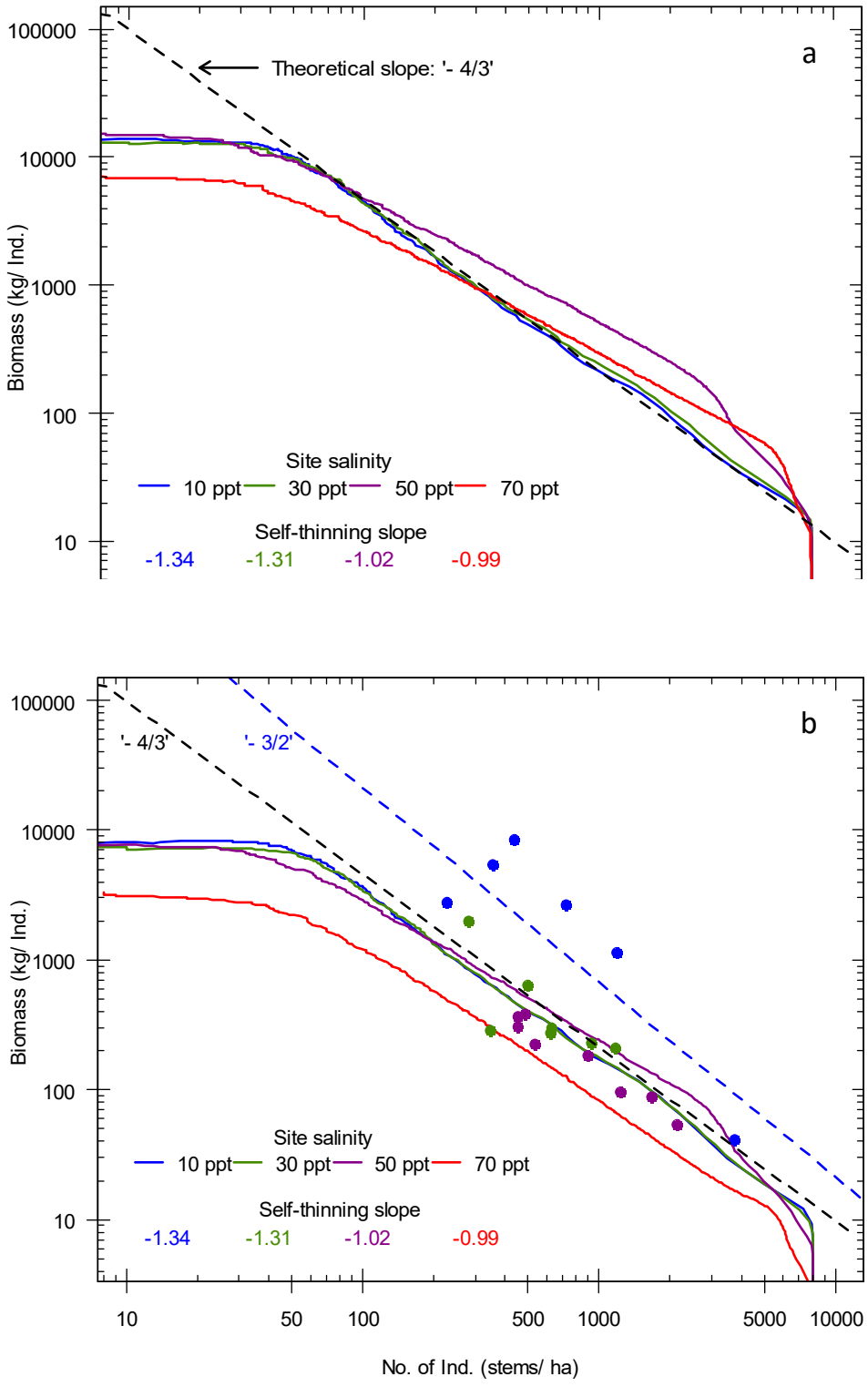


Figure 5-6: Trajectories of plant biomass-density relations ("Self-thinning" process) of simulated stands as influenced by different habitat salinity and water stress conditions. *a. total biomass trajectories, and b. aboveground biomass trajectories in relation to field data*

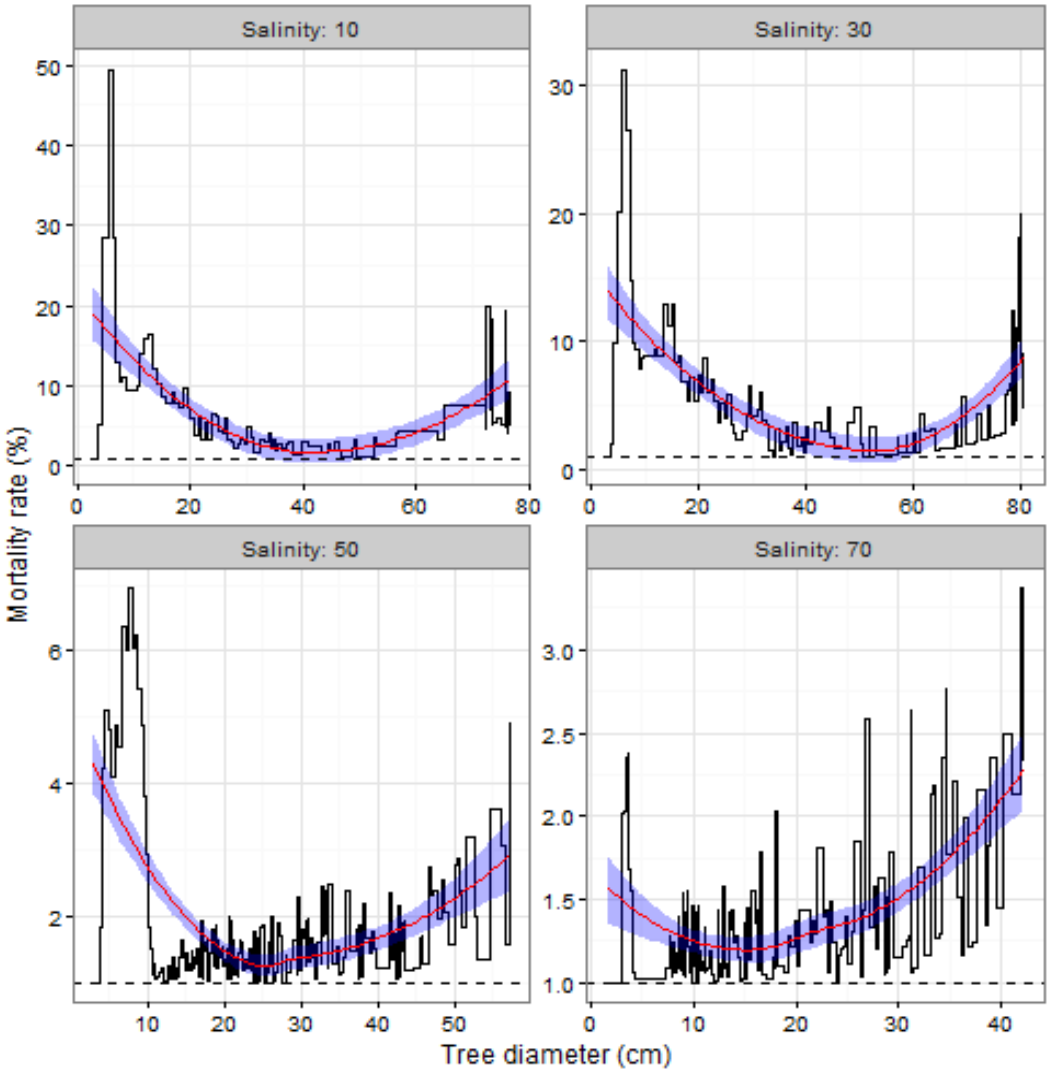


Figure 5-7: Distribution of tree mortality in relation to the diameter size classes in the course of simulated stand development (under "natural forest" scenario) in different habitat salinity-water stress conditions.

In Figure 5-7, we illustrate the changes in the pattern of mortality with increasing tree sizes and the influence of variable ambient environmental conditions. While the mortality rate-size distribution patterns fairly correspond to the empirically known U-shaped curve in general ecology and biostatistics, the rate at which smaller individuals died at the early phase in the successional development decreased significantly with increasing effect of salinity and water stress in the investigated forest stands. In effect, the average mortality rate related to the initial tree density shifted from over 20% to ca. 2% between the 10 ppt and 70 ppt simulated forest stands.

### 5.3.2 *Example model application: relating tree biomass to crown structure*

For a demonstration of the significance of the current modelling approach, we analysed biomass of trees with similar crown projection area (CPA) growing in two stands of contrasting water stress conditions, with site salinity of 30 ppt and 50 ppt respectively. The experiment expound on the hypothesis that tree slenderness and inherent biomass composition are restrained by water stress, that trees with equivalent CPA sizes differ significantly in their aboveground biomass. Apparently, these forest stands showed distinct tree size structure and ditto for crown formations, as presented in the simplified stand mock-ups (Figure 5-8a &b). All trees in the simulated stands were classified into 5 $m^2$ CPA class intervals, and the comparative analysis of tree biomass was restricted to CPA classes with representatives in both stands.

For trees of equivalent crown dimensions, stem diameters differ significantly: trees in the 50 ppt simulated stands displayed as twice the sizes of the counterparts in the 30 ppt site conditions (Figure 5-8c). Meanwhile, the trees in the 50 ppt stands exhibited less slenderness in comparison to individual trees in the 30 ppt stands (Figure 5-8d). Moreover, trees in the 30 ppt stands had 2-fold measures of the ratio of crown diameter to stem diameter (KD-ratio) than trees with similar crown projection area in the simulated 50 ppt stands (Figure 5-8e). Consequently, we recorded significantly different tree biomass (Mann-Whitney-Wilcoxon Test, $p < 0.001$) from trees of equivalent crown dimensions, with a coefficient of variation reaching 23%, between these two simulated stands (Figure 5-8f). In this case, the individuals growing in the high salinity conditions had higher biomass than the low salinity counterparts did.

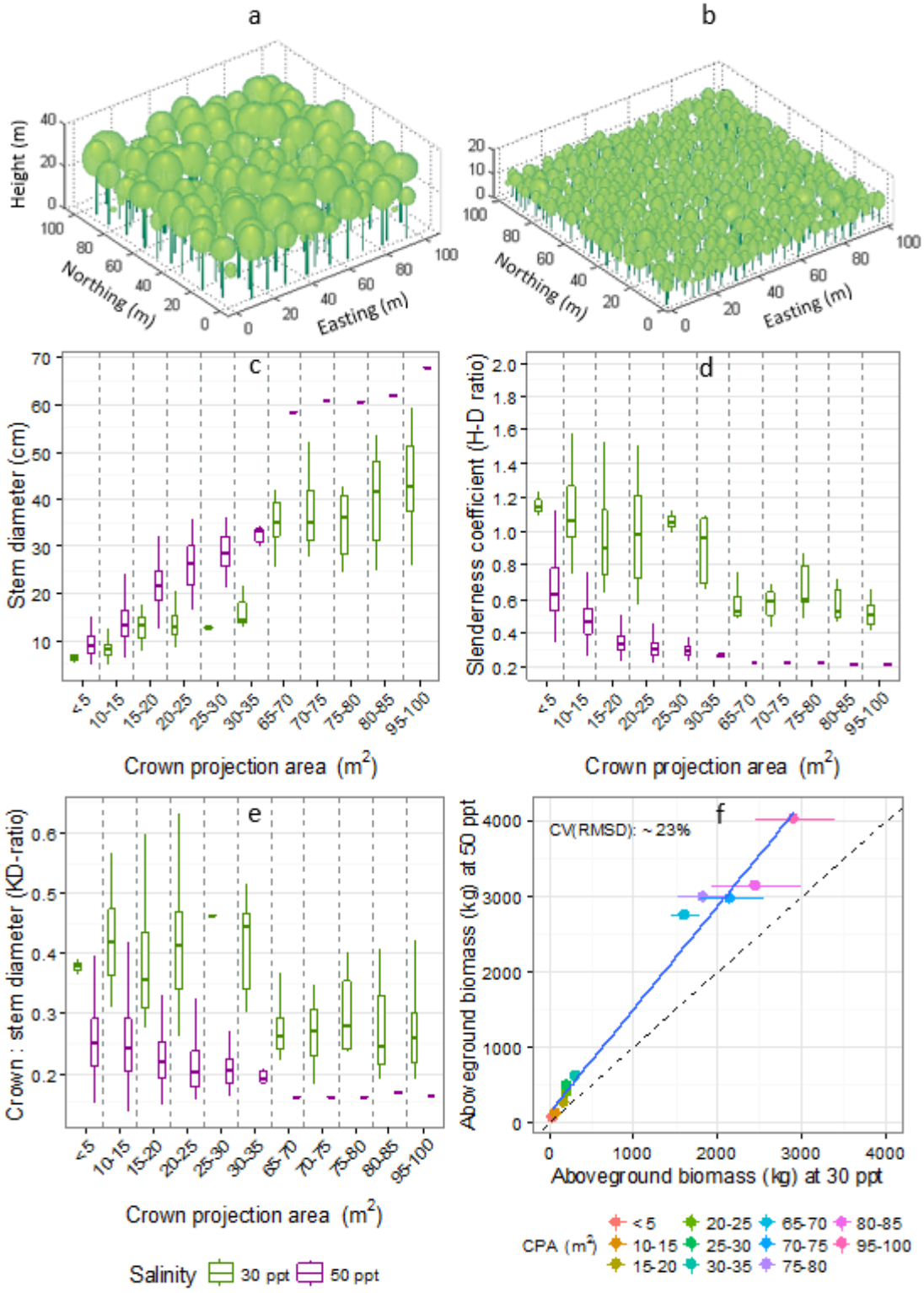


Figure 5-8: Tree structure and biomass distribution in different crown classes under contrasting habitat conditions. *a. & b. provided simple 3D tree mock-ups in the simulated 30 ppt and 50 ppt mangrove forest stands respectively; c. & d. compared the diameters and slenderness coefficient of trees in selected crown classes; and e. compared the average (+/- bidirectional standard errors) of aboveground biomass in corresponding crown classes and the dashed line represents the 1:1 scenario.*

## 5.4 Discussion

Understanding how the environment-induced morphological plasticity of mangrove trees and the underlying ecological processes interplay in the dynamics of forest structural development generally require long-term studies and extensive datasets. The previous chapters, for example, have demonstrated some advancements towards acquiring such datasets using laser scanning (e.g., Olagoke et al. (2016)) and classical inventories supported by 3D processing tools. The precision of these and similar empirical approaches is well acknowledged, but the efforts, costs and time requirements are equally substantial. To this end, we consider stand simulation modelling as a viable complementary approach. The case of BETTINA_IBM presented in this study showcase for the first time the consideration for morphological plasticity in the simulation of structural development of mangrove forests growing in variable environments.

Here, we present the evaluation of the BETTINA_IBM mangrove stand simulator in the objective of demonstrating its suitability to describe how the individual tree's response to changes in abiotic conditions (mainly salinity and water stress) shapes the structural development of mangrove forests. In addition, we demonstrated through the current modelling approach how the accuracy of remotely measured tree biomass through crown metrics can be impacted by the variability of tree slenderness and crown-diameter relation in variable environments. Our simulation results largely suggest that the model reproduced comparable patterns to empirical ecological observations on the plasticity of tree morphology and the associated consequences for stand level forest dynamics in variable environments. The following discussion of our modelling results and observations in informative on the prospect of this model in the study of mangrove forest dynamics.

Mangrove trees typically display high morphological plasticity to salinity, water and nutrient limitations (Ball, 2002; Feller et al., 2010), with several empirical cases recorded in the literature (Lovelock et al., 2006; Vogt et al., 2014; Vovides et al., 2014). From these studies, there emerge a consensus that the metabolic processes and growth rates of individual trees decline with increasing salinity conditions (Ball 2002; Feller et al., 2010), leading to restricted height growth and productivity (Cintron et al., 1978). In a similar manner, the results of our simulation study yielded differential growth rates under varying salinity conditions. The model predicted decreasing height and diameter growth with decreasing biomass productivity along a gradient of increasing salinity. These results equally relate to the behaviour of empirical site quality models for terrestrial forests (e.g., Bowman et al. (2013); Palahí et al. (2008); Uzoh and Oliver (2006)).

According to That simulated trees increase investment in the root components as salinity increases and utilizable water resource becomes less available, places BETTINA_IBM model more in consonance to various empirical observations from mangrove forests (e.g. Nguyen et al. (2015); Castañeda-Moya et al. (2011); Cintron and Schaeffer-Novelli (1984); (Soto, 1988)). Apparently, the description of preferential biomass partitioning to component tree parts at the bottleneck of water uptake (Peters et al., 2014), but also the costs imposed by water transport (hydraulic conductivity) from the root to the leaves (Koch et al., 2004) sufficiently drive trees to divergent architecture and biomass growth across variable salinity conditions in the BETTINA_IBM simulation. This feature, perhaps, marks a key strength of the model as compared to earlier modelling efforts (Berger and Hildenbrandt, 2000; Grueters et al., 2014) that explain tree growth solely by deterministic functions.

Generally, many aspects of forest structure and underlying ecological processes do emerge directly from the expressed architecture of the component trees in the course of their interactions with each other and the ambient environment (Kerkhoff and Enquist, 2007; King, 1990; West et al., 2009). In the case of mangrove forests, Feller et al. (2010) highlighted that high levels of trait plasticity in trees can yield forests of widely divergent structure. In consonance with these assertions, the results from the simulated forest stands under varying salinity and water stress conditions culminated in significantly diverse forest structures. As demonstrated in Figure 5-4, the fits of height – diameter allometry of simulated trees obtained with the current parameterization practically match the overlaid field measurements. Although, the maximum height and diameter values predicted for low salinity conditions (10 – 30 ppt) are relatively lower than observed in some tall mangrove forests (e.g. Fromard et al. (1998); Olagoke et al. (2016)). Refining the model to achieve tree simulation reaching the potential maximum height and diameter under favourable conditions are certainly of interest to improve current model formulations.

As suggested by Grime (1977), and more recent studies in light of the stress gradient hypothesis (e.g., Bertness and Callaway (1994); Maestre et al. (2009)), the intensity of competitive interactions reduces with increasing gradient of stressful environmental cues, and could possibly shift to a facilitative form in more adverse conditions (Callaway et al., 2003). The occurrence of such phenomenon in mangrove forest stands was highlighted in the work of Vogt et al. (2014). In the frame of our simulation experiments, the impact of divergent tree morphological scaling on neighbourhood competition in habitats of contrasting salinity conditions was clearly detectable. First, the importance of asymmetric competition for light reduces as contact between trees decreases with declining biomass investment in crown growth along a gradient of increasing salinity. The second possible explanation

relates to the fact that increasing allocation to the root, when water becomes limiting, would mean an increasing magnitude of belowground symmetric interactions leading to an overall decrease in the effect of competition with increasing site salinity. Though we initiated all stand simulations in a randomly spatial structure, we recorded nearly threefold differences in the magnitude of tree competition intensity between the relatively low- and high salinity conditions. As much as the results appear very reasonable, we still lack sufficient data and published information to validate or generalize on the exactness of the competitive strength obtained under the simulated site conditions.

One interesting results from our simulation experiments appears promising in shedding light to the lingering debates on the "universality" of the trajectories of density-dependent mortality, the so-called "self-thinning rule" in even-aged plant communities. While Yoda et al. (1963) postulated a self-thinning trajectory with a constant slope of '-3/2' on the basis that tree relative to a given growing space shapes in simple Euclidean geometry, the formulations of West et al. (1999) and Enquist et al. (1998) in the frame of metabolic scaling theory suggested a contrasting trajectory with '-4/3' slope. Like demonstrated empirically in Pretzsch (2006), but also in some theoretical works (e.g. Deng et al. (2006); Lin et al. (2013)), the slope of self-thinning line (plant biomass–density relationship) is largely dependent on tree shapes, consequently resulting from the interactions of the abiotic environment and neighbourhood competition. Our analysis resulted in self-thinning slopes ranging from ca. -1.34 in the low salinity (10 ppt) stand to ca. -0.99 in the higher salinity stand (70 ppt). These results generally agree with earlier studies (Deng et al. (2006); Lin et al. (2013)) that the slopes of self-thinning trajectories become shallower with increasing water or nutrient limitations. However, a comparison of the simulation results with field measurements show that self-thinning process could reach steeper slopes in the low salinity conditions, suggesting that the current model formulation under-predicted tree biomass in low salinity conditions.

Relatedly, the analysis of size-dependent rate of tree mortality in the course of stand development displayed the U-shaped mortality curve commonly described in various empirical time-series studies (e.g. Monserud and Sterba (1999); Holzwarth et al. (2013)) as well as earlier simulation studies (e.g. Berger et al. (2004)). Common to all simulated forest stands was the high mortality of small-sized trees at the early successional stage when the asymmetric competition for light is relatively dominant, and declined to the lowest point at the intermediate developmental stage prior to a rise at the later successional stage when much larger individuals died. The rise of mortality in the late successional stage is, however driven by differing factors in our model. While the later rise in the death of larger individuals might have resulted from age-related mortality in the low salinity condition, our results showed that mortality

is consequent to the increasing water limitation and cost of hydraulic conductivity in the high salinity forests.

One aspect in the application of remote sensing technology receiving much attention in the recent time centres on linking canopy structure to tree or forest aboveground biomass (e.g. Popescu et al. (2003); Proisy et al. (2007)) and other forest structural parameters (Barbier et al., 2012; Couteron et al., 2005). Mostly, the available techniques rely on crown-diameter allometric relations for predicting forest parameters of interest on the assumption that the allometry mostly converge at the stand levels (Bohlman and Pacala, 2012; Muller-Landau et al., 2006), or universally constant (West et al., 2009). The challenge remains that the accuracy of these methods can easily be compromised should a change local environmental condition results in a significant change in crown allometry, simply crown plasticity (Grueters et al., 2014; Purves et al., 2007).

With the application of BETTINA_IBM model, we assessed how changes in tree allometric relations under different salinity conditions could influence the accuracy of biomass estimates from crown metrics. Our results clearly demonstrated that trees simulated at 50 ppt salinity conditions are higher in aboveground biomass in comparison to equivalent projected crown-size trees in the lower salinity condition (30 ppt). One clear explanation is that trees in the higher salinity conditions prioritize less biomass to crown development for a given diameter size, and thus the characteristic crown – diameter ratio (KD ratio) of a tree in high salinity becomes relatively lower than in low salinity conditions. These results agree with the findings of Vovides et al. (2014), where a decrease in the KD ratio of *A. germinans* trees with increasing salinity was empirically demonstrated. Based on this analysis, a coupling of mechanistic modelling to the remote sensing methods may thus be a worthwhile effort to benefit the study of forest biomass, but also the dynamics of forest structure at large. While the remote sensing techniques offer potentials to supply data for improved parameterization of mechanistic models, chances are high that mechanistic modelling provides finer calibration for remote measurements.

## 5.5 Conclusion

Conclusively, the BETTINA_IBM model presented here offer new opportunities to link morphological plasticity and biomass allocation with prevailing ambient environmental conditions in realizing observed forest structural patterns in a mechanistic modelling framework. Through this model, chances abound that various factors shaping tree morphological changes and the resulting influence of forest structure and dynamics could be probed and quantified at different temporal and spatial scales. Furthermore, the example demonstration in this study found a footing as the fundamental step in the coupling of mangrove simulation modelling and

remote sensing techniques. While we are optimistic that time series analyses of remotely sensed data could provide additional information to optimize current model parameters and/ or constrain the modelling processes in various scales, the current effort has a prospect for providing relevant information for calibrating some satellite-based observation of forest structure.

## 5.6 References

Baddeley, A., and Turner, R. (2005). spatstat: An R Package for Analyzing Spatial Point Patterns. *Journal of Statistical Software; Vol 1, Issue 6 (2005)*.

Ball, M. C. (2002). Interactive effects of salinity and irradiance on growth: implications for mangrove forest structure along salinity gradients. *Trees-Structure and Function* **16**, 126-139.

Barbier, N., Couteron, P., Gastelly-Etchegorry, J.-P., and Proisy, C. (2012). Linking canopy images to forest structural parameters: potential of a modeling framework. *Annals of Forest Science* **69**, 305-311.

Berger, U., and Hildenbrandt, H. (2000). A new approach to spatially explicit modelling of forest dynamics: spacing, ageing and neighbourhood competition of mangrove trees. *Ecological Modelling* **132**, 287-302.

Berger, U., and Hildenbrandt, H. (2003). The strength of competition among individual trees and the biomass-density trajectories of the cohort. *Plant Ecology* **167**, 89-96.

Berger, U., Hildenbrandt, H., and Grimm, V. (2002). Towards a standard for the individual-based modeling of plant populations: self-thinning and the field of neighborhood approach. *Natural resource modeling* **15**, 39-54.

Berger, U., Hildenbrandt, H., and Grimm, V. (2004). Age-related decline in forest production: modelling the effects of growth limitation, neighbourhood competition and self-thinning. *Journal of Ecology* **92**, 846-853.

Berger, U., Rivera-Monroy, V. H., Doyle, T. W., Dahdouh-Guebas, F., Duke, N. C., Fontalvo-Herazo, M. L., Hildenbrandt, H., Koedam, N., Mehlig, U., Piou, C., and Twilley, R. R. (2008). Advances and limitations of individual-based models to analyze and predict dynamics of mangrove forests: A review. *Aquatic Botany* **89**, 260-274.

Bertness, M. D., and Callaway, R. (1994). Positive interactions in communities. *Trends in Ecology & Evolution* **9**, 191-193.

Bohlman, S., and Pacala, S. (2012). A forest structure model that determines crown layers and partitions growth and mortality rates for landscape-scale applications of tropical forests. *Journal of Ecology* **100**, 508-518.

Bowman, D. M. J. S., Brienen, R. J. W., Gloor, E., Phillips, O. L., and Prior, L. D. (2013). Detecting trends in tree growth: not so simple. *Trends in Plant Science* **18**, 11-17.

Callaway, R. M., Pennings, S. C., and Richards, C. L. (2003). Phenotypic plasticity and interactions among plants. *Ecology* **84**, 1115-1128.

Castañeda-Moya, E., Twilley, R. R., Rivera-Monroy, V. H., Marx, B. D., Coronado-Molina, C., and Ewe, S. M. L. (2011). Patterns of Root Dynamics in Mangrove Forests Along Environmental Gradients in the Florida Coastal Everglades, USA. *Ecosystems* **14**, 1178-1195.

Cintron, G., Lugo, A. E., Pool, D. J., and Morris, G. (1978). Mangroves of Arid Environments in Puerto Rico and Adjacent Islands. *Biotropica* **10**, 110-121.

Cintron, G., and Schaeffer-Novelli, Y. (1984). Methods for studying mangrove structure. *In* "The mangrove ecosystem: research methods" (S. C. Snedaker and J. G. Snedaker,

eds.), pp. 91-113. United Nations Educational, Scientific and Cultural Organization (UNESCO), Paris.

Clark, P. J., and Evans, F. C. (1954). Distance to Nearest Neighbor as a Measure of Spatial Relationships in Populations. *Ecology* **35**, 445-453.

Clough, B. F., Dixon, P., and Dalhaus, O. (1997). Allometric relationships for estimating biomass in multi-stemmed mangrove trees. *Australian Journal of Botany* **45**, 1023-1031.

Couteron, P., Pélissier, R., Nicolini, E., and Paget, D. (2005). Predicting tropical forest stand structure parameters from Fourier transform of very high-resolution remotely sensed canopy figures. *Journal of Applied Ecology* **42**, 1121-1128.

Davey, A. M., and Flores, B. E. (1993). Identification of seasonality in time series: A note. *Mathematical and Computer Modelling* **18**, 73-81.

Deng, J.-M., Wang, G.-X., Morris, E. C., Wei, X.-P., Li, D.-X., Chen, B.-M., Zhao, C.-M., Liu, J., and Wang, Y. U. N. (2006). Plant mass–density relationship along a moisture gradient in north-west China. *Journal of Ecology* **94**, 953-958.

Enquist, B. J., Brown, J. H., and West, G. B. (1998). Allometric scaling of plant energetics and population density. *Nature* **395**, 163-165.

Feller, I. C., Lovelock, C. E., Berger, U., McKee, K. L., Joye, S. B., and Ball, M. C. (2010). Biocomplexity in Mangrove Ecosystems. *Annual Review of Marine Science* **2**, 395-417.

Fromard, F., Puig, H., Mougin, E., Marty, G., Betoulle, J. L., and Cadamuro, L. (1998). Structure, above-ground biomass and dynamics of mangrove ecosystems: new data from French Guiana. *Oecologia* **115**, 39-53.

Giraudoux, P. (2016). pgirmess: Data Analysis in Ecology.

Grime, J. P. (1977). Evidence for the Existence of Three Primary Strategies in Plants and Its Relevance to Ecological and Evolutionary Theory. *The American Naturalist* **111**, 1169-1194.

Grimm, V., Berger, U., Bastiansen, F., Eliassen, S., Ginot, V., Giske, J., Goss-Custard, J., Grand, T., Heinz, S. K., and Huse, G. (2006). A standard protocol for describing individual-based and agent-based models. *Ecological Modelling* **198**, 115-126.

Grimm, V., Berger, U., DeAngelis, D. L., Polhill, J. G., Giske, J., and Railsback, S. F. (2010). The ODD protocol: A review and first update. *Ecological Modelling* **221**, 2760-2768.

Grueters, U., Seltmann, T., Schmidt, H., Horn, H., Pranchai, A., Vovides, A. G., Peters, R., Vogt, J., Dahdouh-Guebas, F., and Berger, U. (2014). The mangrove forest dynamics model mesoFON. *Ecological Modelling* **291**, 28-41.

Holzwarth, F., Kahl, A., Bauhus, J., and Wirth, C. (2013). Many ways to die – partitioning tree mortality dynamics in a near-natural mixed deciduous forest. *Journal of Ecology* **101**, 220-230.

Kerkhoff, A. J., and Enquist, B. J. (2007). The Implications of Scaling Approaches for Understanding Resilience and Reorganization in Ecosystems. *BioScience* **57**, 489-499.

King, D. A. (1990). The Adaptive Significance of Tree Height. *The American Naturalist* **135**, 809-828.

Koch, G. W., Sillett, S. C., Jennings, G. M., and Davis, S. D. (2004). The limits to tree height. *Nature* **428**, 851-854.

Krauss, K. W., Young, P. J., Chambers, J. L., Doyle, T. W., and Twilley, R. R. (2007). Sap flow characteristics of neotropical mangroves in flooded and drained soils. *Tree Physiology* **27**, 775-783.

Lara, R., and Cohen, M. (2006). Sediment porewater salinity, inundation frequency and mangrove vegetation height in Bragança, North Brazil: an ecohydrology-based empirical model. *Wetlands Ecology and Management* **14**, 349-358.

Lin, Y., Berger, U., Grimm, V., Huth, F., and Weiner, J. (2013). Plant Interactions Alter the Predictions of Metabolic Scaling Theory. *PLoS ONE* **8**, e57612.

Lin, Y., Berger, U., Grimm, V., and Ji, Q.-R. (2012). Differences between symmetric and asymmetric facilitation matter: exploring the interplay between modes of positive and negative plant interactions. *Journal of Ecology* **100**, 1482-1491.

Lopez-Portillo, J., Ewers, F. W., Mendez-Alonzo, R., Paredes Lopez, C. L., Angeles, G., Alarcon Jimenez, A. L., Lara-Dominguez, A. L., and Torres Barrera, M. D. (2014). Dynamic control of osmolality and ionic composition of the xylem sap in two mangrove species. *Am J Bot* **101**, 1013-1022.

Lovelock, C. E., Ball, M. C., Choat, B., Engelbrecht, B. M. J., Holbrook, N. M., and Feller, I. C. (2006). Linking physiological processes with mangrove forest structure: phosphorus deficiency limits canopy development, hydraulic conductivity and photosynthetic carbon gain in dwarf Rhizophora mangle. *Plant, Cell & Environment* **29**, 793-802.

Maestre, F. T., Callaway, R. M., Valladares, F., and Lortie, C. J. (2009). Refining the stress-gradient hypothesis for competition and facilitation in plant communities. *Journal of Ecology* **97**, 199-205.

May, F., Grimm, V., and Jeltsch, F. (2009). Reversed effects of grazing on plant diversity: the role of below-ground competition and size symmetry. *Oikos* **118**, 1830-1843.

Monserud, R. A., and Sterba, H. (1999). Modeling individual tree mortality for Austrian forest species. *Forest Ecology and Management* **113**, 109-123.

Muller-Landau, H. C., Condit, R. S., Chave, J., Thomas, S. C., Bohlman, S. A., Bunyavejchewin, S., Davies, S., Foster, R., Gunatilleke, S., Gunatilleke, N., Harms, K. E., Hart, T., Hubbell, S. P., Itoh, A., Kassim, A. R., LaFrankie, J. V., Lee, H. S., Losos, E., Makana, J.-R., Ohkubo, T., Sukumar, R., Sun, I. F., Nur Supardi, M. N., Tan, S., Thompson, J., Valencia, R., Muñoz, G. V., Wills, C., Yamakura, T., Chuyong, G., Dattaraja, H. S., Esufali, S., Hall, P., Hernandez, C., Kenfack, D., Kiratiprayoon, S., Suresh, H. S., Thomas, D., Vallejo, M. I., and Ashton, P. (2006). Testing metabolic ecology theory for allometric scaling of tree size, growth and mortality in tropical forests. *Ecology letters* **9**, 575-588.

Muller, E., Lambs, L., and Fromard, F. (2009). Variations in water use by a mature mangrove of Avicennia germinans, French Guiana. *Annals of Forest Science* **66**, 803-803.

Nguyen, H. T., Stanton, D. E., Schmitz, N., Farquhar, G. D., and Ball, M. C. (2015). Growth responses of the mangrove Avicennia marina to salinity: development and function of shoot hydraulic systems require saline conditions. *Annals of Botany* **115**, 397-407.

Olagoke, A., Proisy, C., Féret, J.-B., Blanchard, E., Fromard, F., Mehlig, U., de Menezes, M. M., dos Santos, V. F., and Berger, U. (2016). Extended biomass allometric equations for large mangrove trees from terrestrial LiDAR data. *Trees* **30**, 935-947.

Palahí, M., Pukkala, T., Kasimiadis, D., Poirazidis, K., and Papageorgiou, A. C. (2008). Modelling site quality and individual-tree growth in pure and mixed Pinus brutia stands in north-east Greece. *Annals of Forest Science* **65**, 501-501.

Peters, R., Vovides, A. G., Luna, S., Grüters, U., and Berger, U. (2014). Changes in allometric relations of mangrove trees due to resource availability – A new mechanistic modelling approach. *Ecological Modelling* **283**, 53-61.

Popescu, S. C., Wynne, R. H., and Nelson, R. F. (2003). Measuring individual tree crown diameter with lidar and assessing its influence on estimating forest volume and biomass. *Canadian Journal of Remote Sensing* **29**, 564-577.

Pretzsch, H. (2006). Species-specific allometric scaling under self-thinning: evidence from long-term plots in forest stands. *Oecologia* **146**, 572-583.

Proisy, C., Couteron, P., and Fromard, F. (2007). Predicting and mapping mangrove biomass from canopy grain analysis using Fourier-based textural ordination of IKONOS images. *Remote Sensing of Environment* **109**, 379-392.

Purves, D. W., Lichstein, J. W., and Pacala, S. W. (2007). Crown Plasticity and Competition for Canopy Space: A New Spatially Implicit Model Parameterized for 250 North American Tree Species. *PLoS ONE* **2**, e870.

R Core Team (2015). R: A language and environment for statistical computing. R Foundation for Statistical Computing, Vienna, Austria.

Soto, R. (1988). Geometry, biomass allocation and leaf life-span of Avicennia germinans L. L. Avicenniaceae along a salinity gradient in Salinas, Puntarenas, Costa Rica. *Revista de Biología Tropical* **36**, 309-328.

Thornley, J. H. M. (1996). Modelling Water in Crops and Plant Ecosystems. *Annals of Botany* **77**, 261-275.

Twilley, R. R., and Rivera-Monroy, V. H. (2005). Developing performance measures of mangrove wetlands using simulation models of hydrology, nutrient biogeochemistry, and community dynamics. *Journal of Coastal Research*, 79-93.

Twilley, R. R., Rivera-Monroy, V. H., Chen, R., and Botero, L. (1999). Adapting an Ecological Mangrove Model to Simulate Trajectories in Restoration Ecology. *Marine Pollution Bulletin* **37**, 404-419.

Uzoh, F. C. C., and Oliver, W. W. (2006). Individual tree height increment model for managed even-aged stands of ponderosa pine throughout the western United States using linear mixed effects models. *Forest Ecology and Management* **221**, 147-154.

Vogt, J., Lin, Y., Pranchai, A., Frohberg, P., Mehlig, U., and Berger, U. (2014). The importance of conspecific facilitation during recruitment and regeneration: A case study in degraded mangroves. *Basic and Applied Ecology* **15**, 651-660.

Vovides, A. G., Vogt, J., Kollert, A., Berger, U., Grueters, U., Peters, R., Lara-Domínguez, A. L., and López-Portillo, J. (2014). Morphological plasticity in mangrove trees: salinity-related changes in the allometry of Avicennia germinans. *Trees* **28**, 1413-1425.

Weiner, J. (2004). Allocation, plasticity and allometry in plants. *Perspectives in Plant Ecology, Evolution and Systematics* **6**, 207-215.

Weiner, J., Stoll, P., Muller-Landau, H., and Jasentuliyana, A. (2001). The Effects of Density, Spatial Pattern, and Competitive Symmetry on Size Variation in Simulated Plant Populations. *The American Naturalist* **158**, 438-450.

West, G. B., Brown, J. H., and Enquist, B. J. (1999). A general model for the structure and allometry of plant vascular systems. *Nature* **400**, 664-667.

West, G. B., Enquist, B. J., and Brown, J. H. (2009). A general quantitative theory of forest structure and dynamics. *Proceedings of the National Academy of Sciences* **106**, 7040-7045.

Yoda, K., Kira, T., Ogawa, H., and Hozumi, K. (1963). Self-thinning in overcrowded pure stands under cultivated and natural conditions. *Journal of Biology, Osaka City University* **14**, 107-129.

## 5.7 Appendix

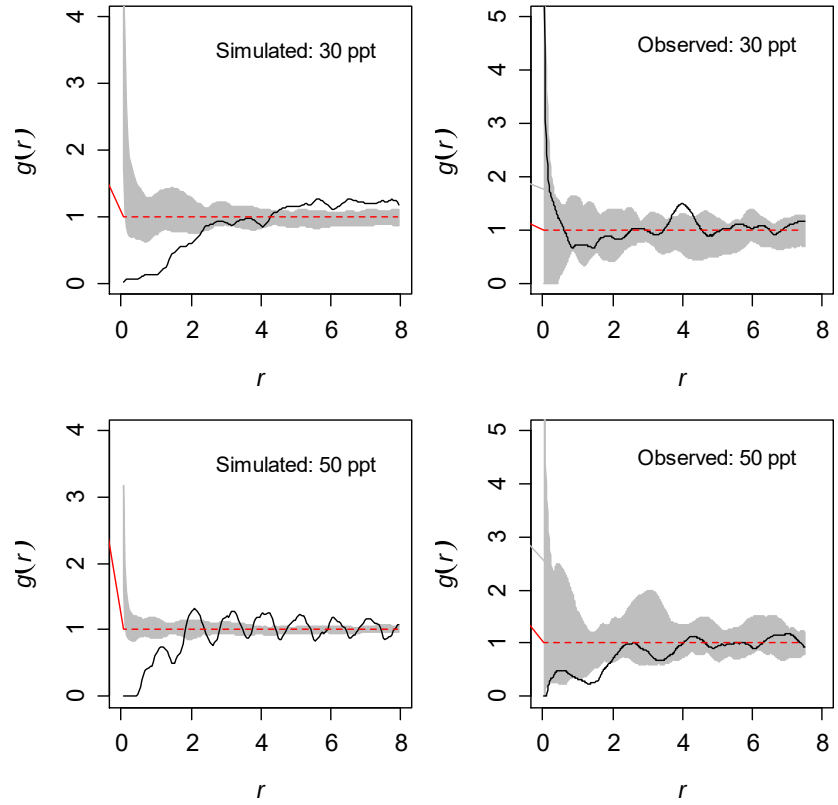


Appendix 5-I: Comparing the spatial patterns of simulated forest stand against field observations in contrasting habitat salinity conditions

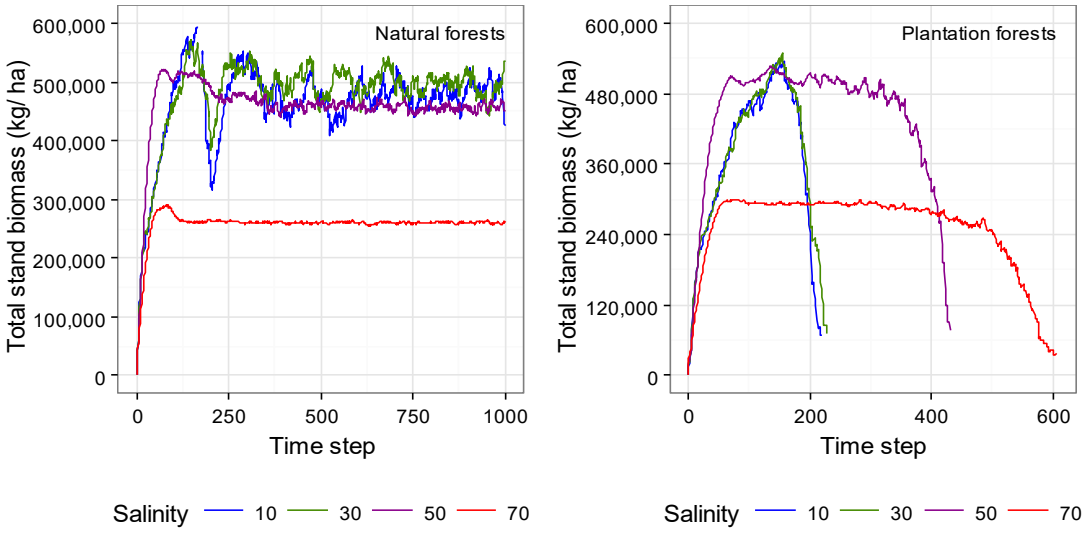


Appendix 5-II: Pattern of stand biomass accumulation under different simulated site conditions in "Natural forest" and "Plantation forest" scenarios. Values represent the sum of aboveground and belowground biomass.

A quasi-equilibrum stand biomass growth can be inferred from these results, where some slight fluctuations in the peak biomass values can be related to the random death of big tree(s) and subsequent stand biomass growth. Given the known empirical pattern or the results of simulation studies, e.g. Berger et al. (2004), tree productivity was expected to increase to reach a climax, and then, decline substantially with tree age. The forest stand simulations from the BETTINA_IBM apparently showed a characteristic decline in the total stand biomass that mimics the age-related decline in biomass productivity. This iconic behaviour can largely be attributed to the death of some "keystone" large trees, which are known for contributing substantial amount of stand biomass.

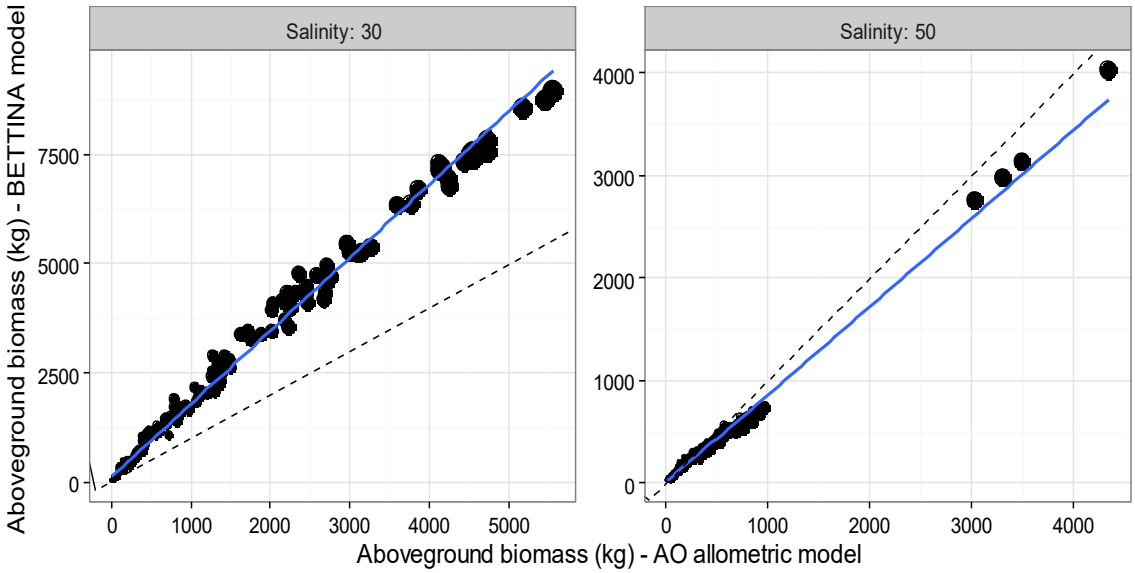


Appendix 5-III: Comparison of aboveground biomass of selected trees based on BETTINA predictions and allometric model (Olagoke et al 2016) estimates. *The size of the dots corresponds to the tree diameters (cm) and the dashed line, being the 1:1 scenario*

**ODD of the BETTINA_IBM Model**

Ronny Peters

May 25, 2016

The model description follows the ODD (Overview, Design concepts, De- tails) protocol for describing individual- and agent-based models (Grimm et al. 2006, 2010).

## 1 Purpose

The BETTINA IBM model is designed as a mangrove stand model for describing the growth and the allometric plasticity of the trees as a response to abiotic con- ditions and the specific competition with neighbours. The underlying single-tree BETTINA approach (Peters et al. 2014) explains the allometric development of an individual tree mechanistically and overcomes the empiric formulation of allometric relations. With this, different individual neighbourhood settings lead to a variation in shape and biomass allocation of the trees.

## 2 Entities, state variables and scales

### 2.1 Agents

The agents of the model are mangrove trees. For now, the model is set up and parametrized for one single species, *Avicennia germinans*. The agents are characterized by the following state variables:

| variable | unit | explanation | initializatio | behaviour |
|---|---|---|---|---|
| x | [m] | x-position | random | constant |
| y | [m] | y-position | random | constant |
| $r_{crown}$ | [m] | crown radius | 0.3 | variable |
| $h_{crown}$ | $[m^3\ m^{-2}]$ | leaf volume per ground | 0.004 | constant |
| $r_{stem}$ | [m] | stem radius | calculated* | variable |
| $h_{stem}$ | [m] | stem height | 0.0001 | variable |
| $r_{root}$ | [m] | root zone radius | calculated* | variable |
| $h_{root}$ | $[m^3\ m^{-2}]$ | fine root vol. per ground | 0.004 | constant |

### 2.2 Collectives

None. Different species may differ in parameters up to now attributed to global variables.

### 2.3 Spatial units

The size of the spatial units (patches), i.e. the spatial resolution can be chosen (size-factor, see global variables).

| variable | unit | explanation | initialisation | behaviour |
|---|---|---|---|---|
| sal | [ppt] | salinity | scenario | constant** |

### 2.4 Temporal resolution

The meaning of a time step is not defined. Nevertheless, there is a parameter controlling the length of a time step: $k_{grow}$. With the current value of 0.05, a time step is in the magnitude of a few months. For a (not yet implemented) seasonal variability of the boundary conditions solar radiation and salinity, this parameter has to be defined properly.

### 2.5 Global variables

Beside $R_{solar}$ (and, if constant in space, salinity *sal*) there are no real environmental variables. As for now, we consider just one single species, the plant parameters are technically global variables.

| variable | unit | explanation | value | behaviour |
|---|---|---|---|---|
| $L_p \times k_{geom}$ *** | [kg $s^{-1}$ $m^{-4}$ ] | fine root permeability × geometric const. | 0.04 | const. |
| $k_{f,sap}$ | [kg $s^{-1}$ $m^{-2}$] | xylem conductivity | 1.48 | const. |
| $R_{solar} \times k_{rel}$*** | [kg $s^{-1}$ $m^{-2}$] | solar radiation × factor (water per light) | 0.038 | const. |
| $psi_{leaf}$ | [MPa] | minimum leaf water potential | -7.86 | const. |
| $k_{maint}$ | [kg $s^{-1}$ $m^{-3}$] | maintenance cost per biomass | 0.28 | const. |
| $k_{r,half\,max}$ | [-] | half of maximum height growth weight | 0.1 | const. |
| $sf_{sig,1}$ | [-] | scaling factor for sigm. function | 0.02 | const. |
| $sf_{sig,2}$ | [-] | scaling fac. for sigm. function (height) | 0.15 | const. |
| $k_{grow}$ | [-] | growth scaling | 0.05 | const. |

*) calculated from other measures to ensure resource equilibrium at initial state for numerical stability.

**) constant in time (no feedback). Spatial variation possible, but not used.

***) these unknown parameters only occur as combinations, and are therefore condensed to one single value.

## 3 Process overview and scheduling

All the individuals act simultaneously. I.e. first, the growth of the plant components of all trees is estimated and then the state variables get updated. Figure 1 shows schematically the information flow for an individual in a single time step.

The individual trees are determined by their location and the allometric measures. These variables determine the competition indices of the individuals' *above_c* and *below_c* and with this, the reduction of resource uptake. This is done within the sub-model **Competition**.

From the allometric measures, the submodel **Resistances** calculates both root surface resistance $r_1$ and sap flow resistance $r_2$.

In **Resources**, the resistances control water uptake, crown size controls light interception and the competition indices *above c* and *below c* account for loss by competition. The available resources $res_{avail}$ are estimated.

From the allometric measures via the determination of the **Volume of Plant Components**, the costs for **Maintenance of Biomass** are estimated.

In **Growth**, the increment of biomass ($growth$) is calculated as the difference between available resources $res_{avail}$ and maintenance costs. (**Growth** and **Maintenance of Biomass** are parts of the sub-module **Resources**.)

Negative values of $growth$ lead to the **Death** of the individual.

The sub-model **Weights** determine, how the biomass increment gets allocated onto the specific plant components. Root and crown radius (as drivers of competition) define the proportion of height growth. Available below- and aboveground resources determine the shares for crown growth and water up- take improvement. For the enhancement of water uptake, the resistances define the distribution into diameter growth and root radius growth.

With the $growth$ of biomass and its distribution to the plant components, the **Increase of Allometric Measures** are calculated. Finally, the allometric measures are updated.

## 4 Design concepts

### 4.1 Basic principles

The considered resources are restricted to light (aboveground) and water (belowground). The model describes resource uptake and growth mechanistically. The resource uptake depends on the allometric measures of the plant. Light interception is proportional to crown area. Water uptake is described with Darcy's law. According to the assumptions of the pipe-model theory (Rennolls, 1994), the characteristics of the vertical flow path is homogeneous along the flow axis.

Further basic assumptions of the model are:

- proportional use of above- and below-ground resources.

- maintenance costs are proportional to the total biomass.

- resources for plant growth are the difference between available resources and maintenance costs.

- growth allocation to improve resource uptake at the bottleneck. (and thus, influencing allometry.)

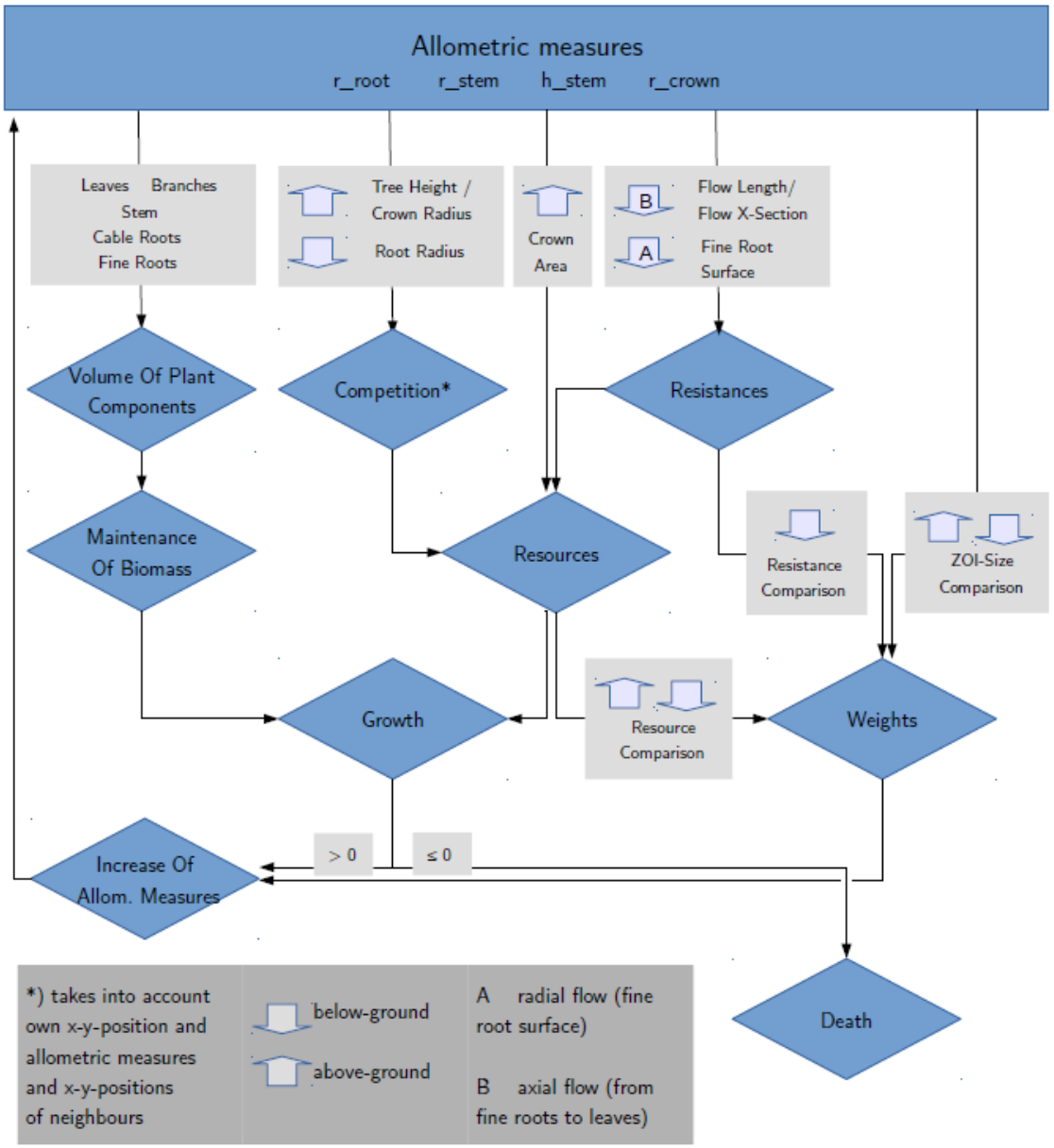


Figure 1: Sub-models and information ow for a time step on the individual scale.

### 4.2 Emergence

The features at the population level, e.g. Clark-Evans-Index and self-thinning trajectories, emerge from the individual growth and death. These are influenced by resource availability due to abiotic variables and competition with neighbours.

### 4.3 Adaptation

Adaptation to the (both biotic and abiotic) environment is a key element of the BETTINA-model (see 'Basic principles'). The shape of the individual con- trols the resource availability. Vice versa, the resource availability controls the allometric measures: they increase in a way to perfectly improve the resource availability regarding the individual's environment.

### 4.4 Objectives

The "objective" of the individual is an equilibrated uptake of below- and above-ground resources. The parameter measuring the disparity of resources and con- trolling growth allocation to balance the availability of the resources is $Q_{res}$.

A secondary objective is to keep both the root surface resistance and the axial flow resistance equal. Measure and control parameter is $Q_r$.

Besides this, (stem) height growth is a feature to get advantages in competition for light. Height growth is controlled by $Q_{rad}$. (For a detailed description of these parameters, see the paragraph on 'weights' in the 'Process overview and scheduling' section.)

### 4.5 Learning

-

### 4.6 Prediction

-

### 4.7 Sensing

-

### 4.8 Interaction

Interaction is taking place as competition. Individuals compete for light (aboveground) and water (belowground). The concept of resource sharing is the Zone of Influence (ZOI, Weiner et al. 2001, May et al. 2009).

*Below-ground competition* The below-ground ZOI radius is equal to $r_{root}$. The competition mode is 'complete symmetry'. I.e., resources on patches claimed by several individual are shared to equal proportions.

*Above-ground competition* The above-ground ZOI radius is equal to $r_{crown}$. The competition mode is 'complete asymmetry'. The better competitor (the "winner") is the taller individual, which is not necessarily the one with the big- ger ZOI-radius. The "winner" gets all of the resources from a competed patch. Deviating from the pure concept of 'complete asymmetry', the model accounts in a very simplified way for the availability of diffuse light penetrating the canopy depending on the share of gaps in the closer environment of an individual. (For a detailed description of these parameters, see the paragraph on 'competition' in the 'Process overview and scheduling' section.)

### 4.9 Stochasticity

The only stochastic component is the random spatial distribution of the individuals at model initialization.

### 4.10 Collectives

-

### 4.11 Observation

Measures related to state variables:

- stem diameter ( $2 \cdot r_{stem}$ )

- tree height ( $h_{stem} + 2 \cdot r_{crown}$ )

Variables describing the growth process of the individual:

- weights for growth allocation

- $growth$

Emerging variables at population level:

- Clark-Evans-Index $CEI$

- average tree volume $\bar{v}_{tree}$

- density of individuals

Measures related to primary state variables of individuals dying at the cur- rent time step:

- stem diameter ( $2 \cdot r_{stem}$ )

- tree height ( $h_{stem} + 2 \cdot r_{crown}$ )

### 5 Initialization

A chosen number of individuals are created and distributed randomly in space. The state variables are initialised as described in the section 'Entities, state vari- ables and scales'. Initial stem radius and root zone radius depend on salinity to provide an

equilibrium in above- and below-ground resources in the beginning. They are calculated using an auxiliary variable $k_{aux}$:

$$K_{aux} = -\frac{\psi_{leaf} + (9.81\ kPa\ m^{-1}).(h_{stem} + 2 \cdot r_{crown}) + (85\ kPa\ ppt^{-1}) \cdot sal}{2 \cdot R_{solar} \cdot \pi \cdot r^2 crown \cdot (9.81\ kPa\ m^{-1})}$$

$$r_{root} = \left( \frac{1}{L_p \times k_{geom} \cdot \pi \cdot \cdot h_{root} \cdot k_{aux}} \right)^{\frac{1}{2}}$$

$$r_{stem} = \left( \frac{2 \cdot r_{crown} + h_{stem} + 2^{-0.5} \cdot r_{root}}{k_{f,sap} \cdot \pi \cdot k_{aux}} \right)^{\frac{1}{2}}$$

## 6 Input data

-

## 7 Sub-models

### 7.1 Competition

The sub-models on competition account for the interactions between the trees and consider the spatial location of the agents. Competition indices for every tree are calculated for both above- and belowground processes. The ZOI- concept is applied. The belowground competition is assumed to be completely symmetric. For the aboveground competition, a modification of the ZOI approach with complete asymmetry is implemented.

*aboveground:*

- set the patch-owned variable *compete above* to the tallest tree being present there. (The criterion of presence is whether the distance between patch and tree is less than the crown radius.)

- set the tree-owned variable *countabove* to the number of patches within the crown radius.

- set the tree-owned variable *win countabove* to the number of patches within the crown radius with the specific tree being the tallest one. (i.e. by comparison of the tree height with *compete above* of the patches)

(To avoid runtime errors the last two steps must at least consider one patch. If spatial resolution is bigger than initial crown radius, there is possibly no patch center (i.e. patch location) within the radius. Therefore at least the patch the tree is on is checked. Note, that in such cases the model is not very precise anyway, at least for small trees. Similar for belowground, see below.)

- calculate the above-ground competition index *above c* of the trees as the ratio of *win_ countabove* and *countabove*

- to account for indirect solar radiation (assumed to be 50% of total), the share of the gap area (patches without presence of any tree's crown) in the radius of 20 meters contribute to light interception of the tree:

$$above\_c = above\_c + (1 - above\_c) \cdot 50\% \cdot \frac{gap\ area\ in 20\ meter\ radius}{area\ in 20\ meter\ radius}$$

*belowground:*

- set the tree-owned variable *countbelow* to the number of patches within the root radius, but at least 1. (if no patch center within distance $\leq r_{root}$)

- set the patch-owned variable *compete_ below* to the reciprocal of the number of trees being present there. (The criterion of presence is whether the distance between patch and tree is less than the root radius.)

- set the tree-owned variable *win countbelow* to the sum of the values *compete_ below* of all the patches in the root zone (distance $\leq r_{root}$), but at least 0.5 (if no patch center within distance $\leq r_{root}$)

- calculate the below-ground competition index *below c* of the trees as the ratio of *win_countbelow* and *countbelow*.

### 7.2 Growth

The individual growth of the plant and the distribution onto the different plant components is the heart of BETTINA. In general, the sub-models accord to the steps as described in section 3. Last, not least there are some explanations about numerical issues.

*Volume of plant components*

- set leaf volume $v_{leaf}$ to the volume of a cylinder with radius $r_{crown}$ and height $h_{crown}$.

- set branch volume $v_{branch}$ to the volume of a cylinder with radius $r_{stem}$ and height $2 \cdot r_{crown}$.

- set stem volume $v_{stem}$ to the volume of a cylinder with radius $r_{stem}$ and height $h_{stem}$.

- set cable root volume $v_{croot}$ to the volume of a cylinder with radius $2^{-0.5} \cdot r_{stem}$ and height $r_{root}$.

- set fine root volume $v_{froot}$ to the volume of a cylinder with radius $r_{root}$

and height $h_{root}$.

- add up all these volumes to total $v_{tree}$

*resistances:*

The resistances for the water crossing the root surface and the axial flow towards the leaves are determined by the species specific (global) parameters $L_p \times k_{geom}$ and $k_{f,sap}$ and the current allometric measures (state variables) of the individuals.

- set root surface resistance $r_1$ to

$$\frac{1}{L_p \times k_{geom} \cdot \pi \cdot r_{root}^2 \cdot h_{root}}$$

- set axial flow resistance $r_2$ to

$$\frac{2 \cdot r_{crown} + h_{stem} + 2^{-0.5} \cdot r_{root}}{k_{f,sap} \cdot \pi \cdot r_{stem}^2}$$

(The term above the fraction line is the length of the flow path.)

*resources:*

The resource uptake is divided into light interception water uptake. Both processes are influenced by the respective competition indices. The available resources are the minimum of both. The part for growing is reduced by biomass- proportional maintenance.

- set the above-ground resources $res_a$ to

$$above\_c \cdot k_{rel} \times R_{solar} \cdot \pi \cdot r_{crown}^2$$

- set the below-ground resources $res_b$ to

$$below\_c \cdot \frac{-\left(\psi_{leaf} + (9.81kPa \cdot m^{-1}) \cdot (h_{stem} + 2 \cdot r_{crown}) + (85kPa \cdot ppt^{-1}) \cdot sal\right)}{(r_1 + r_2) \cdot (9.81kPa \cdot m^{-1})}$$

- set available resources $res_{avail}$ to the minimum of both $res_a$ and $res_b$

- set the total growth variable $growth$ to

$$k_{grow} \cdot (res_{avail} - k_{maint} \cdot v_{tree})$$

- if $growth < 0$ the tree will die. But there is still time for that, we still need the individual for some measurements and plots. Therefore, set *deathflag* of this agent to value 1.

*weights:*

The weights are set to distribute growth mainly in the way to predominately increase specific allometric measures for improving resource uptake at the bottleneck. To define, how strong a mechanism shall be promoted, first some standardized criteria are calculated.

- to quantify, whether the tree lacks either above- or below-ground resources,

$Q_{res}$ is set as the ratio

$$\frac{res_a - res_b}{res_a + res_b}$$

- to quantify, which of the resistances limits water flow, $Q_r$ is set as the ratio

$$\frac{r_1 - r_2}{r_1 + r_2}$$

- Stem height growth is to give advantage for above-ground competition. Assuming, if the crown radius is bigger than the root radius, aboveground competition is expected to be stronger, we set $Q_{rad}$ as the ratio

$$\frac{r_{crown} - r_{root}}{r_{crown} + r_{root}}$$

With these auxiliary variables, the weights are estimated.

- set the weight $wa_2$ (for increasing stem height $h_{stem}$) to

$$\frac{k_r, half\max}{1 + e^{-\frac{Q_{rad}}{sf_{sig,2}}}}$$

- set the weigth $wa_1$ (for increasing crown radius $r_{crown}$) to

$$\frac{1 - wa_2}{1 + e^{-\frac{Q_{res}}{sf_{sig,1}}}}$$

- set the weigth $wb_2$ (for increasing stem radius $r_{stem}$) to

$$\frac{1 - wa_1 - wa_2}{1 + e^{-\frac{Q_r}{sf_{sig,1}}}}$$

- set the weigth $wb_1$ (for increasing root radius $r_{root}$) to

$$1 - wa_1 - wa_2 - wb_2$$

*Increase of allometric measures:*

The remaining resources $growth$ account for a specific increase of biomass (volume). The allometric relations allow for a calculation of the increase respec- tive measure (state variable).

- the stem height $h_{stem}$ increases by

$$\frac{wa_2 \cdot growth}{\pi \cdot r_{stem}^2}$$

- the crown radius $r_{crown}$ increases by

$$\frac{wa_1 \cdot growth}{2 \cdot \pi \cdot (r_{crown} \cdot h_{crown} \cdot r_{stem}^2)}$$

- the root radius $r_{root}$ increases by

$$\frac{wb_1 \cdot growth}{2 \cdot \pi \cdot r_{root} \cdot h_{root} + (2^{-0.5} \cdot \pi \cdot r_{stem}^2)}$$

- the stem radius $r_{stem}$ increases by

$$\frac{wb_2 \cdot growth}{2 \cdot \pi \cdot r_{stem} \cdot (2 \cdot r_{crown} + h_{stem} + 2^{-0.5} \cdot r_{root}^2)}$$

*numerical issues:*

For small trees, when growth is big in comparison to biomass and temporal changes of weights are bigger, numerical instabilities may occur. One way to avoid that is to decrease the growth scaling factor $k_{grow}$. The trees develop almost identically, but it takes more time steps and thus, more computation costs. It should be noted, that if a computation time step is associated to a real time step, this relation would change.

Another opportunity is to add a routine restricting the $growth$ to maximum 2 percent of the tree volume $v_{tree}$ and estimate the share of a time step passed for that growth:

- set the passed fraction of a time step $stepfrac$ to 0

- if growth > $\frac{v_{tree}}{50}$ do not add the calculated increments to the state variables, but instead:

1. calculate *frac* (the applied fraction of both time step and $growth$) as the minimum of $\frac{v_{tree}}{50 \cdot growth}$ and 1 - *stepfrac*

2. set $growth$ to $growth \cdot frac$

3. calculate the increase of allometric measures (see above) with this up- dated $growth$

4. update the allometric measures, the volume of the tree components, resistances, resources and weights.

5. update *stepfrac* with *stepfrac* + $frac$

6. while *stepfrac* < 1, repeat steps 1 to 4.

When *stepfrac* = 1, an entire time step has passed. At early growth stages this routine will be needed, with bigger trees growth will become much smaller than $\frac{v_{tree}}{50}$

### 7.3 Clark-Evans-Index

To measure the deviation from the complete spatial randomness (CSR) at initialization of the model, the Clark-Evans-Index *CEI* was calculated. The *CEI* in the ratio of average minimum distance to nearest neighbouring individual $dist_{min}$ and the expected value for CSR $dist_{min,\,CSR}$

$$CEI = \frac{dist_{\min}}{dist_{\min},CSR}$$

with

$$dist_{\min},CSR = \frac{1}{2} \cdot \sqrt{\frac{A}{n}}$$

*A* is the area of the stand and *n* the number of individuals.

## 8 References

May, F., Grimm, V., Jeltsch, F., 2009. Reversed effects of grazing on plant diversity: the role of below-ground competition and size symmetry. *Oikos* **118**, 1830-1843.

Peters, R., Vovides, A.G., Luna, S., Grüters, U., Berger, U., 2014. Changes in allometric relations of mangrove trees due to resource availability - A new mechanistic modelling approach, *Ecological Modelling* **283**, 53-61, ISSN 0304-3800.

Rennols, K., 1994. Pipe-model theory of stem-profile development. *Forest Ecol. manag*. **69**, 41-55.

Weiner, J., Stoll, P., Muller-Landau, H., Jasentuliyana, A., 2001. The ef- fects of density, spatial pattern, and competitive symmetry on size variation in simulated plant populations. *The American Naturalist* **158**, 438-450.

# 6 CONCLUDING DISCUSSION

*This chapter presents the synthesis of the main findings of the current thesis, focusing on the main contributions, prospects and limits of the different aspects, and general perspectives regarding the study of structural dynamics and functioning of mangrove forests in changing coastal environments.*

## 6.1 Main contributions

In this thesis, the central objective was to contribute to the understanding of the significance of tree morphological plasticity and shifting biomass partitioning for the structural development and dynamics of forest stands, considering the case of mangrove forests in changing environments. To this end, empirical field studies, remotely sensed data and process-based mechanistic modelling were considered as complementary tools. More specifically, the potentials of remotely sensed data using terrestrial laser scanning (TLS) in the measurement of aboveground morphology and biomass distribution of mangrove trees, including very large trees, were elaborated in this thesis. Additionally, the relative contribution of different indicators of morphological plasticity and structural attributes to the dynamics of aboveground biomass of forest stands from local to regional scales was investigated in variable mangrove stands. The proposition of a standardize software tool to facilitate capturing, processing and 3D modelling of forest structure data allows the preparation of our ensemble field data for the calibration and validation of forest stand simulators and remote sensing models. Furthermore, the thesis took benefit of a mechanistic mangrove stand simulator to provide insights into how the interplay of processes underlying morphological changes in the trees and local neighbourhood interactions in shaping structural development and dynamics of mangrove forests. Overall, the contribution of this current thesis found relevance for various aspects of mangrove ecology, from adaptive tree growth, biomass distribution, spatial structure and tree interactions to ecosystem dynamics under changing environmental conditions.

### *6.1.1 Morphological plasticity and allometric analyses at the tree scale*

Given the soft-muddy sediments and frequent tides in mangrove environments (Cintron and Schaeffer-Novelli, 1984), the field survey and detailed measurements of tree traits and forest structural parameters including biomass often present huge difficulties (Komiyama et al., 2008; Proisy et al., 2007). This challenge may partly explain why structural data and biomass of large mangrove trees are rarely available. Meanwhile, tools like terrestrial laser scanning (TLS) and other remote sensing technology have offered possibility for non-destructive and high resolution three-dimensional (3D) structure of trees with relatively low time and labour requirements

(Dassot et al., 2011). These remotely sensed measurements have found extensive applications in various ecological studies, although it is largely unexplored in mangrove studies. In Chapter 2, I have proposed a method to capture tree morphological attributes and biomass of mangrove trees, which was tested for a wide range of tree sizes, up to very large trees. By employing a pixel-based analysis in segmented tree sections, the TLS-based biomass estimation approach presented in this thesis specifically addressed issues of irregular tree shapes or presence of the buttresses that may impact on the overall accuracy (e.g., Nogueira et al. (2006)). Accordingly, it is particularly relevant for extensive application to large mangrove trees, which may present protuberance or buttresses at the lower parts.

Allometric models found applications in various studies concerning the structure and functioning of mangrove forests (Fromard et al., 1998; Kauffman and Donato, 2012; Komiyama et al., 2008). Common to most available allometric models is the fact that they are mostly calibrated based on measurements from small trees for the lack of large tree data. This factor marks a potential source of error propagation, especially when such models are applied to sites dominated by large trees, like the case of French Guiana. Besides, such large trees represent keystone structures explaining variations in forest biomass distributions, stand productivity and ecosystem dynamics (Bastin et al., 2015; Slik et al., 2013). The case is true for the tall mangrove forests common in the equatorial axis (Proisy et al., 2012).

I have integrated the data so obtained via TLS measurements to extend the validity domain of allometric models of *Avicennia germinans* to very large trees up to ca. 125 cm diameter size. In particular, a significant shift found in the partitioning of biomass to different aboveground components between small-moderate diameter size trees and the larger individuals, marks the basis extending allometric models to large trees. Even when the biomass allometric models achieved at this stage significantly improve on the predictive power of the preceding models, it is worth to consider the fact that trees growing in different shape and allocate biomass in a divergent manner to the influence of environmental conditions. This factor establishes the need to move beyond static allometric models into a more mechanistic approach in mangrove biomass modelling. In this direction, the work of Peters et al. (2014) that proposed a single-tree model mechanistically explaining environment-induced changes in tree allometric relations and biomass allocation made the first leap, upon which I built on in my thesis to explore the implications of morphological plasticity and changing biomass partitioning for biomass distributions and forest structure in variable environmental settings (Chapter 5).

Combining structural descriptions of *A. germinans* trees found at both sites, we highlighted the site-specific differences in tree allometries and the implication for

cross-regional biomass modelling (Chapter 3), thanks to the analysis of covariance (ANCOVA). Apparently, our nested ANCOVA (site-dependent) models of allometric relations differed significantly from the joint models obtained through data aggregated from across the study sites. The crown – stem diameter allometry was largely congruent to the tree height – diameter allometric relations in terms of variations, from French Guiana to the two forest classifications in Bragança. This aligns with the behaviours of mangrove trees growing in sites of varying salinity and water stress conditions, earlier documented in other mangrove regions (e.g., Vovides et al. (2014)). Of the two models (power function and logarithmic model) tested for the investigated tree allometries, we selected the model based on the logarithmic transformation of stem diameter. The reasons being that: 1) while power function resulted in over prediction of large tree height and crown diameter, the logarithmic model displayed a good fit for the asymptotic nature of tree growth (Feldpausch et al., 2011; Olagoke et al., 2016); 2) the logarithmic model returned much lower error estimates for trees in the lower and larger diameter size classes than the power model.

Consequently, it was relevant to investigate the extent to which the tree scale plasticity can impact on the accuracy of diameter-biomass allometric equations, when found applications at the cross-regional levels. The parameterization of biomass model that decomposes aboveground tree part into the trunk and crown components (*Sensu.* Ploton et al. (2016)) with the 3D architectural data of selected trees (based on laser scanning and tacheometer measurements) thus became advantageous in this respect. Indeed, local variations in tree morphology significantly impact on aboveground biomass estimates of diameter – biomass allometric models calibrated for French Guiana mangroves when tested against for sites of contrasting tree structure in Bragança, even when sites are located in the same geographical region. Further than the explanation rooted on latitudinal variation in tree biomass (Twilley et al., 1992), morphological plasticity here appears an important factor in the diameter – biomass relationship. The study concludes that regional differences in mangrove tree structure and function could be captured through better description of crown metrics could generate a plus-value in the understanding of mangrove stand dynamics across contrasting coastal environments.

Together, these tree scale allometric studies may facilitate accurate determinations of the biomass for the aboveground parts with potential benefit to the success of the coastal blue carbon projects (Howard et al., 2014) in the effort for conservation of mangrove forests.

### 6.1.2 *Relating morphological plasticity to the structural dynamics of forest stands*

Generally, many aspects of forest structural and functional properties directly relate to the allometric scaling of trees' morphological and physiological traits (Bohlman and Pacala, 2012; Kerkhoff and Enquist, 2007; West et al., 2009). Interestingly, many earlier studies have analyzed and confined such relationships to general (or invariant) allometric models (e.g., Enquist and Niklas (2001); West et al. (1999)) mostly based on the power law of Huxley and Teissier (1936). Nonetheless, controversies abound on this position given the mounting evidence of significant variations in allometric relationships in different environments (Feldpausch et al., 2011; O'Brien et al., 1995; Pretzsch et al., 2014), and the same is true for mangrove species too (Castañeda-Moya et al., 2013; Clough et al., 1997; Vovides et al., 2014). In spite of these tree scale evidences, the implications for forest communities and dynamics seemed rarely explored.

Towards this scope, the study presented in Chapter 3 undertook the analysis of the relative contributions of known attributes (indicators) of morphological plasticity (Vovides et al., 2014) and structural divergence to the dynamics of aboveground biomass in mangrove forest stands. I found that the stand aboveground biomass considerably correlated with the stand basal area, mean quadratic diameter, diameter and height of the dominant trees, but more weakly linked to the median stem diameter and height, and number of trees within the stand (stand density). The negative correlation of stand density with the aboveground biomass is rather not unfounded, given their generally known relationships in the context of self-thinning processes (West et al., 2009; Yoda et al., 1963). Interestingly, the combination of stand basal area, diameter and height of the dominant trees from heterogeneous mangrove stands in French Guiana yielded a parsimonious model that explained up to 90% variance of the stand aboveground biomass. On top, the best-fitted model predicted stand biomass estimates of independent, but contrasting mangrove forests in Bragança to the coefficient of variation values of ca. 88%. Certainly, such collective indicators of morphological plasticity, as identified in Vovides et al. (2014), hold the key for improved predictions of mangrove dynamics in changing environments.

Many datasets and models on tree allometry, biomass and forest structure are available from different mangrove studies in the literature (e.g., Hutchison et al. (2014); Komiyama et al. (2008)). Such datasets would have potential for supporting further studies on the dynamics of mangrove forests beyond the scope presented in this thesis, but for the divergent sampling designs and data presentation. This thesis thus presents a novel tool, named *Lollymangrove*, integrated in the AMAPStudio suite of software for tree architecture, with the objective of maximizing the potential of further field descriptions and modeling works (Chapter 4). The *Lollymangrove*

allows standardized forest data capture, 3D visualization of structural data, aboveground biomass computation from a configurable interface and export formats for forest dynamics and remote sensing models. While the software provides a flexible approach to localized biomass computation over the regular site-specific and general allometric models, the extension for data preparation in formats compatible for integration into forest simulation models gives a greater prospect in advancing data acquisition, modelling and validation towards a better understanding and monitoring of structural development and dynamics of mangrove forests.

### *6.1.3 Predicting morphological plasticity and stand dynamics in changing environments*

Apparently, predicting the influence of morphological plasticity on the structural dynamics of mangrove forests in changing environments through empirical studies would require extensive datasets, achievable over long-term studies. Even at that, the intrinsic tree and stand attributes being observed in various mangrove forests might have resulted from a complex interaction of diverse processes (Cintron and Schaeffer-Novelli, 1984; Proisy et al., 2016; Twilley and Rivera-Monroy, 2005), identifying and describing the interplay of causal processes on shifting tree morphology and stand structure represent an herculean task for empirical studies (Berger et al., 2008). Given the advantage of computer simulation modelling in this regards (Berger and Hildenbrandt, 2000; Berger et al., 2008; Rivera-Monroy et al., 2004), the study presented in Chapter 5 establishes the methodological basis for complementing the empirical analysis of morphological plasticity and the significance for structural dynamics of mangrove forests.

The study took benefit of the BETTINA model (Peters et al., 2014), which was originally designed to factors controlling the individual tree's adaptation to environmental change mechanistically. This lends an opportunity to integrate morphological plasticity in a spatially explicit mangrove stand simulator for the first time. Upon parameterization and subsequent simulation experiments, I made efforts to describe the general model behaviours while considering our field measurements and ecological patterns known to scientific communities as benchmarks. Generally, the simulation experiments revealed insights into the relation between environmental conditions, allometric variations and biomass partitioning of mangrove trees, and stand characteristics. The model describes an important mechanism, namely water uptake limited by salt stress underlying plastic biomass allocation. The results suggest close matches with observed ecological patterns (e.g., the growth patterns, mortality distributions, self-thinning trajectories) under higher salinity. In low salinity conditions, however, the current parameterization underestimates the maximum tree height and diameter, and consequently, aboveground biomass and self-thinning trajectories of forest stands.

In consonance to Grime (1977) and studies highlighting the stress gradient hypothesis (e.g., Brooker and Callaghan (1998); Maestre et al. (2009)), the behaviour of BETTINA_IBM model clearly established a trend of reducing intensity of competitive interactions as salinity-induced water stress increases in the simulated stands. This behaviour equally matches the empirical observations of Vogt et al. (2014) in mangrove forests growing on a gradient of hypersaline conditions. More importantly, the results from simulated monospecific *Avicennia* cohorts shed light on the potential influence of morphological plasticity of trees and subsequent local interactions on the trajectories of plant mass-density relationships in the course of stand development, the so-called "self-thinning rule" in even-aged plant communities. So far, the generalization on the self-thinning process is polarized between two postulations. For Yoda et al. (1963), self-thinning takes place following a constant slope of '-3/2'. The same process, however, was conceptualized as '-4/3' in the frame of metabolic scaling theory (West et al., 1997; West et al., 1999). Based on our simulation results, the contribution of the current thesis is such that slope of self-thinning trajectories can be variable, depending on the realized tree shape and exerting competition intensities. These factors, in turn, are determined by the prevailing environmental conditions.

Certainly, the modelling of mangrove forest dynamics by connecting field measured parameters, remote measurements and individual-based simulation modelling. While current advancements in remote sensing technology offer potentials to provide a basis for improved parameterization of simulation models, chances are high that finer calibration of remote measurements can be achieved through mechanistic modelling. In the anticipation of coupling the simulation modelling to remote sensing observations (e.g., Kasischke and Christensen Jr (1990); Shugart et al. (2015)), I attempted to explore in this thesis the extent to which change in morphological allometries of trees can impact of the estimates of forest parameters made from canopy observations in a simulation experiment. Even when the test was restricted on the aboveground biomass of trees growing in contrasting site conditions, the results clearly suggest that trees of equivalent projected crown areas displayed divergent biomass compositions. This partly explains why forests that may appear similar in structure to remote sensing observations could in reality return varying biomass estimates in direct field measurements (Proisy et al., 2012; Proisy et al., 2007). The next steps would be to complete extensive validation of the simulation modelling approach, decompose the effect of exerting ecological processes on various signals from forest structure in ranges of environmental conditions, and then advance the consolidation to the canopy-based and geospatial approaches the remote sensing can offer while maximizing the *Lollymangrove* initiative.

## 6.2 Methodological issues and perspectives

Generally, the results and conclusion presented in this thesis are based on case studies, and in some instances the sample sizes are relatively small (Chapter 2, 3). This is partly due to the time constraint during field studies, and the challenges of field measurements on soft-muddy sediments in tidal mangrove environments. Other than for the incongruent sampling designs and data presentations, a substantial amount of data already available in published literature could have served for validation and generalization on various approaches presented in this thesis. In the meantime, I have demonstrated the potential of the *Lollymangrove* platform (Chapter 4) in this thesis as a tool to help allay such challenges in subsequent studies.

The TLS-based method implemented in Chapter 2 is very promising, and thus presents a window for non-destructive measurements of tree architecture and biomass in mangrove forests. Potential applications can also be extended to various other aspects of field measurements in coastal wetlands in general. In order to maximize the potential of the TLS-based method proposed in this study, a number of issues are still pending. Due to time limitation, the method was only tested and validated over a very limited scope. It may be worthwhile to ascertain the consistency of the method on further samples, especially in very different terrains. During the scanning operations for the TLS measurements, deflection of tree crowns by wind was clearly an issue for small to medium sized trees. No doubt, this issue marks a potential source of error for estimates so obtained using the TLS approach. I have only controlled instances of such error in my studies by avoiding scanning operations during pronounced wind blowing.

Another issue that may limit the accuracy of biomass measurement with TLS is the likelihood of cavities, occasionally found in large mangrove trees. It is questionable how feasible it is, in a real world scenario, to reliably factor out error due to hollow effect, even in direct 'cut-and-weigh' biomass measurement. Without knowledge of the average volume of the cavities in the different tree size classes and the respective probability of their occurrence, subsequent estimation of biomass from regression models relying on *DBH* surveys will consequently fail, regardless of the calibration technique applied. Advances in the application of ultrasonic tomography (Brancheriau et al., 2008) and Resistograph measurements (Rinn et al., 1996) demonstrate non-destructive detection of volume of cavities in trees. Integrating these measurements with the TLS-based method in the future could address the uncertainty caused by the possible presence of tree cavities.

For the individual based simulations, the results obtained from the current modelling approach and parameter settings yielded are quite encouraging (Chapter 5), and demonstrate the prospects for further applications in mangrove studies. However,

the current parameterization underestimates the maximum tree height and diameter, and consequently, aboveground biomass and self-thinning trajectories of forests under low salinity conditions. This suggests that the morphology of trees under low levels of salinity are explained by further regulation mechanism(s) that still need to be addressed in a subsequent model improvement. Until now, the model assumes a number of parameters; it is most likely that empirical measurements in such instances could significantly drive the model to achieve results that are more realistic in low salinity conditions. For instance, the model can substantially benefit from data on sap flow and hydraulic measurements in microcosm experiments under contrasting salinity conditions. Additional details on current geometric description can also be achieved through the integration of tree architectural measurements from the TLS measurements.

## 6.3 Towards an integrative modelling framework for mangrove dynamics

Achieving reliable forecast of changes in the structure, spatial extent and functioning of mangrove ecosystem largely depends on how well multiple biotic and abiotic factors interplay at the local scale (e.g. Alongi (2009)) to regulate mangrove development are captured in modelling framework. This being that these factors are themselves constrained at varying scales by tides, winds, waves, nearshore currents or sediment transport (e.g. Anthony et al. (2010); Twilley and Rivera-Monroy (2005)). Aspects encapsulated in the current thesis apparently advance the simulation of mangrove growth and structural development to local environmental conditions (abiotic factors) at forest stands scale. The consolidation of the current findings and the demonstrated modelling efforts consist in coupling our forest dynamics models with hindcast, nowcast and forecast scenarios of changing coastal processes being captured in remote sensing observations (Proisy et al., 2016).

The proposition of an integrative, multiscale landscape-modelling framework through the use of Ocelet (Degenne et al., 2009) has good prospects in this regards. Ocelet is a domain-specific language designed for modelling of spatial dynamics within a model-building environment known as the Ocelet Modelling Platform (OMP). This platform allows for a flexible usage of *Interaction graphs*, an approach that distinguishes the Ocelet from other modelling approaches consisted in other system dynamics modelling platforms. Using the concept of *graph* (a set of *vertices* connected with *edges*), elements of a dynamic system are represented in *vertices* linked through the *edges* where *interaction functions* can be applied to change the state of the *entities* connected. This way, relations are built by indicating which entity interacts with which another entity in the graph structure via functions (interaction functions) that are applied when different entities interact. Proisy et al. (2016) provides further description of the ocelet and the potential towards a multiscale simulation of mangrove forest dynamics in changing environments.

The test application of this multiscale modelling approach in French Guiana (Proisy et al., 2016) was quite demonstrative. In this coast, the structural development and dynamics of mangrove forests are largely influenced by the massive discharge fine-grained sediments from the Amazon River (Fromard et al., 2004). Moreover, the hydrodynamics and sedimentary processes regulating the spatial structure, the extent and physiognomy of mangrove forests in this region, like in many mangrove regions are more interlinked in their effects at different spatial and temporal scales. Massive and rapid removal of mangrove forest areas can be observed over several square kilometers in a few years within the inter-bank zones (Anthony et al., 2010). According to these authors, shoreline retreat is mainly attributed to the impact of waves propagating across stretches of coast between banks. Upon continuous consolidation process (Gensac et al., 2015), rapid and extensive colonization of mangrove areas over hundreds of hectares generally follows (Proisy et al., 2009).

Currently, the results of test simulation in the proposed modeling framework largely demonstrate that the descriptions of the underlying processes were suitable enough to explain some of the coastal erosion and subsequent recolonization in the Guiana mangrove shorelines (Proisy et al., 2016). The flexibility of the Ocelet language permits an intuitive establishment of relationships between entities, such as the oceanic processes, the mud banks and the mangrove areas. These entities have rarely been linked in the studies dealing with mangrove changes. When fully developed, a tool capable of spatially explicit modelling of mangrove forest dynamics integrating impacts of large-scale oceanic processes should yield, for example, the timing and location of mangrove colonization, adaptation and erosion processes. More so, high spatial resolution images could be used to detect the initial time (Proisy et al., 2009), the mangrove growth stage (Proisy et al., 2007) and mangrove destruction. In essence, the prospects of this multiscale modelling perspective can be harnessed through interdisciplinary research in forecasting the highly variable fate of mangrove forests in changing coastal environments.

## 6.4 References

Alongi, D. M. (2009). Paradigm shifts in mangrove biology. *In* "Coastal Wetlands: An Integrated Ecosystem Approach" (Perillo G.M.E., E. Wolanski, D. R. Cahoon and M. M. Brinson, eds.), Vol. Chapter 22, pp. 615-640. Elsevier Press, The Netherlands.

Anthony, E. J., Gardel, A., Gratiot, N., Proisy, C., Allison, M. A., Dolique, F., and Fromard, F. (2010). The Amazon-influenced muddy coast of South America: A review of mud-bank-shoreline interactions. *Earth-Science Reviews* **103**, 99-121.

Bastin, J. F., Barbier, N., Réjou-Méchain, M., Fayolle, A., Gourlet-Fleury, S., Maniatis, D., de Haulleville, T., Baya, F., Beeckman, H., Beina, D., Couteron, P., Chuyong, G., Dauby, G., Doucet, J. L., Droissart, V., Dufrêne, M., Ewango, C., Gillet, J. F., Gonmadje, C. H., Hart, T., Kavali, T., Kenfack, D., Libalah, M., Malhi, Y., Makana, J. R., Pélissier, R., Ploton, P., Serckx, A., Sonké, B., Stevart, T., Thomas, D. W., De Cannière, C., and Bogaert, J. (2015). Seeing Central African forests through their largest trees. *Scientific Reports* **5**, 13156.

Berger, U., and Hildenbrandt, H. (2000). A new approach to spatially explicit modelling of forest dynamics: spacing, ageing and neighbourhood competition of mangrove trees. *Ecological Modelling* **132**, 287-302.

Berger, U., Rivera-Monroy, V. H., Doyle, T. W., Dahdouh-Guebas, F., Duke, N. C., Fontalvo-Herazo, M. L., Hildenbrandt, H., Koedam, N., Mehlig, U., Piou, C., and Twilley, R. R. (2008). Advances and limitations of individual-based models to analyze and predict dynamics of mangrove forests: A review. *Aquatic Botany* **89**, 260-274.

Bohlman, S., and Pacala, S. (2012). A forest structure model that determines crown layers and partitions growth and mortality rates for landscape-scale applications of tropical forests. *Journal of Ecology* **100**, 508-518.

Brancheriau, L., Lasaygues, P., Debieu, E., and Lefebvre, J. P. (2008). Ultrasonic tomography of green wood using a non-parametric imaging algorithm with reflected waves. *Annals of Forest Science* **65**, 712-712.

Brooker, R. W., and Callaghan, T. V. (1998). The Balance between Positive and Negative Plant Interactions and Its Relationship to Environmental Gradients: A Model. *Oikos* **81**, 196-207.

Castañeda-Moya, E., Twilley, R. R., and Rivera-Monroy, V. H. (2013). Allocation of biomass and net primary productivity of mangrove forests along environmental gradients in the Florida Coastal Everglades, USA. *Forest Ecology and Management* **307**, 226-241.

Cintron, G., and Schaeffer-Novelli, Y. (1984). Methods for studying mangrove structure. *In* "The mangrove ecosystem: research methods" (S. C. Snedaker and J. G. Snedaker, eds.), pp. 91-113. United Nations Educational, Scientific and Cultural Organization (UNESCO), Paris.

Clough, B. F., Dixon, P., and Dalhaus, O. (1997). Allometric relationships for estimating biomass in multi-stemmed mangrove trees. *Australian Journal of Botany* **45**, 1023-1031.

Dassot, M., Constant, T., and Fournier, M. (2011). The use of terrestrial LiDAR technology in forest science: application fields, benefits and challenges. *Annals of Forest Science* **68**, 959-974.

Degenne, P., Lo Seen, D., Parigot, D., Forax, R., Tran, A., Ait Lahcen, A., Curé, O., and Jeansoulin, R. (2009). Design of a Domain Specific Language for modelling processes in landscapes. *Ecological Modelling* **220**, 3527-3535.

Enquist, B. J., and Niklas, K. J. (2001). Invariant scaling relations across tree-dominated communities. *Nature* **410**, 655-660.

Feldpausch, T. R., Banin, L., Phillips, O. L., Baker, T. R., Lewis, S. L., Quesada, C. A., Affum-Baffoe, K., Arets, E. J. M. M., Berry, N. J., Bird, M., Brondizio, E. S., de Camargo, P., Chave, J., Djagbletey, G., Domingues, T. F., Drescher, M., Fearnside, P. M., França, M. B., Fyllas, N. M., Lopez-Gonzalez, G., Hladik, A., Higuchi, N., Hunter, M. O., Iida, Y., Salim, K. A., Kassim, A. R., Keller, M., Kemp, J., King, D. A., Lovett, J. C., Marimon, B. S., Marimon-Junior, B. H., Lenza, E., Marshall, A. R., Metcalfe, D. J., Mitchard, E. T. A., Moran, E. F., Nelson, B. W., Nilus, R., Nogueira, E. M., Palace, M., Patiño, S., Peh, K. S. H., Raventos, M. T., Reitsma, J. M., Saiz, G., Schrodt, F., Sonké, B., Taedoumg, H. E., Tan, S., White, L., Wöll, H., and Lloyd, J. (2011). Height-diameter allometry of tropical forest trees. *Biogeosciences* **8**, 1081-1106.

Fromard, F., Puig, H., Mougin, E., Marty, G., Betoulle, J. L., and Cadamuro, L. (1998). Structure, above-ground biomass and dynamics of mangrove ecosystems: new data from French Guiana. *Oecologia* **115**, 39-53.

Fromard, F., Vega, C., and Proisy, C. (2004). Half a century of dynamic coastal change affecting mangrove shorelines of French Guiana. A case study based on remote sensing data analyses and field surveys. *Marine Geology* **208**, 265-280.

Gensac, E., Gardel, A., Lesourd, S., and Brutier, L. (2015). Morphodynamic evolution of an intertidal mudflat under the influence of Amazon sediment supply – Kourou mud bank, French Guiana, South America. *Estuarine, Coastal and Shelf Science* **158**, 53-62.

Grime, J. P. (1977). Evidence for the Existence of Three Primary Strategies in Plants and Its Relevance to Ecological and Evolutionary Theory. *The American Naturalist* **111**, 1169-1194.

Howard, J., Hoyt, S., Isensee, K., Pidgeon, E., and Telszewski, M., eds. (2014). "Coastal Blue Carbon: Methods for assessing carbon stocks and emissions factors in mangroves, tidal salt marshes, and seagrass meadows," pp. 1-184. Conservation International, Intergovernmental Oceanographic Commission of UNESCO, International Union for Conservation of Nature, Arlington, Virginia, USA.

Hutchison, J., Manica, A., Swetnam, R., Balmford, A., and Spalding, M. (2014). Predicting Global Patterns in Mangrove Forest Biomass. *Conservation Letters* **7**, 233-240.

Huxley, J. S., and Teissier, G. (1936). Terminology of Relative Growth. *Nature* **137**, 780-781.

Kasischke, E. S., and Christensen Jr, N. L. (1990). Connecting forest ecosystem and microwave backscatter models. *International Journal of Remote Sensing* **11**, 1277-1298.

Kauffman, J. B., and Donato, D. (2012). "Protocols for the measurement, monitoring and reporting of structure, biomass and carbon stocks in mangrove forests," Center for International Forestry Research (CIFOR), Bogor, Indonesia.

Kerkhoff, A. J., and Enquist, B. J. (2007). The Implications of Scaling Approaches for Understanding Resilience and Reorganization in Ecosystems. *BioScience* **57**, 489-499.

Komiyama, A., Ong, J. E., and Poungparn, S. (2008). Allometry, biomass, and productivity of mangrove forests: A review. *Aquatic Botany* **89**, 128-137.

Maestre, F. T., Callaway, R. M., Valladares, F., and Lortie, C. J. (2009). Refining the stress-gradient hypothesis for competition and facilitation in plant communities. *Journal of Ecology* **97**, 199-205.

Nogueira, E. M., Nelson, B. W., and Fearnside, P. M. (2006). Volume and biomass of trees in central Amazonia: influence of irregularly shaped and hollow trunks. *Forest Ecology and Management* **227**, 14-21.

O'Brien, S. T., Hubbell, S. P., Spiro, P., Condit, R., and Foster, R. B. (1995). Diameter, Height, Crown, and Age Relationship in Eight Neotropical Tree Species. *Ecology* **76**, 1926-1939.

Olagoke, A., Proisy, C., Féret, J.-B., Blanchard, E., Fromard, F., Mehlig, U., de Menezes, M. M., dos Santos, V. F., and Berger, U. (2016). Extended biomass allometric equations for large mangrove trees from terrestrial LiDAR data. *Trees* **30**, 935-947.

Peters, R., Vovides, A. G., Luna, S., Grüters, U., and Berger, U. (2014). Changes in allometric relations of mangrove trees due to resource availability – A new mechanistic modelling approach. *Ecological Modelling* **283**, 53-61.

Ploton, P., Barbier, N., Takoudjou Momo, S., Réjou-Méchain, M., Boyemba Bosela, F., Chuyong, G., Dauby, G., Droissart, V., Fayolle, A., Goodman, R. C., Henry, M., Kamdem, N. G., Mukirania, J. K., Kenfack, D., Libalah, M., Ngomanda, A., Rossi, V., Sonké, B., Texier, N., Thomas, D., Zebaze, D., Couteron, P., Berger, U., and Pélissier, R. (2016). Closing a gap in tropical forest biomass estimation: taking crown mass variation into account in pantropical allometries. *Biogeosciences* **13**, 1571-1585.

Pretzsch, H., Biber, P., Schütze, G., Uhl, E., and Rötzer, T. (2014). Forest stand growth dynamics in Central Europe have accelerated since 1870. *Nat Commun* **5**.

Proisy, C., Barbier, N., Guéroult, M., Pélissier, R., Gastellu-Etchegorry, J.-P., Grau, E., and Couteron, P. (2012). Biomass prediction in tropical forests: the canopy grain approach. *In* "Remote Sensing of Biomass: Principles and Applications / Book 1" (T. E. Fatoyinbo, ed.). INTECH publisher.

Proisy, C., Couteron, P., and Fromard, F. (2007). Predicting and mapping mangrove biomass from canopy grain analysis using Fourier-based textural ordination of IKONOS images. *Remote Sensing of Environment* **109**, 379-392.

Proisy, C., Degenne, P., Anthony, E., Berger, U., Blanchard, E., Fromard, F., Gardel, A., Olagoke, A., Santos, V. F., Walcker, R., and Lo Seen, D. (2016). A multiscale simulation approach for linking mangrove dynamics to coastal proceesses using remote sensing observations. *Journal of Coastal Research*, 810-814.

Proisy, C., Gratiot, N., Anthony, E. J., Gardel, A., Fromard, F., and Heuret, P. (2009). Mud bank colonization by opportunistic mangroves: A case study from French Guiana using lidar data. *Continental Shelf Research* **29**, 632-641.

Rinn, F., Schweingruber, F.-H., and Schaer, E. (1996). RESISTOGRAPH and X-ray density charts of wood comparative evaluation of drill resistance profiles and X-ray density charts of different wood species. *Holzforschung* **50**, 303-311.

Rivera-Monroy, V. H., Twilley, R. R., Bone, D., Childers, D. L., Coronado-Molina, C., Feller, I. C., Herrera-Silveira, J., Jaffe, R., Mancera, E., Rejmankova, E., Salisbury, J. E., and Weil, E. (2004). A conceptual framework to develop long-term ecological research and management objectives in the wider Caribbean region. *BioScience* **54**, 843-856.

Shugart, H. H., Asner, G. P., Fischer, R., Huth, A., Knapp, N., Le Toan, T., and Shuman, J. K. (2015). Computer and remote-sensing infrastructure to enhance large-scale testing of individual-based forest models. *Frontiers in Ecology and the Environment* **13**, 503-511.

Slik, J. W. F., Paoli, G., McGuire, K., Amaral, I., Barroso, J., Bastian, M., Blanc, L., Bongers, F., Boundja, P., Clark, C., Collins, M., Dauby, G., Ding, Y., Doucet, J.-L., Eler, E., Ferreira, L., Forshed, O., Fredriksson, G., Gillet, J.-F., Harris, D., Leal, M., Laumonier, Y., Malhi, Y., Mansor, A., Martin, E., Miyamoto, K., Araujo-Murakami, A., Nagamasu, H., Nilus, R., Nurtjahya, E., Oliveira, Á., Onrizal, O., Parada-Gutierrez, A., Permana, A., Poorter, L., Poulsen, J., Ramirez-Angulo, H., Reitsma, J., Rovero, F., Rozak, A., Sheil, D., Silva-Espejo, J., Silveira, M., Spironelo, W., ter Steege, H., Stevart, T., Navarro-Aguilar, G. E., Sunderland, T., Suzuki, E., Tang, J., Theilade, I., van der Heijden, G., van Valkenburg, J., Van Do, T., Vilanova, E., Vos, V., Wich, S., Wöll, H., Yoneda, T., Zang, R., Zhang, M.-G., and Zweifel, N. (2013). Large trees drive forest aboveground biomass variation in moist lowland forests across the tropics. *Global Ecology and Biogeography* **22**, 1261-1271.

Twilley, R. R., Chen, R. H., and Hargis, T. (1992). Carbon sinks in mangroves and their implications to carbon budget of tropical coastal ecosystems. *Water, Air, and Soil Pollution* **64**, 265-288.

Twilley, R. R., and Rivera-Monroy, V. H. (2005). Developing performance measures of mangrove wetlands using simulation models of hydrology, nutrient biogeochemistry, and community dynamics. *Journal of Coastal Research*, 79-93.

Vogt, J., Lin, Y., Pranchai, A., Frohberg, P., Mehlig, U., and Berger, U. (2014). The importance of conspecific facilitation during recruitment and regeneration: A case study in degraded mangroves. *Basic and Applied Ecology* **15**, 651-660.

Vovides, A. G., Vogt, J., Kollert, A., Berger, U., Grueters, U., Peters, R., Lara-Domínguez, A. L., and López-Portillo, J. (2014). Morphological plasticity in mangrove trees: salinity-related changes in the allometry of Avicennia germinans. *Trees* **28**, 1413-1425.

West, G. B., Brown, J. H., and Enquist, B. J. (1997). A General Model for the Origin of Allometric Scaling Laws in Biology. *Science* **276**, 122-126.

West, G. B., Brown, J. H., and Enquist, B. J. (1999). A general model for the structure and allometry of plant vascular systems. *Nature* **400**, 664-667.

West, G. B., Enquist, B. J., and Brown, J. H. (2009). A general quantitative theory of forest structure and dynamics. *Proceedings of the National Academy of Sciences* **106**, 7040-7045.

Yoda, K., Kira, T., Ogawa, H., and Hozumi, K. (1963). Self-thinning in overcrowded pure stands under cultivated and natural conditions. *Journal of Biology, Osaka City University* **14**, 107-129.

# ANCILLARY DOCUMENTS

## Publications

### *Thesis related journal articles and conference presentations*

I. Olagoke, A., Proisy, C., Féret, J.-B., Blanchard, E., Fromard, F., Mehlig, U., de Menezes, M. M., dos Santos, V. F., and Berger, U. (2016). Extended biomass allometric equations for large mangrove trees from terrestrial LiDAR data. *Trees* **30**, 935-947. doi: 10.1007/s00468-015-1334-9

II. Proisy, C., Degenne, P., Anthony, E., Berger, U., Blanchard, E., Fromard, F., Gardel, A., Olagoke, A., Santos, V. F., Walcker, R., and Lo Seen, D. (2016). A multiscale simulation approach for linking mangrove dynamics to coastal processes using remote sensing observations. *Journal of Coastal Research*, Special Issue, No. 75, 810-814, doi: 10.2112/SI75-163.1.

III. Adewole Olagoke, Ronny Peters, Juliane Vogt, Christophe Proisy, Uta Berger (2016). Scaling mangrove tree responses and stand structure dynamics to environmental change: a simulation study, MMM4 Conference holding from 18-22 July 2016 at St. Augustine, Florida (USA) (Accepted abstract for oral presentation)

IV. Olagoke, A.O., C. Proisy, J-B. Feret, F. Fromard and U. Berger (2015). On the potential of Terrestrial Laser Scanning for revising biomass allometric models of mangrove trees, SilviLaser 2015 held at La Grande Motte (France) from 28–30 September 2015 (Invited Talk)/ short paper in proceedings, pp 99 – 101

### *Other relevant publications*

I. Bosire, J.O, Kaino, J.J., **Olagoke, A.O.**, Mwihaki, L.M., Ogendi, G.M.; Kairo, J.G., Berger, U. and Macharia, D. (2014). Mangroves in Peril: unprecedented degradation rates of peri-urban mangroves in Kenya. Biogeosciences, 11: 2623-2634, doi: 10.5194/bgd-10-16371-2013

II. **Olagoke, A.**, Bosire, J. and Berger, U. (2013). Regeneration of Rhizophora mucronata (Lamk.) in degraded mangrove forest: lessons from point pattern analyses of local tree interactions. Acta Oecologica 50: 1-9, http://dx.doi.org/10.1016/j.actao.2013.04.001

III. Olagoke, A., Mwihaki, L., Bosire, J. and Berger, U. (2013). Stand structure and spatial pattern of mangrove regeneration in a degraded peri-urban coastal forest, Tropentag 2013 held at Stuttgart-Hohenheim (Germany) between 17–19 September 2013 (Poster) – Online Abstract

# Résume Etendu (Extended summary in French)

## Vers une meilleure caractérisation de la plasticité morphologique et du partitionnement de la biomasse des palétuviers pour l'étude de la dynamique des forêts de mangroves

**Adewole Olagoke**

*Technische Universitat Dresden (Allemagne)*

*IRD-UMR AMAP/ AgroParisTech, Montpellier (France)*

**Mots clés :** Morphologie des plantes, allocation de biomasse, allometries, structure forestière, modélisation écologique, écosystèmes de mangrove, dynamique côtière

### Introduction

Les changements environnementaux sont souvent sources de stress pour la croissance des plantes. Jusqu'à présent, la plasticité morphologique des arbres, c'est à dire leur capacité à produire des physionomies différentes, n'a été que peu envisagée comme stratégie d'adaptation du peuplement forestier à un environnement stressant. Etant donné la variabilité des physionomies de palétuviers observée y compris au sein d'une même espèce (Figure 1), l'étude des mangroves nous est apparue pertinente à la fois pour aborder la question de l'adaptation des formes de plantes à des environnements changeants mais également pour apprendre sur le fonctionnement de cet écosystème soumis en permanence à des changements environnementaux.

Nous avons focalisé notre étude sur trois objectifs. Le premier était l'amélioration de la caractérisation des morphologies de palétuviers et du partitionnement de biomasse au sein des individus. Le deuxième objectif visait à analyser les différences inter-régionales des allométries et de discuter de leur impact sur le partitionnement de la biomasse. Le dernier objectif était plus théorique et s'intéressait à simuler et comprendre les effets de la plasticité morphologique des palétuviers sur l'émergence de structures et de dynamiques forestières dans différentes contraintes environnementales.

Si l'on considère les difficultés inhérentes aux expérimentations de terrain en mangroves, une originalité de ce travail a été sans aucun doute de tenter de décrire avec un scanner laser terrestre la physionomie de grands palétuviers pour caractériser le partitionnement de biomasse alors qu'il est impossible de prétendre réaliser des coupes et pesées *in situ*.

Une seconde originalité de ce travail vient probablement aussi du développement d'un outil de saisie d'inventaires forestiers proposant une représentation visuelle simplifiée de peuplements de palétuviers et des estimations de biomasse à partir d'une interface configurable. Notre vision à terme est de valoriser l'ensemble des descriptions de structures arborées et forestières afin de simuler à l'aide d'un modèle mécanistique la plasticité morphologique des arbres et le partitionnement en biomasse dans des gradients de salinité et de stress hydrique.


**Figure 1:** Illustration de la variabilité des formes de croissance chez le palétuvier *Avicennia germinans en Guyane Française et dans le nord du Brésil.*

J'ai réalisé des expérimentations de terrain dans deux grandes régions de mangroves situées de part et d'autre de l'embouchure de l'Amazone, à savoir, la Guyane Française et la péninsule de Bragança, dans l'état du Pará au Brésil (Figure 2).

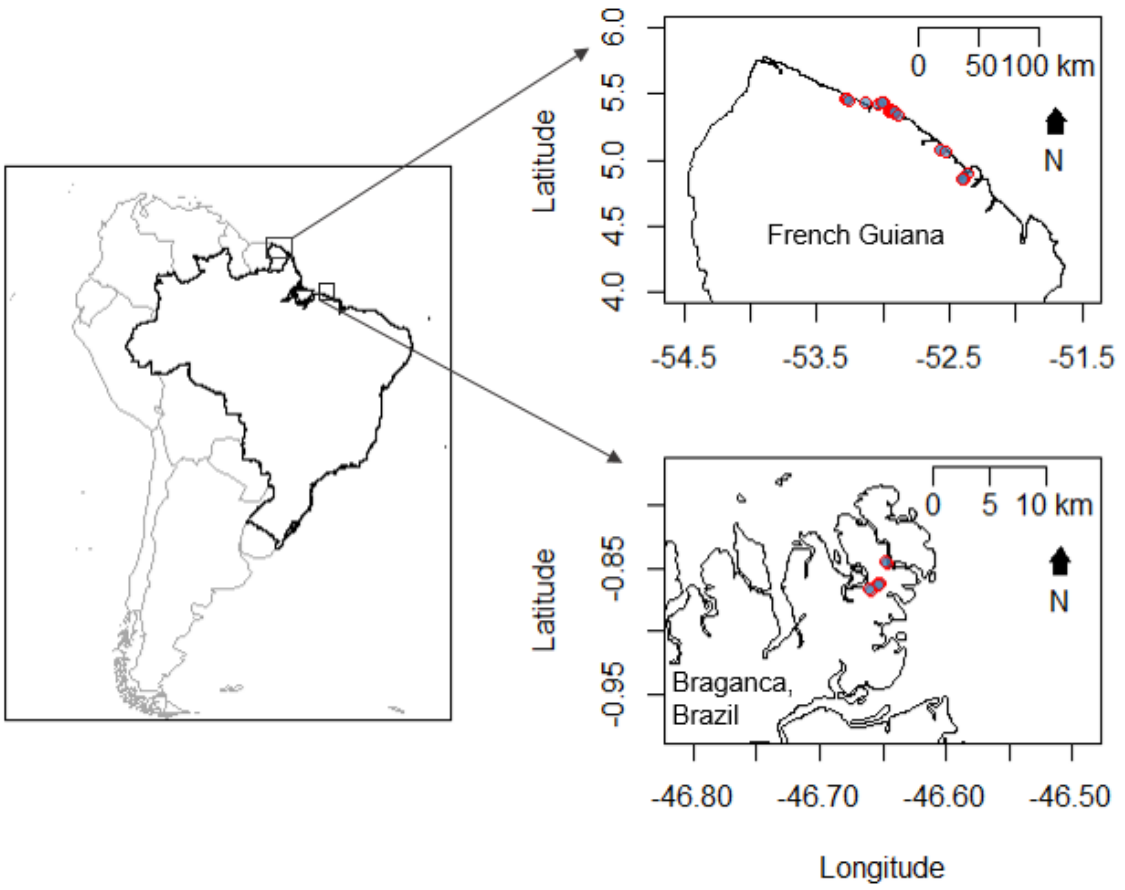


**Figure 2:** Localisation de régions d'étude en Guyane Française (en haut à droite) et dans la péninsule de Bragança, (en bas, à droite), état du Pará, Brésil. Les parcelles forestières inventoriées sont indiquées par les points en couleur.

Le manuscrit de thèse est structuré en 6 chapitres incluant :

1. Une introduction sur les enjeux d'obtenir des meilleures descriptions de la plasticité morphologique des arbres, notamment en mangroves, le détail des objectifs abordés et l'organisation du manuscrit.
2. La description d'une méthode non destructive obtenue à partir de l'analyse de données laser permettant de mieux estimer le partitionnement de biomasse au sein de grands palétuviers avec un focus spécial sur l'espèce *Avicennia germinans*. Ce travail a fait l'objet d'une communication internationale avec acte et d'un article paru dans le journal Trees – Structure and Function.
3. Une analyse inter-régionale des différences de morphologies de palétuviers et de leurs implications pour la dynamique de biomasse des mangroves amazoniennes. L'intérêt d'inclure dans les modèles d'estimation de biomasse épigée des paramètres descripteurs des formes de houppiers a été montré.
4. Le développement d'un logiciel facilitant la de saisie d'inventaires forestiers en mangroves permettant également de produire des représentations visuelles en forme dites de 'sucettes' et qui intègre la possibilité de calculer les biomasses d'arbres et de peuplement

à partir d'une interface configurable. Par ce travail, nous avons renforcé la possibilité de mener des études de modélisation écologique et d'interprétation d'images de télédétection.

5. Une étude théorique basée sur l'emploi d'une modèle mécaniste de l'influence du stress hydrique ou d'un gradient de salinité sur le partitionnement de biomasse au sein d'individus.

6. Une synthèse et une discussion générale des principaux résultats obtenus et comment ils contribuent à mieux lier dynamique forestière en mangrove et dynamique côtière des processus côtiers.

Voici un résumé étendu des 5 derniers chapitres.

## Chapitre 2 : Caractérisation de la structure et de la biomasse de palétuviers à partir de mesures issues d'un scanner laser et extension

La biomasse des grands arbres doit être mieux quantifiée afin de réaliser des bilans corrects de biomasse à l'échelle des massifs forestiers. Cependant, la plupart des modèles allométriques n'a pas été calibrée à partir d'un échantillonnage suffisant de grands arbres. C'est un problème majeur pour l'étude de la dynamique des mangroves de forte biomasse, eu égard à leur rôle dans le stockage de carbone. Nous avons exploré une alternative non destructrice au travail fastidieux et peu envisageable de coupe et de pesée in situ de grands palétuviers grâce à l'utilisation d'un scanner laser terrestre (Figure 3). En Guyane Française, nous avons scanné 36 *palétuviers de l'espèce A. germinans* à partir de positions multiples autour de chaque arbre sélectionné (Figure 3). Ces palétuviers présentaient des hauteurs variant entre 15 m et 45 m pour des diamètres troncs à hauteur de poitrine (DBH) variant entre 13 cm et 124.5 cm. L'idée sous-jacente était d'estimer la biomasse arborées à partir de l'estimation par laser du volume de bois dans le tronc et les grosses branches en utilisant un profil de densité volumique de bois ($kg/m^3$) dépendant de la hauteur de tronc et estimé à partir de carottes de bois prélevées sur une gamme de hauteurs de tronc allant de 0 à 25 m.

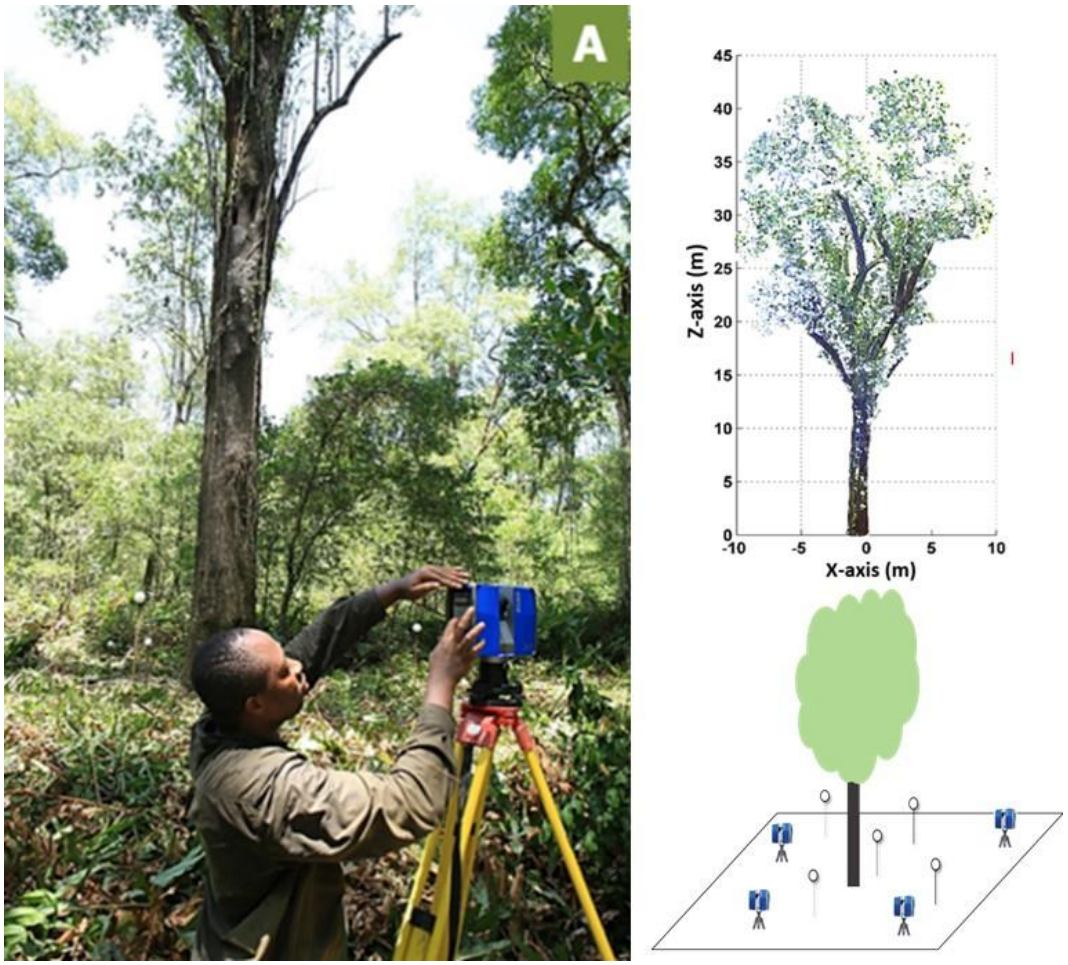


**Figure 3**: Préparation d'un scan laser d'un grand palétuvier avec l'instrument FARO 3D X330 monté sur un trépied en mangroves guyanaises (à gauche). Schéma d'implantation de l'instrument autour de l'arbre (en bas, à droite). Scan résultant d'un grand palétuvier après un premier nettoyage des points externes à l'arbre (en haut, à droite).

De manière à bien calculer les volumes de troncs non cylindriques ou présentant des contreforts, nous avons développé notre propre méthode d'analyse de nuages de points laser en projetant successivement de bas en haut du tronc l'ensemble des échos laser compris dans des sections de 10 cm avant d'utiliser une estimation de surface.

D'une part, nos estimations de biomasse à partir du volume corrèlent à 99% avec les biomasses de référence pesées après avoir coupé des palétuviers de diamètre de troncs inférieurs à 42cm. D'autre part, nous avons établi un nouveau modèle DBH-Biomasse épigée qui présentait un coefficient de corrélation $R^2$ de 0.99 et une erreur quadratique moyenne de 87.6 kg de matière sèche. Notre nouveau modèle, établi sur une plus gamme d'arbres, estime des biomasses totales d'arbres supérieures à ce que propose le modèle de référence. Il suggère que le modèle de référence établi (avant l'avènement des scanners lasers) par pesée pour les individus de DBH<42 cm sous-estime la biomasse des branches alors qu'il surestime la biomasse du tronc. Nous avons conclu qu'il était important de bien caractériser la structure et la biomasse des houppiers dans les grands arbres.

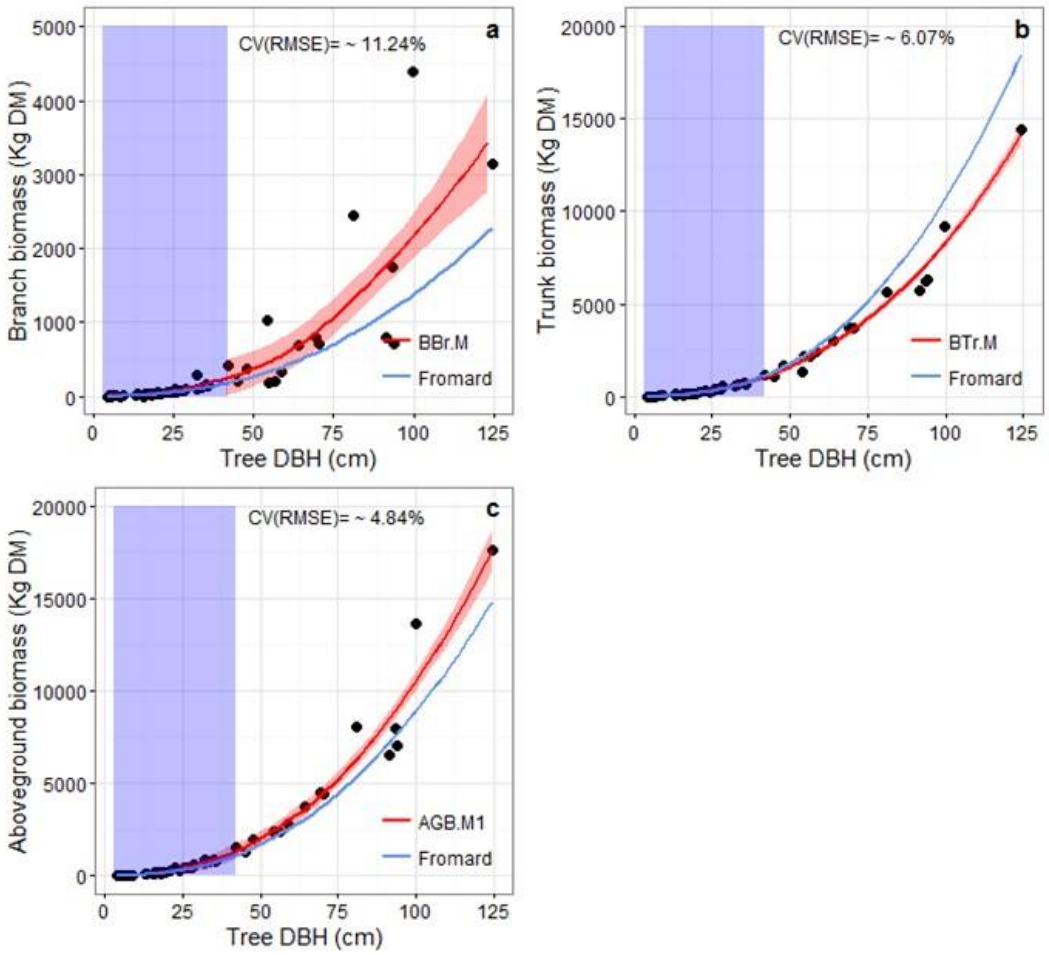


**Figure 4:** Comparaison des estimations de biomasses sur pied estimées par l'approche laser et celles estimées à partir du modèle de référence (Fromard) utilisé au-delà de son domaine de validité (représenté par la bande bleue). Nous distinguons le partitionnement de biomasse suivant: la biomasse des branches (a), la biomasse des troncs (b) et la biomasse totale (c). La ligne rouge donne les estimations du modèle basé sur les mesures laser de volume de bois (et l'intervalle de confiance) alors que la ligne bleue présente les estimations que donnerait le modèle de Fromard pour nos palétuviers scannés.

## Chapitre 4: La plasticité des palétuviers explique bien la dynamique de biomasse observée dans différentes régions de mangroves amazoniennes

Nous avons cherché à évaluer l'influence des variations inter-régionales de physionomies de palétuviers sur les biomasses épigées de peuplements forestiers dans nos deux régions pilotes situées de part et d'autre de l'embouchure de l'Amazone (Figure 5). La base d'inventaires incluait 45 parcelles de structuration diversifiée composée d'arbres de morphologie contrastée. Les différences marquées dans les dimensions de houppier suggèrent clairement une influence régionale sur les relations allométriques entre les mangroves guyanaises et brésiliennes de la région de Bragança (Figure 5).

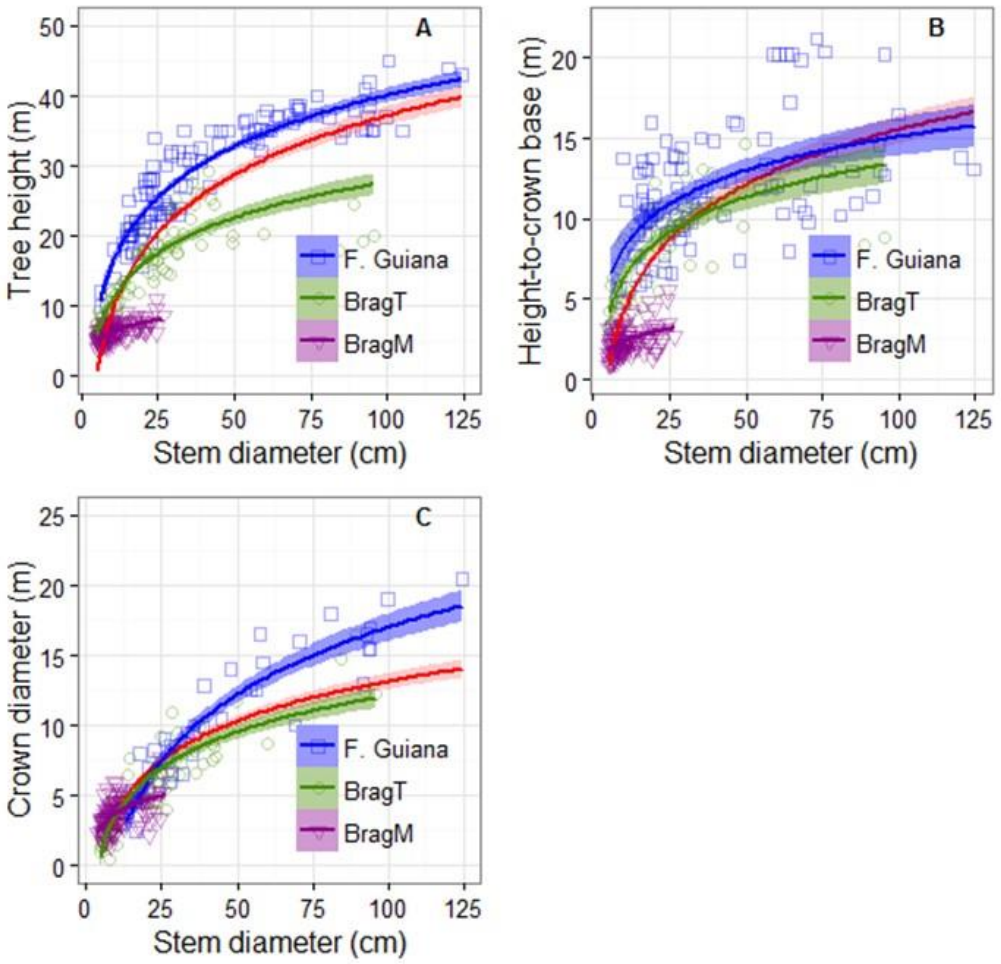


**Figure 5**: Comparaison des relations allométriques entre la Guyane Française (F. Guiana), les forêts de grande taille (BragT) et celles de taille moyenne (BragM) dans la région de Bragança. La courbe rouge indique un modèle régional agrégeant l'ensemble des données.

En prenant l'espèce *Avicennia germinans* comme test, nous avons cherché à optimiser une équation diamètre de tronc-biomasse (AGB.ha) par intégration de la hauteur et des dimensions de houppiers comme variables explicatives supplémentaires. Les résultats issues de l'analyse de covariance menée sur différents modèles basés sur différentes relations telles que hauteur totale *versus* diamètre de tronc, hauteur de houppier *versus* diamètre de tronc ou diamètre de houppier *versus* diamètre de tronc montrent que la variabilité locale des allométries d'arbres explique environ 30% de la variabilité des estimations de biomasse des individus pour tous les types de forêts considérés. Les modèles basés sur la surface terrière (SBA.ha), le diamètre quadratique moyen de tronc (Dq), le diamètre maximal de tronc (Dmax) et la hauteur maximale des individus (Hmax) expliquent jusqu'à 90% de la variabilité des estimations de biomasse produites par le modèle *AGB.ha.* Le meilleur modèle (noté SM.4), combinant SBA.ha, Dq and *Dmax* comme *variables explicatives,* prédit *AGB.ha des mangroves des Bragança avec une erreur RMS de 13.9%.* Par conséquent, ces résultats insistent sur le peu de précision générée par l'application de modèles allométriques régionaux. Par contre, incorporer dans un modèle de biomasse des paramètres descripteurs

de houppiers pourrait aider à rendre compte des différences inter-sites et donc de mieux appréhender les dynamiques structurales des forêts dans différentes régions côtières.


**Figure 6:** Contribution relative des descripteurs de physionomies d'arbres comme variables explicatives de la variabilité des biomasses de peuplements forestiers observée dans nos deux régions d'étude. *SM.1 – SM.4 représentent quatre modèles basés sur différentes combinaisons de descripteurs comme la surface terrière (SBA), le diamètre de tronc quadratique moyen (Dq), le diamètre médian de tronc (Dm), la hauteur maximale de l'arbre (Hmax) et le diamètre maximal de tronc (Dmax).*

## Chapitre 5: Lollymangrove: un logiciel de saisie de données d'inventaires forestiers, de représentation 3D simplifiée de peuplements de palétuviers, de test de différents modèles de biomasse et de couplage avec des modèles écologiques et de télédétection

L'acquisition de données forestières de bonne qualité et suivant des standards bien adaptés est essentielle pour mener des travaux de modélisation et avancer sur notre capacité à prédire les causes et les conséquences des changements dans la structuration des écosystèmes forestiers. Or de plus en plus de données sont collectées au travers le monde réelle harmonisation, ceci empêchant le partage, les comparaisons inter sites et les suivis temporels nécessaires à la compréhension des dynamiques forestiers. Pour le cas mangroves, nous avons décidé de contribuer à

résoudre ce problème via le développement d'un nouveau logiciel nommé 'Lollymangrove' à partir des outils disponibles (et le savoir-faire de nos collègues ingénieurs de l'UMR AMAP) dans la suite logicielle AMAPStudio (http://amapstudio.cirad.fr ; Figure 7).

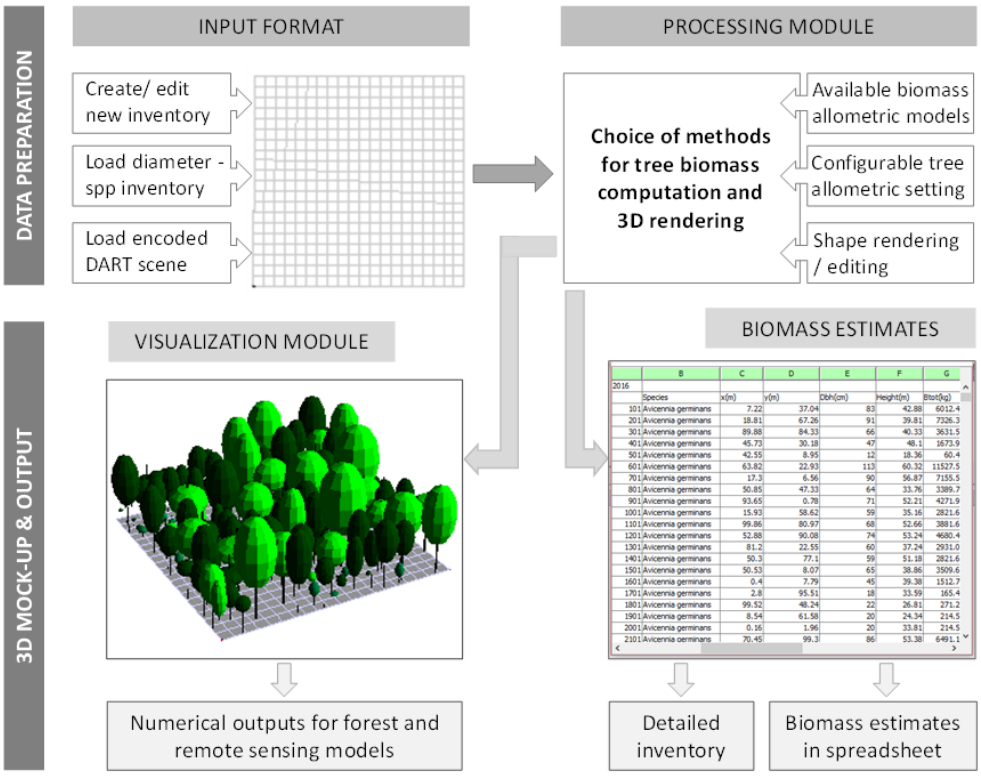


**Figure 7**: Structure de fonctionnement du logiciel Lollymangrove au travers quatre modules principaux qui incluent la saisie ou l'édition d'un inventaire forestier (cf. Input Format), le choix et le paramétrage de modèles allométriques diamètre de tronc-dimensions de houppiers et diamètre de tronc-biomasse pour chaque espèce de l'inventaire et l'ajustement des coefficients du modèle (cf. Processing module), le module de visualisation et d'exportation formatée de fichiers et l'export des calculs de biomasse pour chaque arbre et parcelle (cf. Biomass estimates).

Nous avons mis au point Lollymangrove avec les trois objectifs suivants :

1. Proposer un protocole de saisie d'inventaires forestiers utilisant une interface robuste connectée à une base de données permettant de choisir parmi plus de quarante espèces de palétuviers puis d'ajuster avec des mesures locales disponibles des modèles allométriques 'diamètre de tronc-dimension de houppier-hauteur d'arbres'.
2. Proposer une interface de sélection de modèles de biomasse parmi ceux disponibles dans la littérature permettant d'ajuster les coefficients des modèles choisis pour chacune des espèces présente dans l'inventaire forestier.
3. Proposer une visualisation 3D simplifiée de peuplements forestiers où chaque arbre est représenté sous la forme d'une 'sucette', le houppier correspondant à une ellipsoïde, l'exportation dans des formats variés de descriptions structurales de

peuplements pour assurer un couplage avec des modèles de dynamique forestière (Figure 8, 9) ou des modèles de télédétection et, enfin, des estimations de biomasses totale pour tous les arbres de la parcelle inventoriée.

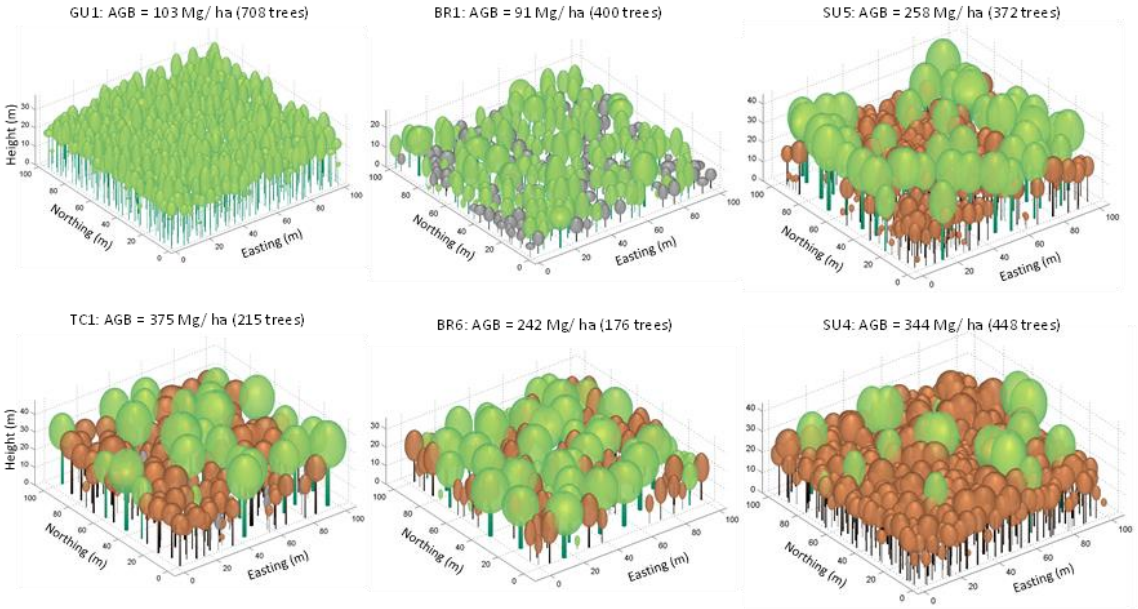


**Figure 8**: Examples 3D forest scene (mock-ups) of forest stands from contrasting mangrove ecosystems in the Amazon-influenced (South America).

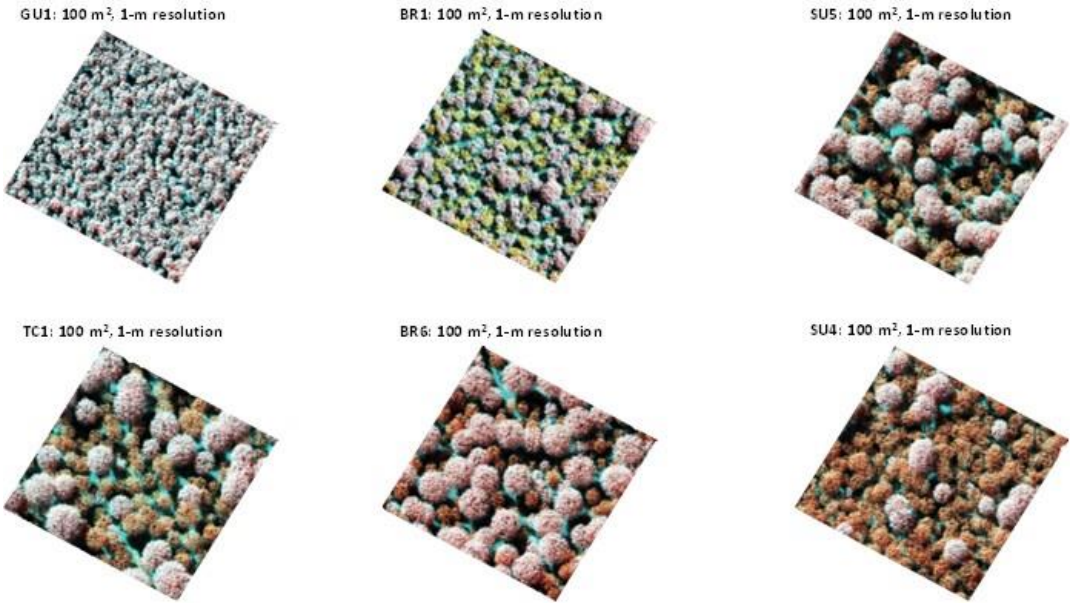


**Figure 9**: Simulated canopy images (from DART model) of the forest scenes presented in Figure 8. Each image corresponds to a multi-spectral (RGB-colored composite) WorldView-2 image acquisition at the configuration of 22.4° Zenith angle and 210° Azimuth angle.

## Chapitre 5: Simulation de l'influence de la plasticité morphologique et du partitionnement de biomasse sur le développement structural des forêts de mangrove

La plasticité morphologique des arbres induit une variabilité du partitionnement de la biomasse aérienne (et probablement souterraine) au fur et à mesure de la croissance de l'individu en fonction des conditions environnementales plus ou moins stressantes en termes d'apports lumineux, de nutriments ou d'eau. En conséquence, la physionomie en cours de modification continue d'un individu va également impactée les interactions de voisinage et les niveaux de compétition inter-arbres au sein d'un peuplement forestier. Afin de mieux comprendre ces interactions complexes, nous avons réalisé un travail théorique de simulation avec le modèle BETTINA_IBM (Figure 10).

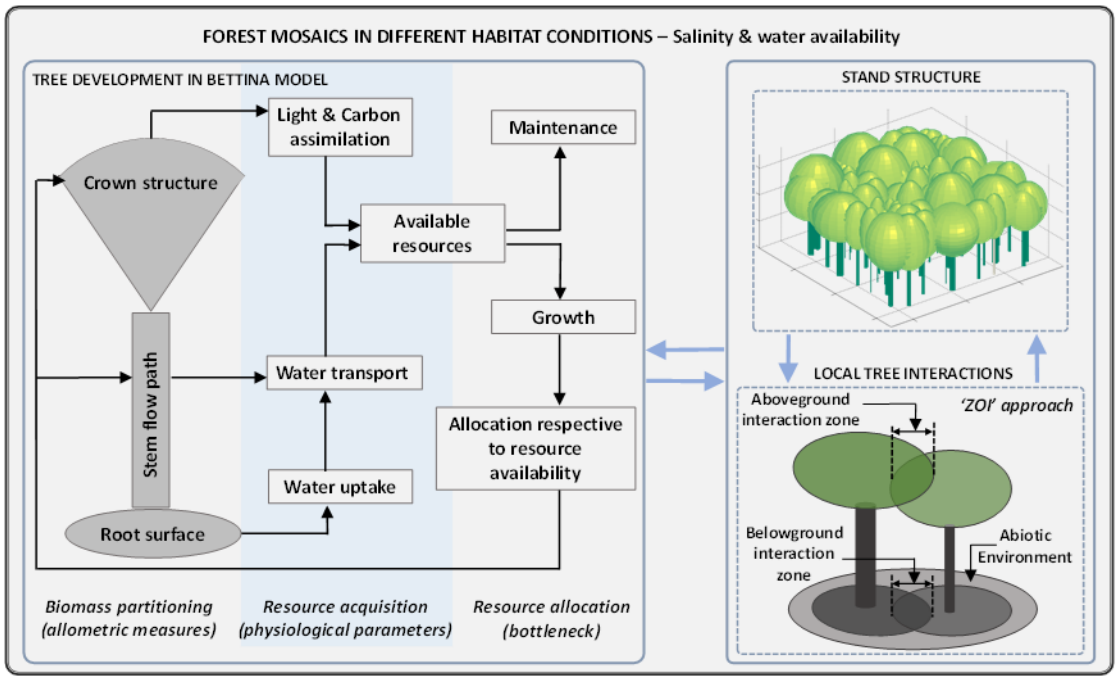


**Figure 9**: Le cadre de modélisation utilisé dans le modèle BETTINA pour simuler la structuration de peuplements de palétuviers en fonction de gradients de salinité et de disponibilité en eau. L'approche ZOI (Zone d'Influence) décrit les interactions locales entre 2 individus voisins au niveau du houppier et du sol.

Ce modèle individu centré et spatialement explicite décrit les mécanismes d'absorption de l'eau sous contraintes de salinité (Figure 11). Il permet d'appréhender les relations entre les conditions environnementales, les variations allométriques, le partitionnement de biomasse dans les palétuviers et la structuration des peuplements forestiers. En conditions de forte salinité, les

résultats sont en bonne adéquation (Figure 12) avec des processus écologiques simples (allométries, trajectoires d'auto-éclaircie, densité de mortalité, etc.). Dans des conditions de faible salinité, le paramétrage actuel sous-estime la hauteur et le diamètre maximaux observés. Les mécanismes de régulation à faible niveau de salinité doivent donc être mieux décrits dans le modèle utilisé.

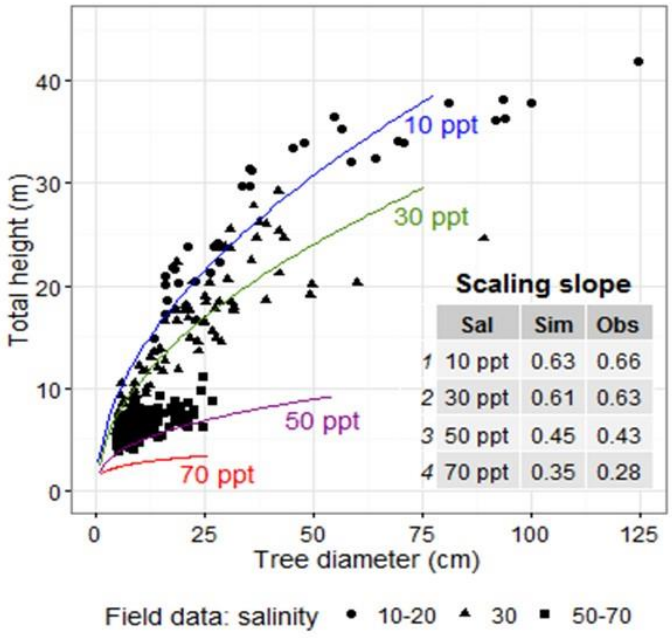


**Figure 11:** Relations allométriques entre le diamètre de tronc et la hauteur totale de l'arbre pour l'ensemble des parcelles inventoriées comparées avec les sorties du modèle BETTINA_IBM pour 4 valeurs de salinité.

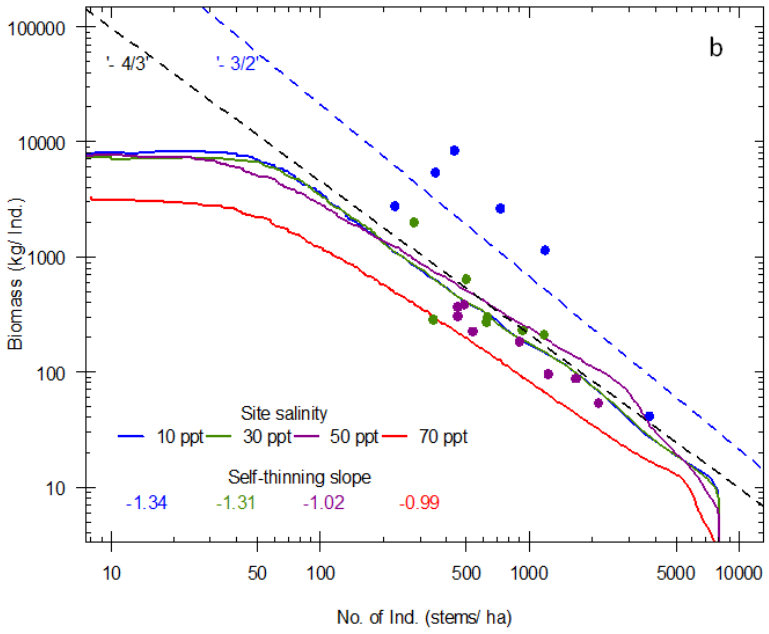


**Figure 12:** Trajectoires d'auto-éclaircie et relations simulées de biomasse aérienne-nombre de tiges sous différentes contraintes de salinité.

## Chapitre 6 : Synthèse

Ce travail de thèse a donné lieu aux publications suivantes.

1. **Olagoke, A.,** Proisy, C., Féret, J.-B., Blanchard, E., Fromard, F., Mehlig, U., de Menezes, M. M., dos Santos, V. F., and Berger, U. (2016). Extended biomass allometric equations for large mangrove trees from terrestrial LiDAR data. *Trees* **30**, 935-947. doi: 10.1007/s00468-015-1334-9
2. Proisy, C., Degenne, P., Anthony, E., Berger, U., Blanchard, E., Fromard, F., Gardel, A., **Olagoke, A.,** Santos, V. F., Walcker, R., and Lo Seen, D. (2016). A multiscale simulation approach for linking mangrove dynamics to coastal processes using remote sensing observations. *Journal of Coastal Research*, Special Issue, No. 75, 810-814, doi: 10.2112/SI75-163.1.
3. **Olagoke, A.,** Peters, R., Juliane Vogt, J., Proisy, C., Berger, U. (2016). Scaling mangrove tree responses and stand structure dynamics to environmental change: a simulation study, MMM4 Conference holding from 18-22 July 2016 at St. Augustine, Florida (USA) (Accepted abstract for oral presentation)
4. **Olagoke, A.,** Proisy, C., Féret, J-B., Fromard, F. and Berger, U. (2015). On the potential of Terrestrial Laser Scanning for revising biomass allometric models of mangrove trees, SilviLaser 2015 held at La Grande Motte (France) from 28–30 September 2015 (Invited Talk)/ short paper in proceedings, pp 99 – 101

En préparation pour une soumission dans le trimestre qui vient, nous avons les articles suivants (par niveau décroissant de finalisation) :

1. **Olagoke, A.**, C. Proisy, U. Berger, S. Costa Neto, G. Estrada, F. Facundes, R. Peters, M. Soares, V. Santos, F. de Coligny (xxxx). Lollymangrove software: A standardized tool for data acquisition and 3D description of mangrove forest structure. *To be submitted to Environmental Modeling and Software.*
2. Olagoke, A., Proisy, C., Mehlig, U., de Menezes, M. M., dos Santos, V. F., and Berger, U. (xxxx). Collective plastic tree attributes explain the dynamics of aboveground biomass in contrasting Amazon-influenced mangrove forests. *To be submitted to Applied Vegetation Science.*
3. Olagoke, A., Peters, R., Vovides, A., Mehlig, U., Proisy, C., and Berger, U. (xxxx). Do plastic morphology and biomass partitioning of trees matter in structural development and functioning of mangrove forests? *To be submitted to Ecological Modelling*

L'ensemble de mon travail, je pense, montre bien le besoin d'élucider comment la plasticité morphologique des palétuviers influence le développement structural et le fonctionnement des forêts de mangroves. Il a établi que la combinaison de mesures TLS et d'analyses de données de structure forestière associée à des efforts de modélisation écologique pouvait fournir des éléments indispensables pour lier dynamique des mangroves et dynamique des processus côtiers (cf. Proisy et al. 2016).

# Declaration of Independent Work

1. I hereby assure that I have produced the present work without inadmissible help from third parties and without aids other than those stated; ideas taken directly or indirectly from external sources are identified as such.

2. When selecting and evaluating the material and also when producing the manuscript, I have received support from the following persons:
   **Uta BERGER, Christophe PROISY, Ronny PETERS, Jean-Baptiste FÉRET, Ulf MEHLIG, François FROMARD, and François de COLIGNY.**

3. No further persons were involved in the intellectual production of the present work. In particular, I have not received help from a commercial doctoral adviser. No third parties have received monetary benefits from me, either directly or indirectly, for work relating to the content of the presented dissertation.

4. The work has not previously been presented in the same or a similar format to another examination body in Germany or abroad, nor has it - unless it is a cumulative dissertation - been published.

5. If this concerns a cumulative dissertation in accordance with Section 10 Para. 2, I assure compliance with the conditions laid down therein.

6. I confirm that I acknowledge the doctoral regulations of the Faculty of Environmental Sciences of the Technische Universität Dresden.

Tharandt, 22.09.2016

Adewole OLAGOKE